Aus dem Institut für Biochemie
Universität Freiburg (Schweiz)

Interaction of *Per* and *Cry* Genes in the Mammalian Circadian Clock

INAUGURAL-DISSERTATION

zur Erlangung der Würde eines *Doctor rerum naturalium*
der Mathematisch-Naturwissenschaftlichen Fakultät
der Universität Freiburg in der Schweiz

vorgelegt von

Henrik Oster
aus
Trier
(Deutschland)

Dissertation Nr. 1396
Erschienen 2002
in Eigendruck

Von der Mathematisch-Naturwissenschaftlichen Fakultät der Universität Freiburg in der Schweiz angenommen, auf Antrag von

Prof. Dr. Urs Albrecht, Universität Freiburg, Leiter der Doktorarbeit,
Priv.-Doz. Dr. Erik Maronde, IPF PharmaCeuticals Hannover, Gutachter,
und Prof. Dr. Ueli Schibler, Universität Genf, Gutachter.

Freiburg, den 8.11.2002

Der Leiter der Doktorarbeit: Der Dekan:

Prof. Urs Albrecht Prof. Dionys Baeriswyl

“The mind is its own place, and in it self
Can make a Heav'n of Hell, a Hell of Heav'n.“

(John Milton, „Paradise Lost“)

Meiner Mutter und meinem Vater.

Contents

Figure List

Table list

Summary

To cope with the daily changes in their environment, in organisms, from cyanobacteria to humans, endogenous clocks have evolved that anticipate these changes and synchronize physiology and behavior accordingly. In mammals, the central circadian pacemaker is located in the *suprachiasmatic nuclei* (SCN) of the hypothalamus. From there subordinated cellular clocks in the peripheral organs are controlled to create the overall rhythm of the organism. Circadian rhythms persist in the absence of external time information with near 24h periods, hence the term "circadian" from the Latin *circa dies* meaning "about one day" (Halberg, 1952). Time signals from the environment (so called *Zeitgeber*) like light, temperature variations, or food intake can phase shift the endogenous oscillator to synchronize the organism to geophysical time.

On the molecular level circadian clocks are built of cellular oscillators. Pacemaker genes like *Clock, Bmal1, mPer1* and *2, mCry1* and *2* or *Casein kinase 1e* are organized in a system of transcriptional/ translational feedback loops creating precise, stabilized 24h rhythms.

In this study we worked with two different model systems. We used transgenic mice (*Mus musculus*) with a targeted disruption of specific genes (*mPer1* and *2, mCry1* and *2*) or a combination of these genes to elucidate their function in the circadian clockwork. In a second project we examined the clock of the blind mole rat superspecies (*Spalax ehrenbergi*). Its isolated subterranean habitat, its adaptive visual and neuronal reorganization, and its polymorphic activity profile makes *Spalax* an extremely interesting model organism to study the evolution of the clock under special environmental conditions.

In mice we show that an additional deletion of the *mCry2* gene in *mPer2* mutants or a deletion of *mCry1* in *mPer1* mutants restores wild-type rhythmicity on the behavioral and the molecular level. This indicates that *mCry2* acts as a non-allelic suppressor of *mPer2* and *mCry1* of *mPer1* in the circadian oscillator. Young *mPer1/ mCry2* double mutants display a very long free-running period and lose rhythmicity with progressing age while *mPer2/ mCry1* mutants have no functional clock at all. This is accompanied by abnormal clock gene and protein regulation in the SCN and the eye.

Based on these findings we developed a model for the interaction of the *mPer* and *mCry* genes in the cellular oscillator providing new insights on how the clock is stabilized and integrates external time information at the molecular level. A multiunit complex of mPER and mCRY proteins forms the negative limb of the autoregulatory feedback loop controlling the periodic activation of clock genes. Specific preferences for homo and heteromeric protein

interactions between all mPER and mCRY proteins form a self-stabilizing oscillator at the transcriptional level. By deleting one or more of its components, the stability of the pacemaker is disturbed and the interaction preferences are altered. If this disturbance exceeds the compensation limits of the clock, the oscillation dampens and the animals become arrhythmic.

In *Spalax* we elucidated the molecular organization of the cellular clockwork by studying gene expression. We show that *Spalax* has a functional circadian clock on the molecular level with pacemaker genes like *Clock, Bmal1, Per1, 2* and *3* as well as two *Crys*. The clockwork of *Spalax* is highly similar to other rodents although some properties show specific adaptation to its subterranean habitat.

Our findings suggest that the hypertrophic Harderian gland surrounding the rudimentary and visually blind eye of these animals plays a functional role in the circadian system probably stabilizing the SCN pacemaker during continuous absence of outside time information.

Spalax can shift from a nocturnal to a diurnal activity pattern. We found that in nocturnal animals the central oscillator is uncoupled from the light driven input pathway indicating a specific control of clock entrainment pathways in both activity types.

Taken together this work provides new insights on redundant as well as distinct functions of the *Per* and *Cry* genes in the molecular mechanism of the circadian clockwork. It demonstrates the conservation of the system of autoregulatory feedback loops to stabilize circadian rhythmicity as well as highlights the evolutional adaptation of external clock regulation to the ecotope of the organism.

Zusammenfassung

Um sich optimal an die periodischen Veränderungen ihres Lebensraums im Verlauf des Tages anzupassen, besitzen die Lebewesen, von den Purpurbakterien bis zum Menschen, eine innere Uhr, die diese Zyklen antizipiert und Stoffwechsel und Verhalten dazu synchronisiert. In Säugetieren sitzt der zentrale innere Schrittmacher im *Nucleus suprachiasmaticus* (SCN) des Hypothalamus'. Von dort werden untergeordnete Uhren in den Organen des Körpers kontrolliert, die dann den Gesamtrhythmus des Organismus erzeugen. Auch wenn der Körper keine Zeitinformationen mehr von außen erhält, bleiben die zirkadianen Rhythmen stabil mit Periodenlängen von ungefähr 24h, daher der Ausdruck „zirkadian" von dem lateinischen *circa dies*, was soviel heißt wie „ungefähr ein Tag". Hinweise über die Tageszeit, so genannte *Zeitgeber*, wie Licht, Temperaturveränderungen oder Nahrungsaufnahme können die Phase des endogenen Oszillators verschieben, um so den Organismus ständig mit der geophysikalischen Zeit zu synchronisieren.

Auf molekularer Ebene besteht die zirkadiane Uhr aus einzelnen zellulären Oszillatoren. Uhrengene wie *Clock*, *Bmal1*, *mPer1* und *2*, *mCry1* und *2* sowie *Caseinkinase 1e* sind in einem System von Transkriptions-/ Translations-Rückkopplungsschleifen organisiert, das einen präzisen und stabilen 24h-Rhythmus generiert.

In der vorliegenden Arbeit haben wir mit zwei unterschiedlichen Modellsystemen gearbeitet. Wir benutzten transgene Mäuse (*Mus musculus*), in deren Erbgut einzelne oder eine Kombination bestimmter Gene (*mPer1* und *2* sowie *mCry1* und *2*) gezielt zerstört wurden, um deren Funktion im zirkadianen Uhrwerk zu bestimmen. In einem zweiten Projekt untersuchten wir die innere Uhr der Blindmaus (*Spalax ehrenbergi*). Sein isoliertes unterirdisches Habitat, eine adaptive visuelle und neuronale Reorganisation sowie sein polyphasisches Aktivitätsprofil machen *Spalax* zu einem äußerst interessanten Modellorganismus zum Studium der Entwicklung innerer Uhren unter besonderen Umweltbedingungen.

An Mäusen zeigen wir, dass eine zusätzliche Deletion des *mCry2*-Gens in *mPer2*-mutanten Tieren sowie eine Deletion von *mCry1* in *mPer1*-Mutanten die wildtyp-artige Rhythmizität auf Verhaltens- sowie auf molekularer Ebene wiederherstellt. Dies deutet darauf hin, dass *mCry2* als nicht-allelischer Suppressor von *mPer2* und *mCry1* als nicht-allelischer Suppressor von *mPer1* im zirkadianen Oszillator fungiert. Junge *mPer1*/ *mCry2*-Doppelmutanten zeigen eine extrem lange Periodenlänge unter Freilaufbedingungen. Sie verlieren ihre Rhythmizität jedoch mit fortschreitendem Alter. *mPer2/ mCry1*-Mutanten dagegen besitzen von Geburt an

keine funktionierende innere Uhr. Dies geht einher mit veränderter Uhrengen- und –proteinregulation im SCN sowie im Auge.

Auf der Grundlage diese Beobachtungen haben wir ein Modell zur Interaktion der *mPer*- und *mCry*-Gene im zellulären Oszillator entwickelt. Ein multimerer Komplex aus mPER- und mCRY-Proteinen bildet den negativen Arm einer autoregulatorischen Rückkopplungsschleife, welche die periodische Aktivierung der Uhrengene kontrolliert. Spezifische Präferenzen für homo- und heteromere Interaktionen zwischen allen mPER- und mCRY-Proteinen generieren einen selbststabilisierenden Oszillator auf transkriptioneller Ebene. Entfernt man eine oder mehrere der Komponenten aus diesem System, wird dessen Stabilität beeinträchtigt und die Interaktionspräferenzen werden verändert. Überschreitet diese Störung die Kompensationsmöglichkeiten der Uhr, wird die Oszillation gedämpft und die Tiere werden arrhythmisch.

An *Spalax* untersuchten wir die molekulare Organisation des zellulären Uhrwerks anhand der Genexpression. Wir zeigen, dass *Spalax* eine funktionelle molekulare Uhr besitzt mit Uhrengenen wie *Clock*, *Bmal1*, *Per1*, *2* und *3* sowie zwei *Crys*. Diese ist dem anderer Nagetiere sehr ähnlich, zeigt aber eine gewisse Anpassung an sein unterirdisches Habitat. Unser Ergebnisse deuten darauf hin, dass die hypertrophe Hardersche Drüse, die das rudimentäre und visuell blinde Auge dieser Tiere umgibt, eine funktionelle Rolle im zirkadianen System übernommen hat und den Schrittmacher im SCN während andauernder Abwesenheit äußerer Zeitinformation stabilisiert. *Spalax* kann von einem tagaktiven zu einem nachtaktiven Verhaltensmuster wechseln. Wir konnten zeigen, dass in nokturnalen Tieren der zentrale Oszillator der Uhr vom Lichteinfluss entkoppelt ist, was auf eine spezifische Kontrolle der Signalwege zur zeitlichen Synchronisierung der Uhr hindeutet.

Zusammengefasst gewährt diese Arbeit neue Einsichten in die redundanten sowie die spezifischen Funktionen der *Per*- und *Cry*-Gene im molekularen Mechanismus der zirkadianen Uhr. Sie betont die Konservierung des Systems autoregulatorischer Rückkopplungsschleifen zur Stabilisierung zirkadianer Rhythmik und zeigt ebenso die evolutionäre Adaption der externen Regulation der Uhr an die Lebensbedingungen des Organismus.

Abbreviations

α	activity phase
αS-ATP	α-thiophospho-adenosine-triphosphate
µg	micrograms
µl	microliters
τ	internal period length
(v/v)	volume per volume
(w/v)	weight per volume
°C	degrees Celsius
2n	number of chromosomes
^{32}P-dCTP	phosphor-32-phosphate labeled deoxy-cytosinetriphosphate
^{35}S-UTP	sulphur-35-sulphate labeled uridinetriphosphate
5-HT	serotonine
ACTH	adrenocorticotropic hormone
AP	accelerator potential
aPVN	autonomic paraventricular nucleus
Art.	article
AVP	arginine vasopressin
Bmal1/2	brain and muscle aryl hydrocarbon receptor nuclear translocator-like 1/2
BSA	bovine serum albumine
Ca^{2+}	calcium cation
CAL	calretinin
cAMP	cyclic adenosine monophosphate
CCG	clock controlled gene
cDNA	copy DNA
cGMP	cyclic guanosine monophosphate
CK1d/e	casein kinase 1 δ/ε
Clock	circadian locomotor output cycles kaput
cm	centimeters
CRE	cAMP responsive elements
CREB	cAMP responsive element binding protein
CRH	corticotrophin-releasing hormone
CT	circadian time
Dbp	D-albumine binding protein
DD	constant darkness
DMH	dorsomedial hypothalamic nucleus
DNA	deoxy-ribonucleic acid
EAP	experimental accelerator potentials
EDTA	ethylene-diamine-tetra-acetic acid
ER	endoplasmatic reticulum
ES cells	embryonic stem cells
et al.	and co-workers
FASPS	familial advanced sleep phase syndrome
Fig.	figure
GABA	γ-amino butyric acid
GH	gonadotropic hormone
GHT	geniculohypothalamic tract
GnRH	gonadotrophin-releasing hormone
GRP	gastrin-releasing peptide
h	hours
HCl	hydrochloric acid
Hprt	hypoxanthine phosphoribosyltransferase gene
IGL	intergeniculate leaflet
IML	intermediolateral column of the spinal chord
ir	immunoreactive
kb	kilobases
LD	light dark cycle
LGN	lateral geniculate nucleus
LL	constant light
Lx	lux

M	mole per liter
MAP	mitogen activated protein
ME	β-mercaptoethanol
min	minutes
min	minutes
mm	millimeters
mM	millimole per liter
MOP3/9	member of PAS superfamily 3/9
MOPS	3-morpholino-propanesulfonic acid
MPN	medial preoptic nucleus
mRNA	messenger ribonucleic acid
NaCl	sodium chloride
NOS	nitric oxide synthase
NPAS2	neuronal PAS domain protein 2
NPY	neuropeptide Y
OAP	overall accelerator potential
ON	over night
PAS	period / aryl hydrocarbon receptor nuclear translocator / singleminded
PBS	phosphate buffered saline
PFA	paraformaldehyde
PHI	phospho-histidine
PK2	prokineticin 2
PKA	protein kinase A
PKG	protein kinase G
PVN	paraventricular nuclei of the hypothalamus
RE	regression error
RHT	retinohypothalamic tract
RT	room temperature
RT-PCR	reverse transcription-polymerase chain reaction
s	seconds
SCG	superior cervical ganglion
SCN	suprachiasmatic nuclei
SDS	sodium dodecylsulfate
sPVN	sub-paraventricular nucleus
SS	somatostatin
TAB	theoretical overall accelerator potential
Tab.	table
TK	*Herpes simplex* virus thymidine kinase gene
TNT	Tris normal saline Tween 20 buffer
TPA	12-O-tetradecanoylphorbol-13-acetate
Tris	Tris-(hydroxymethy)-aminomethane
TTL	transcriptional/ translational feedback loop
UV	ultra-violet
V	Volt
VIP	vasoactive intestinal peptide
WT	wild-type
ZT	*Zeitgeber* time

Chapter 1

Introduction

1.1. The Internal Clock

In 1729, the French astronomer Jean-Jaques Dortous de Mairan discovered that the diurnal closing and opening rhythm of *Mimosa* leaves continues with a nearly 24h (=*"circadian"*) period when these plants are kept isolated from outside time information (so called "*Zeitgeber*", in this case the sun) in a closed cupboard. This was the birth of modern chronobiology, the research on biological rhythms. Circadian rhythmicity has since then not only been observed in leaves but at all levels of organization, from the behavior of mammals, flies, and single cells down to the activity of enzymes and the transcription of specific genes (Pittendrigh, 1993).

Internal clocks have evolved throughout all *phyla* and species, from ancient cyanobacteria to the modern *Homo sapiens* (Dunlap, 1999). The purpose of these internal timekeepers is to anticipate regular changes in the environment and synchronize the status of the whole organism to maximally benefit from the temporal availability of natural resources. The most prominent environment-shaping factor of our world is the succession of day and night and the easiest way to keep track of it is to monitor the rising and setting of the sun. Although for most species – with the exception maybe of photosynthetic organisms – the mere presence or absence of light is not an important parameter itself, secondary phenomena like the diurnal or nocturnal occurrence of predators, prey, the temperature difference or the varying efficiency of certain sensual organs at different times have driven evolution to develop circadian clocks (Rensing et al., 2001).

But why does *Mimosa* keep on closing and opening its leaves in total darkness? Or: Why do we need a self-sustaining clock, when it would be enough to evolve a sensory system for the presence or absence of light? The first answer is anticipation. If our body would merely react to the presence of light we would lose a certain amount of time every morning when it is already bright outside but our physiology is still in transition from "night"-status to "day" or

from "inactive" to "active". This is especially true for most animals living at least temporally in environments isolated from outside time information, e.g. in caves or buildings (Nevo et al., 1982). By anticipating these transitions the organism saves energy because the physiology can be prepared in an economic way. Additionally the timed availability of internal resources serves to maximally benefit from temporally restricted resources granting an important advantage under evolutional pressure.

The second aspect of the autonomous internal pacemaker points to its role as a synchronizer of different physiological aspects of the organism. In order to work efficiently, e.g. using as little energy as possible, the activity of the organs responsible for physiological aspects of the body has to be temporally organized. The time information given by the circadian oscillator serves to harmoniously orchestrate the interplay of the different meta- and catabolic pathways by linking them to the central clock (Akhtar et al., 2002; Panda et al., 2002a; Storch et al., 2002).

For most organisms light is the prominent *Zeitgeber* transferring outside time information to the internal pacemaker because of its high reliability and easy way of detection. However, different *Zeitgeber* exist like temperature, humidity as well as social factors like stress and pheromonal communication and for some species these might be even dominant to the daily cycle of the sun (Hastings et al., 1995; see as well Oster et al., below).

1.2. Physiological Aspects

In mammals the central circadian clock is located in the *suprachiasmatic nuclei* of the hypothalamus (SCN). Many if not all major physiological processes of the body are under circadian control (Panda et al., 2002a; Storch et al., 2002). The clock coordinates the different pathways with regard to the solar cycle *via* two distinct mechanisms, the endocrine system and the direct regulation of the activity of pace setting enzymes (Buijs and Kalsbeek, 2001). The SCN directs the endocrine system partly by secretion of melatonin from the pineal and partly *via* the hypothalamus. Several pathways lead from the SCN to the pineal: There is innervation *via* the *paraventricular nuclei* (PVN), extracerebral pathways including the intermediolateral column of the spinal chord (IML) and the superior cervical ganglion (SCG) as well as direct signaling (reviewed in Schwartz et al., 2001).

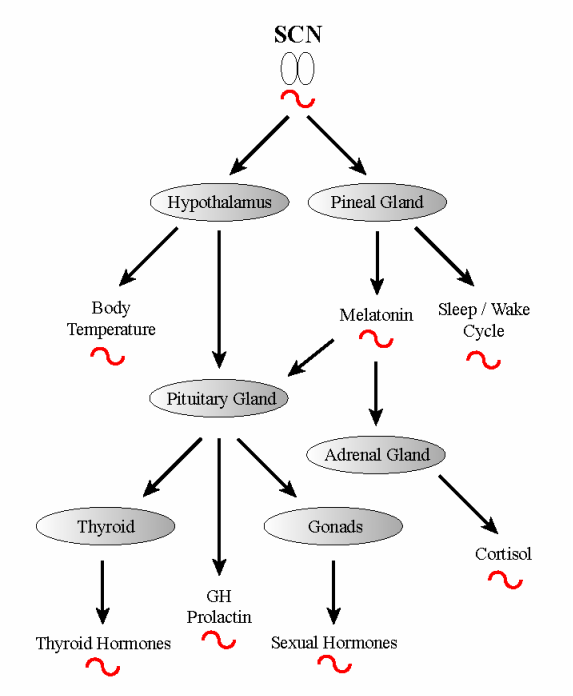

Fig. 1: Regulation of the mammalian endocrine system by the circadian clock. Grey spheres show endocrine glands influenced by the central oscillator in the SCN.
Red waves depict cycling hormonal levels and physiological parameters under circadian control (modified from http://www.rpi.edu/~hrushw/).

From the pineal, feedback to the SCN is provided by melatonin reception as well as nervous signaling in the brain. Melatonin levels are high during the night. It is involved in the regulation of the sleep/ wake cycle, influences the pituitary gland (see below) and controls the secretion of cortisols in the adrenal gland (Malpaux et al., 2001). The hypothalamus directs the daily variation of the body temperature and confers clock signaling to the pituitary gland. The pituitary gland releases hormones like GH, prolactin and ACTH and stimulates endocrine glands like the thyroid and the gonads which themselves produce a set of additional hormones (Goldman, 2001).

Recent studies using gene expression profiling in the SCN and peripheral tissues demonstrate that the activation of a high number of rate-limiting enzymes of key physiological pathways is under circadian control. The set of these genes / enzymes varies from tissue to tissue creating an organ specific pattern orchestrated by the central pacemaker (Akhtar et al., 2002; Panda et al., 2002a; Storch et al., 2002).

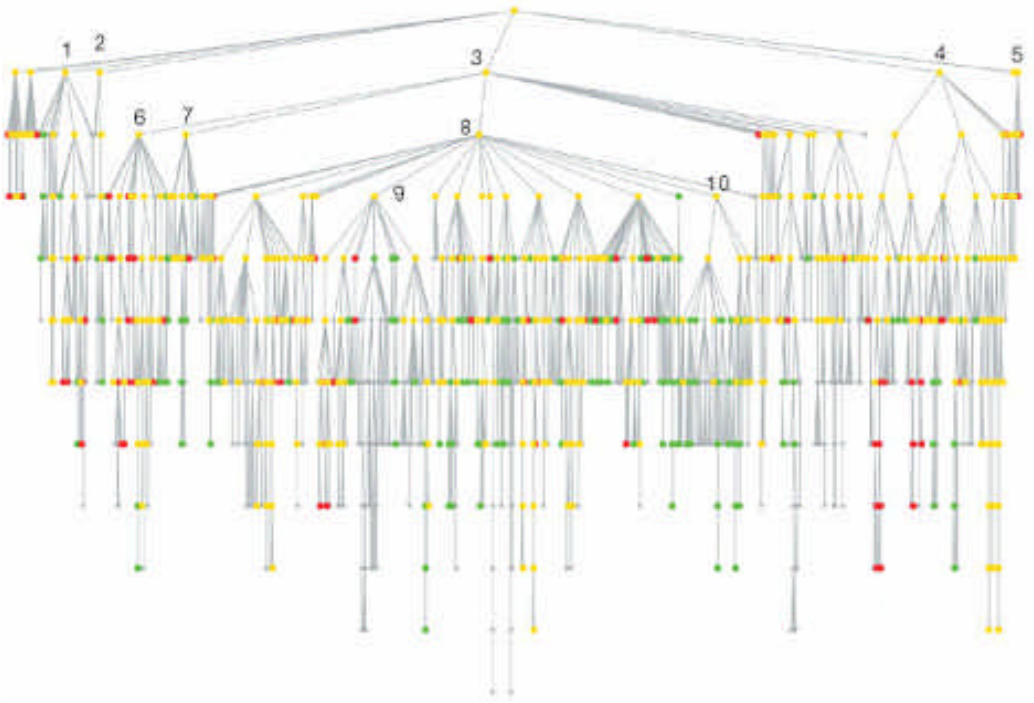

Fig. 2: Global comparison of biological processes associated with the genes exhibiting circadian expression in liver and heart. The tree (gray dots and connecting paths) represents those categories (dots) in the gene ontology hierarchy for biological process that match genes expressed in liver (green) or heart (red) or both (yellow). Selected examples of biological process categories are indicated by the following numbers: 1, developmental process; 2, death; 3, cell growth and/or maintenance; 4, cell communication; 5, behavior; 6, transport; 7, stress response; 8, metabolism; 9, (metabolism) nucleobase/ nucleoside/ nucleotide; 10, (metabolism) amino-acid derivative (modified from Storch et al., 2002)

1.3. The Internal Clockwork

1.3.1. The Central Oscillator

The master circadian clock of the mammalian organism resides in the *suprachiasmatic nuclei* of the anterior hypothalamus (Klein et al., 1991). It is composed of a few thousand densely packed, parvocellular neurons. The pacemaker of the SCN maintains its rhythmicity even in the absence of outside time information with a period of nearly but not exactly 24h (hence the term "circadian" from lat. "circa" = approximately and "dies" = the day). Generally nocturnal species like mice have an internal period (τ) of less, diurnal species like man of more than 24h in constant darkness (DD) (see (Pittendrigh and Daan, 1976). Under natural conditions however, the clock is not free running but periodically synchronized to the external daycycle. Environmental parameters linked to daytime, so called "Zeitgeber", confer time information to the central clock and reset its phase to match the external conditions. From the central clock, time information is conferred to the body. Subordinated clocks in peripheral organs receive information from the SCN *via* the activation of clock controlled genes ('CCGs'). Thereby the whole organism is synchronized with the solar cycle (reviewed in Herzog and Tosini, 2001 and Balsalobre, 2002).

1.3.2. Clock Input

Neurons in the ventrolateral part of the SCN receive glutamatergic input from the retina *via* the retinohypothalamic tract (RHT) (Moore and Lenn, 1972), neuropeptide Y (NPY) input from the intergeniculate leaflet (IGL) of the lateral geniculate nucleus (LGN) *via* the geniculohypothalamic tract (GHT) (Swanson and Cowan, 1975), and serotonergic (5-HT) input from the *Raphé nuclei* (Bosler and Beaudet, 1985; Francois-Bellan and Bosler, 1992). Neurons in the dorsomedial part of the SCN receive modest non-photic input from the cortex, basal forebrain and the hypothalamus (Moga and Moore, 1997).

The RHT conveys information about external lighting conditions to the SCN. Non-visual photoreceptors in the retina – the specific molecules are unknown, although good candidates are opsin based proteins like melanopsin located in the nuclear ganglion cell layer (Berson et al., 2002; Gooley et al., 2001; Hattar et al., 2002; Provencio et al., 2002) – activate monosynaptic projections to the SCN. Glutamate release at the synaptic terminals of the RHT

activate glutamate receptors resulting in a calcium influx in SCN neurons (reviewed in (Gillette and Mitchell, 2002)). This leads to an activation of calcium-dependent kinases, proteases and transcription factors (Xia et al., 1996). At the begin of the dark phase, light exposure causes phase delays (Pittendrigh and Daan, 1976). The downstream actions of calcium likely include activation of calmodulin, MAP kinases and PKA leading to a phosphorylation of the cAMP responsive element binding protein (CREB) which itself can activate *mPer* transcription *via* cAMP responsive elements (CRE) in the promoter (Gau et al., 2002; Gillette and Tischkau, 1999; Obrietan et al., 1998). In the late night light exposure *in vivo* (or glutamate receptor activation *in vitro*) causes phase advances *via* the activation of nitric oxide synthase (NOS) and cGMP dependent kinase (PKG) resulting in a phosphorylation of CREB (Ding et al., 1997; Gau et al., 2002).

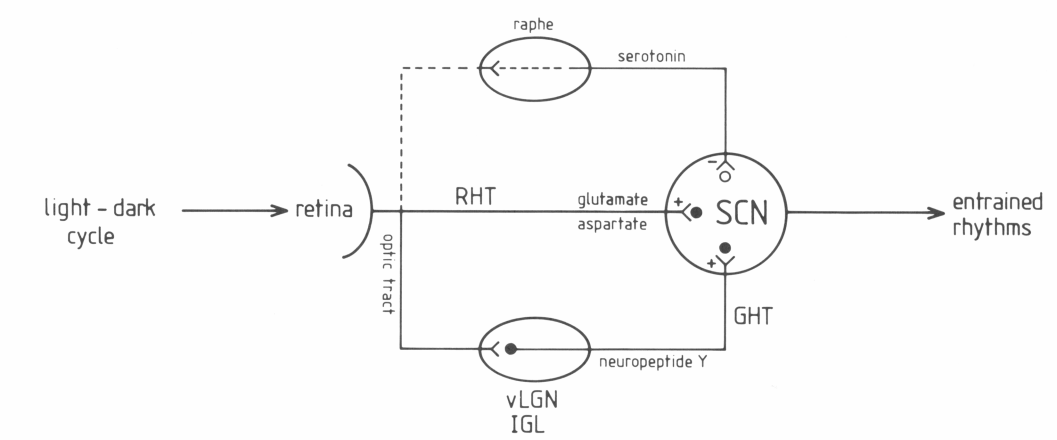

Fig. 3: Photic afferents to the SCN. Light/ dark information is conferred *via* the retina, the RHT and the IGL to the SCN. Main neurotransmitters of the RHT are glutamate and aspartate, while the GHT signals *via* NPY. Serotonergic efferents from the *Raphé nuclei* negatively modulate photic signaling in the SCN (RHT, retinohypothalamic tract; GHT, geniculohypothalamic tract; +, excitatory; -, inhibitory; ·, light responsive cells; ° cells may not be light-responsive (from Meijer, 1991).

A second pathway of photic signaling is formed by projections from the retina *via* NPY-reactive neurons in the IGL (Jacob et al., 1999). NPY levels in the ventrolateral SCN show a biphasic diurnal pattern with peaks at both light/ dark and dark/ light transitions. This rhythm however, is absent in DD suggesting a mere modulator function of the IGL in the responsiveness of the circadian system to light stimuli (Shinohara et al., 1993).

The serotonergic input from the *Raphé nuclei* seems to be tightly interlocked with the signaling from the retina (Cagampang and Inouye, 1994). Destruction of the 5-HT system increases light induced phase-shifts (Bradbury et al., 1997) while administration of the 5-HT precursor tryptophane inhibits photic phase shifts during subjective night (Glass et al., 1995).

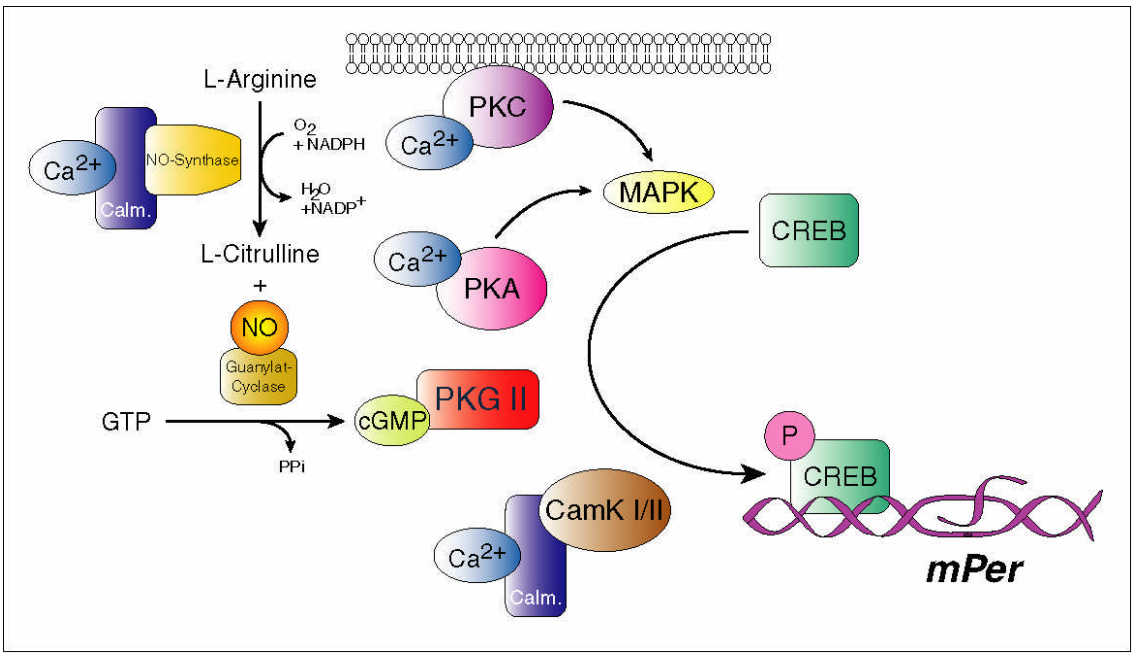

Fig. 4: Calcium mediated signaling to the circadian clock. Elevated calcium levels after nocturnal light stimulation activate calcium dependent kinases leading to a phosphorylation of the transcription factor CREB which induces *mPer* gene expression.

Apart from light there exist so-called "non-photic" stimuli which are able to reset the circadian clock (Hastings et al., 1997). An increase of the activity level in nocturnal animals during the inactive period by a dark pulse, forced wheel-running or benzodiazepine injection result in large phase advances (Gannon and Rea, 1995; Van Reeth and Turek, 1989; Wickland and Turek, 1991). Non-photic phase shifts seem to be mediated by NPY *via* the IGL (Biello et al., 1994; Janik and Mrosovsky, 1994; Maywood et al., 1997). The cellular signal transduction cascade of these stimuli is largely unknown. It does not affect CREB phosphorylation, but a role for serum cortisol through arousal-induced adrenocortical activation has been suggested (Sumova et al., 1994).

1.3.3. Clock Output

The projection pattern from the SCN is predominantly ipsilateral consisting of mainly six anatomical components of intra- and extra-hypothalamic origin. First there are rostrally directed fibers to the preoptic area, namely the anteroventricular periventricular nucleus and the anteroventral periventricular nucleus. Secondly there is projection to the paraventricular nucleus of the hypothalamus, the dorsomedial nucleus and finally into the posterior hypothalamic area and the periaquaeductal gray. A third line of efferent connections project

caudally to terminate in the region between the arcuate and the ventromedial nuclei. An additional projection is directed into the paraventricular nucleus of the thalamus and the paratenial nucleus. A small pathway leads to the intermediate lateral septal nucleus and a last one terminates in the intergeniculate leaflet of the lateral geniculate nucleus (Watts, 1991).

The individual SCN neurons contain different neuropeptides like AVP, VIP, GRP and somatostatin (reviewed in (Buijs and Kalsbeek, 2001)). Additionally about 30% of the SCN axons contain glutamate or GABA and a peptide transmitter (Castel and Morris, 2000; Hermes et al., 1996). The presence of these large number of transmitters in different combinations demonstrates the variety in SCN controlled signaling. GABA and AVP are essential for transmitting the daytime message of the SCN. GABA itself inhibits melatonin secretion from the pineal, which is the main signal of night time to the body.

The major target of efferent projections from the SCN is the paraventricular nucleus of the hypothalamus, an integrative center concerned with neuroendocrine, autonomic and behavioral processes (Swanson et al., 1987). It can influence the secretions of the anterior and posterior lobes of the pituitary gland as well as descending projections to the brain stem and the spinal cord. The PVN additionally controls the secretion of ACTH and thereby corticosterone. The extrahypothalamic projections are still poorly described functionally (Kalsbeek and Buijs, 2002).

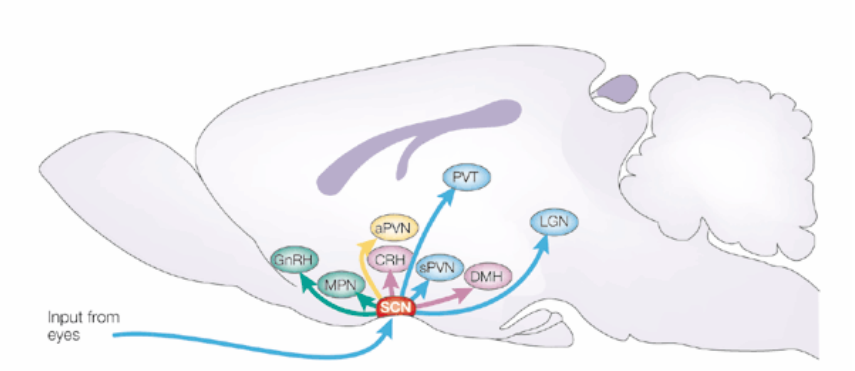

Fig. 5: Projective targets of the SCN. The SCN uses four important means to organize hormonal secretion: first, by direct contact with neuroendocrine neurons containing gonadotrophin-releasing hormone (GnRH) or corticotrophin-releasing hormone (CRH); second, by contact with neuroendocrine neurons *via* intermediate neurons like those of the medial preoptic nucleus (MPN), the dorsomedial hypothalamic nucleus (DMH) or the sub-paraventricular nucleus (sPVN); third, by projections to the autonomic PVN (aPVN) to influence the autonomic nervous system, preparing the endocrine organs for the arrival of hormones; and fourth, by influencing its own feedback. (from Buijs and Kalsbeek, 2001).

1.3.4. SCN Architecture

The *suprachiasmatic nuclei* are bilaterally paired tiny *nuclei* located just above the optic chiasm (therefore the name). They consist of small neurons, neuropile and glial elements, particularly astrocytes (van den Pol et al., 1992). Most neurons of the SCN are GABAergic although a large variety of neuropeptides are synthesized throughout the whole nucleus (Okamura et al., 1990). So far four different types of SCN neurons have been identified: monopolar, radial, simple bipolar, and curly bipolar (Pennartz et al., 1997). The simple bipolar cells, which have the highest number of all types, form the efferent projections from the *nuclei* (Pennartz et al., 1998). Axon immunoreactivity for many compounds is higher in the nucleus than in adjacent areas of the hypothalamus (Van Den Pol, 1991). The main neuroactive substances found in the SCN are reviewed in Moore et al., 2002):

γ-Amino butergic acid: GABA is the major neurotransmitter within the SCN and in SCN efferent projections. Therefore much of the local interaction within the SCN seems to be governed by inhibitory circuits. Stimulation of axons projecting into the periventricular region indeed results in a general depression of cells in the targeted area (Kow and Pfaff, 1984).

Gastrin-releasing Peptide: GRP is involved in the hypothalamic control of thermoregulation and homeostasis (Brown and Vale, 1979). GRP immunoreactivity is mainly found ventral and lateral in the medial part of the nucleus. GRPir neurons are the smallest neurons in the SCN.

Vasoactive Intestinal Peptide: VIP positive neurons are found in the same area as GRPir cells overlapping visual and *Raphé* afferents. VIPir neurons seem to be located slightly more ventral than the GRPir neurons. Together both cells comprise about 39% of all SCN neurons.

Vasopressin: AVP-containing neurons are found throughout the whole body of the SCN with some higher concentration in the dorsomedial part. They comprise about 37% of all SCN neurons and co-localize in part with angiotensin II positive cells.

Calretinin: CALir neurons are found mainly in the dorsolateral part and in adjacent hypothalamic areas of the SCN. Their number comes up to 14% of all SCN neurons.

Somatostatin: SS is well expressed in the shell of the SCN near to the shell/ core border. Somatostatin application modulates the firing activity of SCN neurons and depresses activity of neurons in the hypothalamic ventromedial nucleus (van den Pol, 1991).

While serotonin-mediated afferents do not terminate in a specific area of the SCN, photic signaling *via* glutamate and NPY mainly terminates in the ventrolateral part of the *nuclei*. Although there exist several neuronal connections between both *nuclei* of the SCN (Van Den Pol, 1980), both rhythms can be separated as seen in hamsters with a split locomotor activity.

In this case the *nuclei* oscillate in anti-phase (de la Iglesia et al., 2000). Ablation of one of the nuclei eliminates the split rhythm (Pickard and Turek, 1983).

SCN glial cells have mostly been omitted from models of cellular interactions underlying circadian rhythms. However, they make up a large part of the total cell number of the SCN. Astrocytes in the SCN seem to be metabolically active and show an increase in calcium levels on neurotransmitter release in the synaptic cleft indicating intraglial signaling probably mediated *via* GAP junctions upon neurotransmitter stimulation (van den Pol, 1991).

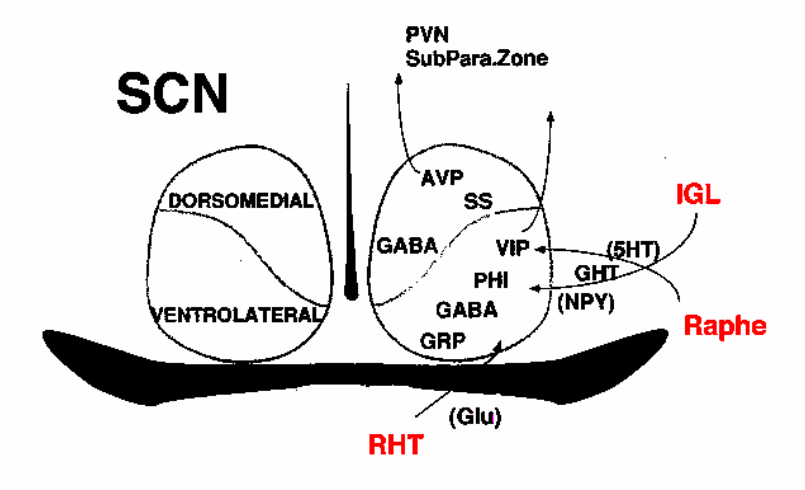

Fig. 6: Anatomical organization of the SCN. Indicated are afferent and efferent neuronal projections and the major neuroactive substances detected in the core and the shell of the SCN (AVP: arginine vasopressin; GABA: g-amino butyric acid; Glu: glutamate; GRP: gastrin-releasing peptide; GHT: geniculohypothalamic tract; 5HT: 5-hydroxythryptamine (serotonin); IGL: intergeniculate leaflet; NPY: neuropeptide Y; PHI: phospho-histidine; PVN: paraventricular nucleus of the hypothalamus; RHT: retinohypothalamic tract; SS: somatostatin; VIP: vasoactive intestinal protein; modified from www.aasmnet.org/MEDSleep/ rhythmslides.htm).

1.4. The Cellular Clockwork

The dominant role of the SCN in the control of circadian rhythms has been identified by lesion experiments in the early seventies (Moore and Eichler, 1972; Stephan and Zucker, 1972). The origin of its circadian firing rate activity has been traced from small unit recordings (Groos and Hendriks, 1982) down to the rhythmicity of single neurons (Welsh et al., 1995). Therefore it seems that the rhythmic signal from the SCN is an integration of a large population of single cellular clocks connected to each other but each cell has a principally self-sustaining rhythm. Chimaeric mice with SCNs composed of two cell types of different internal period lengths indeed show a variety of circadian phenotypes with a period range depending on the relative number of each cell type in the SCN (Low-Zeddies and Takahashi, 2001). On the other hand in *Clock* mutant mice which become arrhythmic after some time in DD, it has been demonstrated that the isolated SCN neurons retain a rhythmic firing rate even when the animal has already lost its internal rhythm. Therefore the arrhythmicity in these mice seems to be a problem of cell communication rather than a breakdown of the cellular clockwork itself (Nakamura et al., 2002).

With the discovery of the first clock gene *period* in *Drosophila melanogaster* (Konopka and Benzer, 1971) research started on the molecular aspects of the circadian clock. Until now a growing number of clock and clock related genes have been discovered in species throughout all *phyla*. Most of these genes found in animals and fungi are listed in table 1 below.

The molecular clockwork can be divided into three parts: Input, pacemaker and output. The pacemaker genes are important for the maintenance of rhythmicity under constant conditions. Their inactivation manifests as altered or disrupted rhythmicity in DD. Mutations or loss of input genes uncouples the internal clock from outside time information thereby de-synchronizing the organism with respect to the solar cycle. Output genes transmit time information from the SCN to the body. A loss of an output gene results in the disruption of peripheral rhythms subordinated to the signaling pathway of that gene. Some of these genes have partially redundant functions in the internal clockwork. Therefore the disruption of one single gene can often be compensated by others making it difficult to define a clear phenotype in the single mutant organism.

Table 1 | **Clock genes in animals and fungi**

Gene	Organism	Characteristics of protein product	Function (in the circadian system)
Input genes			
cry	*Drosophila*	Similar to DNA photolyases	Conveys photic information to PER–TIM
Immediate early genes (*c-fos*)?	Mammals	Transcription factors	Induced by light in the suprachiasmatic nucleus; important for photic entrainment
per1, 2	Mammals	PAS domain	Induced by light in the SCN; *Per1* important for photic entrainment
wc-1	*Neurospora*	PAS domain; GATA transcription factor	Required for light-induced *frq* expression
Pacemaker genes			
clock	Mammals, birds, fish, amphibians	bHLH–PAS factor	Dimerizes with BMAL1 and activates clock and clock-controlled gene expression
per	Mammals (3 genes), fish, insects	PAS domain	Negatively regulates CLOCK–BMAL1-driven transcription; positively regulates *bmal* (mammals) or *clock* (*Drosophila*) expression
tim	Mammals (?), fish *Drosophila*		In *Drosophila*, dimerizes with PER to repress CLOCK–BMAL1-driven transcription and activate clock expression
bmal1 (*cycle*)	Mammals (2 genes?) Fish (2 genes) *Drosophila*	bHLH–PAS factor	Dimerizes with CLOCK and activates CLOCK and CLOCK-controlled gene expression (function of MOP9, a close human homologue, is not defined)
cry	Mammals (2 genes) *Drosophila*	Similar to DNA photolyases	In *Drosophila*, binds TIM and inhibits PER–TIM dimer In mammals, negatively regulates CLOCK–BMAL1-driven transcription; translocates PER to the nucleus
CKIε (*doubletime*)	Mammals *Drosophila*	Serine/threonine protein kinase	Phosphorylates and destabilizes PER (at least PER1 in mammals)
vrille?	*Drosophila*	Similar to PAR leucine-zipper factors	Affects *per* and *tim* expression
dbp?	Mammals	PAR leucine-zipper transcription factor	May be involved in *per1* expression
frq	*Neurospora*		Negatively regulates WC-1/WC-2-driven transcription of its own gene; positively regulates WC-1 expression
wc-1	*Neurospora*	PAS domain; GATA transcription factor	Dimerizes with WC-2 and activates *frq* expression
wc-2	*Neurospora*	PAS domain; GATA transcription factor	Dimerizes with WC-1 and activates *frq* expression
Output genes			
pdf	*Drosophila*	Neuropeptide	Links the molecular clock to behaviour
avp	Mammals	Vasopressin peptide	Controls the activity of various output pathways
vrille	*Drosophila*	Similar to PAR leucine-zipper factors	Indirectly controls PDF peptide oscillation
dbp	Mammals	PAR leucine-zipper transcription factor	Controls rhythmic expression of various genes; influences circadian behaviour
CREM	Mammals	bZip transcription factor	The repressor isoform ICER is involved in the rhythmic expression of NAT, the key enzyme in melatonin synthesis
takeout	*Drosophila*	Similarity to ligand-binding proteins	Involved in output pathways that link the clock to feeding

Table 1: Clock genes in animals and fungi (from Cermakian and Sassone-Corsi, 2000)

The basic principle underlying all cellular clocks described so far is the transcriptional/ translational feedback loop (reviewed in Panda et al., 2002b). In it's simplest form it consists of an oscillator gene and its protein product (see Fig 7 below). The activation of the oscillator gene results in the production of the corresponding mRNA, which is translocated to the endoplasmatic reticulum where its message is translated into the cytoplasmic oscillator protein. When the concentration of the oscillator protein in the cytoplasm reaches a certain threshold, it re-translocates back into the nucleus where it can interfere with its own transcription machinery thereby inhibiting the activation of the oscillator gene. Subsequently the oscillator protein levels decrease due to constitutive degradation in the cytoplasm and in the nucleus. With the oscillator protein levels the inhibition of the oscillator gene transcription is reduced and the cycle starts again.

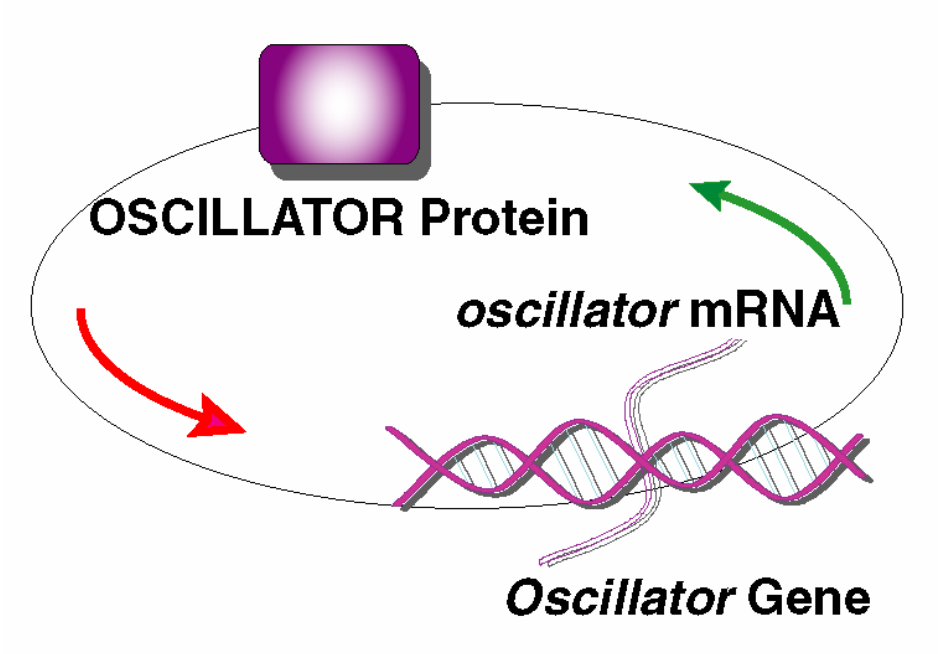

Fig. 7: The principle of the transcriptional/ translational feedback loop (TTL). The activation of an oscillator gene leads to the production of oscillator protein. High oscillator protein levels inhibit their own transcription resulting in a decrease of oscillator protein and the cycle starts again.

This basic principle seems to be preserved throughout all *phyla.* Some of the genes involved - like the *Cryptochromes* found in plants, insects, fishes, amphibia and mammals (reviewed in Sancar, 2000) - appear in many organisms studied so far. But the role these genes play in the clockwork underlies some variation. This has caused confusion in the beginning of molecular chronobiology and led to some likely misinterpretations due to inappropriate experimental setups (Cermakian et al., 2002; Sangoram et al., 1998; Yagita et al., 2000). In the following part I will therefore focus on the mammalian system. Although studies were done predominantly in nocturnal rodents like mice, rats and hamsters, the rodent clock believed to essentially follow the same organization as the human counterpart. As can be seen in the second part of this work, clock gene regulation is indeed highly similar in nocturnal and diurnal mammals (Avivi et al., 2001; Avivi et al., 2002). Additionally there are studies emerging on clock gene polymorphism and mutations in humans with phenotypes expected from the corresponding mouse mutants (Toh et al., 2001).

Clock was the first clock gene cloned in mammals (King et al., 1997). Clock mutants – identified in a chemical mutagenesis screen – show an abnormally long period in constant darkness (DD) finally causing arrhythmicity in homozygous animals (Vitaterna et al., 1994). CLOCK protein forms heterodimers with BMAL1 (or MOP3). Both proteins contain a PAS domain (from *per/ arnt/ sim*) important for protein/ protein interactions, a motif conserved in many proteins involved in the generation of circadian rhythms (Gu et al., 2000; Kay, 1997;

Reppert, 1998). Additionally both have a basic helix-loop-helix motif (bHLH) for protein/ DNA interaction. The CLOCK/ BMAL1 complex can bind to E-boxes containing the nucleotide sequence CACGTG found in the promoter regions of several other clock related genes like *mPer1, mPer2, mCry1, mCry2, Dbp, AVP* among others (Darlington et al., 1998; Gekakis et al., 1998; Hogenesch et al., 1998; Jin et al., 1999; Kume et al., 1999). The mutated CLOCK protein can still bind BMAL1 but the transcriptional activation of other clock genes is deficient (Gekakis et al., 1998).

BMAL1 and the highly similar BMAL2 (also known as MOP9) can both form heterodimers with CLOCK. Together they can drive transcription from E-box elements and are co-expressed in neurons of the SCN (Gekakis et al., 1998; Hogenesch et al., 1998; Hogenesch et al., 2000; Honma et al., 1998; Ikeda et al., 2000; Jin et al., 1999; Ripperger et al., 2000). Mice with a targeted deletion in the *Bmal1* gene show an impaired entrainment to an LD cycle with comparably high activity levels during the day and a variable onset of activity after "lights off". Upon release into constant darkness (DD) the animals immediately become arrhythmic indicating a complete disruption of the circadian clockwork. Additionally it was shown that in these mutants *mPer* and *Dbp* gene expression is not cyclic anymore. Therefore CLOCK alone is not sufficient to activate E-box driven transcription nor can *MOP9* compensate the loss of *Bmal1* in these animals (Bunger et al., 2000).

If the transcriptional activation of clock genes by CLOCK/ BMAL1 is the positive arm of the transcriptional/ translational feedback loop the inhibition of CLOCK/ BMAL1 by the products of these clock genes constitutes its negative counterpart.

Both *Cryptochromes* (mCRY1 and mCRY2) and *Period* proteins have the ability to inhibit CLOCK/ BMAL1 with the CRYs having by far the biggest inhibitory effect *in vitro*. *mCry1* mRNA levels are cycling with a circadian period while *mCry2* transcript shows only slight variations throughout the day. mCRY2 protein however, is prominently oscillating in the SCN. Both proteins are predominantly localized in the nucleus where they can interfere with the CLOCK/ BMAL1 heterodimer (Kume et al., 1999). Mice with a targeted disruption of the *mCry1* gene show a shortened free-running period (τ) in DD while a loss of *mCry2* results in a prolonged τ under constant conditions. A simultaneous deletion of both genes however, leads to a complete loss of rhythmicity in these animals indicating a complementary but essential role for both *Cry* genes in the TTL of the central pacemaker (van der Horst et al., 1999; Vitaterna et al., 1999).

The transcripts of all three known *mPer* genes oscillate with a 24h period in the SCN and most peripheral tissues (see below; Albrecht et al., 1997b; Shearman et al., 1997; Sun et al.,

1997; Takumi et al., 1998; Tei et al., 1997; Zylka et al., 1998b). All PER proteins contain PAS domains, which seem to play a role in PER/ PER protein interactions (Yagita et al., 2000). Additionally *in vitro* studies suggest an interaction between both PER and CRY proteins (Griffin et al., 1999; Kume et al., 1999; Yagita et al., 2001). A partial deletion of the PAS domain of *mPer2* results in a shortened free-running period in homozygous mice. Moreover these mice completely lose their rhythm after some time in constant darkness (Bae et al., 2001; Zheng et al., 1999). In contrast, *mPer1* mutants do not get arrhythmic although their free-running period is reduced and destabilized (Bae et al., 2001; Cermakian et al., 2001; Zheng et al., 2001). *mPer1/ mPer2* double mutants do not show any circadian rhythm in DD indicating a complete disruption of the circadian pacemaker (Bae et al., 2001; Zheng et al., 2001). The deletion of *mPer3* has only minor effects on the circadian phenotype in mice. Therefore *mPer3* seems not to play a role in the central oscillator but may still be part of some clock regulated output pathway (Shearman et al., 2000a).

Low levels of clock gene transcripts in *mPer* mutant mice lead to the discovery of a second role of *mPer2* in the TTL: It seems to have a positive influence on *Bmal1* transcription (Shearman et al., 2000b). *In vitro* studies indicate that mPER2 as well as mCRY1 and mCRY2 can activate *Bmal1* promoter driven transcription (Yu et al., 2002). Other studies suggest *Rev-erbα* as a transcriptional inhibitor of *Bmal1* that in turn can be inhibited by interaction with PER2 (Preitner et al., 2002). This second loop in the central oscillator is believed to stabilize the clock to ensure a precise and constant rhythmicity in the absence of regular *Zeitgeber* input (Hastings, 2000).

A third role of the two *mPer* genes lies in their transcriptional activation by light. While *mPer1* expression can be induced throughout the night *mPer2* is light sensitive only at the beginning of the dark phase (Albrecht et al., 1997b). Thus the *mPers* seem to form the link between the central oscillator and the input pathways to the clock. It has been demonstrated that *mPer* mutant mice show impaired resetting of their activity rhythms in response to nocturnal light pulses (Albrecht et al., 2001). While *mPer2* mutants have deficiencies in clock delaying after a light pulse at the begin of the night, *mPer1* mutants are not able to phase advance after light exposure before sunrise. This corresponds with the differential light inducibility of both *mPer* genes by light with *mPer2* being light responsive only at the begin of the night (Albrecht et al., 1997b).

The *mPer1* promoter contains CRE motifs capable of binding the phosphorylated form of the cAMP responsive element binding protein (CREB) (Shigeyoshi et al., 1997) activated by the Ca^{2+} mediated light signaling pathways in the SCN (see above). In addition, the *hPer1*

promoter has been shown to integrate signaling from other second messenger pathways like Protein kinase A, C, G and mitogen activated kinases (Akashi and Nishida, 2000; Lee et al., 1999; Motzkus et al., 2002; Motzkus et al., 2000; Prosser and Gillette, 1989; Sanada et al., 2000; Schak and Harrington, 1999; Tischkau et al., 2000). Thus the regulated transcription of the *mPer* genes can act as a molecular integrator of cellular signaling to the circadian clockwork.

Some reviews still place *mTim*, the mammalian homologue of *Drosophila timeless*, in the central oscillator. Though *mTim* is expressed at low levels in the SCN, it is not rhythmic nor does it respond to light as expected from *Drosophila* (Field et al., 2000; Hastings et al., 1999). mTIM does not interact with any mPER protein *in vivo* (Zylka et al., 1998a) although it co-immunoprecipitates with mCRY in over-expression studies (Field et al., 2000). Moreover, a targeted disruption of *mTim* results in a defective kidney development resulting in the death of homozygous embryos before midgestation. Heterozygous mice show a normal circadian phenotype (Gotter et al., 2000). Thus *mTim* is a developmental gene without substantial circadian function (Reppert and Weaver, 2001a).

Taken together the current understanding of the mammalian TTL works as follows:

CLOCK/ BMAL1 heterodimer binds to *mPer* and *mCry* promoters at the end of the night / begin of the day and activates their transcription. In the course of the day mPER and mCRY proteins accumulate in the cytoplasm and re-translocate back into the nucleus. There they form a multimeric complex that inhibits CLOCK/ BMAL1 activated transcription. Additionally mPER2 and/or mCRY1/2 activate *Bmal1* transcription. During the night, while *mPer/ mCry* transcription is low, mPER/ mCRY protein levels decrease due to degradation (see below) and BMAL1 levels rise. At dawn the critical relation between BMAL1 and mPER/ mCRY levels is reached, new active CLOCK/ BMAL1 heterodimers are formed and *mPer/ mCry* transcription is initiated again.

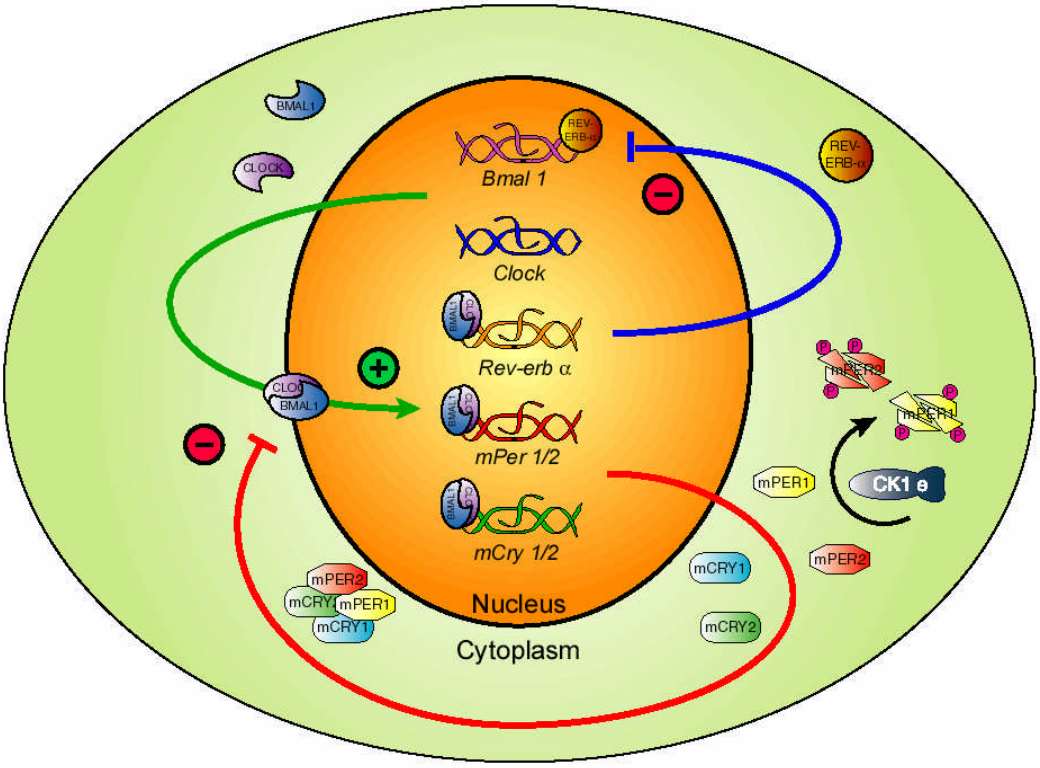

Fig. 8: Model of the circadian clockwork within an individual SCN neuron. The CLOCK/ BMAL1 heterodimer activates *mPer* and *mCry* transcription. mPER and mCRY proteins form a multimeric complex and inhibit CLOCK/ BMAL1. Both loops are linked by Rev-erb α, which is activated by CLOCK/ Bmal1 but inhibits Bmal1 transcription. *Casein kinase 1e* phosphorylates the PER proteins which ultimately leads to their degradation. For further explanations see text above.

Additional aspects of the circadian clockwork with special respect to influences of photoperiod are discussed below.

Phosphorylation, proteolysis and the re-translocation into the nucleus of mPER and mCRY proteins are likely to be crucial for imparting a 24h time constant to the SCN clockwork (Lee et al., 2001; Young and Kay, 2001). One protein kinase which is able to phosphorylate both mPER and mCRY proteins and BMAL1 is Casein Kinase 1ε (CK1ε) (Eide et al., 2002; Keesler et al., 2000; Lowrey et al., 2000; Vielhaber et al., 2000). The "tau hamster" carrying a mutation in the CK1ε gene has a severely shortened free-running period of about 20h (Lowrey et al., 2000). Additionally, over-expression experiments suggest a role of CK1ε or CK1δ in the nuclear translocation of mPER proteins (Vielhaber et al., 2000). A recent study by Yagita and colleagues (Yagita et al., 2002) brings together all the three aspects of post-translational processing connected to the circadian machinery so far. In an elegant set of cell system based experiments the authors suggest a mechanism by which the timed interaction between mPER2, mCRY protein and CK1ε regulates the nuclear abundance of an mPER/ mCRY complex capable of interacting with the CLOCK/ BMAL1 transcription machinery.

They show that mPER2 contains functional nuclear import and export signals allowing the protein to shuttle freely between the nucleus and the cytoplasm. In the nucleus mPER2 interacts with mCRY1 or mCRY2 thereby protecting each other from degradation by the proteasome after phosphorylation by CK1ε.

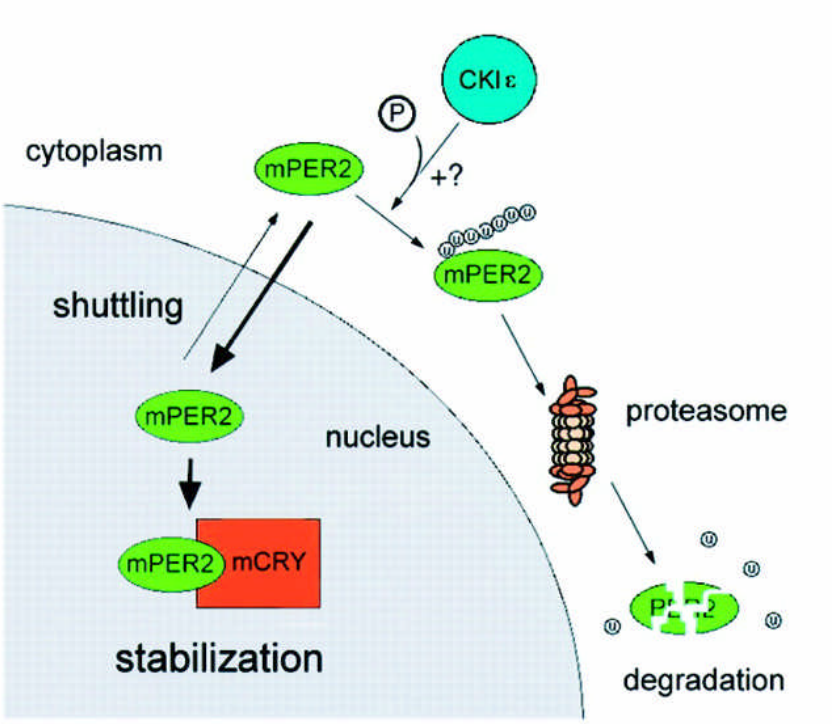

Fig. 9: Working model for mCRY-mediated nuclear accumulation of mPER2. mCRY keeps shuttling mPER2 in the nucleus and protects it from phosphorylation by CK1ε and subsequent degradation by the proteasome (taken from (Yagita et al., 2000)).

This corresponds well with the data from *mCry1/ mCry2* double mutant mice where *mPer* transcript levels are high but mPER protein cannot be detected (Shearman et al., 2000b) and results from a human circadian disease, the familial advanced sleep phase syndrome (FASPS). FASPS patients carry a mutation of the *hPer2* gene in the region of the CK1ε phosphorylation site (Toh et al., 2001). Decreased phosphorylation would lead to higher PER levels in the nucleus thereby accelerating the speed of the clock. This is exactly what is seen in FASPS patients and in the tau hamster (Jones et al., 1999; Ralph and Menaker, 1988).

1.5. Peripheral Clocks

Clock genes are not only expressed in the SCN but appear in several tissues outside the brain indicating the existence of peripheral circadian clocks subordinated to the central pacemaker of the hypothalamus (for review see Balsalobre, 2002 and Herzog and Tosini, 2001). Analysis of clock gene expression in different tissues like liver, kidney, heart or muscle revealed that most of their transcript levels indeed show a circadian profile (Balsalobre et al., 1998; Lee et al., 2001; McNamara et al., 2001; Nonaka et al., 2001; Oishi et al., 1998; Zylka et al., 1998a). Essentially all peripheral organs seem to be capable of generating circadian rhythmicity. However, circadian gene expression in peripheral cell types is delayed about 4h when compared to the SCN (Balsalobre et al., 1998). The regulative mechanisms of peripheral clocks seem identical to those present in the SCN, although a recent study in *Clock* mutant mice suggests a different impact of the *Clock* mutation on central and peripheral oscillators (Oishi et al., 2000). This probably reflects the presence of clock gene homologues in non-SCN tissues (like NPAS-2 in the forebrain (Reick et al., 2001)), which can compensate for the loss or misfunction of some of the "classical" clock genes.

Additionally peripheral oscillators dampen without continuing stimulation (Balsalobre et al., 1998). Therefore the clocks of the body need to be regularly synchronized to the master time teller of the brain. This synchronization most probably occurs *via* diffusible factors (Silver et al., 1996) – although neural signals seem also important for some outputs (Kalsbeek and Buijs, 2002) - probably released *via* the bloodstream (Oishi et al., 1998). This would explain the 4h lag of peripheral clock gene expression. SCN neurons have been shown to directly synchronize cultured fibroblasts (Allen et al., 2001). Recent work by Cheng and colleagues demonstrates that Prokineticin 2, which is synthesized in the SCN, is essential for the control of locomotor activity. PK2 receptors are found in several brain *nuclei* involved in output signaling from the clock. Therefore these *nuclei* might as well produce the humoral signals synchronizing the periphery (Cheng et al., 2002).

Several candidates exist for timing ligands in the blood. Glucocorticoids induce circadian gene expression in fibroblasts and induce phase shifts in liver, kidney and heart (Balsalobre et al., 2000a). However, the disruption of the glucocorticoid receptor does not affect circadian gene expression in the periphery indicating that glucocorticoids cannot be the only signaling compound. Fibroblast rhythmicity can be induced as well by forskolin, adenylate cyclase agonists, TPA and calcimycin (Akashi and Nishida, 2000; Balsalobre et al., 2000b; Motzkus et al., 2002; Motzkus et al., 2000; Nonaka et al., 2001; Yagita and Okamura, 2000). Retinoids

seem to be important for circadian gene expression in the vascular system (McNamara et al., 2001). But the general mechanism by which peripheral clocks are reset remains unclear. It has been shown that during light phase restricted feeding the temperature of mice was affected suggesting an impact of body temperature on the resynchronization of peripheral clocks (Damiola et al., 2000). Rutter and colleagues (Rutter et al., 2001) show that the redox state of the cell influences the efficiency of CLOCK/ BMAL1 driven transcriptional activation. Since the cell redox state is affected by metabolism, restricted feeding may thus directly reset peripheral clocks through metabolic activity (reviewed in Schibler et al., 2001).

1.6. Photoperiodism

1.6.1. Publication: “The Circadian Clock as a Molecular Calendar”

Henrik Oster, Erik Maronde, and Urs Albrecht

Chronobiology International, 19(3), 507-516 (2002)

CHRONOBIOLOGY INTERNATIONAL, 19(3), 507–516 (2002)

MINIREVIEW

THE CIRCADIAN CLOCK AS A MOLECULAR CALENDAR

Henrik Oster,[1] Erik Maronde,[2] and Urs Albrecht[1,*]

[1]Institute of Biochemistry, University of Fribourg, Rue du Musée 5, CH-1700 Fribourg, Switzerland
[2]IPF Pharmaceuticals GmbH, Feodor-Lynen-Str. 31, D-30625 Hannover, Germany

ABSTRACT

There are two dominant environmental oscillators shaping the living conditions of our world: the day–night cycle and the succession of the seasons. Organisms have adapted to these by evolving internal clocks to anticipate these variations. An orchestra of finely tuned peripheral clocks slaved to the master pacemaker of the suprachiasmatic nuclei (SCN) synchronizes the body to the daily 24h cycle. However, this circadian clockwork closely interacts with the seasonal time-teller.

Recent experiments indeed show that photoperiod—the dominant *Zeitgeber* of the circannual clock—might be deciphered by the organism using the tools of the circadian clock itself. From the SCN, the photoperiodic signal is transferred to the pineal where it is decoded as a varying secretion of melatonin.

Different models have been proposed to explain the mechanism by which the circadian clock measures day-length. Recent work using mutant mice suggests a set of two molecular oscillators tracking dusk and dawn, respectively, thereby translating day-length to the body. However, not every aspect of photoperiodism is covered by this theory and major adjustments will need to be made to establish a widely acceptable uniform model of circadian/circannual timekeeping. (*Chronobiology International, 19(3), 507–516, 2002*)

Key Words: Seasons; *Per*; *Cry*; Melatonin; Oscillator; Suprachiasmatic nuclei (SCN)

*Corresponding author. E-mail: urs.albrecht@unifr.ch

INTRODUCTION

Life in most areas of the world is under the regime of two major periodic variations, the day–night cycle and the seasons. Organisms have learned to adapt to these oscillations by evolving mechanisms to keep track of the time thereby anticipating upcoming environmental changes. This synchronization of physiology and behavior to the environment serves to maximally benefit from the limited availability of resources in nature.

The timekeeping devices that have evolved to optimally adapt animals to the environment are the circadian clock to predict daily events and the circannual clock to enable an organism to foresee the seasons. While in the last years a vast amount of data has been accumulated about the molecular mechanism of the circadian clock, knowledge about the nature of the circannual clock remains sparse. Recent findings indicate that there might not even be a distinct circannual oscillator, but that the circadian clock itself could measure seasonal time [reviewed in Ref. (1)].

Circadian clocks are found in many organisms throughout all *phyla* [reviewed in Ref. (2)]. However, seasonal timekeeping has been reported only in a few species, which is not astonishing given the fact that many organisms just do not live long enough to be forced to adapt to a circannual rhythm. Nevertheless, some short-lived animals like insects [reviewed in Ref. (3)] and fungi [reviewed in Ref. (4)] show day-length adaptations.

In this review, we will focus on mechanisms of circadian and circannual timekeeping in mammals. We will give an overview of recent insights into clockwork function and model a molecular calendar that is based on the circadian clock.

CENTRAL AND PERIPHERAL CLOCKS IN MAMMALS

The mammalian organism uses more than one clock to keep track of time. In fact, almost every cell of our body holds all the components necessary to build a functional biological oscillator. Circadian rhythms were found in many tissues like the brain, liver, eyes, kidneys, skin, muscle, and even in fibroblasts. All these peripheral clocks do not run independently, but are driven by the master circadian pacemaker in the suprachiasmatic nuclei (SCN) of the hypothalamus [reviewed in Ref. (5)].

The cells of the SCN receive light information from the retina directly via the retinohypothalamic tract (RHT) and indirectly via the intergeniculate leaflet (IGL) (6). Unknown nonvisual photoreceptors in the eye transfer light/dark information via glutamatergic nerves to the SCN [reviewed in Ref. (7)]. In the pacemaker cells of the SCN, a set of light inducible genes, namely *Per1* and *Per2*, refers daytime information to the molecular clockwork (8,41). In analogy to experiments in *Drosophila*, it is hypothesized that the Period (PER) proteins together with the two Cryptochromes (CRYs) influence their own transcriptional activation by interfering with the CLOCK/BMAL1 transcriptional activation complex. However, there is evidence that

the regulation of the mammalian clock is different from that described in *Drosophila* (9–11). Nuclear abundance of PER and CRY proteins varies in a 24h rhythm (12). CLOCK/BMAL1 activation and deactivation cycles also control a set of clock-dependent genes whose proteins transfer the time information to the body and to the peripheral organic clocks, which themselves govern the physiological processes of the body [reviewed in Refs. (13,14)].

So far, the primary transmission pathway from the SCN to the periphery, which could either be neuronal or endocrine, remains elusive. However, most experiments favor transmission by diffusible factors (15), which would explain why the peripheral clocks normally follow the SCN with a lag of several hours. One factor that is secreted by the SCN in a diurnal fashion is TGFalpha, which has been identified as a likely inhibitor of locomotion (16). It has also been shown that glucocorticoids are able to reset vascular clocks (17), but the main resetting mechanism might be of a more indirect nature as well.

There are connections between different peripheral clocks as well as feedback to the SCN [reviewed in (18)]. Restricted feeding schedules are able to reset the clock in the liver, but not in the SCN (19). In contrast, forced activity schedules are known to reset the central pacemaker in hamsters (20).

The orchestrated interaction of interwoven cellular clocks creates the variation of the physiological status over the 24h day/night cycle, and over the seasonal cycle as well.

PHOTOPERIODICITY IN MAMMALS

Seasonality evolved to adapt the organism to expect environmental changes through the course of the year. Photoperiod is a *proximate* but not an *ultimate* factor meaning that the adaptation to the photoperiod itself does not have any evolutional advantages (like the adaptation to temperature changes and the knowledge of variations in food and water abundance) (21). However, nature chose this readout for the time of the year because of its easy accessibility and relative accuracy.

The photoperiod is transmitted to the body via the secretion of nocturnal melatonin by the pineal gland. The duration of melatonin release is reciprocal to the day-length: Short days mean longer melatonin release and vice versa (22). Melatonin-sensitive tissues convert this signal into those overt circannual rhythms we observe in most mammals like the reproductive status and activity schedules [reviewed in Refs. (23,24)].

Melatonin and the pineal seem essential for seasonality. Pineal-ectomized hamsters do not react to photoperiodic changes anymore (25). Infusions of external melatonin can mimic different photoperiods in these animals (26).

One remaining problem in reproductive photoperiodism in rodents is the occurrence of nonresponders. The adaptive value of this phenomenon is unclear, but it has been speculated that under certain environmental conditions,

nonresponsiveness to photoperiodically gated seasonality may be of adaptive benefit for the species [reviewed in Ref. (27)]. It is tempting to speculate that one reason for such variation may be mutations or polymorphisms in clock genes.

Seasonality in humans has long been debated. Nowadays, there is mutual agreement that seasonality in, e.g., birthrate can be found from the times before the inventions of artificial nocturnal illumination [reviewed in Ref. (28)].

THE ROLE OF THE SUPRACHIASMATIC NUCLEI IN PHOTOPERIODIC TIME MEASUREMENT

The SCN is a major contributor to photoperiodism because SCN lesions in rodents lead to a complete loss in photoperiodicity (29). However, this did not rule out the possibility of a secondary clockwork independent of the circadian in the same nucleus.

First evidence for a direct involvement of the circadian system in photoperiodic time measurement (PTM) came from three different experimental setups: night breaks, resonance light cycles, and T cycles. All these setups use short light periods to provoke long-day phenotypes in hamsters (30–32). They clearly show that the duration of light does not tell the body the time of the year, but the phase of light input in respect to the phase of the circadian cycle. The SCN is integrating the light signals to form photoperiodic information. From the SCN, the pineal gets its instructions to release melatonin into the body [reviewed in Ref. (33)]. In Fig. 1, we give an overview about photoperiodic signaling pathways in the brain.

There are some complications in this simplistic scheme. The SCN does not show a gradual response in firing rate corresponding to variations in melatonin occurrence under different day-lengths (34). Additionally true circannual rhythms like the body mass variation of ground squirrels are not touched by SCN lesions (35), but the SCN is involved in the photo-entrainment of this rhythm (36) and the onset of hibernation (37). Both experiments indicate a role of the SCN downstream of the pineal.

HOW THE SCN MEASURES DAY-LENGTH

Two models have been proposed to describe PTM in mammals. The external coincidence model (38) postulates that light—besides its effect in resetting the circadian system—induces long-day responses when present in certain photo-inductive phases of the circadian cycle. This implies a kind of phase response curve for photoperiodism.

Secondly, the model of internal coincidence (39) postulates that two distinct oscillators in the circadian clock lock to different events of the day cycle, namely, dawn and dusk. So when the days get longer during springtime, the phase angle

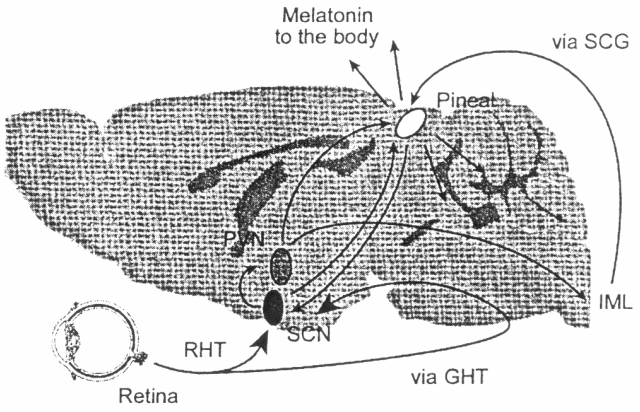

Figure 1. Photoperiodic signaling pathways in the mammalian brain. Light exposure is transmitted from the retina via the retinohypothalamic tract (RHT) and indirectly via the geniculohypothalamic tract (GHT) to the suprachiasmatic nuclei (SCN) where it is decoded into day-length information. Several pathways lead from the SCN to the pineal where melatonin is secreted. There is innervation via the paraventricular nuclei (PVN), extracerebral pathways including the intermediolateral column of the spinal chord (IML) and the superior cervical ganglion (SCG) as well as direct signaling. From the pineal feedback to the SCN is provided by melatonin reception as well as nervous signaling in the brain.

between those two oscillators is growing while in fall, both get closer together again. These oscillators where termed M (morning) and E (evening) oscillator with E inducing melatonin production in the pineal and M switching off the melatonin in the morning [(39); see Fig. 2a].

In the last year, some proposals have been made in which components of the circadian clock might form these oscillators and now first data emerge to solidify these postulations. In a paper by Daan et al. (40), the authors try to flesh out the old two-oscillator model derived from splitting phenomena in hamsters with assigning certain genes as M or E components. They postulate that *Per1* together with *Cry1* forms the morning oscillator indicated by the peak of expression of *Per1* in the early morning. *Per2* and *Cry2* form E, indicated by the late afternoon maximum of *Per2* expression and the restricted light inducibility of *Per2* to the early night proposing a role of *Per2* in the delaying mechanism of the clock. Experiments from our group (41) indeed show that *Per1* mutant mice are not able to phase-advance in response to a short light pulse while *Per2* mutants cannot phase-delay. Additionally *Per2* mutants are not following Aschoff's rule of the *tau* increase with higher light intensity in constant light (LL) (42). According to the E/M model, these animals run only on the morning oscillator and are thereby not able to properly delay the clock in reaction to stronger light exposition.

In situ analysis of clock gene expression in the SCN of mice kept in long- and short-day photoperiods shows a broadening of the expression maxima of *Per1* and *Per2* with a maximum of *Per1* in the middle of the day and of *Per2* in the early evening implicating an approximation of both maxima in short days (42). In wild

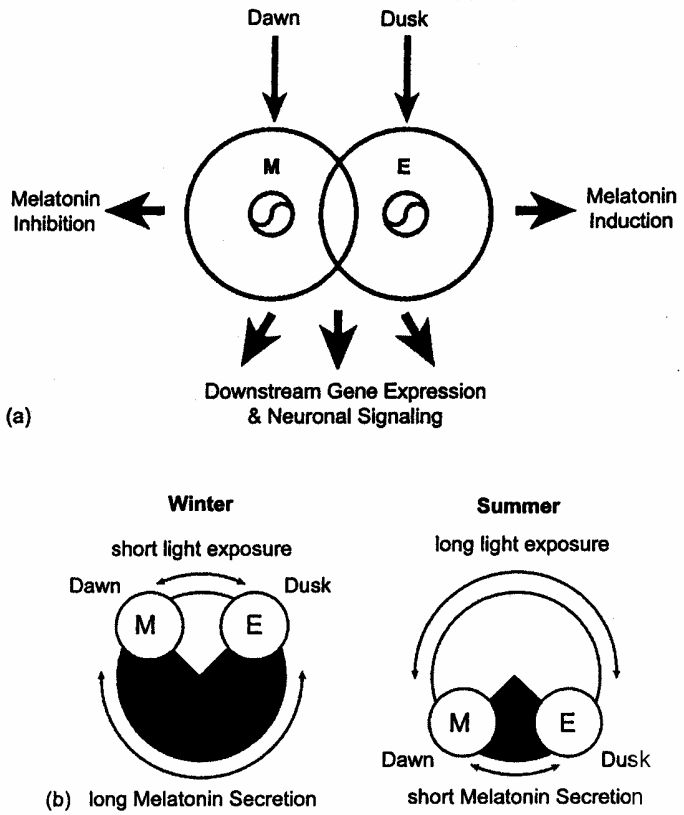

Figure 2. (a) Schematic illustration of hypothetical day-length encoding in the circadian clock. Two molecular oscillators are coupled to dusk and dawn, respectively. The M (morning) oscillator inhibits melatonin secretion in the pineal while the E (evening) oscillator induces melatonin at the start of the night. The phase angle between M and E determines day-length. (b) Phase angle variations between M and E oscillator in winter (short days) and summer (long days). While short light exposure reduces the difference between M and E during the day, prolonged melatonin expression is mediated by the nightly time span between E (melatonin induction) and M (melatonin inhibition). This effect is inverted in summer where the interval between E and M is shortened by the long light exposure during the day.

type animals *Per1* and *Per2* gene expression seem to be coupled. *Per1* gene expression in *Per2* mutant mice shifted to times around dawn, whereas *Per2* gene expression in *Per1* mutant mice became linked to dusk (42). Hence, an uncoupling of *Per1* and *Per2* gene expression occurred in *Per* mutant mice. These data are consistent with the two-oscillator model in which *Per1* would be part of the M oscillator and *Per2* of the E oscillator.

This model gives an easy mechanism by which the organism can adapt to varying day-length throughout the year (Fig. 2b) by changing the phase-angle between both oscillators. However, it still shows several shortcomings. For example, the mRNA oscillations in other species like the Siberian hamster do not

show the same variations with different day-length as mice (43,44). This might be due to the feedback on the clock by the strong melatonin rhythm in these animals. But if the genetic clock does not work in seasonal animals, of what relevance is it elsewhere?

Another paradigm in which gene expression is monitored while animals are adapting to a shifted light–dark cycle shows a rapid change of *Per1* and *Per2* expression followed by a slow adaptation in *Cry1* and *Cry2* mRNA rhythms suggesting a functional unity of both *Per*s and *Cry*s, respectively (45). Still possible is a functional compartmentalization of the SCN cells into morning and evening oscillators. For example, multiunit recordings from horizontal SCN slices show a bimodal firing rate maximum with peaks in the morning and in the evening (46).

CONCLUSION

With the enormous progress made in the field of circadian timekeeping, the mystery of circannual clocks is slowly getting unraveled as well. Work on photoperiodic mammals like hamsters and on mutant mouse strains gave new molecular insight on old theories about the nature of the internal calendar.

An important question remains about the impact of photoperiod on the human organism. Despite a seasonal variation in vasopressin (VP) and melatonin levels (47,48) as well as slightly altered fertility throughout the year (49,50), there is not much noted about human seasonalism [reviewed in Ref. (28)].

However, the molecular aspects of the periodic function of the circadian clock offer a simple and intriguing explanation for such common-day phenomena like seasonal affective disorder: When during the short days of winter M and E oscillators of the circadian clock get close together, this may result in clockwork disturbances with psychological impact.

How the internal clock and our psychological well-being are linked and which molecules play a role in photoperiodic signaling of the body are only sparsely understood [reviewed in Refs. (51,52)]. But more and more gaps are closed and the increasing understanding of the mechanisms underlying our circadian system will soon lead towards a better comprehension of seasonal timekeeping as well.

REFERENCES

1. Goldman, B.D. Mammalian Photoperiodic System: Formal Properties and Neuroendocrine Mechanisms of Photoperiodic Time Measurement. J. Biol. Rhythms **2001**, *16* (4), 283–301.
2. Dunlap, J.C. Molecular Bases for Circadian Clocks. Cell **1999**, *96* (2), 271–290.
3. Vaz Nunes, M.; Saunders, D. Photoperiodic Time Measurement in Insects: A Review of Clock Models. J. Biol. Rhythms **1999**, *14* (2), 84–104.

4. Roenneberg, T.; Merrow, M. Seasonality and Photoperiodism in Fungi. J. Biol. Rhythms **2001**, *16* (4), 403–414.
5. Herzog, E.D.; Tosini, G. The Mammalian Circadian Clock Shop. Semin. Cell Dev. Biol. **2001**, *12* (4), 295–303.
6. Jacob, N.; Vuillez, P.; Lakdhar-Ghazal, N.; Pevet, P. Does the Intergeniculate Leaflet Play a Role in the Integration of the Photoperiod by the Suprachiasmatic Nucleus? Brain Res. **1999**, *828* (1–2), 83–90.
7. Morin, L.P. The Circadian Visual System. Brain Res. Rev. **1994**, *19* (1), 102–127.
8. Albrecht, U.; Sun, Z.S.; Eichele, G.; Lee, C.C. A Differential Response of Two Putative Mammalian Circadian Regulators, *mPer1* and *mPer2*, to Light. Cell **1997**, *91* (7), 1055–1064.
9. Field, M.D.; Maywood, E.S.; O'Brien, J.A.; Weaver, D.R.; Reppert, S.M.; Hastings, M.H. Analysis of Clock Proteins in Mouse SCN Demonstrates Phylogenetic Divergence of the Circadian Clockwork and Resetting Mechanisms. Neuron **2000**, *25* (2), 437–447.
10. Bae, K.; Jin, X.; Maywood, E.S.; Hastings, M.H.; Reppert, S.M.; Weaver, D.R. Differential Functions of *mPer1*, *mPer2* and *mPer3* in the SCN Circadian Clock. Neuron **2001**, *30*, 525–536.
11. Zheng, B.; Albrecht, U.; Kaasik, K.; Sage, M.; Lu, W.; Vaishnav, S.; Li, Q.; Sun, Z.S.; Eichele, G.; Bradley, A.; Lee, C.C. Nonredundant Roles of the *mPer1* and *mPer2* Genes in the Mammalian Circadian Clock. Cell **2001**, *105* (5), 683–694.
12. Lee, C.; Etchegaray, J.P.; Cagampang, F.R.; Loudon, A.S.; Reppert, S.M. Posttranslational Mechanisms Regulate the Mammalian Circadian Clock. Cell **2001**, *107* (7), 855–867.
13. King, D.P.; Takahashi, J.S. Molecular Genetics of Circadian Rhythms in Mammals. Annu. Rev. Neurosci. **2000**, *23*, 713–742.
14. Albrecht, U. Circadian Rhythms: A Fine C(l)ocktail! Curr. Biol. **2001**, *11* (13), R517–R519.
15. Silver, R.; Romero, M.T.; Besmer, H.R.; Leak, R.; Nunez, J.M.; LeSauter, J. Calbindin-D28K Cells in the Hamster SCN Express Light-Induced Fos. Neuroreport **1996**, *7* (6), 1224–1228.
16. Kramer, A.; Yang, F.C.; Snodgrass, P.; Li, X.; Scammell, T.E.; Davis, F.C.; Weitz, C.J. Regulation of Daily Locomotor Activity and Sleep by Hypothalamic EGF Receptor Signaling. Science **2001**, *294* (5551), 2511–2515.
17. Balsalobre, A.; Brown, S.A.; Marcacci, L.; Tronche, F.; Kellendonk, C.; Reichardt, H.M.; Schutz, G.; Schibler, U. Resetting of Circadian Time in Peripheral Tissues by Glucocorticoid Signaling. Science **2000**, *289* (5488), 2344–2347.
18. Pando, M.P.; Sassone-Corsi, P. Signaling to the Mammalian Circadian Clocks: In Pursuit of the Primary Mammalian Circadian Photoreceptor. Sci. STKE **2001**, *2001* (107), RE16, 1–9.
19. Damiola, F.; Le Minh, N.; Preitner, N.; Kornmann, B.; Fleury-Olela, F.; Schibler, U. Restricted Feeding Uncouples Circadian Oscillators in Peripheral Tissues from the Central Pacemaker in the Suprachiasmatic Nucleus. Genes Dev. **2000**, *14* (23), 2950–2961.
20. Maywood, E.S.; Mrosovsky, N.; Field, M.D.; Hastings, M.H. Rapid Down-Regulation of Mammalian Period Genes During Behavioral Resetting of the Circadian Clock. Proc. Natl Acad. Sci. USA **1999**, *96* (26), 15211–15216.

21. Baker, J. The Evolution of Breeding Seasons. In *Evolution*; DeBeer, J., Ed.; Clarendon: Oxford, 1938; 161–177.
22. Carter, D.S.; Goldman, B.D. Antigonadal Effects of Timed Melatonin Infusion in Pinealectomized Male Djungarian Hamsters (*Phodopus sungorus sungorus*): Duration is the Critical Parameter. Endocrinology **1983**, *113* (4), 1261–1267.
23. Bartness, T.J.; Powers, J.B.; Hastings, M.H.; Bittman, E.L.; Goldman, B.D. The Timed Infusion Paradigm for Melatonin Delivery: What Has It Taught Us About the Melatonin Signal, Its Reception, and the Photoperiodic Control of Seasonal Responses? J. Pineal Res. **1993**, *15* (4), 161–190.
24. Malpaux, B.; Migaud, M.; Tricoire, H.; Chemineau, P. Biology of Mammalian Photoperiodism and the Critical Role of the Pineal Gland and Melatonin. J. Biol. Rhythms **2001**, *16* (4), 336–347.
25. Czyba, J.C.; Girord, C.; Durand, N. Sur L'antagonisme Epiphyseo-Hypophysaire et les Variations Saisonnieres de la Spermatogenese Chez le Hamster Dore (*Mesocricetus auratus*). CR Soc. Biol. **1964**, *158*, 742–745.
26. Goldman, B.D.; Nelson, R.J. Melatonin and Seasonality in Mammals. In *Melatonin: Biosynthesis, Physiological Effects and Clinical Applications*; Reiter, H.-S.Y.R., Ed.; CRC Press: Boca Raton, FL, 1993; 225–252.
27. Prendergast, B.J.; Kriegsfeld, L.J.; Nelson, R.J. Photoperiodic Polyphenisms in Rodents: Neuroendocrine Mechanisms, Costs, and Functions. Q. Rev. Biol. **2001**, *76* (3), 293–325.
28. Wehr, T.A.; Aeschbach, D.; Duncan, W.C., Jr. Evidence for a Biological Dawn and Dusk in the Human Circadian Timing System. J. Physiol. **2001**, *535* (Pt 3), 937–951.
29. Rusak, B.; Morin, L.P. Testicular Responses to Photoperiod are Blocked by Lesions of the Suprachiasmatic Nuclei in Golden Hamsters. Biol. Reprod. **1976**, *15* (3), 366–374.
30. Hoffmann, K. Photoperiodic Effects in the Djungarian Hamster: One Minute of Light During Darktime Mimics Influence of Long Photoperiods on Testicular Recrudescence, Body Weight and Pelage Colour. Experientia **1979**, *35* (11), 1529–1530.
31. Lerchl, A. Sustained Response of Pineal Melatonin Synthesis to a Single One-Minute Light Pulse During Night in Djungarian Hamsters (*Phodopus sungorus*). Neurosci. Lett. **1995**, *198* (1), 65–67.
32. Elliott, J.A. Circadian Rhythms and Photoperiodic Time Measurement in Mammals. Fed. Proc. **1976**, *35* (12), 2339–2346.
33. Stehle, J.H.; von Gall, C.; Schomerus, C.; Korf, H.W. Of Rodents and Ungulates and Melatonin: Creating a Uniform Code for Darkness by Different Signaling Mechanisms. J. Biol. Rhythms **2001**, *16* (4), 312–325.
34. Mrugala, M.; Zlomanczuk, P.; Jagota, A.; Schwartz, W.J. Rhythmic Multiunit Neural Activity in Slices of Hamster Suprachiasmatic Nucleus Reflect Prior Photoperiod. Am. J. Physiol. Regul. Integr. Comp. Physiol. **2000**, *278* (4), R987–R994.
35. Zucker, I.; Boshes, M.; Dark, J. Suprachiasmatic Nuclei Influence Circannual and Circadian Rhythms of Ground Squirrels. Am. J. Physiol. **1983**, *244* (4), R472–R480.
36. Lee, T.M.; Zucker, I. Suprachiasmatic Nucleus and Photic Entrainment of Circannual Rhythms in Ground Squirrels. J. Biol. Rhythms **1991**, *6* (4), 315–330.

37. Ruby, N.F.; Dark, J.; Heller, H.C.; Zucker, I. Ablation of Suprachiasmatic Nucleus Alters Timing of Hibernation in Ground Squirrels. Proc. Natl Acad. Sci. USA **1996**, *93* (18), 9864–9868.
38. Bünning, E. Circadian Rhythms and Time Measurement in Photoperiodism. Cold Spring Harbor Symp. Quant. Biol. **1960**, *25*, 249–256.
39. Illnerova, H. The Suprachiasmatic Nucleus and Rhythmic Pineal Melatonin Production. In *The Suprachiasmatic Nucleus: The Mind's Clock*; Klein, R.M.D.C., Reppert, S.M., Eds.; Oxford University Press: New York, 1991; 197–216.
40. Daan, S.; Albrecht, U.; van der Horst, G.T.; Illnerova, H.; Roenneberg, T.; Wehr, T.A.; Schwartz, W.J. Assembling a Clock for All Seasons: Are There M and E Oscillators in the Genes? J. Biol. Rhythms **2001**, *16* (2), 105–116.
41. Albrecht, U.; Zheng, B.; Larkin, D.; Sun, Z.S.; Lee, C.C. *mPer1* and *mPer2* are Essential for Normal Resetting of the Circadian Clock. J. Biol. Rhythms **2001**, *16* (2), 100–104.
42. Steinlechner, S.; Jacobmeier, B.; Scherbarth, F.; Dernbach, H.; Kruse, F.; Albrecht, U. Robust Circadian Rhythmicity of *Per1* and *Per2* Mutant Mice in Constant Light and Dynamics of *Per1* and *Per2* Gene Expression Under Long and Short Photoperiods. J. Biol. Rhythms **2002**, in press.
43. Messager, S.; Hazlerigg, D.G.; Mercer, J.G.; Morgan, P.J. Photoperiod Differentially Regulates the Expression of *Per1* and ICER in the Pars Tuberalis and the Suprachiasmatic Nucleus of the Siberian Hamster. Eur. J. Neurosci. **2000**, *12* (8), 2865–2870.
44. Nuesslein-Hildesheim, B.; O'Brien, J.A.; Ebling, F.J.; Maywood, E.S.; Hastings, M.H. The Circadian Cycle of *mPer* Clock Gene Products in the Suprachiasmatic Nucleus of the Siberian Hamster Encodes Both Daily and Seasonal Time. Eur. J. Neurosci. **2000**, *12* (8), 2856–2864.
45. Hastings, M.H.; Follett, B.K. Toward a Molecular Biological Calendar? J. Biol. Rhythms **2001**, *16* (4), 424–430.
46. Jagota, A.; de la Iglesia, H.O.; Schwartz, W.J. Morning and Evening Circadian Oscillations in the Suprachiasmatic Nucleus In Vitro. Nat. Neurosci. **2000**, *3* (4), 372–376.
47. Hastings, M.H.; Walker, A.P.; Herbert, J. Effect of Asymmetrical Reductions of Photoperiod on Pineal Melatonin, Locomotor Activity and Gonadal Condition of Male Syrian Hamsters. J. Endocrinol. **1987**, *114* (2), 221–229.
48. Hofman, M.A.; Purba, J.S.; Swaab, D.F. Annual Variations in the Vasopressin Neuron Population of the Human Suprachiasmatic Nucleus. Neuroscience **1993**, *53* (4), 1103–1112.
49. Roenneberg, T.; Aschoff, J. Annual Rhythm of Human Reproduction: II. Environmental Correlations. J. Biol. Rhythms **1990**, *5* (3), 217–239.
50. Roenneberg, T.; Aschoff, J. Annual Rhythm of Human Reproduction: I. Biology, Sociology, or Both? J. Biol. Rhythms **1990**, *5* (3), 195–216.
51. Parry, B.L.; Newton, R.P. Chronobiological Basis of Female-Specific Mood Disorders. Neuropsychopharmacology **2001**, *25* (Suppl. 5), S102–S108.
52. Pacchierotti, C.; Iapichino, S.; Bossini, L.; Pieraccini, F.; Castrogiovanni, P. Melatonin in Psychiatric Disorders: A Review on the Melatonin Involvement in Psychiatry. Front. Neuroendocrinol. **2001**, *22* (1), 18–32.

1.7. Aim of this Work

The goal of this project was to further characterize the role of the *Period* and *Cryptochrome* genes and their interaction in the mammalian circadian clockwork. Although the importance of the four genes *mPer1*, *mPer2*, *mCry1* and *mCry2* as components of the central transcriptional/ translational feedback loop has convincingly been demonstrated, the exact nature of the interactions of these genes and their specific roles in the stabilization and maintenance of the cellular oscillator remains to be discovered (Albrecht, 2002; Okamura et al., 2002).

One aspect is the putative redundancy of the *mPers* and the *mCrys* in the circadian system. Some work has been performed on the distinct role of the two *mPer* genes (Bae et al., 2001; Zheng et al., 2001). However, *mCry1* and *mCry2* are still believed to be mutually exchangeable despite the fact that the corresponding null mutant mice show clearly different circadian phenotypes (van der Horst et al., 1999; Vitaterna et al., 1999).

Another point of debate is the role of the *mPers* and *mCrys* in the resetting pathway of the clock. While the light inducibility of the *mPer* genes and resetting deficiencies in the corresponding mouse mutants make them likely candidates for the connection between the pacemaker and the environment (Albrecht et al., 1997b; Albrecht et al., 2001), it is still not clear whether the *mCrys* are important in light signaling (like their plant and *Drosophila* homologues) or not (Barinaga, 1999; Sancar, 2000).

Additionally, much of the functional data regarding the circadian system was generated using more or less artificial experimental setups. However, it is very difficult to mimic the clockwork depending on interactions organized in spatial and temporal manners *in vitro*. And indeed many of the proposed mechanisms were demonstrated to be of no significant relevance when it came to *in vivo* studies using transgenic animals (Gotter et al., 2000; Shearman et al., 2000a).

Therefore we chose to study *mPer/ mCry* interactions directly in the living animal. We crossed *mPer* and *mCry* mutant mice to produce animals lacking different combinations of the genes. This allowed us to assess *mPer* and *mCry* functional interaction under physiological conditions and deduce the different roles of these genes in the circadian clockwork.

In the second part we elucidated the molecular circadian clockwork of the blind mole rat *Spalax ehrenbergi* superspecies. Although the circadian behavior of *Spalax* has been broadly examined (Ben-Shlomo et al., 1995; Goldman et al., 1997; Rado and Terkel, 1989; Tobler et al., 1998) only sparse work has been performed on the molecular level so far (Negroni et al.,

1997; Tobler et al., 1998). The total visual blindness of the mole rats with extreme ocular degradation (Cooper et al., 1993) makes *Spalax* a highly interesting system for chronobiological studies. Additionally the ability of *Spalax* to change between a predominantly diurnal to a nocturnal activity pattern allowed us to examine differences in the clock mechanism of nocturnal and diurnal organisms in one species.

Chapter 2

Results

2.1. Publication: "Disruption of *mCry2* restores circadian rhythmicity in *mPer2* mutant mice"

Henrik Oster, Akira Yasui, Gijsbertus T.J. van der Horst, and Urs Albrecht

Genes & Development 2002, 16: 2633-2638

RESEARCH COMMUNICATION

Disruption of *mCry2* restores circadian rhythmicity in *mPer2* mutant mice

Henrik Oster,[1,2] Akira Yasui,[4] Gijsbertus T.J. van der Horst,[3] and Urs Albrecht[1,2,5]

[1]Max Planck Institute for Experimental Endocrinology, 30625 Hannover, Germany; [2]Department of Medicine, Division of Biochemistry, University of Fribourg, 1700 Fribourg, Switzerland; [3]Department of Cell Biology and Genetics, Erasmus Medical Center Rotterdam, 3000 DR Rotterdam, The Netherlands; [4]Department of Molecular Genetics, Institute of Development, Aging and Cancer, Tohoku University, 980-8575 Sendai, Japan.

Many biochemical, physiological, and behavioral processes display daily rhythms generated by an internal timekeeping mechanism referred to as the circadian clock. The core oscillator driving this clock is located in the ventral part of the hypothalamus, the so called *suprachiasmatic nuclei* (SCN). At the molecular level, this oscillator is thought to be composed of interlocking autoregulatory feedback loops involving a set of clock genes. Among the components driving the mammalian circadian clock are the *Period* 1 and 2 (*mPer1* and *mPer2*) and *Cryptochrome* 1 and 2 (*mCry1* and *mCry2*) genes. A mutation in the *mPer2* gene leads to a gradual loss of circadian rhythmicity in mice kept in constant darkness (DD). Here we show that inactivation of the *mCry2* gene in *mPer2* mutant mice restores circadian rhythmicity and normal clock gene expression patterns. Thus, *mCry2* can act as a nonallelic suppressor of *mPer2*, which points to direct or indirect interactions of PER2 and CRY2 proteins. In marked contrast, inactivation of *mCry1* in *mPer2* mutant mice does not restore circadian rhythmicity but instead results in complete behavioral arrhythmicity in DD, indicating different effects of *mCry1* and *mCry2* in the clock mechanism

Received April 10, 2002; revised version accepted August 6, 2002.

The mammalian *Period* (*mPer*) and *Cryptochrome* (*mCry*) genes are major components of the circadian pacemaker (King and Takahashi 2000; Albrecht 2002). mCRY proteins are part of the negative limb in the transcriptional/translational feedback loop, whereas mPER2 is thought to act positively on *Bmal1* expression (Shearman et al. 2000). In vitro studies point to multiple physical interactions between all mPER and mCRY proteins and posttranslational modifications such as phosphorylation and ubiquitylation, thereby offering a variety of putative regulation points for timed accumulation and nuclear appearance of clock proteins (Griffin et al. 1999; Kume et al. 1999; Field et al. 2000; Shearman et al. 2000; Yagita et al. 2000; Lee et al. 2001; Miyazaki et al. 2001; Vielhaber et al. 2001; Zheng et al. 2001; Yu et al. 2002). In particular there is evidence that mPER2 (GFP-tagged) shuttles between cytoplasm and nucleus and is ubiquitylated and degraded by the proteasome unless it is retained in the nucleus by mCRY proteins (Yagita et al. 2002). These findings implicate a regulatory effect of mCRY proteins on mPER2. However, the time course of protein availability, modification, and localization is difficult to resolve in model systems such as cell or slice cultures (Jagota et al. 2000; Hamada et al. 2001; Lee et al. 2001). In bacteria, yeast, *Caenorhabditis elegans*, and *Drosophila*, interactions of proteins have frequently been found through nonallelic supressor screens, that is, the restoration of a phenotype by introducing a mutation in another gene (Maine and Kimble 1989; Amin et al. 1999; Nakano et al. 2000; Grandin and Charbonneau 2001; LaJeunesse et al. 2001; Roy et al. 2002). We decided to further elucidate the functional relationship between *mPer* and *mCry* genes by studying their genetic interactions in the living animal. To this end, we inactivated the *mCry1* or *mCry2* gene in an *mPer2* mutant mouse strain.

[*Keywords*: Circadian clock; Per; Cry; nonallelic suppressor]
[5]**Corresponding author.**
E-MAIL urs.albrecht@unifr.ch; FAX 41-26-300-9735.
Article and publication are at http://www.genesdev.org/cgi/doi/10.1101/gad.233702.

Results and Discussion

$Per2^{Brdm1}$ mice, carrying a mutant *mPer2* gene with a deletion in the PAS domain thought to be important for protein–protein interactions (Zheng et al. 1999), were crossed with $mCry1^{-/-}$ or $mCry2^{-/-}$ mice (van der Horst et al. 1999). The double-heterozygous offspring was intercrossed to produce wild-type and homozygous mutant animals. $Per2^{Brdm1}/mCry2^{-/-}$ and $Per2^{Brdm1}/mCry1^{-/-}$ mice (representative genotyping shown in Fig. 1a) were obtained at the expected Mendelian ratios, appeared fertile, and were morphologically indistinguishable from wild-type animals.

To determine the influence of inactivation of either *mCry1* or *mCry2* on circadian behavior of $Per2^{Brdm1}$ mice, mutant and wild-type animals were individually housed in circadian activity-monitoring chambers (Albrecht and Oster 2001) for detection of wheel-running activity, an accurate measure of circadian rhythmicity. Mice were kept in a 12-h light:12-h dark cycle (LD 12:12, or LD) for several days to establish entrainment, and were subsequently kept in constant darkness (DD). Under LD conditions, homozygous $Per2^{Brdm1}$, $Per2^{Brdm1}/mCry2^{-/-}$ and $Per2^{Brdm1}/mCry1^{-/-}$ animals displayed activity patterns similar to that of wild-type mice (Fig. 1b–e). In constant darkness, $Per2^{Brdm1}$ mutant animals lost circadian rhythmicity after a few days (Fig. 1c), as described previously (Zheng et al. 1999, 2001; Bae et al. 2001). In contrast, $Per2^{Brdm1}/mCry1^{-/-}$ mice lost circadian rhythmicity immediately upon release into DD (Fig. 1d), as also observed for $mPer1^{-/-}/Per2^{Brdm1}$ and $mCry1^{-/-}/mCry2^{-/-}$ double mutant mice (van der Horst et al. 1999; Vitaterna et al. 1999; Bae et al. 2001; Zheng et al. 2001). Surprisingly, $Per2^{Brdm1}/mCry2^{-/-}$ animals maintained a circadian rhythm in DD (Fig. 1e). Determination of the period length (τ) by χ^2 periodogram analysis

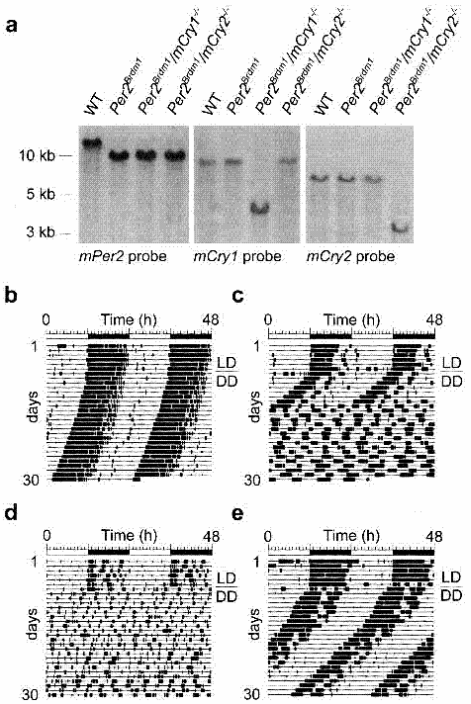

Figure 1. Generation of *mPer/mCry* double mutant mice and representative locomotor activity records. (*a*) Southern blot analysis of wild-type (WT), $Per2^{Brdm1}$, $Per2^{Brdm1}/mCry1^{-/-}$, and $Per2^{Brdm1}/mCry2^{-/-}$ tail DNA. The *Per2* probe hybridizes to a 12-kb wild-type and a 10-kb mutant fragment of *Bam*HI-digested genomic DNA. The *mCry1* probe detects a 9-kb wild-type and a 4-kb *Nco*I-digested fragment of the targeted locus. In *mCry2* mutants, the wild-type allele is detected by hybridization of the probe to a 7-kb *Eco*RI fragment, whereas the mutant allele yields a 3.5-kb fragment. The *left panel* indicates size of DNA fragments. (*b*) Representative locomotor activity records of wild-type (WT), $Per2^{Brdm1}$, $Per2^{Brdm1}/mCry1^{-/-}$, and $Per2^{Brdm1}/mCry2^{-/-}$ mice. All animals were kept in a 12-h light:12-h dark cycle (LD) for at least 7 d before release into constant darkness (DD, indicated by the line over the DD). Activity is represented by black bars (three plot heights, >1, >10, and >20 wheel revolutions per 5-min period) and is double-plotted. The top bar indicates light and dark phases in LD. For the first 5 d in DD, wheel rotations per day were 20,021 ± 2,524 (n = 22) for wild-type animals, 17,656 ± 3,301 (n = 17) for $Per2^{Brdm1}$ mutants, 16,025 ± 3,201 (n = 12) for $Per2^{Brdm1}/mCry1^{-/-}$ mutants, and 17,859 ± 2,703 (n = 15) for $Per2^{Brdm1}/mCry2^{-/-}$ mutants.

(using activity record intervals in which the circadian periodicity appeared stable on the activity record) revealed an average circadian period length of 23.8 ± 0.1 h (mean ± S.D., n = 22) for wild-type mice, 22.1 ± 0.3 h (n = 17) for $Per2^{Brdm1}$ mice and 23.4 ± 0.2 h (n = 15) for $Per2^{Brdm1}/mCry2^{-/-}$ animals. Interestingly, the period length of $Per2^{Brdm1}/mCry2^{-/-}$ animals is the average of that of $mCry2^{-/-}$ mice (24.6 ± 0.1 h, van der Horst et al. 1999) and $Per2^{Brdm1}$ mice. However, this might be coincidental. Wild-type and mutant mice all showed comparable levels of total wheel-running activity (see Fig. 1b legend), indicating that circadian period measurements were not influenced by aberrant running behavior.

To unravel whether the rescue of circadian rhythmicity in $Per2^{Brdm1}$ mutant animals by additional inactivation of the *mCry2* gene was reflected at the molecular level, we examined the expression patterns of the *mPer1*, *mPer2*, *mCry1*, and *Bmal1* clock genes in the SCNs of wild-type and mutant animals under DD (Fig. 2 a–d) and LD (Fig. 2 e–h) conditions. In situ hybridization experiments revealed that *mPer1* expression in wild-type mice peaks at CT6, which is in line with previous reports (Sun et al. 1997; Tei et al. 1997). In $Per2^{Brdm1}$ mutant animals, this rhythmicity is severely blunted (Fig. 2a). As might be expected from the behavioral data, *mPer1* gene ex-

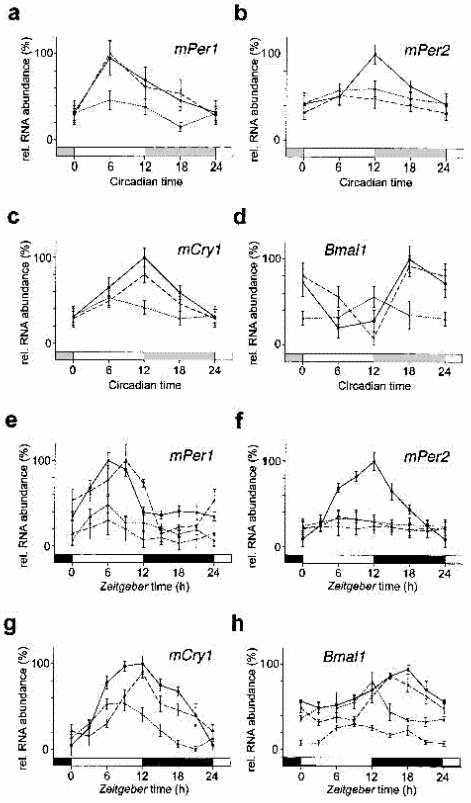

Figure 2. In situ hybridization profiles of cycling clock genes in the SCN of wild-type (solid line), $Per2^{Brdm1}$ (pointed line), $Per2^{Brdm1}/mCry2^{-/-}$ (dashed line), and $Per2^{Brdm1}/mCry1^{-/-}$ (point/dash line) mice kept in DD (*a–d*) or in a 12-h:12-h LD cycle (*e–h*). Each value is the mean ± S.D. (n = 3). Data at circadian time (CT) and *Zeitgeber* time (ZT) 0/24 are double-plotted. Bars on *X*-axis indicate light and dark phase. (*a*) *mPer1* expression in DD; (*b*) *mPer2* expression in DD; (*c*) *mCry1* expression in DD; (*d*) *Bmal1* expression in DD; (*e*) *mPer1* expression in LD; (*f*) *mPer2* expression in LD; (*g*) *mCry1* expression in LD; (*h*) *Bmal1* expression in LD.

pression was back to a normal amplitude, reaching a maximum at CT6 in $Per2^{Brdm1}/mCry2^{-/-}$ mutants (Fig. 2a). Thus, circadian expression of *mPer1* in $Per2^{Brdm1}$ mutants is rescued by inactivation of *mCry2*. A similar rescue was observed for *mCry1* expression: both amplitude and timing of *mCry1* oscillation in $Per2^{Brdm1}/mCry2^{-/-}$ mutant animals was not significantly different from that observed in wild-type animals (Fig. 2c). $Per2^{Brdm1}$ mutant mice displayed abnormal *Bmal1* mRNA rhythms, as evident from the reduced amplitude and shift of maximal expression levels to earlier CT times (Fig. 2d; Shearman et al. 2000). In the $Per2^{Brdm1}/mCry2^{-/-}$ mutants, however, both the phase and amplitude of *Bmal1* expression were comparable to those of the wild-type animals (Fig. 2d). Oscillation of mutant *mPer2* expression was not rescued in $Per2^{Brdm1}/mCry2^{-/-}$ mutants (Fig. 2b). Taken together, these data strongly indicate that normal circadian behavior and core oscillator performance is possible in the absence of functional *mPer2* and *mCry2* genes (Fig. 1e).

We also found a rescue of the amplitude of *mPer1*, *mCry1*, and *Bmal1* expression profiles in $Per2^{Brdm1}/mCry2^{-/-}$ animals kept under LD conditions (Fig. 2 e,g,h), whereas *mPer2* mRNA levels remained low as in the $Per2^{Brdm1}$ mice (Fig. 2f). These results are comparable to the expression patterns observed under DD conditions (Fig. 2 a–d), except that in the $Per2^{Brdm1}$ mutant mice, the amplitude of *Bmal1* expression was almost as high as in wild-type animals (there is no statistically significant difference between both maxima; Fig. 2h; Shearman et al. 2000). The phase advance of *Bmal1* expression in $Per2^{Brdm1}$ mice compared to wild-type mice, which might explain the frequently observed early onset of wheel running activity before the beginning of the dark phase (Zheng et al. 1999), is also lost in $Per2^{Brdm1}/mCry2^{-/-}$ animals (Fig. 2d). These data further underline the correction of the circadian phenotype of $Per2^{Brdm1}$ mice by inactivation of *mCry2*.

As shown above, $Per2^{Brdm1}/mCry1^{-/-}$ mice are arrhythmic in DD. To investigate whether these animals lack a circadian clockwork, we studied the expression patterns of the *mPer1*, *mPer2*, and *Bmal1* clock genes under LD conditions. We found that in $Per2^{Brdm1}/mCry1^{-/-}$ mutant animals, none of these genes is rhythmically expressed and mRNA levels are very low (Fig. 2e,f,h). This indicates that these animals lack a functional clock and that their diurnal behavioral activity under LD conditions (Fig. 1d) is most likely driven by the light/dark cycle. The loss of cyclic *Bmal1* expression in the $Per2^{Brdm1}$ mutant mice following inactivation of *mCry1* suggests that *mCry1* might play a role in transcriptional regulation of *Bmal1*.

The experiments described above indicate that an inactivation of *mCry2* in $Per2^{Brdm1}$ mice rescues circadian rhythmicity at the behavioral level as well as at the molecular level in the SCN. To determine whether this is also valid for peripheral clocks, we performed Northern blot analysis on kidney tissue. The expression profiles of *mPer1*, *mPer2*, *mCry1*, and *Bmal1* (Fig. 3a–d) under DD conditions are comparable to those observed in the SCN (Fig. 2 a–d), except that peak expression of these genes is delayed by several hours in the kidney (Zheng et al. 2001). Thus, rescue of circadian gene expression and probably clock function is also manifest in the periphery.

Inactivation of *Bmal1* causes immediate arrhythmicity, indicating that its gene product is crucial for circa-

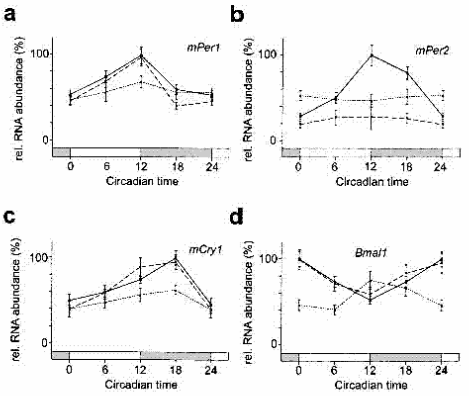

Figure 3. Quantificaion of Northern blots identifying clock genes in the kidney of wild-type (solid line), $Per2^{Brdm1}$ (pointed line), and $Per2^{Brdm1}/Cry2^{-/-}$ (dashed line) mice kept in DD. Each value is the mean ± S.D. of two (mutants) or four (wild-type) different experiments. Data at circadian time (CT) 0/24 is double-plotted. Bars on *X*-axis indicate subjective night (gray) and day (white). (*a*) *mPer1* expression in DD; (*b*) *mPer2* expression in DD; (*c*) *mCry1* expression in DD; (*d*) *Bmal1* expression in DD.

dian rhythmicity (Bunger et al. 2000). Since in $Per2^{Brdm1}$ mutant animals, *Bmal1* mRNA cycling seems to be dampened under DD conditions (Figs. 2d, 3d), we investigated expression levels of the latter transcript at CT18 (wild-type and $Per2^{Brdm1}/mCry2^{-/-}$ animals) and CT12 ($Per2^{Brdm1}$ mice) at 0, 3, 5, and 10 d after transfer of animals to constant darkness conditions. We found that in wild-type and $Per2^{Brdm1}/mCry2^{-/-}$ mice, *Bmal1* expression is maintained, whereas in $Per2^{Brdm1}$ animals, this mRNA rhythm decreases gradually until it disappears after 5–10 d (Fig. 4a). This observation parallels the gradual loss of circadian rhythmicity of *mPer2* mutant mice in DD (Fig. 1c; Zheng et al. 1999, 2001; Bae et al. 2001) and further supports the idea that the mPER2 protein is involved in regulating *Bmal1* expression (Shearman et al. 2000). The mCRY1 and mCRY2 proteins were recently reported to activate the *Bmal1* promoter in vitro (Yu et al. 2002). Because only $mCry1^{-/-}/mCry2^{-/-}$ and $mPer1^{-/-}/Per2^{Brdm1}$ double mutant mice, but not the corresponding single mutant animals, display an immediate loss of circadian rhythmicity in constant darkness, neither mCRY1 and mCRY2 proteins alone nor mPER1 and mPER2 proteins alone are likely to be responsible for rhythmic *Bmal1* transcriptional activation. Rather, *Bmal1* gene expression appears to be regulated by a combination of *mPer* and *mCry* gene products. Analogous to $mCry1^{-/-}/mCry2^{-/-}$ (van der Horst et al. 1999; Vitaterna et al. 1999) and $mPer1^{-/-}/Per2^{Brdm1}$ double mutant mice (Bae et al. 2001; Zheng et al. 2001), inactivation of both *mPer2* and *mCry1* leads to immediate loss of circadian rhythmicity (Fig. 1d). This implies that $Per2^{Brdm1}/mCry1^{-/-}$ mutant mice are lacking a circadian clock and that mPER1 and mCRY2 proteins are not sufficient for maintenance of circadian rhythmicity and expression of clock genes such as *Per1*, *Cry2*, and *Bmal1* (Figs. 2a,b,d; 3a,b,d). However, mice with inactivated *mPer2* and *mCry2* genes display stable circadian rhythmicity and

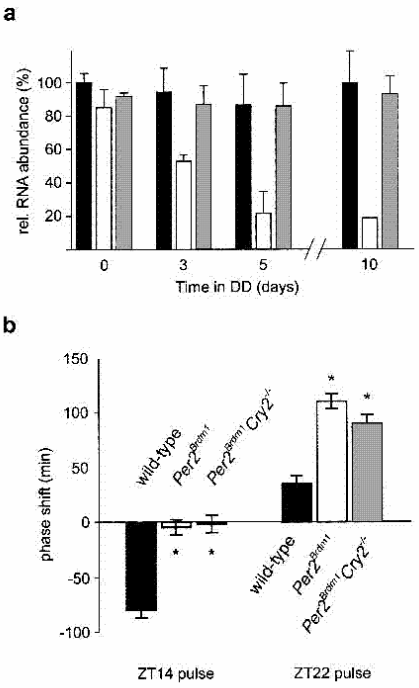

Figure 4. (*a*) *Bmal1* maximal expression in the SCN of wild-type (black column), $Per2^{Brdm1}$ (white column), and $Per2^{Brdm1}/mCry2^{-/-}$ (gray column) mice released into DD. Mice were adapted to a 12-h: 12-h LD cycle and subsequently put into DD for 3, 5, or 10 subjective days. Only rhythmic animals were sacrificed at time points of maximal *Bmal1* expression (CT18 for wild-type and $Per2^{Brdm1}/mCry2^{-/-}$; CT12 for $Per2^{Brdm1}$ mice). Each value is the mean ± S.D. of three animals (except for day 10 in $Per2^{Brdm1}$ mice with only one rhythmic animal). (*b*) Light-induced activity phase shifts in wild-type (black column), $Per2^{Brdm1}$ (white column), and $Per2^{Brdm1}/mCry2^{-/-}$ (gray column) mice. After entrainment to a 12-h:12-h LD cycle, animals were exposed to a 15-min light pulse (400Lux) at the beginning (ZT14) or at the end (ZT22) of the night and subsequently relased into DD. Negative values represent phase delays, and positive values phase advances. Each value is the mean ± S.D. of 10–14 animals. Only animals which remained rhythmic for at least 7 consecutive days in DD were used for quantification. Significance as indicated by asterisks was determined by one-way ANOVA with subsequent Bonferroni posttest ($p < 0.05$).

normal *Bmal1 mRNA* cycling, indicating that mPER1 and mCRY1 proteins can maintain circadian rhythmicity and rhythmic *Bmal1* expression in the absence of functional *mPer2* and *mCry2* genes. These data suggest that in $Per2^{Brdm1}$ single mutant mice, the functional *mCry2* gene product interferes with mPER1 and/or mCRY1, which leads to a gradual loss of circadian rhythmicity. Thus, *mPer1* only in combination with *mCry1* and in the absence of a functional *mCry2* gene seems to be able to sustain the circadian clock in vivo. However, the resetting defect observed in $Per2^{Brdm1}$ single mutant mice (Albrecht et al. 2001) was not rescued in $Per2^{Brdm1}/mCry2^{-/-}$ mice (Fig. 4b). This indicates that in $Per2^{Brdm1}/mCry2^{-/-}$ mice, PER1 can substitute PER2 in the core clock mechanism but not in the light input signaling pathway. As a note of caution, one should keep in mind that the phenotypic effect of genetic modifications of genetically altered animals in a nonhomogeneous genetic background are prone to epigenetic effects. However, we tried to minimize this risk by using double heterozygous animals throughout the crossings from which the wild-type and mutants were derived. Thus the wild-type control animals in this study have a mixed background similar to that of the mutants.

Our observations would be compatible with a hypothesis that there is a hierarchy of "activity potentials" for the four members of the negative limb (*mPer1, mPer2, mCry1, mCry2*) of the clock mechanism. It seems that CRY1 is a stronger repressor than CRY2, and PER2 is a more potent repressor than PER1. The activity potentials on the negative limb will have effects on the positive limb of the clock mechanism as well. Thus one could envisage a similar hierarchy of activity potentials for the positive limb or more precisely on activation of *Bmal1*. Assuming that all four CRY and PER proteins can be assembled into a protein complex with two CRY and two PER proteins, the activity potential of this complex is dependent on its composition. For example, a complex of two PER1 proteins and two CRY2 proteins would have a lower repressor potential than a complex composed of two PER2 and two CRY1 proteins. In turn, a complex that only forms in a wild-type animal composed of PER1, PER2, CRY1, and CRY2 would have an intermediate repressor potential. Assuming that circadian clocks are based on limit cycles of feedback-transcription to generate circadian rhythms (Glass and Mackey 1988; Leloup et al. 1999), too-low or too-high repressor potentials will destabilize the limit cycle, and the system will fall into equilibrium and become arrhythmic. Such a model might be further supported by the gene dosage effects observed in *mCry* double mutant mice. For instance, knocking out one *mCry1* allele in $mCry2^{-/-}$ mice normalizes the behavioral rhythm, and knocking out one *mCry2* allele in $mCry1^{-/-}$ mice further disturbs rhythmicity (van der Horst et al. 1999). In $mPer1^{-/-}$ animals, both PER subunits would be PER2 proteins with a high repressor potential, which accelerates the feedback loop, as has been observed (Zheng et al. 2001). However, the overall repressor potential is still compatible with the parameters of the limit cycle, and therefore the $mPer1^{-/-}$ mice are still rhythmic. In $Per2^{Brdm1}$ mutant animals, both PER subunits are PER1 proteins that are weak repressors, and therefore the feedback loop is slowed down to a degree that is no longer compatible with the limit cycle; thus, $Per2^{Brdm1}$ mice become arrhythmic. In $Per2^{Brdm1}/mCry2^{-/-}$ mice, however, the repressor complex is composed of two CRY1 proteins (strong repressors) and two PER1 proteins (weak repressors). The overall repressor potential of this complex would approach that of the wild-type complex and is thus compatible with the parameters of the limit cycle. $Per2^{Brdm1}/mCry2^{-/-}$ mice would therefore be rhythmic, which is compatible with our observations.

Taken together, our findings suggest that *mCry2* can act as a nonallelic suppressor of *mPer2* and that there might exist PER/CRY complexes with different transcriptional activity potentials, some of which are compatible with the parameters of a limit cycle whereas others are not.

Materials and methods

Generation of mPer and mCry mutant mice

We crossed *mPer2*^{Brdm1} mice (Zheng et al. 1999) with *mCry1* and *mCry2* knockout animals (van der Horst et al. 1999). The genotype of the offspring was determined by Southern blot analysis as described (Ramirez-Solis et al. 1993). Hybridization probes were for *mPer2* as described by Zheng et al. (1999) and for *mCry1* and *mCry2* as described by van der Horst et al. (1999). Matching wild-type control animals were produced by back-crossing heterozygous animals.

Locomotor activity monitoring and circadian phenotype analysis

Mice housing and handling were performed as described (Albrecht and Oster 2001). For LD–DD transitions, lights were turned off at the end of the light phase and not turned on again the next morning. Activity records are double plotted so that each day cycle's activity is shown both to the right and below that of the previous day cycle. Activity is plotted in threshold format with three different thresholds set to >1, >10, and >20 wheel revolutions per 5-min period (Fig. 1). For activity counting, we used the ACS program of Simon Fraser University. For actograms and period determination, we used the Circadia program of Simon Fraser University. Period length was assessed by χ^2 periodogram analysis using mice running in constant darkness for at least 10 d (5 d for *Per2*^{Brdm1}).

For light-induced phase shifts, we used the Aschoff Type II protocol as described (Albrecht et al. 2001). We chose this protocol because *mPer2*^{Brdm1} mice become arrhythmic in constant darkness, precluding the determination of circadian times. Animals were entrained to an LD cycle for at least 7 d before the light administration [15 min bright white light (400Lux) at *Zeitgeber* time (ZT)14 or ZT22] and subsequently released into DD. The phase shift was determined by eye-fitting a line through at least 7 consecutive d of onset of activity in LD before the light pulse and in DD after the light pulse. The difference between the two lines on the day of the light pulse determined the value of the phase shift.

In situ hybridization

Mice were sacrificed by cervical dislocation under ambient light conditions at ZT6 and ZT12 and under a 15W safety red light at ZT18 and ZT0/24 as well as at circadian time (CT) 0, 6, 12, and 18. For DD conditions, animals were kept in the dark for 3 d before decapitation. Specimen preparation, ^{35}S-UTP labeled riboprobe synthesis, and hybridization steps were performed as described (Albrecht et al. 1998). The probes for *mPer1* and *mPer2* were as described (Albrecht et al. 1997). The *mCry1* probe was made from a cDNA corresponding to nucleotides 190–771 (accession no. AB000777) and the *Bmal1* probe corresponding to nucleotides 654–1290 (accession no. AF015953). The *mPer2* probe is located outside the region deleted in the mutant. Quantification was performed by densitometric analysis of autoradiograph films (Amersham Hyperfilm MP) using the NIH Image program after conversion into the relative optical densities by the ^{14}C-autoradiographic microscale (Amersham). Data from the SCN were normalized with respect to the signal intensities in an equal area of the lateral hypothalamus. Three sections per SCN were analyzed. "Relative mRNA abundance" values were calculated by defining the highest value of each experiment as 100%.

Northern blot analysis

Rhythmic animals were sacrificed at the specified circadian time points on the third day in DD. Total RNA from kidney was extracted using RNAzol B (WAK Chemie). Northern analysis was performed using denaturing formaldehyde gels (Sambrook and Russel 2001) with subsequent transfer to Hybond-N membrane (Amersham). For each sample, 20µg of total RNA was used. cDNA probes were the same as described for in situ hybridization. Labeling of probes was done using the random prime labeling kit (Pharmacia) incorporating [P^{32}]dCTP to a specific activity of 10^8 cpm/µg. Blots were hybridized using QuickHyb solution (Stratagene) containing 100 µg/mL salmon sperm DNA. The membrane was washed at 60°C in 0.1× SSC and 0.1% SDS. Subsequently, blots were exposed to phosphoimager plates (Bio-Rad) for 20 h, and signals were quantified using Quantity One 3.0 software (Bio-Rad). Signal intensities were normalized by comparison of the 18S ribosomal RNA bands' methylene blue staining on the blotted membrane. The highest clock gene signal was determined as 100% for each experiment.

Acknowledgments

We thank E. Maronde for comments on the manuscript. This work was supported by the Max-Planck-Society and grants from the Deutsche Forschungsgemeinschaft, the Swiss National Science Foundation, the Novartis Foundation (U.A.), and a SPINOZA premium from the Netherlands Organization for Scientific Research (NWO; G.T.J. v. d. H.).

The publication costs of this article were defrayed in part by payment of page charges. This article must therefore be hereby marked "advertisement" in accordance with 18 USC section 1734 solely to indicate this fact.

References

Albrecht, U. 2002. Invited Review: Regulation of mammalian circadian clock genes. *J. Appl. Physiol.* **92:** 1348–1355.

Albrecht, U. and Oster, H. 2001. The circadian clock and behavior. *Behav. Brain Res.* **125:** 89–91.

Albrecht, U., Sun, Z.S., Eichele, G., and Lee, C.C. 1997. A differential response of two putative mammalian circadian regulators, mper1 and mper2, to light. *Cell* **91:** 1055–1064.

Albrecht, U., Lu, H.-C., Revelli, J.-P., Xu, X.-C.-, Lotan, R., and Eichele, G. 1998. Studying gene expression on tissue sections using *in situ* hybridization. In *Human genome methods* (ed. K.W. Adolph), pp. 93–119. CRC Press, NY.

Albrecht, U., Zheng, B., Larkin, D., Sun, Z.S., and Lee, C.C. 2001. *mPer1* and *mPer2* are essential components for normal resetting of the circadian clock. *J. Biol. Rhythms* **16:** 100–104.

Amin, N.S., Tuffo, K.M., and Holm, C. 1999. Dominant mutations in three different subunits of replication factor C suppress replication defects in yeast PCNA mutants. *Genetics* **153:** 1617–1628.

Bae, K., Jin, X., Maywood, E.S., Hastings, M.H., Reppert, S.M., and Weaver, D.R. 2001. Differential functions of mPer1, mPer2 and mPer3 in the SCN circadian clock. *Neuron* **30:** 525–536.

Bunger, M.K., Wilsbacher, L.D., Moran, S.M., Clendenin, C., Radcliffe, L.A., Hogenesch, J.B., Simon, M.C., Takahashi, J.S., and Bradfield, C.A. 2000. Mop3 is an essential component of the master circadian pacemaker in mammals. *Cell* **103:** 1009–1017.

Field, M.D., Maywood, E.S., O'Brien, J.A., Weaver, D.R., Reppert, S.M., and Hastings, M.H. 2000. Analysis of clock proteins in mouse SCN demonstrates phylogenetic divergence of the circadian clockwork and resetting mechanisms. *Neuron* **25:** 437–447.

Glass, L. and Mackey, M.C. 1988. *From clocks to chaos. The rhythms of life.* pp. 22–25. Princeton University Press, Princeton, NJ.

Grandin, N. and Charbonneau, M. 2001. Hsp90 levels affect telomere length in yeast. *Mol. Genet. Genomics.* **265:** 126–134.

Griffin, E.A., Jr., Staknis, D., and Weitz, C.J. 1999. Light-independent role of CRY1 and CRY2 in the mammalian circadian clock. *Science* **286:** 768–771.

Hamada, T., LeSauter, J., Venuti, J.M., and Silver, R. 2001. Expression of Period genes: Rhythmic and nonrhythmic compartments of the suprachiasmatic nucleus pacemaker. *J. Neurosci.* **21:** 7742–7750.

Jagota, A., de la Iglesia, H.O., and Schwartz, W.J. 2000. Morning and evening circadian oscillations in the suprachiasmatic nucleus in vitro. *Nat. Neurosci.* **3:** 372–376.

King, D.P. and Takahashi, J.S. 2000. Molecular genetics of circadian rhythms in mammals. *Annu Rev Neurosci* **23:** 713–742.

Kume, K., Zylka, M.J., Sriram, S., Shearman, L.P., Weaver, D.R., Jin, X., Maywood, E.S., Hastings, M.H., and Reppert, S.M. 1999. mCRY1 and mCRY2 are essential components of the negative limb of the circadian clock feedback loop. *Cell* **98:** 193–205.

LaJeunesse, D.R., McCartney, B.M., and Fehon, R.G. 2001. A systematic screen for dominant second-site modifiers of Merlin/NF2 phenotypes reveals an interaction with blistered/DSRF and scribbler. *Genetics* **158:** 667–679.

Lee, C., Etchegaray, J.P., Cagampang, F.R., Loudon, A.S., and Reppert, S.M. 2001. Posttranslational mechanisms regulate the mammalian circadian clock. *Cell* **107:** 855–867.

Leloup, J.C., Gonze, D., and Goldbeter, A. 1999. Limit cycle models for circadian rhythms based on transcriptional regulation in Drosophila and Neurospora. *J. Biol. Rhythms* **14:** 433–448

Maine, E.M. and Kimble, J. 1989. Identification of genes that interact with glp-1, a gene required for inductive cell interactions in Cae-

norhabditis elegans. *Development* **106:** 133–143.
Miyazaki, K., Mesaki, M., and Ishida, N. 2001. Nuclear entry mechanism of rat PER2 (rPER2): Role of rPER2 in nuclear localization of CRY protein. *Mol. Cell. Biol.* **21:** 6651–6659.
Nakano, M.M., Zhu, Y., Liu, J., Reyes, D.Y., Yoshikawa, H., and Zuber, P. 2000. Mutations conferring amino acid substitutions in the C-terminal domain of RNA polymerase alpha can suppress clpX an clpP with respect to developmentally regulated transcription in Bacillus subtilis. *Mol. Microbiol.* **37:** 869–884.
Ramirez-Solis, R., Zheng, H., Whiting, J., Krumlauf, R., and Bradley, A. 1993. Hoxb-4 (Hox-2.6) mutant mice show homeotic transformation of a cervical vertebra and defects in the closure of the sternal rudiments. *Cell* **73:** 279–294.
Roy, F., Laberge, G., Douziech, M., Ferland-McCollough, D., and Therrien, M. 2002. KSR is a scaffold required for activation of the ERK/MAPK module. *Genes & Dev.* **16:** 427–438.
Sambrook, J. and Russel, D.W. 2001. *Molecular cloning.* Cold Spring Harbor Laboratory Press, Cold Spring Harbor, NY.
Shearman, L.P., Sriram, S., Weaver, D.R., Maywood, E.S., Chaves, I., Zheng, B., Kume, K., Lee, C.C., van der Horst, G.T., Hastings, M.H., et al. 2000. Interacting molecular loops in the mammalian circadian clock. *Science* **288:** 1013–1019.
Sun, Z.S., Albrecht, U., Zhuchenko, O., Bailey, J., Eichele, G., and Lee, C.C. 1997. RIGUI, a putative mammalian ortholog of the Drosophila period gene. *Cell* **90:** 1003–1011.
Tei, H., Okamura, H., Shigeyoshi, Y., Fukuhara, C., Ozawa, R., Hirose, M., and Sakaki, Y. 1997. Circadian oscillation of a mammalian homologue of the Drosophila period gene. *Nature* **389:** 512–516.
van der Horst, G.T., Muijtjens, M., Kobayashi, K., Takano, R., Kanno, S., Takao, M., de Wit, J., Verkerk, A., Eker, A.P., van Leenen, D., et al. 1999. Mammalian Cry1 and Cry2 are essential for maintenance of circadian rhythms. *Nature* **398:** 627–630.
Vielhaber, E.L., Duricka, D., Ullman, K.S., and Virshup, D.M. 2001. Nuclear export of mammalian PERIOD proteins. *J. Biol. Chem.* **8:** 8.
Vitaterna, M.H., Selby, C.P., Todo, T., Niwa, H., Thompson, C., Fruechte, E.M., Hitomi, K., Thresher, R.J., Ishikawa, T., Miyazaki, J., et al. 1999. Differential regulation of mammalian period genes and circadian rhythmicity by cryptochromes 1 and 2. *Proc. Natl. Acad. Sci.* **96:** 12114–12119.
Yagita, K., Yamaguchi, S., Tamanini, F., van Der Horst, G.T., Hoeijmakers, J.H., Yasui, A., Loros, J.J., Dunlap, J.C., and Okamura, H. 2000. Dimerization and nuclear entry of mPER proteins in mammalian cells. *Genes & Dev.* **14:** 1353–1363.
Yagita, K., Tamanini, F., Yasuda, M., Hoeijmakers, J.H., van Der Horst, G.T., and Okamura, H. 2002. Nucleocytoplasmic shuttling and mCRY-dependent inhibition of ubiquitylation of the mPER2 clock protein. *EMBO J.* **21:** 1301–1314.
Yu, W., Nomura, M., and Ikeda, M. 2002. Interactivating feedback loops within the mammalian clock: BMAL1 is negatively autoregulated and upregulated by CRY1, CRY2, and PER2. *Biochem. Biophys. Res. Commun.* **290:** 933–941.
Zheng, B., Larkin, D.W., Albrecht, U., Sun, Z.S., Sage, M., Eichele, G., Lee, C.C., and Bradley, A. 1999. The mPer2 gene encodes a functional component of the mammalian circadian clock. *Nature* **400:** 169–173.
Zheng, B., Albrecht, U., Kaasik, K., Sage, M., Lu, W., Vaishnav, S., Li, Q., Sun, Z.S., Eichele, G., Bradley, A., et al. 2001. Nonredundant roles of the mPer1 and mPer2 genes in the mammalian circadian clock. *Cell* **105:** 683–694.

2.2. Publication: “Loss of circadian rhythmicity in ageing *mPer1*$^{-/-}$*mCry2*$^{-/-}$ mutant mice”

Henrik Oster, Stéphanie Baeriswyl, Gijsbertus T. J. van der Horst,and Urs Albrecht

in preparation

Abstract

The *mPer1*, *mPer2* and *mCry1*, *mCry2* genes play a central role in the molecular mechanism driving the central pacemaker of the mammalian circadian clock, located in the *suprachiasmatic nuclei* (SCN) of the hypothalamus. *In vitro* studies suggest a close interaction of all mPER and mCRY proteins. We investigated mPER and mCRY interactions *in vivo* by generating different combinations of *mPer/mCry* double mutant mice. We previously showed that *mCry2* acts as a non-allelic suppressor of *mPer2* in the core clock mechanism. Here we focus on the circadian phenotypes of *mPer1/mCry* double mutant animals and find a decay of the clock with age in *mPer1*$^{-/-}$*mCry2*$^{-/-}$ mice at the behavioural and the molecular level. Our findings indicate that complexes consisting of different combinations of mPER and mCRY proteins are not redundant *in vivo* and have different potentials in transcriptional regulation in the system of autoregulatory feedback loops driving the circadian clock.

Introduction

The earth's rotation around the sun has strongly influenced temporal organisation of the mammalian organism manifested by near 24 hour rhythms of biological processes (Pittendrigh, 1993) including the sleep-wake cycle, energy metabolism, body temperature, renal activity and blood pressure. These rhythms are maintained even in the absence of external time signals (*Zeitgeber*). They are driven by a central clock located in the *suprachiasmatic nuclei* (SCN) of the ventral hypothalamus (Ralph et al., 1990; Rusak and Zucker, 1979). Since the internal period length generated by this pacemaker is not exactly 24 hours (hence the term 'circadian', from the Latin *circa dies* which translates to 'about one day'), the clock has to be reset every day by an input pathway synchronising the organism's biological processes with geophysical time. This is accomplished by monitoring the daily variation in light intensity by photoreceptors in the eye that project directly *via* the retinohypothalamic tract (RHT; Rusak and Zucker, 1979) or indirectly *via* the intergeniculate leaflet (IGL; Jacob et al., 1999) to the SCN. The oscillations generated in the SCN are translated into overt rhythms in behaviour and physiology through output pathways that probably involve both chemical and electrical signals. These signals are essential for the maintenance of overt circadian rhythms, but most cells of peripheral tissues possess a functional circadian oscillator with a molecular organisation very similar to that of SCN neurons (Balsalobre et al., 1998; Yamazaki et al., 2000).

At the molecular level, circadian rhythms are generated by the integration of autoregulatory transcriptional/translational feedback loops (TTLs; Albrecht, 2002; Allada et al., 2001; Reppert and Weaver, 2002). In the mammalian system, the TTL can be subdivided into a positive and a negative limb. The positive limb is constituted by the PAS helix-loop-helix transcription factors CLOCK and BMAL1 that bind upon heterodimerisation to enhancer elements termed E-boxes regulating transcription of *Period (mPer)* and probably also *Cryptochrome (mCry)* genes. The mPER and mCRY proteins are components of the negative limb that attenuate the CLOCK/BMAL1-mediated activation of their own genes and hence generate a negative feedback. There is evidence that a mPER/mCRY complex interacts directly with the CLOCK/BMAL1 complex bound to chromatin (Lee et al., 2001). A number of posttranslational events such as phosphorylation, ubiquitylation, degradation and intracellular transport seem to be critical for the generation of oscillations in clock gene products and the stabilisation of a 24h period (Kume et al., 1999; Lee et al., 2001; Miyazaki et al., 2001; Vielhaber et al., 2001; Yagita et al., 2002; Yagita et al., 2000; Yu et al., 2002).

Additionally, the two limbs of the TTL are linked by the nuclear orphan receptor REV-ERBα, which is under the influence of *mPer* and *mCry* genes and controls transcription of *Bmal1* (Preitner et al., 2002). In mammals three *Per* genes, *mPer1* (Sun et al., 1997; Tei et al., 1997), *mPer2* (Albrecht et al., 1997; Shearman et al., 1997), and *mPer3* (Zylka et al., 1998) and two *Cry* genes, *mCry1* and *mCry2* (Miyamoto and Sancar, 1998) have been identified. While *mPer3* seems not to be necessary for the generation of circadian rhythmicity (Shearman et al., 2000), *mPer1*, *mPer2* and both *mCry* genes have been demonstrated to play essential roles in the central oscillator as well as in the light driven input pathway to the clock (Albrecht et al., 2001; Bae et al., 2001; Cermakian et al., 2001; van der Horst et al., 1999; Vitaterna et al., 1999; Zheng et al., 2001; Zheng et al., 1999).

The molecular mechanism of clock autoregulation has largely been studied *in vitro* (Gekakis et al., 1998; Kume et al., 1999; Miyazaki et al., 2001; Vielhaber et al., 2001; Yagita et al., 2002; Yagita et al., 2000; Yu et al., 2002). These studies point to multiple physical interactions between all mPER and mCRY proteins. However, the time course of protein availability, modification and localisation is difficult to resolve in cell and slice cultures (Hamada et al., 2001; Jagota et al., 2000; Lee et al., 2001). To elucidate the functional relationship between the *mPer* and *mCry* genes *in vivo*, we started to inactivate different combinations of *mPer* and *mCry* genes in mice. Disruption of *mCry2* restores circadian rhythmicity in *mPer2* mutant mice, suggesting that *mCry2* can act as a non-allelic suppressor of *mPer2* (Oster et al., 2002b). In contrast, additional inactivation of *mCry1* in *mPer2* mutant animals leads to an immediate loss of circadian rhythmicity (Oster et al., 2002b).

Here we show that *mPer1*$^{-/-}$*mCry1*$^{-/-}$ mice maintain a functional circadian clock and that *mPer1*$^{-/-}$*mCry2*$^{-/-}$ mice initially display circadian rhythmic behaviour and gene expression. After a few months however, the rhythm of *mPer1*$^{-/-}$*mCry2*$^{-/-}$ mice breaks down. This loss of rhythmicity is accompanied by altered regulation of expression of core clock components. Additionally, the light responsiveness of the clock in *mPer1*$^{-/-}$*mCry2*$^{-/-}$ mice is affected at the behavioural and molecular levels. Interestingly, this defect seems to have its roots in the signal transduction pathway of the ganglion cell layer in the retina. Taken together with previous observations, our results indicate that the amount of mPER and mCRY proteins and hence the composition of mPER/mCRY complexes are critical for generation and maintenance of circadian rhythms. The destabilisation of these complexes in *mPer1*$^{-/-}$*mCry2*$^{-/-}$ mice disrupts the ability of the TTL to compensate age-related changes in transcriptional and posttranscriptional efficiency resulting in a disruption of the circadian clock in older animals.

Results

mPer1 acts as a non-allelic suppressor of mCry1

To begin to understand the *in vivo* function of the *mPer* and *mCry* genes in the clock mechanism, we generated mice with disruptions in both the *mPer1/mCry1* and *mPer1/mCry2* genes respectively. Mice with a deletion of the *mPer1* gene (Zheng et al., 2001) were crossed with *mCry1*$^{-/-}$ or *mCry2*$^{-/-}$ mice, respectively (van der Horst et al., 1999). The double-heterozygous offspring was intercrossed to produce wild-type and homozygous mutant animals. *mPer1*$^{-/-}$*mCry1*$^{-/-}$ and *mPer1*$^{-/-}$*mCry2*$^{-/-}$ mice (representative genotyping shown in Fig. 1A) were obtained at the expected Mendelian ratios and were morphologically indistinguishable from wild-type animals. The animals appeared normal in fertility, although in *mPer1/mCry* double mutant mice the intervals between two litters seem to increase significantly with progressing age (data not shown).

To determine the influence of inactivation of either the *mCry1* or *mCry2* gene on circadian behaviour of *mPer1*$^{-/-}$ mice, mutant and wild-type animals were individually housed in circadian activity-monitoring chambers (Albrecht and Oster, 2001) for analysis of wheel-running activity, an accurate measure of circadian rhythmicity. Mice were kept in a 12 hour light/ 12 hour dark cycle (LD 12:12, or LD) for several days to establish entrainment, and were subsequently kept in constant darkness (DD). Under LD and DD conditions *mPer1*$^{-/-}$ *mCry1*$^{-/-}$ animals displayed activity patterns and expression patterns of clock components similar to that of wild-type mice (Fig. 1 B, C and supplemental Fig. 2). Under DD conditions *mPer1*$^{-/-}$*mCry1*$^{-/-}$ mutant mice displayed a period length (τ) of 23.7 $\pm$ 0.2 h (mean $\pm$ S.D., n=15) which is similar to that of wild-type animals (τ = 23.8 $\pm$ 0.1 h; n=17). Thus an additional deletion of *mPer1* rescues the short period phenotype of *mCry2* deficient mice (van der Horst et al., 1999) indicating that *mPer1* acts as a non-allelic suppressor of *mCry1*.

Loss of circadian wheel running activity rhythms in ageing mPer1$^{-/-}$*mCry2*$^{-/-}$ *double mutant mice*

mPer1$^{-/-}$*mCry2*$^{-/-}$ animals that were between 2 and 6 months old ('young' *mPer1*$^{-/-}$ *mCry2*$^{-/-}$ mice) displayed a diurnal activity pattern like wild-type animals under LD conditions. However, onset of activity was delayed and highest activity could be observed in the second half of the night (Fig. 1D). Interestingly, *mPer1*$^{-/-}$*mCry2*$^{-/-}$ animals that were more

than six months old ('old' *mPer1*$^{-/-}$*mCry2*$^{-/-}$ mice) showed a disturbed diurnal activity pattern under LD conditions (Fig. 1F), but a faint 24 hour rhythm could still be detected when applying χ^2 periodogram analysis (Fig. 1G). Under DD conditions young *mPer1*$^{-/-}$*mCry2*$^{-/-}$ mice display a long period (τ) of 25.3 $\pm$ 0.2 h (mean $\pm$ S.D., n=14) compared to wild-type animals (τ = 23.8 $\pm$ 0.1 h; n=17) (Fig. 1D and E). In contrast to young *mPer1*$^{-/-}$*mCry2*$^{-/-}$ mice, old *mPer1*$^{-/-}$*mCry2*$^{-/-}$ mice were arrhythmic under DD conditions (Fig. 1F and I). The transition from a rhythmic to an arrhythmic phenotype, however, did not occur in all animals at the same age, but age is correlated with loss of circadian wheel-running activity (Fig. 1H). *mPer1*$^{-/-}$*mCry2*$^{-/-}$ mice that are between two and six months old all display circadian activity patterns, whereas only about 60 % of animals between six and twelve months of age maintain circadian rhythmicity. Interestingly, 87% of the *mPer1*$^{-/-}$*mCry2*$^{-/-}$ mice older than twelve months are arrhythmic. We did not observe a comparable age-related loss of rhythmicity in wild-type, *mPer1*$^{-/-}$ and *mCry2*$^{-/-}$ mice (Fig. 1 H and supplemental Fig. 1). However, we cannot completely rule out that arrhythmicity could be observed sometime in ageing single mutants as well but the stability of rhythmicity appears dramatically decreased in the double knock out context. Following this observation we divided all double mutant animals into two groups for use in subsequent experiments. Rhythmic animals are referred to as 'young *mPer1*$^{-/-}$*mCry2*$^{-/-}$' and arrhythmic animals are referred to as 'old *mPer1*$^{-/-}$*mCry2*$^{-/-}$'. This does not necessarily correspond with the physical age of each individual because all animals used for mRNA and protein analyses were between 6 and 12 months old and the onset of arrhythmicity does not occur at the same age in every animal. However, since there is a clear correlation between age and rhythmicity the average age of 'old' animals is higher than of the 'young'.

Alterations in expression levels of clock components in ageing mPer1$^{-/-}$*mCry2*$^{-/-}$ *double mutant mice*

To investigate whether the loss of circadian rhythmicity in ageing *mPer1*$^{-/-}$*mCry2*$^{-/-}$ mutant mice was reflected at the molecular level, we examined the expression patterns of the *mPer2*, *mCry1* and *Bmal1* genes. Under LD and DD conditions *mPer2* mRNA expression in the SCN was comparable in young *mPer1*$^{-/-}$*mCry2*$^{-/-}$ mice and wild-type animals with peak levels at *Zeitgeber* time (ZT) or circadian time (CT) 12 (Fig. 2A and B). Interestingly, *mPer2* mRNA expression was markedly reduced in old *mPer1*$^{-/-}$*mCry2*$^{-/-}$ mice at ZT12 with the diurnal expression pattern almost not detectable (Fig. 2A). In the kidney, a similar reduction of

mPer2 mRNA expression in old *mPer1*$^{-/-}$*mCry2*$^{-/-}$ mice could be observed with a maximum of expression at ZT12 in wild-type animals (Cermakian et al., 2001; Zheng et al., 2001) and young *mPer1*$^{-/-}$*mCry2*$^{-/-}$ mice (Fig. 2D and E). Expression patterns of old *mPer1*$^{-/-}$*mCry2*$^{-/-}$ mice in DD were not determined because these mice loose circadian rhythm and no circadian times can be determined. To justify that the observed changes are related to the double knock out status of the animals we looked for *mPer2* expression in *mPer1*$^{-/-}$ and *mCry2*$^{-/-}$ mice of the same age. *mPer2* oscillation appeared to be normal in both LD and DD in the single mutants with no detectable reduction in the amplitude (supplemental figure 3 A and B).

To investigate whether the reduced *mPer2* mRNA expression in old *mPer1*$^{-/-}$*mCry2*$^{-/-}$ mice was manifested at the protein level, we examined the presence of mPER2 protein in the SCN by immunohistochemistry. In wild-type and young *mPer1*$^{-/-}$*mCry2*$^{-/-}$ mice protein levels are high between ZT12 and ZT18 (Fig. 2C; Field et al., 2000) which is a few hours later than mRNA expression (Fig. 2A). In old *mPer1*$^{-/-}$*mCry2*$^{-/-}$ mice however, protein levels are low comparable to mRNA expression (Fig. 2A and C).

There is evidence that mPER1/2 and mCRY1/2 can indirectly activate *Bmal1* expression (Preitner et al., 2002; Yu et al., 2002) *via* the inhibition of *Rev-Erbα*. *REV-ERBα* protein inhibits the transcription of *Bmal1* and possibly *Clock*. On the other hand CLOCK/BMAL1 protein activates *Rev-Erbα* expression (Preitner et al., 2002). mPER1/2 and mCRY1/2 proteins can interfere with CLOCK/BMAL1 mediated transcriptional activation. Therefore we investigated the expression pattern of *mCry1* and *Bmal1* in the SCN. In wild-type, *mPer1*$^{-/-}$, *mCry2*$^{-/-}$ and young *mPer1*$^{-/-}$*mCry2*$^{-/-}$ mice *mCry1* mRNA expression was similar in LD and DD with a maximum at ZT12 or CT12, respectively (Fig. 3A, B and supplemental figure 3 C-F). This is consistent with previous reports on wild-type animals (Okamura et al., 1999). Interestingly, *mCry1* mRNA expression was normal in old *mPer1*$^{-/-}$*mCry2*$^{-/-}$ mice in LD (Fig. 3A), which is in marked contrast to the reduced *mPer2* mRNA expression in these mice (Fig. 2A and B). Therefore we examined mCRY1 protein levels in the SCN by immunohistochemistry. mCRY1 protein levels were cycling in wild-type animals with peak expression between ZT12 and ZT18 (Fig. 3C) as reported previously (Field et al., 2000). Similarly, young *mPer1*$^{-/-}$*mCry2*$^{-/-}$ mice displayed cycling expression of mCRY1 protein, but the expression levels at ZT0 (24) were notably higher than in wild-type animals (Fig. 3C). The elevated expression of mCRY1 protein at ZT0 (24) became even more pronounced in old *mPer1*$^{-/-}$*mCry2*$^{-/-}$ mice leading to almost constant high levels of mCRY1 protein throughout the 24 hour LD cycle (Fig. 3C). In age matched *mPer1*$^{-/-}$ and *mCry2*$^{-/-}$ mice however, mCRY1 protein cycling was observed (see Suppl Fig. 3) indicating that the abnormal regulation of the

mCRY1 protein in old *mPer1*$^{-/-}$*mCry2*$^{-/-}$ mice is due to the inactivation of both *mPer1* and *mCry2*. Next, we looked at *Bmal1* mRNA expression in the SCN under LD and DD conditions. In wild-type and *mPer1*$^{-/-}$ animals a maximum was seen at ZT and CT 18 (supplemental figure 3 E and F) as previously observed (Honma et al., 1998). In *mCry2*$^{-/-}$ animals the maximum of *Bmal1* expression was slightly delayed (supplemental figure 3 E and F). Young *mPer1*$^{-/-}$*mCry2*$^{-/-}$ animals displayed a similar expression pattern, although the levels tended to be slightly decreased (Fig. 3D and E). In old *mPer1*$^{-/-}$*mCry2*$^{-/-}$ mice *Bmal1* mRNA levels were significantly reduced in LD ($p < 0.05$) (Fig. 3D) which is comparable to the low *mPer2* mRNA expression observed in old *mPer1*$^{-/-}$*mCry2*$^{-/-}$ animals (Fig. 2A). Taken together it seems that *mPer2* mRNA levels as well as protein levels are normal in young *mPer1*$^{-/-}$ *mCry2*$^{-/-}$ animals, whereas in old *mPer1*$^{-/-}$*mCry2*$^{-/-}$ mice the amounts are strongly reduced. The same was observed for *Bmal1* mRNA but not for *mCry1* mRNA. However, mCRY1 protein levels are constitutively high in old *mPer1*$^{-/-}$*mCry2*$^{-/-}$ mice.

From the expression data in old *mPer1*$^{-/-}$, *mCry2*$^{-/-}$ and *mPer1*$^{-/-}$*mCry2*$^{-/-}$ mice described above it is reasonable to assume that the circadian phenotype observed in *mPer1*$^{-/-}$ *mCry2*$^{-/-}$ mice is a consequence of the simultaneous inactivation of the *mPer1* and *mCry2* genes in these animals. Therefore we focussed in the following studies on the comparison between wild-type and double mutant animals.

Loss of light inducibility of mPer2 mRNA and effect on delaying the clock phase in mPer1$^{-/-}$ *mCry2*$^{-/-}$ *mice*

As described above, the amplitude of cyclic *mPer2* mRNA expression declines with progressing age. In addition to CLOCK-BMAL1-driven circadian expression, phase-resetting light stimuli are known to induce *mPer* expression *via* a cAMP-responsive element in the promoter (Motzkus et al., 2000; Travnickova-Bendova et al., 2002). To investigate whether ageing affects light inducibility of the *mPer2* gene in the SCN of *mPer1*$^{-/-}$*mCry2*$^{-/-}$ mice, we applied a 15 minutes nocturnal light pulse at ZT14 to the animals. Wild-type mice displayed a significant increase of *mPer2* mRNA (Fig. 4A and B) as described previously (Albrecht et al., 1997). Interestingly, induction of *mPer2* mRNA was significantly impaired in young *mPer1*$^{-/-}$ *mCry2*$^{-/-}$ mice compared to wild-type animals ($p < 0.05$; Fig. 4A and B). This observation was even more pronounced in old *mPer1*$^{-/-}$*mCry2*$^{-/-}$ mice ($p<0.001$; Fig. 4A and B) indicating that the light signal transduction pathway might be defective. Therefore we set out to investigate light dependent phosphorylation of CREB at position 133 (CREB-Ser^{133}). We found that in

wild-type animals phosphorylation at CREB-Ser^{133} was induced by light (Fig. 4C and D) as described previously (von Gall et al., 1998). Young *mPer1*$^{-/-}$*mCry2*$^{-/-}$ animals tended to show slightly reduced (but statistically not significant) phosphorylation of CREB-Ser^{133} (Fig. 4C and D). In contrast, old *mPer1*$^{-/-}$*mCry2*$^{-/-}$ mice hardly displayed phosphorylation at CREB-Ser^{133} ($p<0.001$; Fig. 4C and D) suggesting a degeneration of the light input pathway to the clock. In a next step we wanted to investigate, whether the observed reduction of *mPer2* mRNA induction and CREB-Ser^{133} phosphorylation in *mPer1*$^{-/-}$*mCry2*$^{-/-}$ mice had behavioural consequences. We monitored wheel-running activity before and after a 15min light pulse at ZT14 and 22 as well as at CT14 and 22 and measured the phase shifts (Fig. 4E and F). In wild-type animals we observed a phase delay at ZT14 of 82 $\pm$ 10 min (mean $\pm$ S.D., n=14) and 87.3 $\pm$ 9.3 min (n=14) at CT 14 and a phase advance of 35 $\pm$ 6.7 min (n=14) at ZT22 and 39.3 $\pm$ 6.7 min (n=14) at CT22. In *mPer1*$^{-/-}$*mCry2*$^{-/-}$ animals only the phase shifts for young animals could be determined because old animals are arrhythmic in DD, which precludes determination of phase shifts. *mPer1*$^{-/-}$*mCry1*$^{-/-}$ mice delayed their phase at ZT14 similar to wild-type animals (86.5 +/- 12min; n=11; Fig 4E). Remarkably, in *mPer1*$^{-/-}$*mCry2*$^{-/-}$ mice phase delays at CT14 tended to be reduced (60 $\pm$ 13 min; with p=0.0539 (n=10) missing the criterion of $p < 0.05$ for significance; Fig. 4F). However, at ZT22 and CT22 phase advances in both *mPer1/mCry1* (1.3 $\pm$ 13 min; n=11) and *mPer1*/*mCry2* (7.3 $\pm$ 10.5 min; n=10) double mutant animals were abolished (Fig. 4E and F), which is comparable to the inability of *mPer1*$^{-/-}$ mice to advance clock phase after a 15min light pulse (Albrecht et al., 2001). These results suggest that the defect in advancing clock phase is due to a lack of *mPer1* in both *mPer1*$^{-/-}$*mCry1*$^{-/-}$ and *mPer1*$^{-/-}$*mCry2*$^{-/-}$ mice. The impairment of delaying clock phase in *mPer1*$^{-/-}$*mCry2*$^{-/-}$ mice at CT14 is probably due to a reduction of phosphorylation in CREB-Ser^{133} and reduced expression of *mPer2* mRNA. This is in line with previous findings that *mPer2* mutant mice are defective in delaying clock phase (Albrecht et al., 2001).

CREB phosphorylation at Ser 133 is decreased in the eye of mPer1$^{-/-}$*mCry2*$^{-/-}$ *mice*

The sloppy onset of wheel running activity in LD and the strong reduction in CREB phosphorylation at Ser 133 in the SCN of old *mPer1*$^{-/-}$*mCry2*$^{-/-}$ mice indicated that light signalling from the eye to the SCN might be defective. We therefore performed a detailed (immuno)histochemical analysis of the retinas from wild-type, *mPer1*$^{-/-}$, *mCry2*$^{-/-}$ and *mPer1*$^{-/-}$ *mCry2*$^{-/-}$ mice, respectively (Fig. 5). Using the Gomori staining procedure we could not detect overt morphological differences between wild-type, *mPer1*$^{-/-}$, *mCry2*$^{-/-}$, young and old *mPer1*$^{-}$

$^{-/-}$mCry2$^{-/-}$ retinas (Fig. 5A). To reveal cell death in the different layers of the retina, we performed lipofuscin staining. We did not observe any difference between wild-type, *mPer1$^{-/-}$*, *mCry2$^{-/-}$*, young and old *mPer1$^{-/-}$mCry2$^{-/-}$* mice (Fig. 5B), indicating that the retinas of all mice were intact. Additionally, we performed lipofuscin as well as Congo red histological staining in different regions of the brain with a focus on areas involved in the machinery of the circadian clock. We did not detect any amyloid plaques and *mPer1$^{-/-}$mCry2$^{-/-}$* mice did not show any differences to wild-type animals (data not shown). Thus, the observed effects of ageing are restricted to the functionality of the circadian system and do not originate from aberrant development or age-related morphological changes in the retina of *mPer1$^{-/-}$mCry2$^{-/-}$* animals.

Next we investigated phosphorylation of CREB at serine residue 133 in the retina by using an anti Ser^{133} P-CREB antibody (Fig. 5C). In wild-type animals, in the absence of light stimuli, Ser^{133} P-CREB was detected in the inner nuclear layer. A light pulse given at ZT14 has been shown to result in increased numbers of immunoreactive nuclei in the inner nuclear layer and ganglion cell layer (Gau et al., 2002). In *mPer1$^{-/-}$*, *mCry2$^{-/-}$* and young *mPer1$^{-/-}$ mCry2$^{-/-}$* mice a similar immunoreactivity was seen (Fig. 5C). Old *mPer1$^{-/-}$mCry2$^{-/-}$* animals however, displayed a reduced number of immunoreactive nuclei in the inner nuclear layer after a light pulse, whereas Ser^{133} P-CREB staining could hardly be observed in the ganglion cell layer (Fig. 5C). This indicates that phosphorylation of serine 133 in CREB is affected in the retina of old *mPer1$^{-/-}$mCry2$^{-/-}$* mice. Taken together, these results demonstrate that the profound loss of circadian wheel running behaviour of old *mPer1$^{-/-}$mCry2$^{-/-}$* mice under LD conditions (Fig. 1F) is due to impaired light signal transduction pathway performance.

Discussion

Interaction of clock components has predominantly been investigated in cultured cells, transiently (over)expressing clock components and E-box-containing reporter constructs (Gekakis et al., 1998; Kume et al., 1999; Yagita et al., 2002; Yagita et al., 2000). Such assays revealed that mPER and mCRY proteins can *in vitro* interact with themselves or each other, thereby forming stabilised complexes that influence nuclear transport of clock proteins or transcriptional regulation of clock genes. In contrast, it is not known to which extent complexes composed of various combinations of mPER and mCRY proteins contribute to circadian oscillator performance *in vivo*. We thus started to conduct genetic experiments by crossing mouse strains with inactivated *mPer* or *mCry* genes and subsequent analysis of circadian behaviour, clock gene and protein expression. We found that *mCry2* can act as a non-allelic suppressor of *mPer2* in the core clock mechanism and hence the presence of only *mPer1* and *mCry1* genes is sufficient to maintain circadian rhythmicity of the clock *in vivo* (Oster et al., 2002b). In this study we investigated the consequences of the absence of *mPer1* in combination with *mCry1* or *mCry2* on the circadian clock.

$mPer1^{-/-}mCry1^{-/-}$ mice display normal circadian rhythmicity but show impaired ability to phase advance the clock

Inactivation of *mPer1* and *mCry1* leads to a behavioural phenotype under LD and DD conditions similar to wild-type animals. *$mPer1^{-/-}mCry1^{-/-}$* mice display a period length comparable to wild-type littermates (Fig 1B, C). In comparison to *$mCry1^{-/-}$* mice however, it seems that the additional loss of *mPer1* in *$mCry1^{-/-}$* mice leads to an increase in period length to near normal values in DD (23.7 $\pm$ 0.2 h for *$mPer1^{-/-}mCry1^{-/-}$* mice *vs.* 22.51 + 0.06h for *$Cry1^{-/-}$* mice). This indicates that the loss of *mPer1* rescues the phenotype observed in *$mCry1^{-/-}$* mice and that the mPER2 and mCRY2 proteins seem to be sufficient to maintain a circadian rhythm with a period that is comparable to wild-type animals. This is also reflected at the molecular level, where *mPer2* and *Bmal1* mRNA rhythms are comparable to the expression patterns in wild-type animals under both LD and DD conditions (see supplemental figure 2). Hence it seems that *mPer1* is a non-allelic suppressor of *mCry1* (or *vice versa*). Interestingly, application of a 15 minute light pulse at ZT22 does not lead to a phase advance as observed in wild-type animals (Fig. 4E). This inability of *$mPer1^{-/-}mCry1^{-/-}$* mice to advance clock phase is

comparable to the defect observed in *mPer1*$^{-/-}$ animals (Albrecht et al., 2001). It seems that only circadian core clock functionality is rescued by an inactivation of *mCry1* in *mPer1*$^{-/-}$ mice but not the resetting properties of the clock. This is similar to the observations made in *mPer2*^{Brdm1}*mCry2*$^{-/-}$ mice, which appear to have a normal circadian rhythm but display a defect in delaying clock phase similar to *mPer2*^{Brdm1} mice (Oster et al., 2002b). Taken together it seems that deletion of *mCry1* in *mPer1*$^{-/-}$ mice and *mCry2* in *mPer2*^{Brdm1} mice rescues circadian phenotype without affecting the light driven resetting mechanism indicating that mPER1 interacts predominantly with mCRY1 and mPER2 with mCRY2 *in vivo.*

Breakdown of the clock in ageing mPer1$^{-/-}$*mCry2*$^{-/-}$*mice*

Circadian organisation changes with age (Valentinuzzi et al., 1997; Yamazaki et al., 2002). Typical changes include decrease in the amplitude of wheel-running activity, fragmentation of the activity rhythm, decreased precision in onset of daily activity and alterations in the response to the phase-shifting effects of light (Valentinuzzi et al., 1997). Within the SCN histological changes have been reported in aged rats and electrical activity rhythms in SCN slice cultures have lower amplitude and are less precise than in SCN cultures prepared from young animals (Aujard et al., 2001; Satinoff et al., 1993; Watanabe et al., 1995). At the molecular level age diminishes the amplitude of *Per2* but not *Per1* expression in mice (Weinert et al., 2001). However in rats similar expression patterns of molecular clock components in the SCN of young and old rats have been reported (Asai et al., 2001). The above mentioned studies have investigated the effects of ageing on the clock. Here we show evidence that a defective clock has an influence on ageing. Inactivation of *mPer1* and *mCry2* in mice leads in young *mPer1*$^{-/-}$*mCry2*$^{-/-}$ animals (2-6 months old) to a decreased precision in onset of daily activity compared to wild type mice (Fig. 1D, E). Onset of activity is markedly delayed with a sharp offset at the dark/light transition probably reflecting masking (Mrosovsky, 1999). In ageing *mPer1*$^{-/-}$*mCry2*$^{-/-}$ mice the decreased precision in onset of daily activity is even more pronounced (Fig. 1F). Additionally, a fragmentation of the activity rhythm is observed under LD conditions and a daily rhythm is barely detectable (Fig. 1G). In constant darkness old *mPer1*$^{-/-}$*mCry2*$^{-/-}$ mice do not display a circadian rhythm and the amplitude of wheel-running activity is decreased compared to wild type and young *mPer1*$^{-/-}$ *mCry2*$^{-/-}$ mice (Fig. 1F, I). All these phenotypes are not observed in *mPer1*$^{-/-}$ and *mCry2*$^{-/-}$ single mutant mice (van der Horst et al., 1999; Zheng et al., 2001) (supplemental Fig. 1). Interestingly, *mPer1*$^{-/-}$*mCry2*$^{-/-}$ mice display an altered response to the phase-shifting effects of

light (see below and Fig. 4). All the above described observations indicate that the clock seems to break down in ageing *mPer1*$^{-/-}$*mCry2*$^{-/-}$ mice and, as a consequence, can accelerate some aspects of ageing. The breakdown of the circadian rhythm does not occur in all *mPer1*$^{-/-}$ *mCry2*$^{-/-}$ mice at the same time indicating that additional genes or genetic background may contribute to the ageing process. However, the percentage of arrhythmic *mPer1*$^{-/-}$*mCry2*$^{-/-}$ animals increases with age (Fig. 1H) supporting the notion that the *mPer1* and *mCry2* genes in combination influence some aspects of the ageing process. Most probably transcriptional and posttranscriptional fidelity decreases with age and the absence of *mPer1* and *mCry2* renders the animal more prone to this infidelity. This view is supported by our observation that *mPer2* and *Bmal1* mRNA levels are strongly reduced in the SCN and in the kidney of old *mPer1*$^{-/-}$*mCry2*$^{-/-}$mice (Figs. 2 and 3D). Additionally, mCRY1 protein levels are elevated (Fig. 2C) pointing to an impaired degradation pathway of mCRY1. Interestingly, *mCry1* mRNA cycling is not affected in contrast to *mPer2* and *Bmal1* transcripts indicating that regulation of *mCry1* differs from *mPer2* and *Bmal1* transcriptional regulation.

The loss of circadian wheel running behaviour in old *mPer1*$^{-/-}$*mCry2*$^{-/-}$ mice is not a gradual process but occurs rapidly within a period of 3 days (see supplemental Fig. 4). This probably reflects the bimodality of transcriptional and posttranscriptional processes that are likely to act as "on/off" switches lacking intermediate states. Transcription is initiated by multimeric protein complexes (Beato, 1996; Freedman, 1999) and hence the components of transcriptional complexes have to be orchestrated in order to be present at a specific time and place in the cell. It seems that in young *mPer1*$^{-/-}$*mCry2*$^{-/-}$mice the critical amplitude in the level of PER2/CRY1 heterodimers to regulate the clock is just barely reached. With progressing age synthesis and processing of these proteins are reduced. The amplitude of PER2/CRY1 heterodimer oscillation falls below a critical threshold leading to a deregulation of the clock (Fig. 6 B), probably resulting in the uncoordinated cellular and physiological events we observe in old *mPer1*$^{-/-}$*mCry2*$^{-/-}$mice.

Light sensitivity is impaired in ageing mPer1$^{-/-}$*mCry2*$^{-/-}$*mice*

Old *mPer1*$^{-/-}$*mCry2*$^{-/-}$mice are very poorly synchronised to the light dark cycle (Fig. 1F). Therefore we hypothesised that these animals would be defective in light driven resetting of the circadian clock. A light pulse at ZT14 revealed a reduced inducibility of *mPer2* in young and even more pronounced in old *mPer1*$^{-/-}$*mCry2*$^{-/-}$mice (Fig. 4 A, B). Therefore we tested whether CREB, an essential factor for numerous transcriptional processes, was activated by

phosphorylation in response to a light pulse (Motzkus et al., 2000; Travnickova-Bendova et al., 2002). CREB phosphorylation was only slightly lowered in young *mPer1*$^{-/-}$*mCry2*$^{-/-}$mice but was significantly impaired in old animals (Fig. 4C, D) indicating a defect in light signalling in the SCN of these mice. At the behavioural level we could only measure the phase shifts of young *mPer1*$^{-/-}$*mCry2*$^{-/-}$mice, because old animals immediately became arrhythmic in DD (thus precluding the determination of phase shifts). The young *mPer1*$^{-/-}$ *mCry2*$^{-/-}$mice resemble *mPer1*$^{-/-}$ animals in that they were not able to advance clock phase (Fig. 4F) (Albrecht et al., 2001), suggesting that this anomaly is due to the lack of *mPer1*. Interestingly, phase delays in *mPer1*$^{-/-}$*mCry2*$^{-/-}$ mice were also affected although the criterion of significance was barely missed (p= 0.0539). The reduced inducibility of *mPer2* by light in young *mPer1*$^{-/-}$*mCry2*$^{-/-}$mice and the reduction in delaying clock phase in those animals is consistent with the previous finding that *mPer2* mutant mice are defective in delaying clock phase (Albrecht et al., 2001).

The impaired light response of *mPer1*$^{-/-}$*mCry2*$^{-/-}$mice might be a consequence of a defect in transmitting light information from the eye to the SCN. To test this possibility we looked for anatomical malformations in the retina. Neither young nor old *mPer1*$^{-/-}$*mCry2*$^{-/-}$mice displayed overt abnormalities (Fig. 5A) indicating that the animals were not visually blind. Cell death as a reason for malfunction of the retina could most possibly be excluded, since lipofuscin staining (Fig. 5B) and Congo red staining (data not shown) did not reveal dead cells in the retina. Comparable to the SCN however, light dependent phosphorylation of CREB at Ser 133 was affected in old *mPer1*$^{-/-}$*mCry2*$^{-/-}$mice (Fig. 5C). As a consequence light perceived by the eye is probably not processed properly to induce a cellular signalling cascade coding for the light signal. The reason for the impaired transmission of the light signal is most likely not a developmental defect, since young *mPer1*$^{-/-}$*mCry2*$^{-/-}$mice show phosphorylation of CREB at Ser 133. Therefore the defect is probably of transcriptional or posttranscriptional nature. For example CREB kinases might be regulated by some clock components. Candidates would be mouse homologues of the Drosophila kinase mothers against decapentaplegic (*Mad*). The mouse homologues, termed *Madh1* and *Madh2*, are expressed in a circadian manner in the SCN (Panda et al., 2002) suggesting that their transcription is influenced by the clock and hence would phosphorylate CREB in a clock dependent manner.

The transcriptional potential of mPER and mCRY protein complexes and their temporal abundance determines circadian rhythmicity

The precise regulation of the circadian oscillator requires an exact choreography of clock protein synthesis, interaction and posttranslational modification. The positive limb of circadian clock gene activation is influenced by the negative limb, probably through a complex consisting of mPER and mCRY proteins (Albrecht, 2002; Okamura et al., 2002). Such a mPER/mCRY complex would be composed of those PER and CRY proteins which are most abundant at a given time. Figure 6A depicts the temporal abundance of cycling *mPer1*, *mPer2*, *mCry1* and *mCry2* mRNA in the SCN illustrating that the amount of mRNA of these genes differs with time (Albrecht et al., 1997; Okamura et al., 1999; Reppert and Weaver, 2002; Yan and Okamura, 2002). Because the clock components of the negative limb (*Per* and *Cry*) are probably regulating their own transcription, the mRNA cycling is likely to reflect the activity of the corresponding proteins. The active forms of PER and CRY proteins seem to be cycling with a delay of 4-6 hours compared to mRNA (Field et al., 2000).

Interestingly, not all PER/CRY complexes seem to be equally important *in vivo* (Oster et al., 2002b) (this study). *mPer2*^{Brdm1}*mCry2*$^{-/-}$ mutant but not *mPer2*^{Brdm1}*mCry1*$^{-/-}$ mutant mice display circadian rhythmic behaviour, indicating that mPER1/mCRY1 but not mPER1/mCRY2 are sufficient to drive the circadian clock (Oster et al., 2002b). Our observations presented in this study indicate that mPER2/mCRY2 but - at least in older mice - not mPER2/mCRY1 can sustain circadian rhythms. Additionally, *mPer1*$^{-/-}$*mPer2*^{Brdm1} and *mCry1*$^{-/-}$*mCry2*$^{-/-}$ double mutant mice do not show circadian rhythmicity, indicating that mPER or mCRY homodimers are not sufficient to maintain circadian rhythmicity. Based on these observations we propose abundance and timing of PER/CRY complexes as illustrated in figure 6B. According to this model the complexes composed of mPER1/mCRY1 and mPER2/mCRY2 would be the most abundant ones with a difference in their maximal presence of about 2 hours. The abundance of these complexes is higher than a critical threshold level necessary to drive clock regulation (green horizontal line in Fig. 6 B). In contrast, mPER1/mCRY2 complexes formed in *Per2/Cry1* mutant mice do not reach this critical threshold. The reason for this might be that the timing of expression of these two proteins is not synchronised and/or the affinity between mPER1 and mCRY2 is low. As a consequence *Per2/Cry1* mutant mice lose clock function (Oster et al., 2002b). The complex formed between mPER2 and mCRY1 seems to just reach the critical threshold necessary for clock regulation as illustrated by the circadian wheel-running behaviour of young *mPer1*$^{-/-}$ *mCry2*$^{-/-}$ mice (Fig. 1D, E). However, with the progressing infidelity of transcription in ageing mice the presence of this complex falls below the critical threshold level and hence, older

mPer1$^{-/-}$*mCry2*$^{-/-}$ mice lose circadian wheel-running behaviour (Fig. 1F, I). *mPer2*^{Brdm1} mutant mice lose circadian rhythmicity after a few days in constant darkness. In these animals only functional mPER1/mCRY1 and mPER1/mCRY2 complexes can form, which should in principle be able to drive circadian rhythm. This seems to be the case for the first few days in constant darkness, but then competition between mCRY1 and mCRY2 for PER1 could lead to equal amounts of PER1/CRY1 and PER1/CRY2 complexes. The abundance of each of these complexes seems to fall below the threshold critical for normal clock function.

Taken together it seems that PER/CRY complexes have different potentials to regulate the circadian clock. In wild type animals theoretically all complexes can form but the formation of PER/CRY complexes is probably not random and depends on temporal abundance and strength of interaction between the complex forming partners (Fig. 6B). The sum of the regulatory potential of PER/CRY complexes over time displays a robust circadian cycling as illustrated in figure 6C. The robustness of this cycling is probably ensured by the different phasing of the oscillation of the two strong regulatory complexes PER1/CRY1 and PER2/CRY2. This notion is supported by theoretical considerations indicating that an overt oscillation is stabilised by two oscillators that are slightly out of phase (Glass and Mackey, 1988; Roenneberg and Merrow, 2001).

A model composed of two coupled molecular oscillators has been proposed by Daan and coworkers (2001). This model states that *mPer1* and *mCry1* are part of a morning (M) oscillator (comparable to the dark blue curve in Fig. 6B) whereas *mPer2* and *mCry2* are components of an evening (E) oscillator (light blue curve in Fig. 6B). Hence a deletion of the M oscillator (inactivation of *mPer1* and *mCry1*) leaves the E oscillator untouched. The E oscillator (*mPer2* and *mCry2*) would then drive the circadian clock alone, which would result in circadian rhythmicity. This is consistent with our observation that *mPer1*$^{-/-}$*mCry1*$^{-/-}$ mice display a circadian rhythm (Fig. 1C). Conversely, an inactivation of the E oscillator (*mPer2* and *mCry2*) would leave the M oscillator (*mPer1* and *mCry1*) alone to drive the circadian clock. In fact, inactivation of both *mPer2* and *mCry2* leads to normal circadian wheel running activity in mice (Oster et al., 2002b), and the rhythm seems to be stable. But what is the advantage of having two oscillators when a stable rhythm is observed with only the M or E oscillator alone? The answer lies in the adaptation of clock phase to changing environmental conditions (e.g. seasonal variation in day length) (Oster et al., 2002a; Steinlechner et al., 2002). Our results show that deletion of either the putative M or E oscillator results in normal circadian rhythmicity, but resetting in these mutant mice is not normal. Mice with inactivated mPER2 and mCRY2 proteins display a defect in delaying clock phase in response to a light

pulse (Oster et al., 2002b) whereas *mPer1*$^{-/-}$*mCry1*$^{-/-}$mice are not able to phase advance the clock (Fig. 4E). Since these resetting phenotypes are similar to the resetting phenotypes observed in *mPer2*^{Brdm1} and *mPer1*$^{-/-}$ single mutant mice respectively, we can conclude that both the M and E oscillators have to be intact in order to reset clock phase properly. Interestingly, hampering the M and E oscillators by inactivating *Per1* and *Cry2* or *Per2* and *Cry1* leads to loss of circadian rhythmicity. This takes several months in *mPer1*$^{-/-}$*mCry2*$^{-/-}$ mice (Fig. 1H) but is immediate in *mPer2*^{Brdm1}*mCry1*$^{-/-}$ animals (Oster et al., 2002b). The reason for this difference might be that *mPer2* and *mCry1* have a greater transcriptional potential than *mPer1* and *mCry2* (see above).

Taken together our *in vivo* studies support a model based on two coupled oscillators (Fig. 6). It is reasonable to conclude that not all interactions between PER and CRY proteins are equal *in vivo.* Although these proteins seem to be partially redundant, all of them are necessary for a functional circadian clock that can predict time and thereby being adaptable to changing environmental conditions. The importance of the PER1/CRY2 complex only becomes apparent in *mPer1*$^{-/-}$*mCry2*$^{-/-}$ mice half a year after birth illustrating a connection between the clock and aspects of ageing.

Materials and Methods

Generation of mPer and mCry mutant mice.

We crossed *mPer1*$^{-/-}$ mice (Zheng et al., 2001) with *mCry1*$^{-/-}$ and *mCry2*$^{-/-}$ animals (van der Horst et al., 1999). The genotype of the offspring was determined by southern blot analysis as described (Oster et al., 2002b). Hybridisation probes were for *mPer1* as described in (Zheng et al., 2001) and for *mCry1* and *mCry2* as described in (van der Horst et al., 1999). Matching wild-type control animals were produced by back-crossing heterozygous animals derived form the *mPer1*$^{-/-}$ and *mCry*$^{-/-}$ matings to minimise epigenetic effects. However, we can not completely rule out such effects and epistatic interactions between different gene clusters that could have clouded our observations.

Locomotor activity monitoring and circadian phenotype analysis.

Mice housing and handling were performed as described (Albrecht and Oster, 2001). For LD-DD transitions lights were turned off at the end of the light phase and not turned on again the next morning. Activity records are double plotted so that each light/dark cycle's activity is shown both to the right and below that of the previous light/dark cycle. Activity is plotted in threshold format for 5-minute bins. For activity counting and evaluation we used the ClockLab software package (Actimetrics). Rhythmicity and period length were assessed by χ^2 periodogram analysis and Fourier transformation using mice running in LD or in constant darkness for at least 10 days.

For light induced phase shifts we used the Aschoff Type I (for *mPer1*$^{-/-}$*mCry1*$^{-/-}$ animals) or the Type II protocol (for *mPer1*$^{-/-}$*mCry2*$^{-/-}$ animals) as described (Albrecht and Oster, 2001; Albrecht et al., 2001). We originally chose Type II protocol because of the convenient set-up for high numbers of animals and for comparison with *mPer2*^{Brdm1} mice (Albrecht et al., 2001; Oster et al., 2002b) which become arrhythmic in constant darkness precluding the determination of circadian times. However, the unstable onset of activity of *mPer1*$^{-/-}$*mCry2*$^{-/-}$ mice in LD and the long period length of these animals in DD resulted in very high variations when determining the phase shifts with Type II protocol. Therefore we repeated the experiments using a Type I set-up with animals free running in DD before light administration. For Type II protocol animals were entrained to an LD cycle for at least 7 days before light administration (15 min bright white light (400 Lux) at ZT14 or ZT22) and subsequently released into DD. The phase shift was determined by drawing a line through at least 7 consecutive days of onset of activity in LD before the light pulse and in DD after the

light pulse as determined by the ClockLab program. The difference between the two lines on the day of the light pulse determined the value of the phase shift. For Type I protocol animals were kept in DD for at least ten days before the light pulse (at CT14 or CT22 respectively). The phase shift was determined by drawing lines through at least 7 consecutive days before and after the light pulse using the ClockLab software. The first one or two days following the light administration were not used for the calculation since animals were thought to be in transition between both states.

In situ hybridisation

Mice were sacrificed by cervical dislocation under ambient light conditions at ZT6 and ZT12 and under a 15W safety red light at ZT18 and ZT0/24 as well as at CT0/24, 6, 12 and 18. For DD conditions animals were kept in the dark for 3 days before decapitation. For light induction experiments animals were exposed to a 15min light pulse (400 Lux) at ZT14 and killed at ZT15; controls were killed at ZT15 without prior light exposure. Specimen preparation, ^{35}S-rUTP labelled riboprobe synthesis and hybridisation steps were performed as described (Albrecht et al., 1998). The probe for *mPer2* was as described (Albrecht et al., 1997). The *mCry1* and the *Bmal1* probes were as described (Oster et al., 2002). Quantification was performed by densitometric analysis of autoradiograph films (Amersham Hyperfilm MP) as described (Oster et al., 2002b). For each time point three animals were used and three sections per SCN were analysed. "Relative mRNA abundance" values were calculated by defining the highest value of each experiment as 100%.

Immunohistochemistry

Animals were killed and tissue prepared as described for *in situ* hybridisation. Eye lenses were removed before cutting. Sections were boiled in 0.01M sodium citrate (pH 6) for 10 min to unmask hidden antigen epitopes and processed for immunohistochemical detection using the Vectastain Elite ABC system (Vector Laboratories) and diaminobenzidine with nickel amplification as chromogenic substrate. Immunostained sections were inspected with an Axioplan microscope (Zeiss) and the area of the SCN determined by comparison to Nissl stained parallel sections. Semiquantitative analysis for mCRY1, mPER2 and ^{Ser133}P-CREB immunoreactivity in the SCN was performed using NIH Image program. Images were digitised; background staining was used to define a lower threshold. Within the whole area of the SCN all cell nuclei exceeding the threshold value were marked. Three sections of the

intermediate aspect of the SCN were chosen at random for further analysis. Values presented are the mean of three different experiments +/- SD. Primary antibodies against mCRY1 (Alpha Diagnostics, order number CRY11-A), against CREB (Cell Signalling Technology, order number 9192), against CREB, phosphorylated at the residue Ser^{133} (New England Biolabs, order number 9191S), and against mPER2 (Santa Cruz Biotechnology, order number sc-7729) were used at dilutions of 1:200, 1:500, 1:1000, and 1:200, respectively.

Northern Blot Analysis

Rhythmic animals were sacrificed at the specified time points. Total RNA from kidney was extracted using RNAzol B (WAK Chemie). Northern analysis was performed using denaturing formaldehyde gels (Sambrook and Russel, 2001) with subsequent transfer to Hybond-N^+ membrane (Amersham). For each sample 20 µg of total RNA was used. cDNA probes were the same as described for *in situ* hybridisation. Labelling of probes was done using the Rediprime II labelling kit (Pharmacia) incorporating [P^{32}]dCTP to a specific activity of 10^8 cpm/µg. Blots were hybridised using UltraHyb solution (Ambion) containing 100 µg/ml salmon sperm DNA. The membrane was washed at 60°C in 0.1x SSPE and 0.1 % SDS. Subsequently, blots were exposed to phosphoimager plates (Bio-Rad) for 20 hours and signals quantified using Quantity One 3.0 software (Bio-Rad). For comparative purposes, the same blot was stripped and re-used for hybridisation. The relative level of RNA in each lane was determined by hybridisation with mouse *Gapdh* cDNA.

Histology

All histological staining was performed as described (Burkett et al., 1993). For Gomori's trichrome staining PFA fixed, paraffin embedded sections were de-waxed, post-fixed with Bouin's fluid at 56°C for 30 min, and nuclei stained with ferric haematoxyline (according to Weigert) for 10 min. After washing in water, slides were incubated for 15 min with trichrome stain (Chromotrope 2R (0.6% (w/v)) and Light Green (0.3% (w/v)) in 1% (v/v) acetic acid and 0.8% (w/v) phosphotungstic acid). After washing with 0.5% acetic acid and 1% (v/v) acetic acid/ 0.7% (w/v) phosphotungstic acid, slides were rinsed with water, dehydrated and mounted with Canada balsam/ methyl salycilate.

For lipofuscin staining slides were de-waxed and colorised with 0.75% (w/v) ferric chloride/ 0.1% (w/v) potassium ferricyanide (Aldrich) for 5 min. After washing with 1% (v/v) acetic acid and water, slides were incubated with 1% (w/v) Neutral Red for 3-4 min and

subsequently washed with water, de-hydrated and mounted with Dpx mounting media (Fluka). All reagents were from Sigma if not stated otherwise.

Statistical analysis

Statistical analysis of all experiments was performed using GraphPad Prism software (GraphPad). Significant differences between groups were determined with one-way ANOVA, followed by Bonferroni's *post*-test. Values were considered significantly different with $p<0.05$ (*), $p<0.01$ (**) or $p<0.001$ (***).

References

Albrecht, U. (2002). Invited Review: Regulation of mammalian circadian clock genes, J Appl Physiol *92*, 1348-55.

Albrecht, U., Lu, H.-C., Revelli, J.-P., Xu, X.-C.-., Lotan, R., and Eichele, G. (1998). Studying Gene Expression on Tissue Sections Using *In Situ* Hybridization. In Human Genome Methods, K. W. Adolph, ed. (New York, CRC Press), pp. 93-119.

Albrecht, U., and Oster, H. (2001). The circadian clock and behavior, Behav Brain Res *125*, 89-91.

Albrecht, U., Sun, Z. S., Eichele, G., and Lee, C. C. (1997). A differential response of two putative mammalian circadian regulators, mper1 and mper2, to light, Cell *91*, 1055-64.

Albrecht, U., Zheng, B., Larkin, D., Sun, Z. S., and Lee, C. C. (2001). mper1 and mper2 are essential for normal resetting of the circadian clock, J Biol Rhythms *16*, 100-4.

Allada, R., Emery, P., Takahashi, J. S., and Rosbash, M. (2001). Stopping time: the genetics of fly and mouse circadian clocks, Annu Rev Neurosci *24*, 1091-119.

Asai, M., Yoshinobu, Y., Kaneko, S., Mori, A., Nikaido, T., Moriya, T., Akiyama, M., and Shibata, S. (2001). Circadian profile of Per gene mRNA expression in the suprachiasmatic nucleus, paraventricular nucleus, and pineal body of aged rats, J Neurosci Res *66*, 1133-9.

Aujard, F., Dkhissi-Benyahya, O., Fournier, I., Claustrat, B., Schilling, A., Cooper, H. M., and Perret, M. (2001). Artificially accelerated aging by shortened photoperiod alters early gene expression (Fos) in the suprachiasmatic nucleus and sulfatoxymelatonin excretion in a small primate, Microcebus murinus, Neuroscience *105*, 403-12.

Bae, K., Jin, X., Maywood, E. S., Hastings, M. H., Reppert, S. M., and Weaver, D. R. (2001). Differential Functions of *mPer1*, *mPer2* and *mPer3* in the SCN Circadian CLock, Neuron *30*, 525-536.

Balsalobre, A., Damiola, F., and Schibler, U. (1998). A serum shock induces circadian gene expression in mammalian tissue culture cells, Cell *93*, 929-37.

Beato, M. (1996). Chromatin structure and the regulation of gene expression: remodeling at the MMTV promoter, J Mol Med *74*, 711-24.

Burkett, H. G., Young, B., and Heath, J. W. (1993). Wheather's Functional Histology, 3 edn (London, Churchill Livingstone).

Cermakian, N., Monaco, L., Pando, M. P., Dierich, A., and Sassone-Corsi, P. (2001). Altered behavioral rhythms and clock gene expression in mice with a targeted mutation in the Period1 gene, Embo J *20*, 3967-74.

Daan, S., Albrecht, U., van der Horst, G. T., Illnerova, H., Roenneberg, T., Wehr, T. A., and Schwartz, W. J. (2001). Assembling a clock for all seasons: are there M and E oscillators in the genes?, J Biol Rhythms *16*, 105-16.

Field, M. D., Maywood, E. S., O'Brien, J. A., Weaver, D. R., Reppert, S. M., and Hastings, M. H. (2000). Analysis of clock proteins in mouse SCN demonstrates phylogenetic divergence of the circadian clockwork and resetting mechanisms, Neuron *25*, 437-47.

Freedman, L. P. (1999). Increasing the complexity of coactivation in nuclear receptor signaling, Cell *97*, 5-8.

Gau, D., Lemberger, T., von Gall, C., Kretz, O., Le Minh, N., Gass, P., Schmid, W., Schibler, U., Korf, H. W., and Schutz, G. (2002). Phosphorylation of CREB Ser142 Regulates Light-Induced Phase Shifts of the Circadian Clock, Neuron *34*, 245-53.

Gekakis, N., Staknis, D., Nguyen, H. B., Davis, F. C., Wilsbacher, L. D., King, D. P., Takahashi, J. S., and Weitz, C. J. (1998). Role of the CLOCK protein in the mammalian circadian mechanism, Science *280*, 1564-9.

Glass, L., and Mackey, M. C. (1988). From Clocks to Chaos - The Rhythms of Life (Princeton, New Jersey, Princeton University Press).

Hamada, T., LeSauter, J., Venuti, J. M., and Silver, R. (2001). Expression of Period genes: rhythmic and nonrhythmic compartments of the suprachiasmatic nucleus pacemaker, J Neurosci *21*, 7742-50.

Honma, S., Ikeda, M., Abe, H., Tanahashi, Y., Namihira, M., Honma, K., and Nomura, M. (1998). Circadian oscillation of BMAL1, a partner of a mammalian clock gene Clock, in rat suprachiasmatic nucleus, Biochem Biophys Res Commun *250*, 83-7.

Jacob, N., Vuillez, P., Lakdhar-Ghazal, N., and Pevet, P. (1999). Does the intergeniculate leaflet play a role in the integration of the photoperiod by the suprachiasmatic nucleus?, Brain Res *828*, 83-90.

Jagota, A., de la Iglesia, H. O., and Schwartz, W. J. (2000). Morning and evening circadian oscillations in the suprachiasmatic nucleus in vitro, Nat Neurosci *3*, 372-6.

Kume, K., Zylka, M. J., Sriram, S., Shearman, L. P., Weaver, D. R., Jin, X., Maywood, E. S., Hastings, M. H., and Reppert, S. M. (1999). mCRY1 and mCRY2 are essential components of the negative limb of the circadian clock feedback loop, Cell *98*, 193-205.

Lee, C., Etchegaray, J. P., Cagampang, F. R., Loudon, A. S., and Reppert, S. M. (2001). Posttranslational mechanisms regulate the mammalian circadian clock, Cell *107*, 855-67.

Miyamoto, Y., and Sancar, A. (1998). Vitamin B2-based blue-light photoreceptors in the retinohypothalamic tract as the photoactive pigments for setting the circadian clock in mammals, Proc Natl Acad Sci U S A *95*, 6097-102.

Miyazaki, K., Mesaki, M., and Ishida, N. (2001). Nuclear entry mechanism of rat PER2 (rPER2): role of rPER2 in nuclear localization of CRY protein, Mol Cell Biol *21*, 6651-9.

Motzkus, D., Maronde, E., Grunenberg, U., Lee, C. C., Forssmann, W., and Albrecht, U. (2000). The human PER1 gene is transcriptionally regulated by multiple signaling pathways, FEBS Lett *486*, 315-319.

Mrosovsky, N. (1999). Masking: history, definitions, and measurement, Chronobiol Int *16*, 415-29.

Okamura, H., Miyake, S., Sumi, Y., Yamaguchi, S., Yasui, A., Muijtjens, M., Hoeijmakers, J. H., and van der Horst, G. T. (1999). Photic induction of mPer1 and mPer2 in cry-deficient mice lacking a biological clock, Science *286*, 2531-4.

Okamura, H., Yamaguchi, S., and Yagita, K. (2002). Molecular machinery of the circadian clock in mammals, Cell Tissue Res *309*, 47-56.

Oster, H., Maronde, E., and Albrecht, U. (2002a). The circadian clock as a molecular calendar, Chronobiol Int *19*, 507-16.

Oster, H., Yasui, A., van der Horst, G. T., and Albrecht, U. (2002b). Disruption of *mCry2* retores circadian in *mPer2* mutant mice, Genes Dev *16*, 2633-2638.

Panda, S., Antoch, M. P., Miller, B. H., Su, A. I., Schook, A. B., Straume, M., Schultz, P. G., Kay, S. A., Takahashi, J. S., and Hogenesch, J. B. (2002). Coordinated transcription of key pathways in the mouse by the circadian clock, Cell *109*, 307-20.

Pittendrigh, C. S. (1993). Temporal organization: reflections of a Darwinian clock-watcher, Annu Rev Physiol *55*, 16-54.

Preitner, N., Damiola, F., Lopez-Molina, L., Zakany, J., Duboule, D., Albrecht, U., and Schibler, U. (2002). The Orphan Nuclear Receptor REV-ERBalpha Controls Circadian Transcription within the Positive Limb of the Mammalian Circadian Oscillator, Cell *110*, 251-60.

Ralph, M. R., Foster, R. G., Davis, F. C. and Menaker M. (1990). Transplanted suprachiasmatic nucleus determines circadian period, Science *247*, 975-978.

Reppert, S., and Weaver, D. (2002). Coordination of circadian timing in mammals, Nature *418*, 935-941.

Roenneberg, T., and Merrow, M. (2001). Circadian systems: different levels of complexity, Philos Trans R Soc Lond B Biol Sci *356*, 1687-96.

Rusak, B., and Zucker, I. (1979). Neural regulation of circadian rhythms, Physiol Rev *59*, 449-526.

Sambrook, J., and Russel, D. W. (2001). Molecular Cloning, Vol 1, 3 edn (Cold Spring Harbour, USA, Cold Spring Harbour Laboratory Press).

Satinoff, E., Li, H., Tcheng, T. K., Liu, C., McArthur, A. J., Medanic, M., and Gillette, M. U. (1993). Do the suprachiasmatic nuclei oscillate in old rats as they do in young ones?, Am J Physiol *265*, R1216-22.

Shearman, L. P., Jin, X., Lee, C., Reppert, S. M., and Weaver, D. R. (2000). Targeted Disruption of the mPer3 Gene: Subtle Effects on Circadian Clock Function, Mol Cell Biol *20*, 6269-6275.

Shearman, L. P., Zylka, M. J., Weaver, D. R., Kolakowski, L. F., Jr., and Reppert, S. M. (1997). Two period homologs: circadian expression and photic regulation in the suprachiasmatic nuclei, Neuron *19*, 1261-9.

Steinlechner, S., Jacobmeier, B., Scherbarth, F., Dernbach, H., Kruse, F., and Albrech, U. (2002). Robust circadian rhythmicity of Per1 and Per2 mutant mice in constant light, and dynamics of Per1 and Per2 gene expression under long and short photoperiods, J Biol Rhythms *17*, 202-9.

Sun, Z. S., Albrecht, U., Zhuchenko, O., Bailey, J., Eichele, G., and Lee, C. C. (1997). RIGUI, a putative mammalian ortholog of the Drosophila period gene, Cell *90*, 1003-11.

Tei, H., Okamura, H., Shigeyoshi, Y., Fukuhara, C., Ozawa, R., Hirose, M., and Sakaki, Y. (1997). Circadian oscillation of a mammalian homologue of the Drosophila period gene, Nature *389*, 512-6.

Travnickova-Bendova, Z., Cermakian, N., Reppert, S. M., and Sassone-Corsi, P. (2002). Bimodal regulation of mPeriod promoters by CREB-dependent signaling and CLOCK/BMAL1 activity, Proc Natl Acad Sci U S A *14*, 14.

Valentinuzzi, V. S., Scarbrough, K., Takahashi, J. S., and Turek, F. W. (1997). Effects of aging on the circadian rhythm of wheel-running activity in C57BL/6 mice, Am J Physiol *273*, R1957-64.

van der Horst, G. T., Muijtjens, M., Kobayashi, K., Takano, R., Kanno, S., Takao, M., de Wit, J., Verkerk, A., Eker, A. P., van Leenen, D., *et al.* (1999). Mammalian Cry1 and Cry2 are essential for maintenance of circadian rhythms, Nature *398*, 627-30.

Vielhaber, E. L., Duricka, D., Ullman, K. S., and Virshup, D. M. (2001). Nuclear export of mammalian PERIOD proteins, J Biol Chem *8*, 8.

Vitaterna, M. H., Selby, C. P., Todo, T., Niwa, H., Thompson, C., Fruechte, E. M., Hitomi, K., Thresher, R. J., Ishikawa, T., Miyazaki, J., *et al.* (1999). Differential regulation of mammalian period genes and circadian rhythmicity by cryptochromes 1 and 2, Proc Natl Acad Sci U S A *96*, 12114-9.

von Gall, C., Duffield, G. E., Hastings, M. H., Kopp, M. D., Dehghani, F., Korf, H. W., and Stehle, J. H. (1998). CREB in the mouse SCN: a molecular interface coding the phase-adjusting stimuli light, glutamate, PACAP, and melatonin for clockwork access, J Neurosci *18*, 10389-97.

Watanabe, A., Shibata, S., and Watanabe, S. (1995). Circadian rhythm of spontaneous neuronal activity in the suprachiasmatic nucleus of old hamster in vitro, Brain Res *695*, 237-9.

Weinert, H., Weinert, D., Schurov, I., Maywood, E. S., and Hastings, M. H. (2001). Impaired expression of the mPer2 circadian clock gene in the suprachiasmatic nuclei of aging mice, Chronobiol Int *18*, 559-65.

Yagita, K., Tamanini, F., Yasuda, M., Hoeijmakers, J. H., van der Horst, G. T., and Okamura, H. (2002). Nucleocytoplasmic shuttling and mCRY-dependent inhibition of ubiquitylation of the mPER2 clock protein, Embo J *21*, 1301-14.

Yagita, K., Yamaguchi, S., Tamanini, F., van Der Horst, G. T., Hoeijmakers, J. H., Yasui, A., Loros, J. J., Dunlap, J. C., and Okamura, H. (2000). Dimerization and nuclear entry of mPER proteins in mammalian cells, Genes Dev *14*, 1353-63.

Yamazaki, S., Numano, R., Abe, M., Hida, A., Takahashi, R., Ueda, M., Block, G. D., Sakaki, Y., Menaker, M., and Tei, H. (2000). Resetting central and peripheral circadian oscillators in transgenic rats, Science *288*, 682-5.

Yamazaki, S., Straume, M., Tei, H., Sakaki, Y., Menaker, M., and Block, G. D. (2002). Effects of aging on central and peripheral mammalian clocks, Proc Natl Acad Sci U S A *99*, 10801-6.

Yan, L., and Okamura, H. (2002). Gradients in the circadian expression of Per1 and Per2 genes in the rat suprachiasmatic nucleus, Eur J Neurosci *15*, 1153-62.

Yu, W., Nomura, M., and Ikeda, M. (2002). Interactivating feedback loops within the mammalian clock: BMAL1 is negatively autoregulated and upregulated by CRY1, CRY2, and PER2, Biochem Biophys Res Commun *290*, 933-41.

Zheng, B., Albrecht, U., Kaasik, K., Sage, M., Lu, W., Vaishnav, S., Li, Q., Sun, Z. S., Eichele, G., Bradley, A., and Lee, C. C. (2001). Nonredundant roles of the mPer1 and mPer2 genes in the mammalian circadian clock, Cell *105*, 683-94.

Zheng, B., Larkin, D. W., Albrecht, U., Sun, Z. S., Sage, M., Eichele, G., Lee, C. C., and Bradley, A. (1999). The mPer2 gene encodes a functional component of the mammalian circadian clock, Nature *400*, 169-73.

Zylka, M. J., Shearman, L. P., Weaver, D. R., and Reppert, S. M. (1998). Three period homologs in mammals: differential light responses in the suprachiasmatic circadian clock and oscillating transcripts outside of brain, Neuron *20*, 1103-10.

Figures

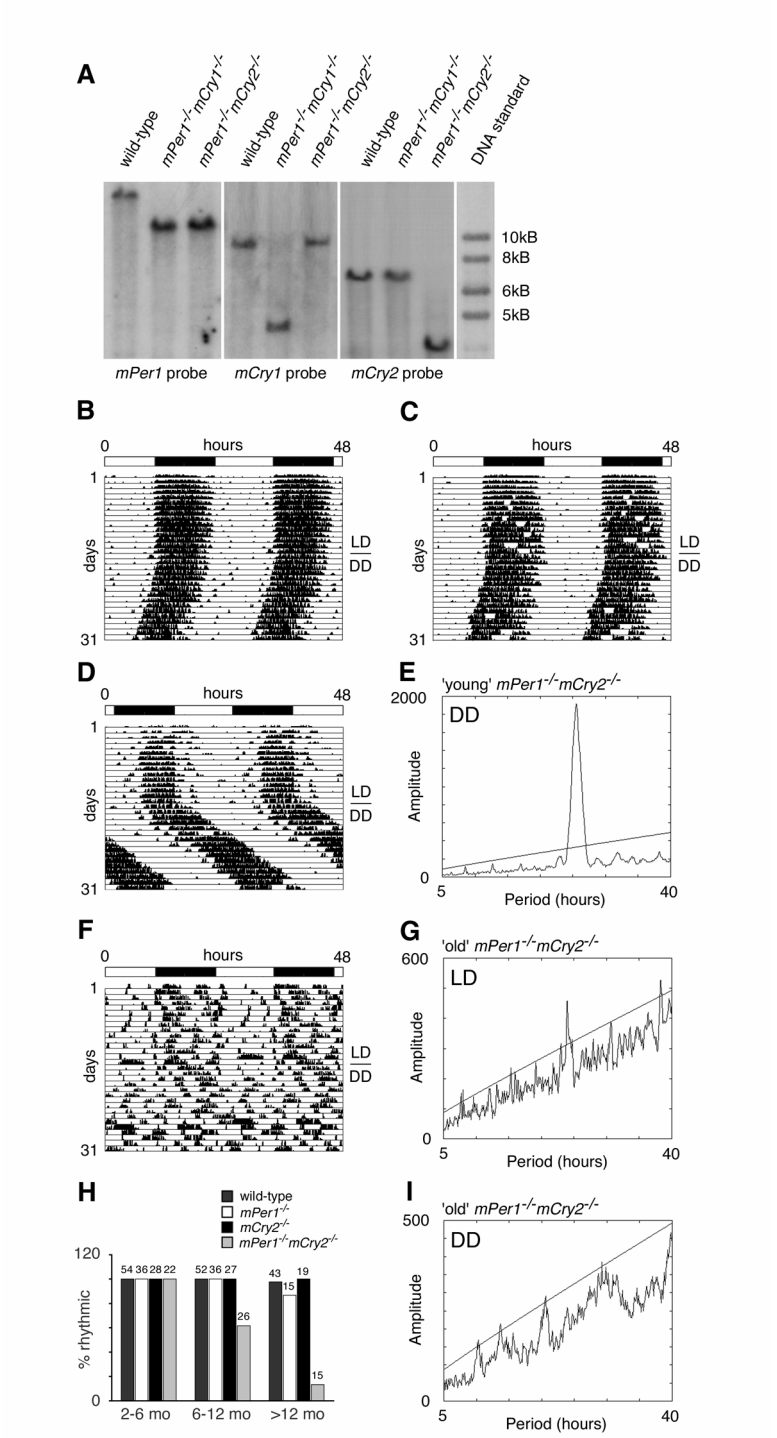

Figure 1 Generation of *mPer1mCry* double mutant mice and representative locomotor activity records. (A) Southern blot analysis of wild-type, *mPer1*$^{-/-}$*mCry1*$^{-/-}$,and *mPer1*$^{-/-}$*mCry2*$^{-/-}$ tail DNA. The *mPer1* probe hybridises to a 20kb wild-type and a 11.8kb mutant fragment of *EcoR* I digested genomic DNA. The *mCry1* probe detects a 9kb wild-type and a 4kb *Nco* I digested fragment of the targeted locus. In *mCry2* mutants the wild-type allele is detected by hybridisation of the probe to a 7kb *EcoR* I fragment whereas the mutant allele yields a 3.5kb fragment. (B-D, F) Representative locomotor activity records of wild-type (B), *mPer1*$^{-/-}$*mCry1*$^{-/-}$ (C), young *mPer1*$^{-/-}$*mCry2*$^{-/-}$ (D), and old *mPer1*$^{-/-}$*mCry2*$^{-/-}$ (F) animals kept in a 12h light 12h dark (LD) cycle and in constant darkness (DD; transition indicated by the horizontal line). Activity is represented by black bars and is double-plotted with the activity of the following light/dark cycle plotted to the right and below the previous light/dark cycle. The top bar indicates light and dark phases in LD. For the first five days in DD, wheel rotations per day were 20,000 ± 2,500 (n=17) for wild type animals, 21,500 ± 7,300 (n=15) for *mPer1*$^{-/-}$*mCry1*$^{-/-}$ mutants, 25,100 ± 6,200 (n=14) for young *mPer1*$^{-/-}$*mCry2*$^{-/-}$ mutants, and 17,200 ± 7,900 (n=9) for old *mPer1*$^{-/-}$*mCry2*$^{-/-}$ mutants. (E, G, I) Periodogram analysis of young *mPer1*$^{-/-}$*mCry2*$^{-/-}$ animals in DD (E corresponds to activity plot in D), and old *mPer1*$^{-/-}$*mCry2*$^{-/-}$ animals in LD (G corresponds to activity plot in F) and DD (I corresponds to activity plot in F). Analysis was performed on 10 consecutive days in LD or DD after animals were allowed to adapt 5 days to the new light regimen. The ascending straight line in the periodograms represents a statistical significance of $p < 0.001$ as determined by the ClockLab program. (H) Age dependence of rhythmicity in wild-typed (dark grey bar), *mPer1*$^{-/-}$ (white bar), *mCry2*$^{-/-}$ (black bar), and *mPer1*$^{-/-}$*mCry2*$^{-/-}$ (light grey bar) mice. Animals tested were divided into three groups according to their age (2-6 months, 6-12months and more than 12 months old). Rhythmicity in DD was determined by periodogram analysis. Values on top of each bar indicate total numbers of animals tested per group and genotype.

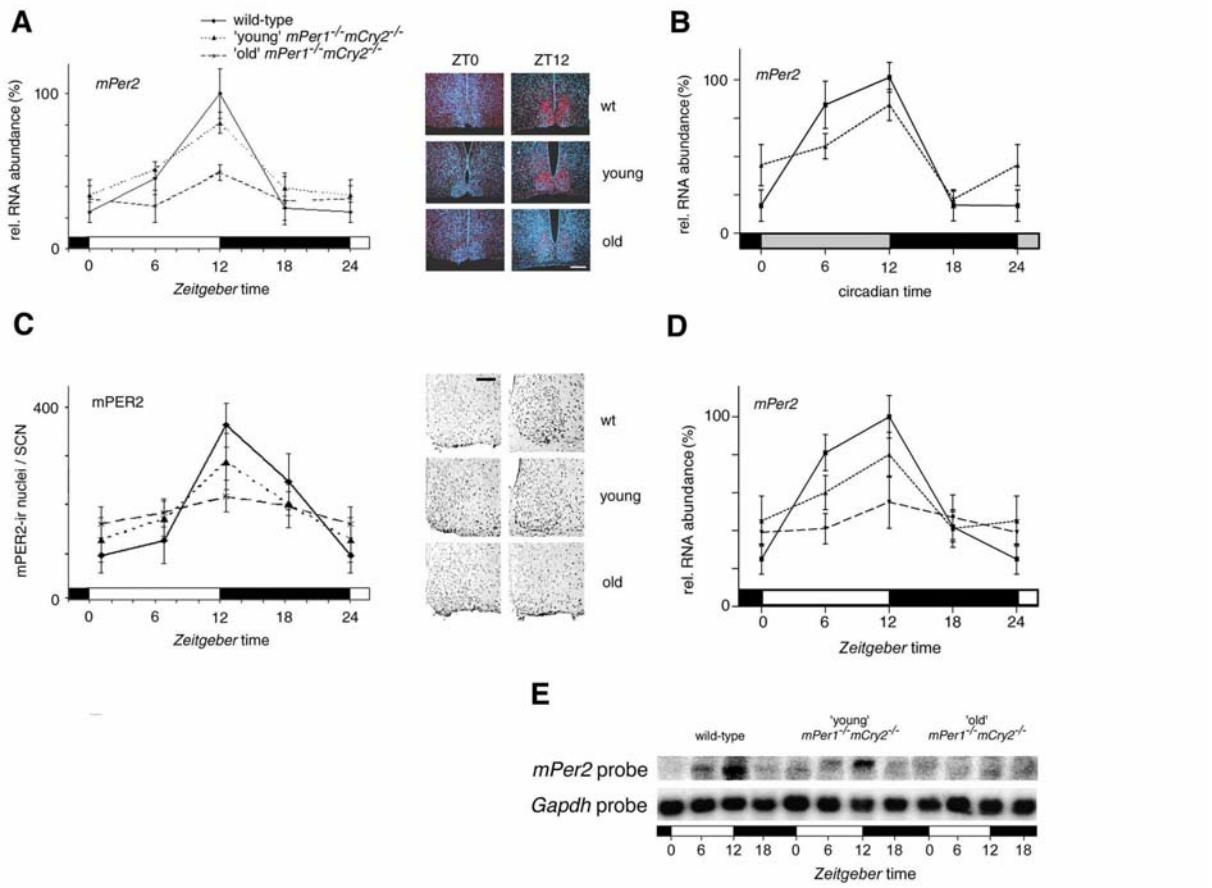

Figure 2 ***mPer2*****/ mPER2 expression profiles of young and old** ***mPer1*** $^{-/-}$ ***mCry2*** $^{-/-}$ **mice. (A) Diurnal expression of** ***mPer2*** **in the SCN of wild-type (solid line), young** ***mPer1*** $^{-/-}$ ***mCry2*** $^{-/-}$ **(pointed line), and old** ***mPer1*** $^{-/-}$ ***mCry2*** $^{-/-}$ **(dashed line) mice in LD. In old double mutants** ***mPer2*** **cycling is significantly dampened ($p < 0.05$). Black and white bars on x-axis indicate dark and light phase respectively. All data presented are mean +/- S.D. for three different experiments. Right panels show representative micrographs of SCN probed with** ***mPer2*** **antisense probe at time points of minimal (ZT0) and maximal (ZT12) expression. Tissue was visualised by Hoechst dye nuclear staining (blue); silver grains are artificially coloured (red) for clarification. White bar indicates 200 µm.**
(B) Circadian expression of ***mPer2*** **in the SCN of wild-type (solid line) and young** ***mPer1*** $^{-/-}$ ***mCry2*** $^{-/-}$ **(pointed line) mice on the fourth day in DD. Grey and black bars on x-axis indicate subjective day and night respectively. (C) Diurnal variation of mPER2 immunoreactivity in the SCN of wild-type (solid line), young** ***mPer1*** $^{-/-}$ ***mCry2*** $^{-/-}$ **(pointed line), and old** ***mPer1*** $^{-/-}$ ***mCry2*** $^{-/-}$ **(dashed line) mice in LD. Quantification was performed by counting immunoreactive nuclei in the area of the SCN. In old double mutants oscillation of mPER2 immunoreactivity is significantly dampened ($p < 0.05$) with medium numbers of immunoreactive nuclei. Right panels show representative micrographs of immunostained SCN at time points of minimal (ZT0) and maximal (ZT12) immunoreactivity. Black bar indicates 100 µm. (D) Northern analysis of diurnal expression of** ***mPer2*** **in the kidney of wild-type (solid line), young** ***mPer1*** $^{-/-}$ ***mCry2*** $^{-/-}$ **(pointed line), and old** ***mPer1*** $^{-/-}$ ***mCry2*** $^{-/-}$ **(dashed line) mice in LD. (E) Representative Northern blot from kidney tissue from wild-type (left), young** ***mPer1*** $^{-/-}$ ***mCry2*** $^{-/-}$ **(middle) and old** ***mPer1*** $^{-/-}$ ***mCry2*** $^{-/-}$ **(right) mice sequentially hybridised with** ***mPer2*** **(top row) and** ***Gapdh*** **(bottom row) antisense probe. Black and white bars bellow blots indicate dark and light phase respectively.**

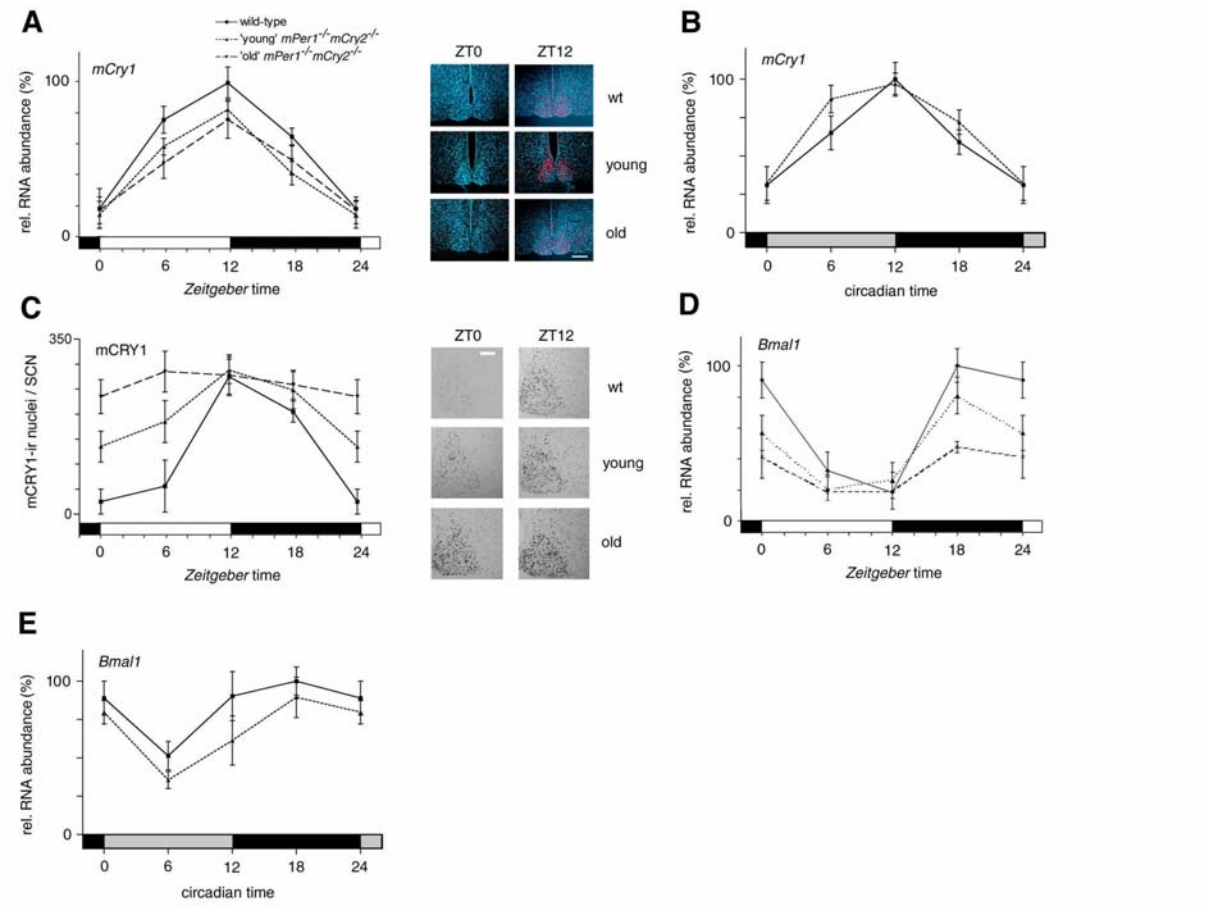

Figure 3 *mCry1*/ mCRY1 and *Bmal1* expression profiles of young and old *mPer1*$^{-/-}$*mCry2*$^{-/-}$ mice. (A) Diurnal expression of *mCry1* in the SCN of wild-type (solid line), young *mPer1*$^{-/-}$*mCry2*$^{-/-}$ (pointed line), and old *mPer1*$^{-/-}$*mCry2*$^{-/-}$ (dashed line) mice in LD. Black and white bars on x-axis indicate dark and light phase respectively. All data presented are mean +/- S.D. for three different experiments. Right panels show representative micrographs of SCN probed with *mCry1* antisense probe at time points of minimal (ZT0) and maximal (ZT12) expression. Tissue was visualised by Hoechst dye nuclear staining (blue); silver grains are artificially coloured (red) for clarification. White bar indicates 200µm. (B) Circadian expression of *mCry1* in the SCN of wild-type (solid line) and young *mPer1*$^{-/-}$*mCry2*$^{-/-}$ (pointed line) mice on the fourth day in DD. Grey and black bars on x-axis indicate subjective day and night respectively. (C) Diurnal variation of mCRY1 immunoreactivity in the SCN of wild-type (solid line), young *mPer1*$^{-/-}$*mCry2*$^{-/-}$ (pointed line), and old *mPer1*$^{-/-}$*mCry2*$^{-/-}$ (dashed line) mice in LD. Quantification was performed by counting immunoreactive nuclei in the area of the SCN. In old double mutants oscillation of mCRY1 immunoreactivity is significantly dampened ($p < 0.05$) with constantly high numbers of immunoreactive nuclei throughout the LD cycle. Right panels show representative micrographs of immunostained SCN at time points of minimal (ZT0) and maximal (ZT12) immunoreactivity. White bar indicates 100µm. (D) Diurnal expression of *Bmal1* mRNA expression in the SCN of wild-type (solid line), young *mPer1*$^{-/-}$*mCry2*$^{-/-}$ (pointed line), and old *mPer1*$^{-/-}$*mCry2*$^{-/-}$ (dashed line) mice in LD. In old double mutants *Bmal1* cycling is significantly dampened ($p < 0.05$). (E) Circadian expression of *Bmal1* mRNA in the SCN of wild-type (solid line) and young *mPer1*$^{-/-}$*mCry2*$^{-/-}$ (pointed line) mice on the fourth day in DD.

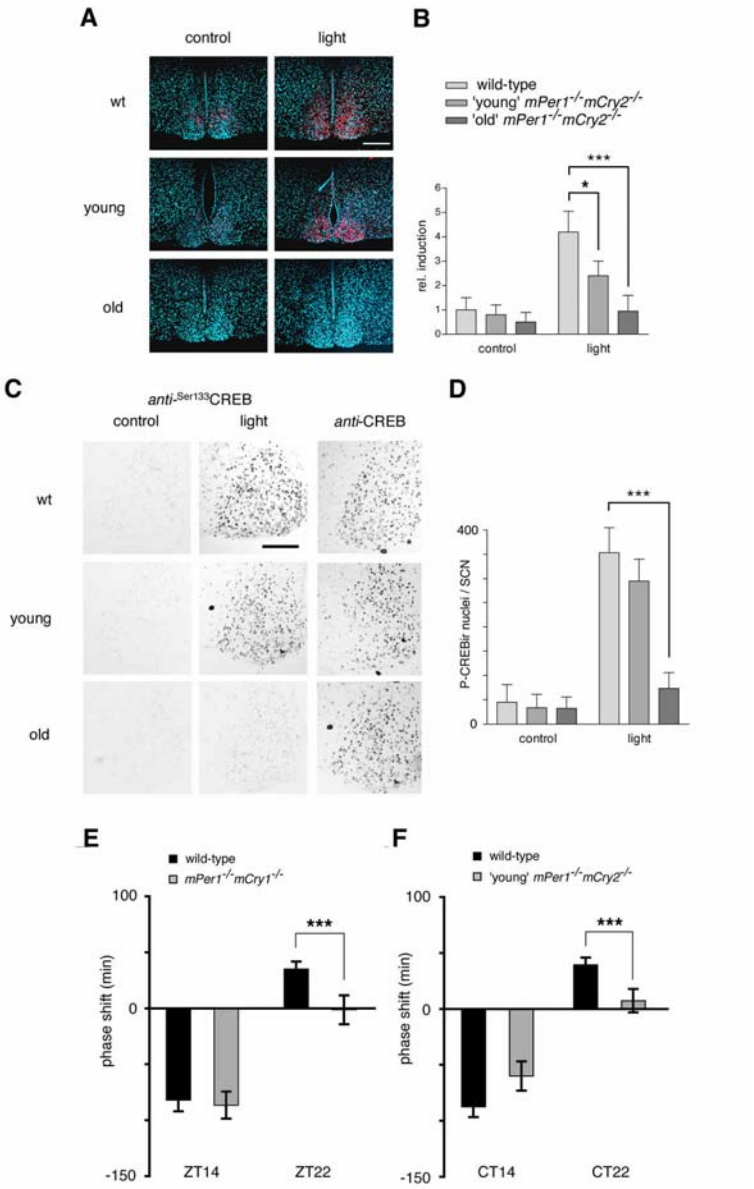

Figure 4 Light responsiveness in the SCN of young and old *mPer1*$^{-/-}$*mCry2*$^{-/-}$ mice. (A) *In situ* hybridisation analysis of *mPer2* light inducibility in the SCN of wild-type (wt, upper row), young *mPer1*$^{-/-}$*mCry2*$^{-/-}$ (middle row), and old *mPer1*$^{-/-}$*mCry2*$^{-/-}$ mice (lower row). Shown are representative micrographs of SCN probed with *mPer2* antisense probe with (light) or without light administration (control) at ZT14 (15min light pulse, 400Lux; animals were sacrificed one hour later). Tissue was visualised by Hoechst dye nuclear staining (blue); silver grains are artificially coloured (red) for clarification. White bar indicates 200µm. (B) Quantification of *mPer2* induction after a light pulse at Z14. Left panel shows control animals without light exposure. Right panel shows relative *mPer2* mRNA induction after light exposure (wild-type control was set as 1). Data presented are mean +/- S.D. of three different animals each. Statistical significance is indicated by asterisks (*, $p < 0.05$; ***, $p < 0.001$). (C) Immunohistochemistry analysis of CREB Ser-133 phosphorylation by light in the SCN of wild-type (wt, upper row), young *mPer1*$^{-/-}$*mCry2*$^{-/-}$ (middle row), and old *mPer1*$^{-/-}$*mCry2*$^{-/-}$ mice (lower row). Shown are representative micrographs of SCN sections immunostained for ^{Ser133}P-CREB with (light) or without light administration (control) at ZT14. As a control SCN sections for all genotypes were stained for CREB (unphosphorylated) at the same time points. (D) Quantification of CREB phosphorylation after a light pulse at ZT14. Panels show numbers of ^{Ser133}P-CREB immunoreactive nuclei in the SCN with or without light exposure (*, $p < 0.001$). (E) Light induced phase shifts in *mPer1*$^{-/-}$*mCry1*$^{-/-}$ mice using Aschoff Type II protocol to assess phase shifts. Animals were kept for at least 10 days in LD and released into DD after a light pulse at ZT14 or ZT22. Negative values indicate phase delays, positive values indicate phase advances. Data presented are mean +/- S.D. of 10 to 14 animals (***, $p < 0.001$). (F) Light induced phase shifts in young *mPer1*$^{-/-}$*mCry2*$^{-/-}$ mice using Aschoff Type I protocol to assess phase shifts. Animals were kept for at least 10 days in DD before a light pulse at CT14 or CT22. Data presented are mean +/- S.D. of 10 to 13 animals.**

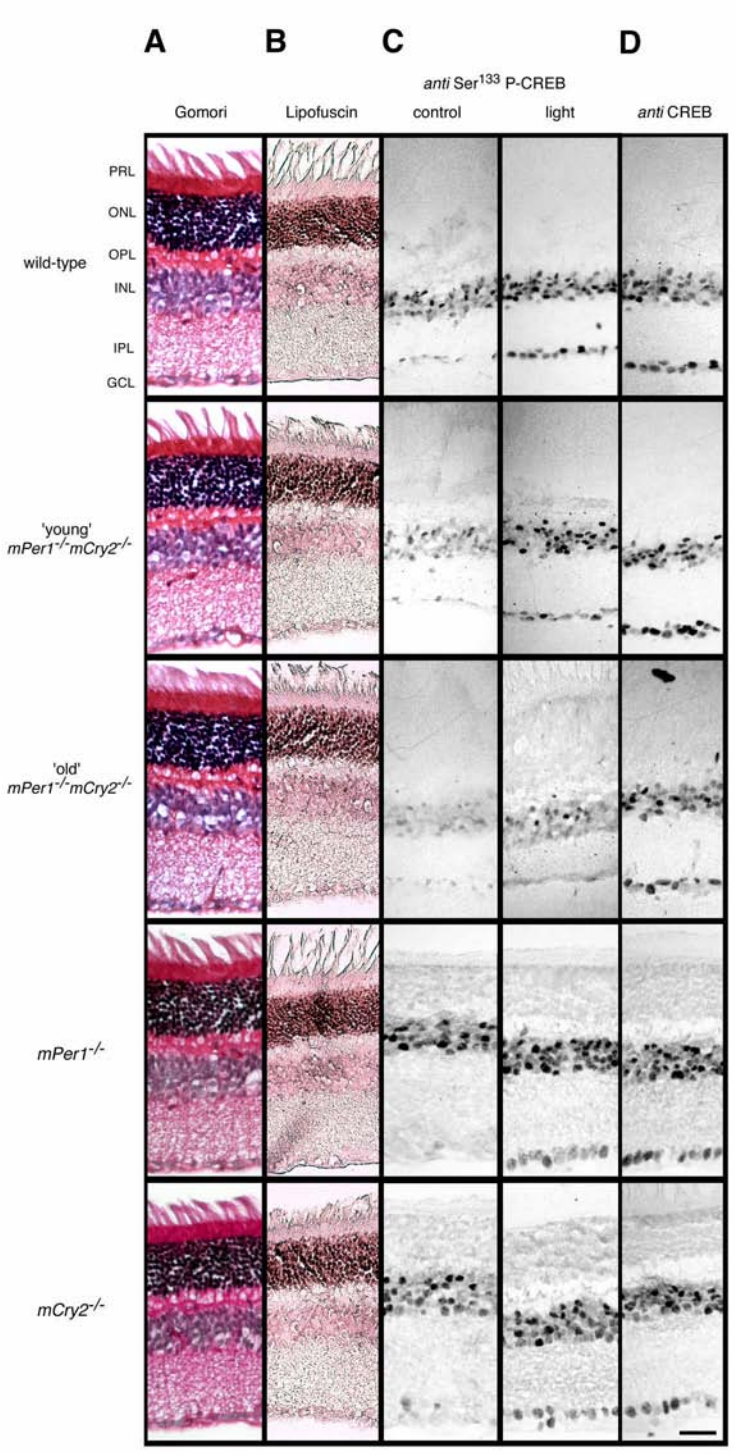

Figure 5 Histology and light responsiveness in the retina of wild type, young and old mPer1$^{-/-}$mCry2$^{-/-}$ mice. (A) Gomori trichrome and (B) lipofuscin staining of retinal sections of wild-type (upper row), young mPer1$^{-/-}$mCry2$^{-/-}$ (middle row), and old mPer1$^{-/-}$mCry2$^{-/-}$ mice (lower row). Retinal layers are indicated on the left (PRL, photoreceptor layer; ONL, outer nuclear layer; OPL, outer plexiform layer; INL, inner nuclear layer; IPL, inner plexiform layer; GCL, ganglion cell layer). (C) Immunohistochemistry analysis of light induced CREB Ser-133 phosphorylation in the retina. Left panels show immunostained retinal sections of control animals without light exposure right panels of animals 1hr after light exposure (400Lux, 15min) at ZT14. (D) Immunohistochemistry analysis for (unphosphorylated) CREB in the retina at ZT14. Black bar indicates 10 µm.

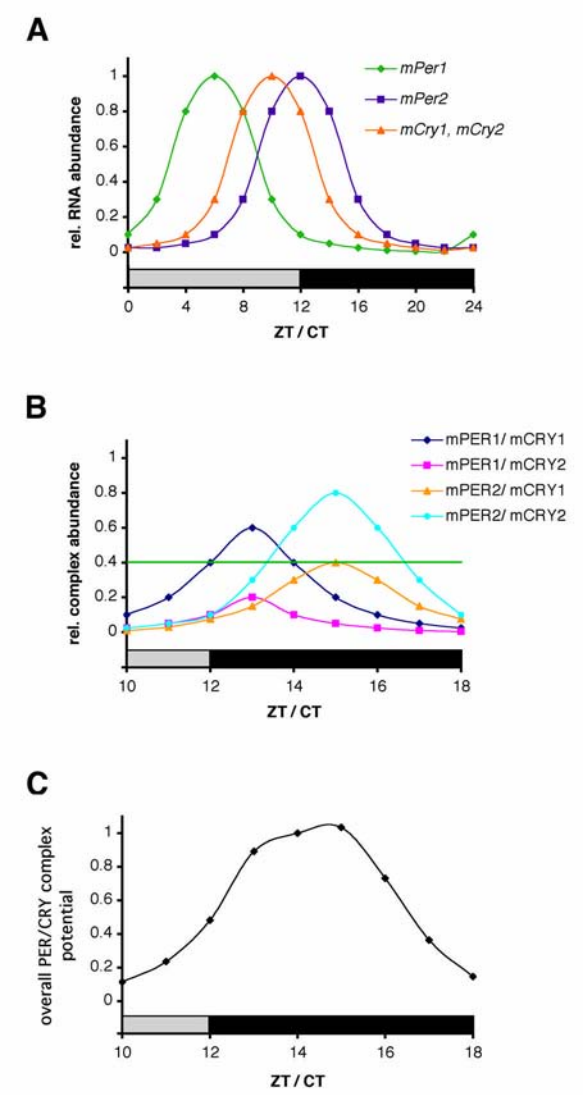

Figure 6 ***Working model for PER/CRY driven inhibition of CLOCK/BMAL1*****. (A)** ***mPer*** **and** ***mCry*** **transcripts show diurnal / circadian cycling in the SCN. While** ***mPer1*** **expression peaks between ZT/ CT 4 to 8,** ***mCry1*** **and** ***mPer2*** **mRNA rhythms have their maxima at ZT/ CT10 to ZT/ CT12, respectively (Fig. 2 & 3; see as well Oster et al. 2002; Yan et al. 2002; Kume et al. 1999). Note that** ***mCry2*** **is also expressed in the SCN but without a clearly defined rhythm (Kume et al. 1999). Protein peaks are delayed by about 4-6 hours with regard to mRNA (Field et al., 2000; King and Takahashi 2000; Reppert and Weaver 2002). (B) mPER and mCRY proteins form heterodimeric complexes that form with certain preferences according to protein-protein affinity and temporal abundance. The complexes are colour coded with mPER1/mCRY1 and mPER2/mCRY2 representing the most abundant ones. The green horizontal line indicates a threshold above which a PER/CRY complex is abundant enough to influence CLOCK/BMAL1 transcription. (C) Time course of the overall inhibitory potential of the mPER/ mCRY heterodimers on CLOCK/ BMAL1 activity. The strong inhibition of CLOCK/ BMAL1 during (subjective) night corresponds to the low transcriptional activity of (CLOCK/ BMAL1 induced)** ***mPer*** **and** ***mCry*** **genes.**

2.3. Additional Data

2.3.1. Breeding Statistics

To check if the deletion of certain combinations of *mPer* and/ or *mCry* genes has an impact on the viability and fertility of the animals we analyzed the data obtained from our breeding colonies. In the heterozygous F1 generation we checked if the different genotypes of the F2 offspring occurred in the expected distribution according to the Mendelian laws of inheritance.

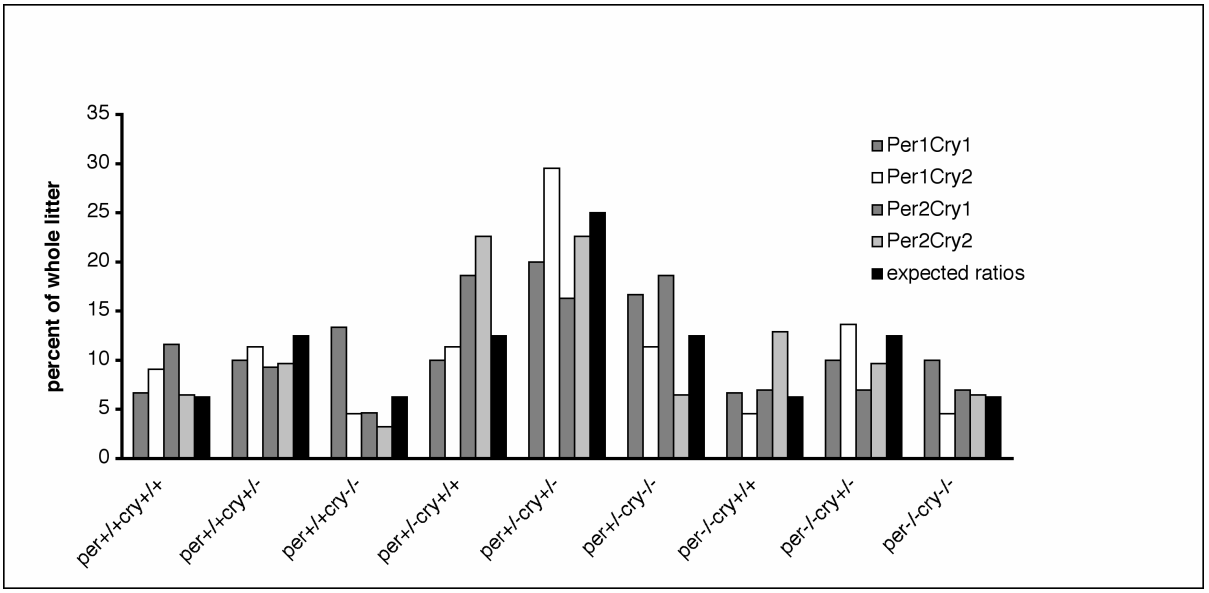

Fig. 22: Genotypic distribution in the F2 generation of the different *mPer/ mCry* double mutant strains. Shown are the experimental values together with the ideal (expected) numbers (black bars) of different genotypes obtained from double heterozygous parents.

With minor variations all F2 genotypic ratios appeared as expected. Differences between ideal and experimental values are results of the relatively small number of F1 breedings because the colony was set up for breeding efficiency and as soon as homozygous F2 breeding pairs were available these were used to replace the F1 generation.

Once these F2 breeding pairs were established, parents were kept together as long as possible to prevent unnecessary genetic drift due to relatively small founder populations. We checked homozygous breedings for litter size and frequency.

There was no significant difference in the litter size for all strains of double and triple mutant mice with the exception of the *mPer1/2/ mCry1* and the *mPer1/ mCry1/2* mutants which never bread. *mPer1/2/ mCry2* mutants never had more than one litter per mating.

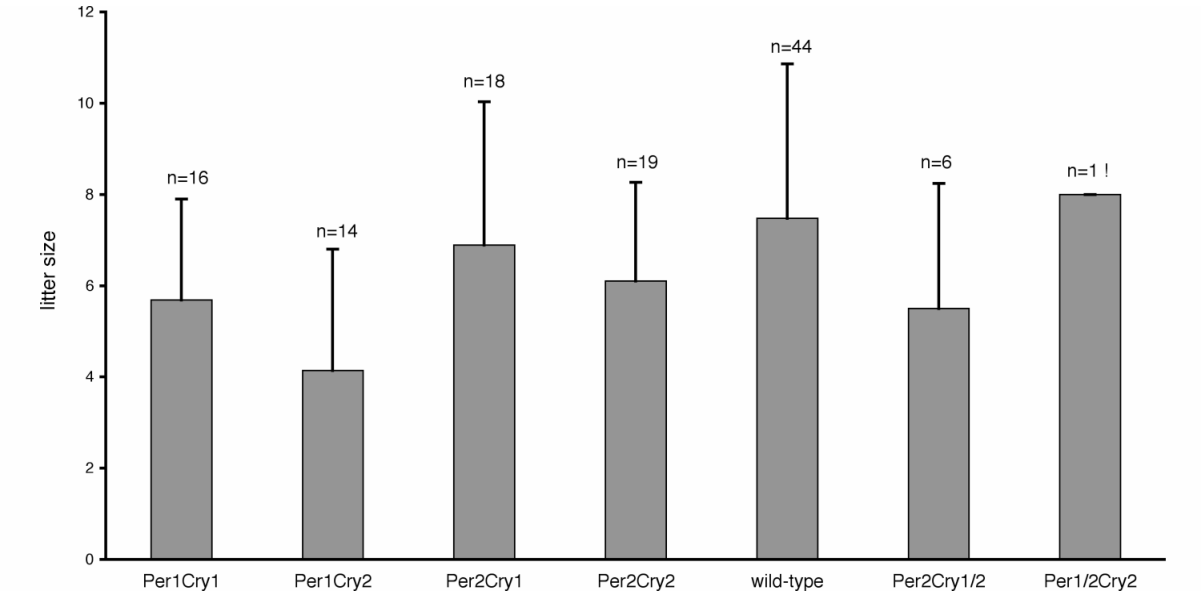

Fig. 23: Average litter size of homozygous *mPer/ mCry* double and triple mutant matings. Values on top indicate the absolute number of breeding pairs for each strain.

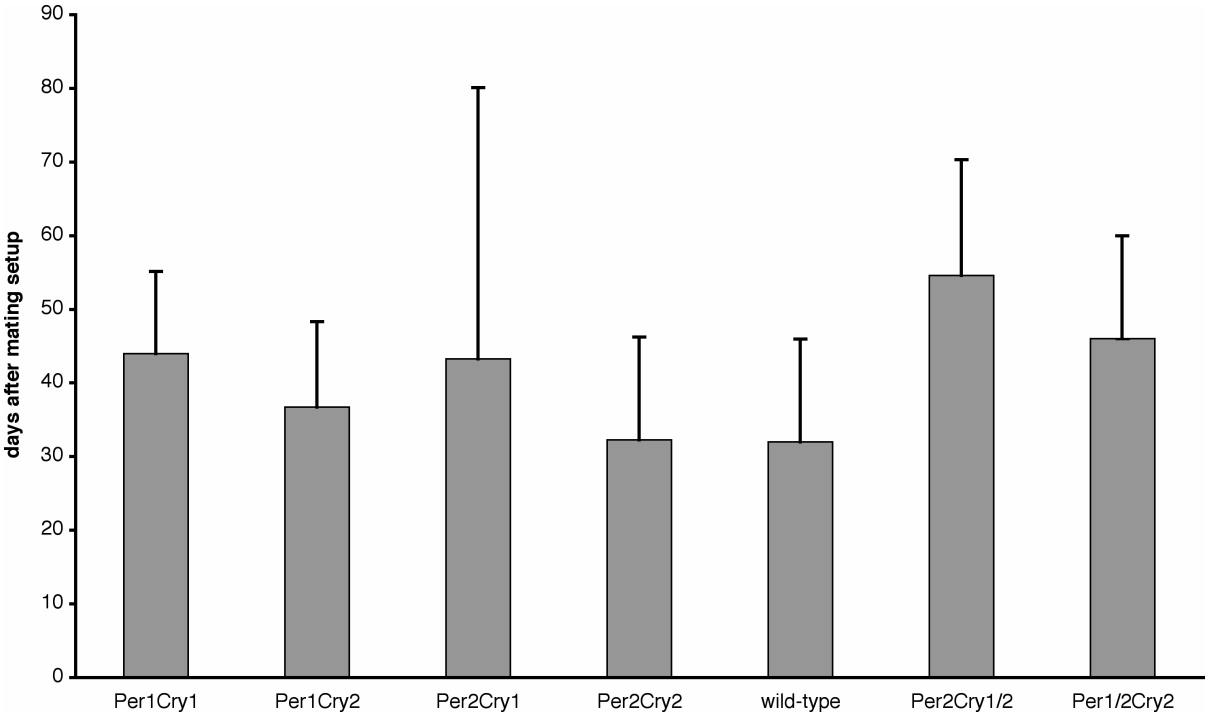

Fig. 24: Birthday of the first litter after mating setup of homozygous *mPer/ mCry* double and triple mutants.

While there were no significant differences in litter intervals and stability of breeding intervals between all fertile strains, wild-type breedings were generally more stable and regular but with rather high variations between different matings.

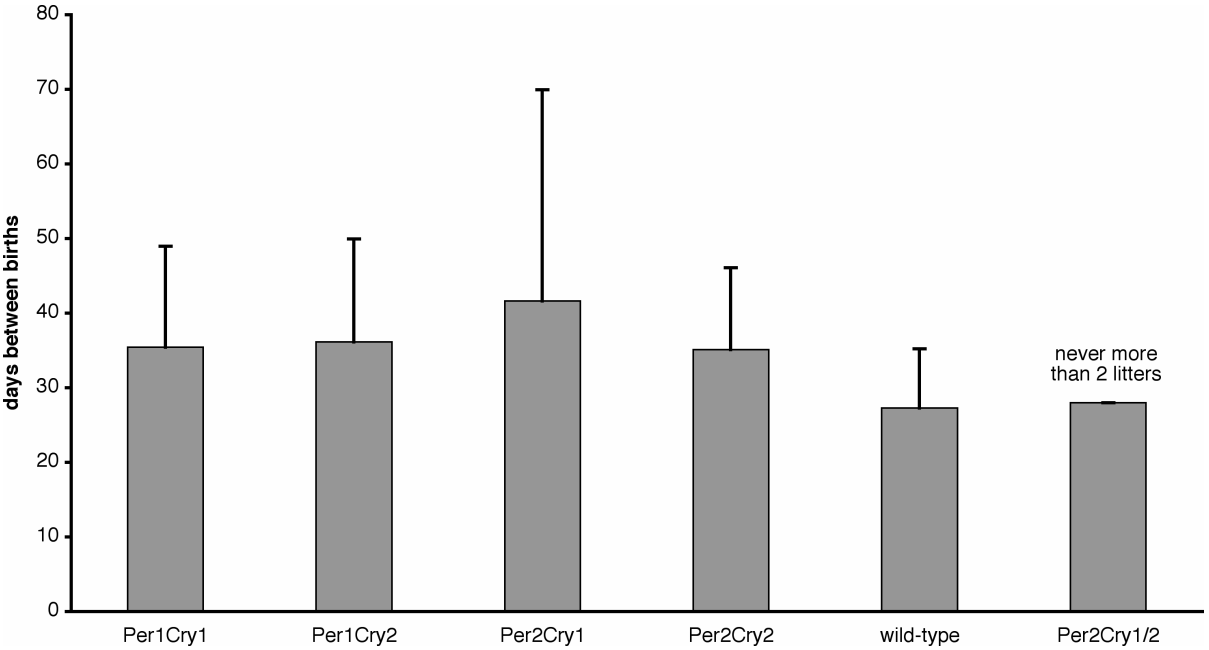

Fig. 25: Litter frequency of homozygous *mPer/ mCry* double and triple mutant matings.

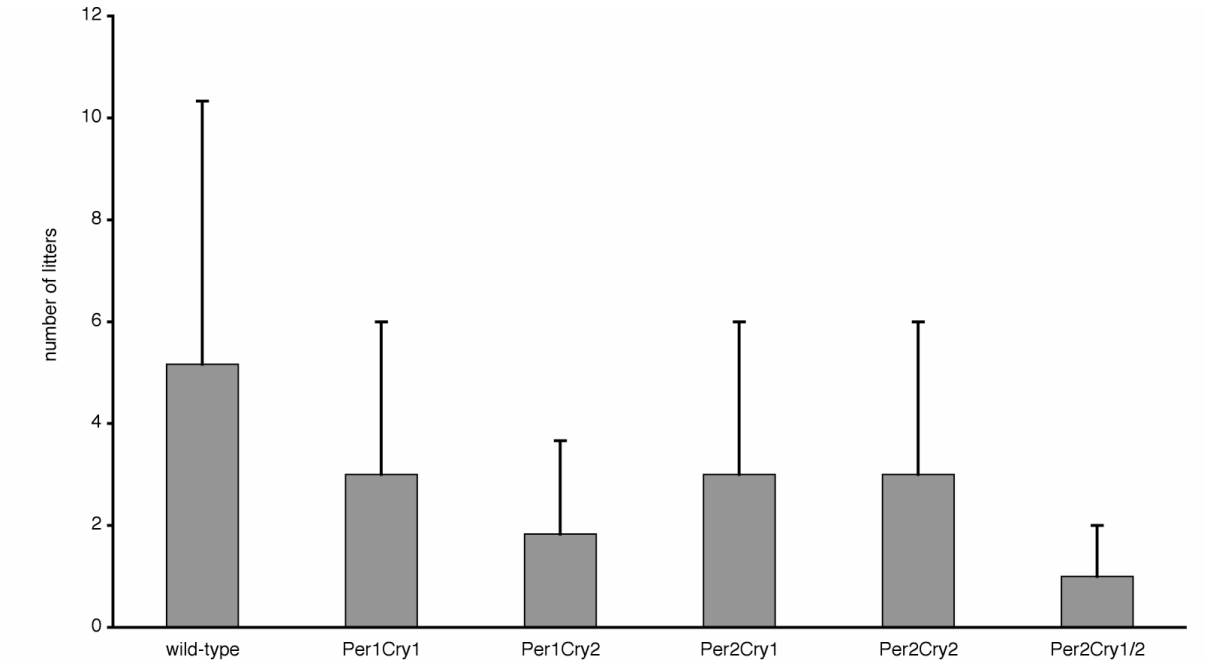

Fig. 26: Average number of litters from homozygous *mPer/ mCry* double and triple mutant matings per 6 months.

All triple mutant breedings were rather unreliable with small litters, irregular breeding intervals and high death numbers after birth. Since the estrous cycle is known to be linked to the circadian clock (Alleva et al., 1971) it seems obvious that females with a disrupted circadian clock may have difficulties with regard to their fertility.

Although the triple mutants generally appeared smaller and less aggressive and a notable number of animals showed a tendency to spastic seizures upon arousal the total numbers used in this study were insufficient to allow a scientific investigation.

2.3.2. Activity monitoring

Besides the double mutant strains presented in the publications above we generated three *mPer/ mCry* triple mutant strains. The fourth possible combination of triple mutation, *mPer1/ mCry1/2* was not fertile and probably caused some additional defects we could not examine since the F1 matings (8 pairs) did not give enough homozygous offspring. The few animals we tested however, were arrhythmic under constant conditions (DD, LL) like all the other three triple mutant strains.

Generally, triple mutants run less than their wild-type littermates. They immediately lose their rhythm in DD and LL indicating a completely disrupted circadian clockwork.

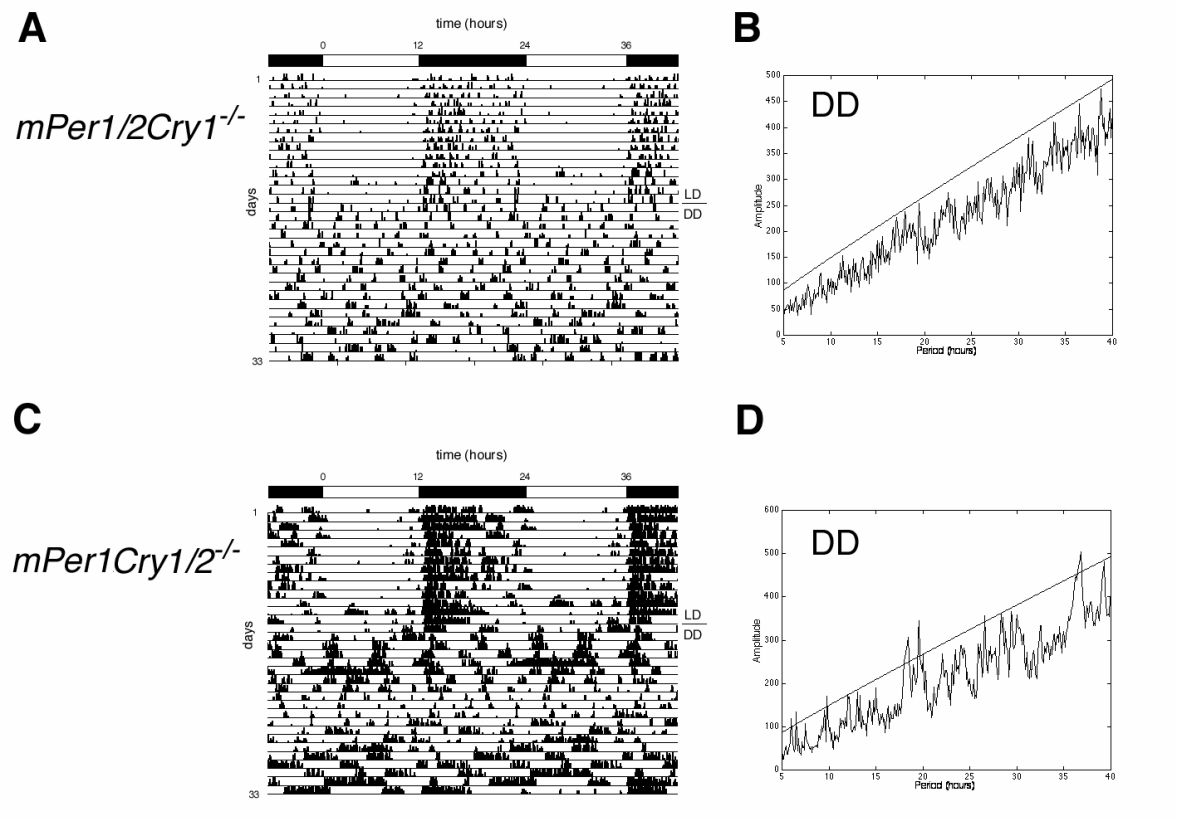

(Legend: see next page)

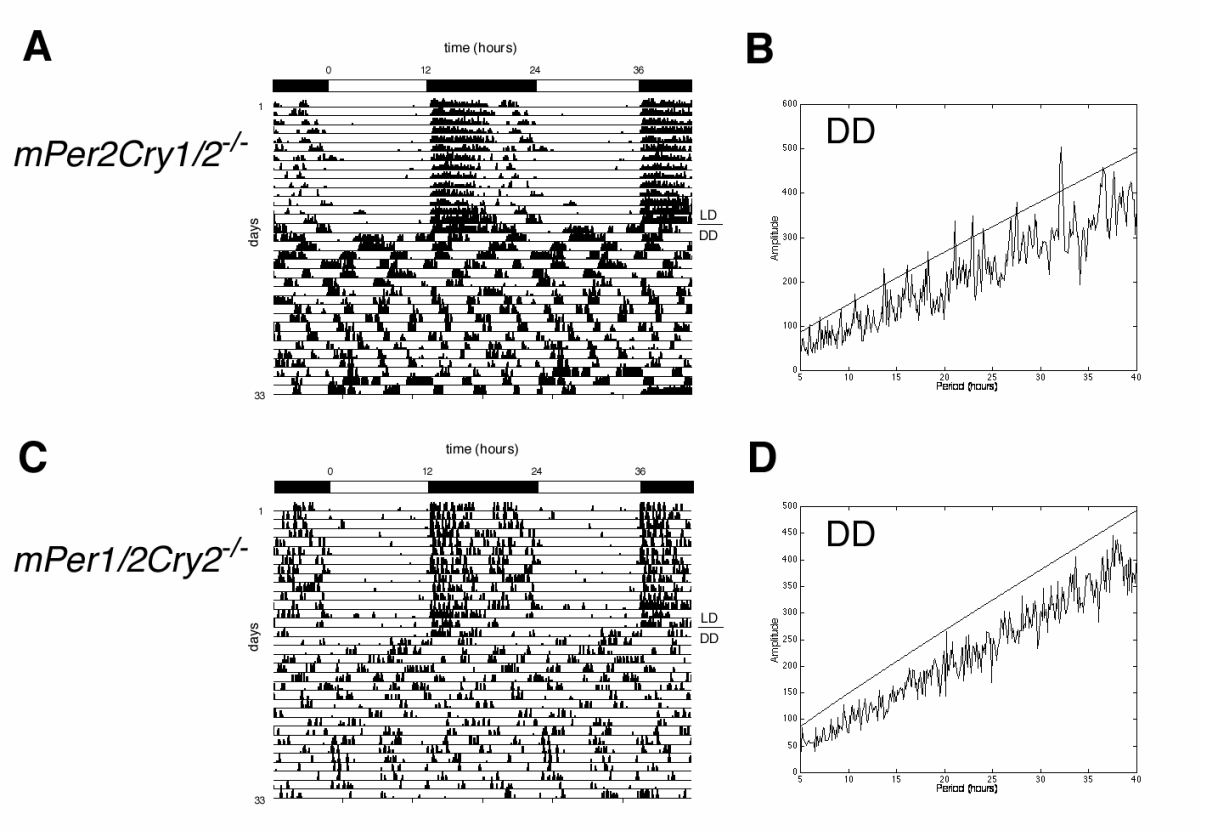

Fig. 27: Activity profiles of *mPer/ mCry* triple mutant mice in LD and DD. Left panels show representative actograms of *mPer1/2/ mCry1*$^{-/-}$, *mPer1/ mCry1/2*$^{-/-}$, *mPer1/2/ mCry2*$^{-/-}$, and *mPer2/ mCry1/2*$^{-/-}$ mice in LD and DD (transition indicated by the line below LD). Black and white bars on top indicate light and dark phase in LD. Right panels show periodograms of the same animals in DD. The diagonal line depicts significance as given by the ClockLab program.

When released into constant light both double and triple mutants generally run less than in LD or DD demonstrating the activity suppressing ("masking") effect of light on nocturnal animals. Interestingly, *mPer1mCry2*$^{-/-}$ mice lost their rhythmicity in LL while at least the young animals show a stable rhythm of activity in DD. Even more surprising was the fact that in *mPer2mCry1* mutant mice rhythmicity could be rescued by high light intensities in LL while the animals were totally arrhythmic in DD. One explanation might be the light inducibility of *mPer1*: While in DD mPER1 and mCRY2 protein levels and distribution do not overlap spatially and temporally an increased *mPer1* expression in LL enables mPER1 protein to interact with mCRY2. The combination of both is enough to restart the TTL, although with a very short period.

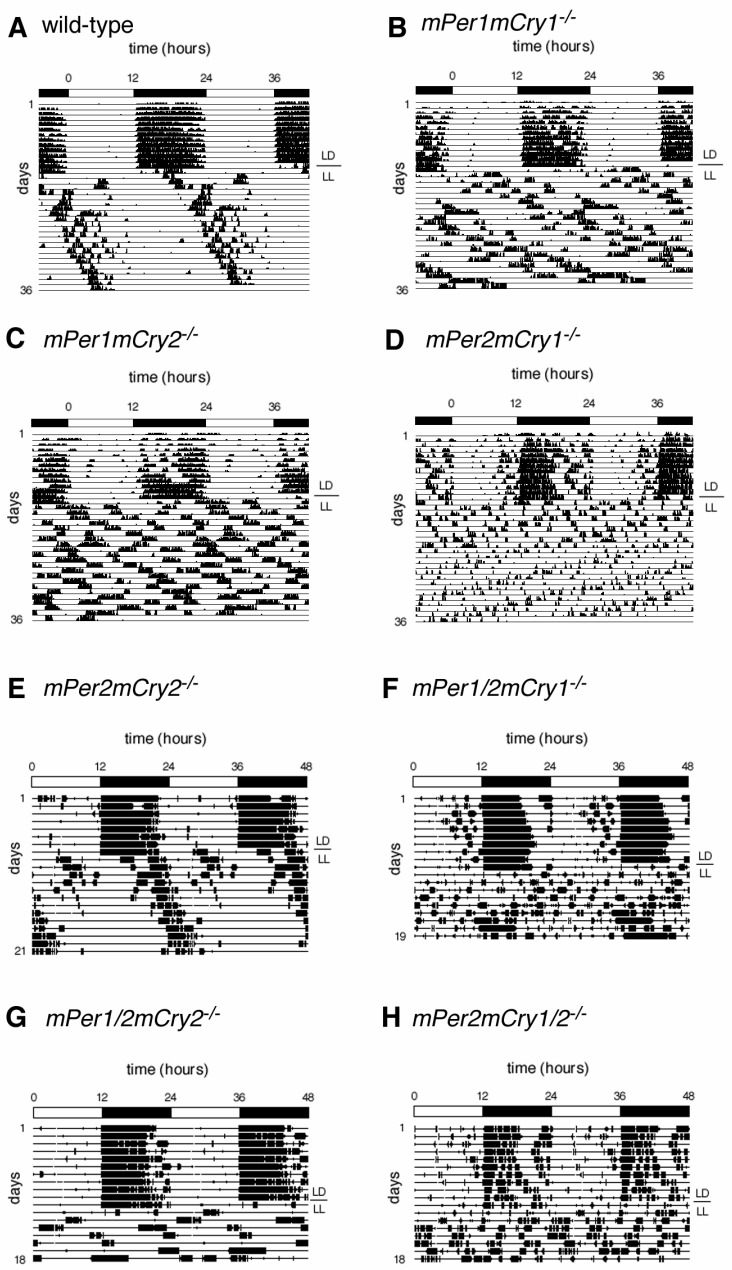

Fig. 28: Activity profiles of *mPer/ mCry* double and triple mutant mice in LD and LL. Panels show representative actograms of wild-type (A), *mPer1/ mCry1*$^{-/-}$ (B), 'young' *mPer1/ mCry2*$^{-/-}$ (C), *mPer2/ mCry1*$^{-/-}$ (D), *mPer2/ mCry2*$^{-/-}$ (E), *mPer1/2/ mCry1*$^{-/-}$ (F), *mPer1/2/ mCry2*$^{-/-}$ (G), and *mPer2/ mCry1/2*$^{-/-}$ mice (H) in LD and LL (400Lx bright white light; transition indicated by the line below LD). Black and white bars on top indicate light and dark phase in LD.

To further investigate the influence of masking on the wheel running activity, we exposed the animals to a 8h shifted LD cycle and monitored the time the animals needed to adapt to the new light regimen. While the double mutants needed a few days to adjust the triple mutants did not suffer from that "jet lag" like experience but changed their activity patterns immediately after the transition. This indicates that the rhythmicity these animals show in LD is merely driven by the masking effect of light and not by an endogenous pacemaker.

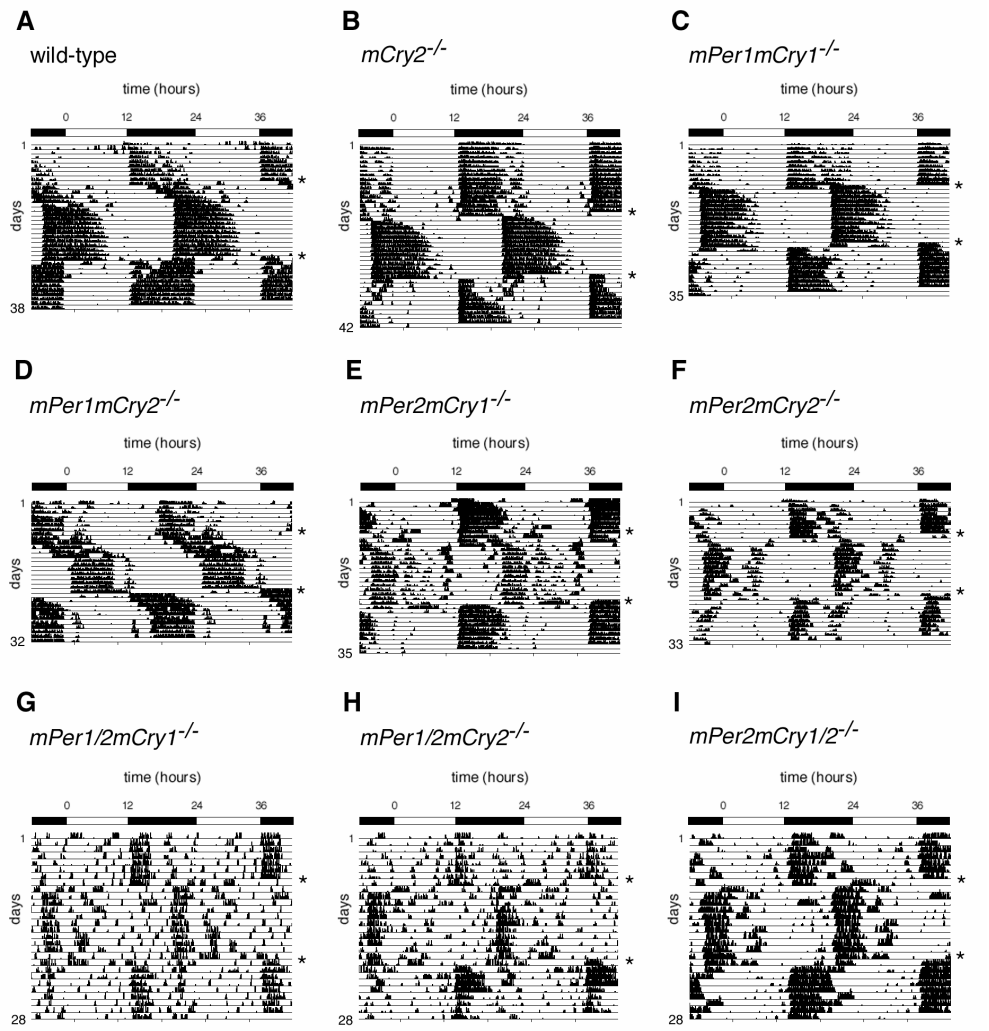

Fig. 29: Activity profiles of *mPer/ mCry* double and triple mutant mice after a shifted LD cycle. Panels show representative actograms of wild-type (A), *mCry2*$^{-/-}$ (B), *mPer1/ mCry1*$^{-/-}$ (C), 'young' *mPer1/ mCry2*$^{-/-}$ (D), *mPer2/ mCry1*$^{-/-}$ (E), *mPer2/ mCry2*$^{-/-}$ (F), *mPer1/2/ mCry1*$^{-/-}$ (G), *mPer1/2/ mCry2*$^{-/-}$ (H), and *mPer2/ mCry1/2*$^{-/-}$ mice (I) in LD, LD 8h shifted backwards (indicated by the upper asterisk), and LD 8h shifted forwards (indicated by the lower asterisk). Black and white bars on top indicate light and dark phase of the first LD cycle.

The table below summarizes the data obtained by the general activity profile analysis of all *mPer/ mCry* double and triple mutant strains in this study.

Genotype	Activity onset (hours after 'lights off')	Overall Activity (rev/day)	Covered Distance (km/day)	relative light phase activity (%)	duration of activity a (hours)	n
wild-type	0.29 +/- 0.22	19600 +/- 3000	7.14	3.4 +/- 2.1	7.7 +/- 0.7	10
mPer1mCry1-/-	0.25 +/- 0.34	20600 +/- 6700	7.51	3.2 +/- 3.5	8.2 +/- 0.6	10
mPer1mCry2-/-	5.79 +/- 0.67	17400 +/- 9600	6.34	10.7 +/- 11.3	7.4 +/- 0.3	8
mPer2mCry1-/-	-0.16 +/- 0.35	18000 +/- 3700	6.56	12.5 +/- 5.3	7.6 +/- 0.8	10
mPer2mCry2-/-	0.18 +/- 0.14	18000 +/- 2600	6.56	3.5 +/- 2.9	10.1 +/- 0.5	10
mPer1/2mCry1-/-	0.08 +/- 0.4	4200 +/- 2500	1.53	1.8 +/- 1.8	10.4 +/- 2.0	10
mPer1/2mCry2-/-	0.02 +/- 0.47	6300 +/- 1500	2.30	2.7 +/- 1.1	10.6 +/- 1.5	6
mPer2mCry1/2-/-	0.19 +/- 0.21	4600 +/- 2500	1.68	0.9 +/- 0.6	9.5 +/- 0.4	4

Table 2: Activity profiles of *mPer/ mCry* double and triple mutant mice in LD. All data are mean +/- SD; total numbers used for statistical evaluation are given in the right column.

Genotype	period length t (hours)	Overall Activity (rev/day)	Covered Distance (km/day)	duration of activity a (hours)	n
wild-type	23.8 +/- 0.1	20000 +/- 2500	7.29	9.5 +/- 0.4	10
mPer1mCry1-/-	23.7 +/- 0.2	21500 +/- 7300	7.83	10.5 +/- 0.6	7
mPer1mCry2-/-	25.3 +/- 0.2	25100 +/- 6200	9.15	11.4 +/- 0.5	6
mPer2mCry1-/-	arrhythmic	16000 +/- 3200	5.83	n.a.	9
mPer2mCry2-/-	23.4 +/- 0.1	18000 +/- 2700	6.56	10.5 +/- 0.4	10
mPer1/2mCry1-/-	arrhythmic	4500 +/- 2400	1.64	n.a.	8
mPer1/2mCry2-/-	arrhythmic	6800 +/- 1600	2.48	n.a.	6
mPer2mCry1/2-/-	arrhythmic	8500 +/- 1800	3.10	n.a.	3

Table 3: Activity profiles of *mPer/ mCry* double and triple mutant mice in DD. All data are mean +/- SD; total numbers used for statistical evaluation are given in the right column.

Genotype	period length t (hours)	Overall Activity (rev/day)	Covered Distance (km/day)	duration of activity a (hours)	n
wild-type	24.5 +/- 0.2	12300 +/- 3500	4.48	6.5 +/- 0.5	10
mPer1mCry1-/-	26.8 +/- 0.3	10800 +/- 2600	3.94	*	7
mPer1mCry2-/-	24.5 +/- 0.2	13500 +/- 1800	4.92	6.3 +/- 0.6	6
mPer2mCry1-/-	19.9 +/- 0.2	6500 +/- 1400	2.37	10.4 +/- 1.8	9
mPer2mCry2-/-	arrhythmic	1900 +/- 1300	0.69	n.a.	5
mPer1/2mCry1-/-	arrhythmic	3500 +/- 2300	1.28	n.a.	8
mPer1/2mCry2-/-	arrhythmic	1500 +/- 1200	0.55	n.a.	6
mPer2mCry1/2-/-	arrhythmic	4200 +/- 1400	1.53	n.a.	3

n.a.: not available

** : activity was too scattered to determine alpha*

Table 4: Activity profiles of *mPer/ mCry* double and triple mutant mice in LL. All data are mean +/- SD; total numbers used for statistical evaluation are given in the right column.

In order to investigate the role of the *mPer* and the *mCry* genes in the light input pathway to the clock we examined phase shifting effects of nocturnal light. For most strains we applied the Aschoff Type 2 protocol (see chapter 4) for practical reasons. For *mPer1mCry2* mutants however, the evaluation of these experiments turned out to be very difficult due to the long period of the free running rhythm in DD. Therefore we decided to apply the Type 1 protocol to this strain. Since we had to include wild-type animals as reference we could compare results from Type 1 and 2 protocols and show that there are no significant differences in the values obtained from both protocols.

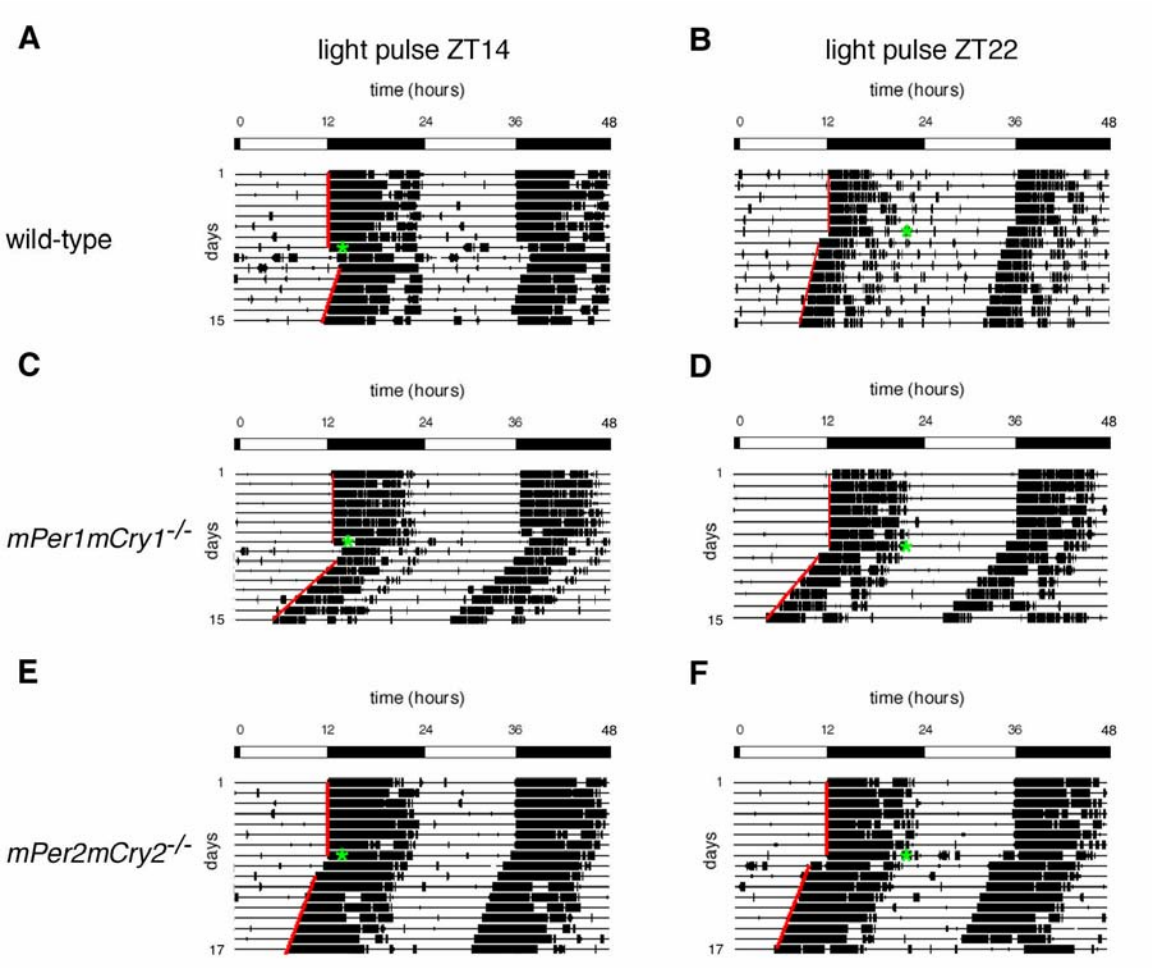

Fig. 30: Nocturnal light pulses phase shift the rhythm of *mPer1/ mCry1* and *mPer2/ mCry2* mutant mice. Animals were subjected to a 15min light pulse at ZT14 (left panels) or ZT22 (right panels), indicated by the green asterisk, before release into DD. Upper row, wild-type; middle row, *mPer1/ mCry1*, and lower row, *mPer2/ mCry2* mutants. Black and white bars on top indicate light and dark phases in LD.

The data obtained from the double mutants reflected the results obtained from *mPer1* and *mPer2* single mutants (Albrecht et al., 2001) with *mPer1* necessary for light induced phase advances and *mPer2* for light induced phase delays. This corresponds to the differential inducibility of both genes by light at different time points during the night (Albrecht et al., 1997b). The double mutant data further supports experiments indicating that the *mCrys* are dispensable for light entrainment but have their role in the central TTL of the circadian oscillator (Griffin et al., 1999; van der Horst et al., 1999).

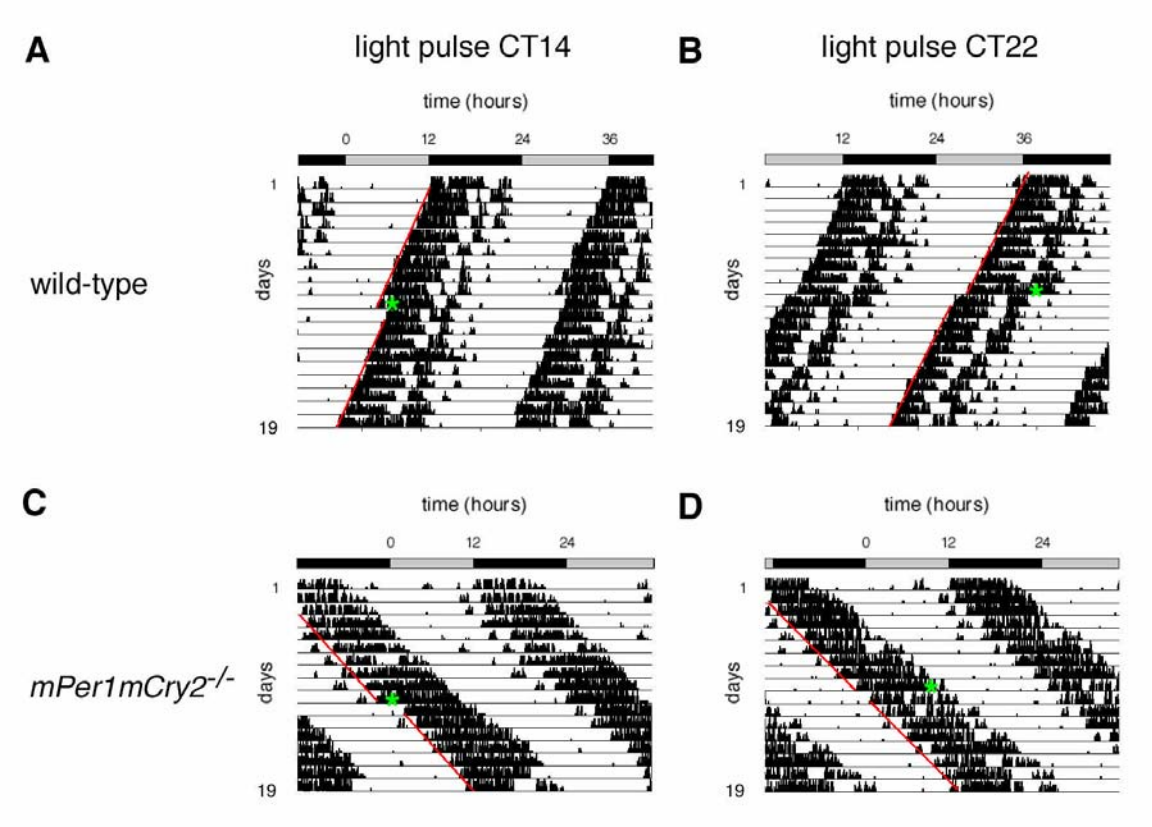

Fig. 31: Nocturnal light pulses phase shift the rhythm of *mPer1/ mCry2* mutant mice. Animals were subjected to a 15min light pulse at CT14 (left panels) or CT22 (right panels), indicated by the green asterisk, in DD. Upper row, wild-type; lower row, *mPer1/ mCry2* mutants. Grey and black bars on top indicate subjective night and day of the first day recorded.

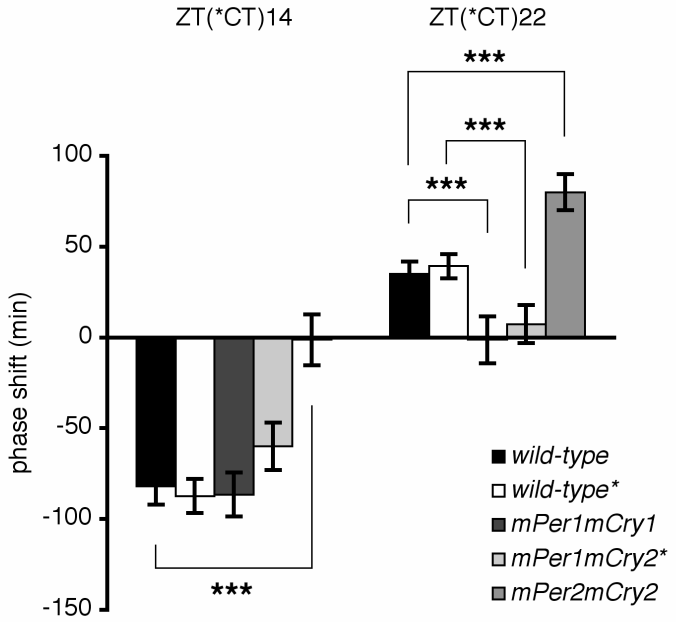

Fig. 32: Light induced activity phase shifts in mPer/ mCry double mutant mice. Shown are results from Aschoff Type 1 (marked with an asterisk) and Type 2 protocols. Left panel shows phase delays after a 15min light pulse early in the night; right panel shows phase advances after a light pulse in the late night (*, p<0.001).**

2.3.3. Clock gene expression

To see if the disrupted activity rhythm is accompanied by an absence of clock gene oscillation in the SCN of *mPer/ mCry* triple mutants we examined the diurnal expression of *mPer2* and *Bmal1* transcripts in these animals. Surprisingly *mPer2* mRNA levels still cycle in all three strains but *Bmal1* oscillation is blunted below significance. The reason might be that *mPer2* transcription is still reactive to light. So we expect this oscillation to dampen upon release into DD. We could not define the transcript levels under constant conditions however, since the arrhythmicity of the animals excludes the determination of circadian times. Since the *mPer2* gene was mutated in all three strains examined, the absence of *Bmal1* induction is a further argument that the truncated mPER2 protein translated in the $mPer2^{Brdm1}$ mutant has no function in the circadian clockwork anymore.

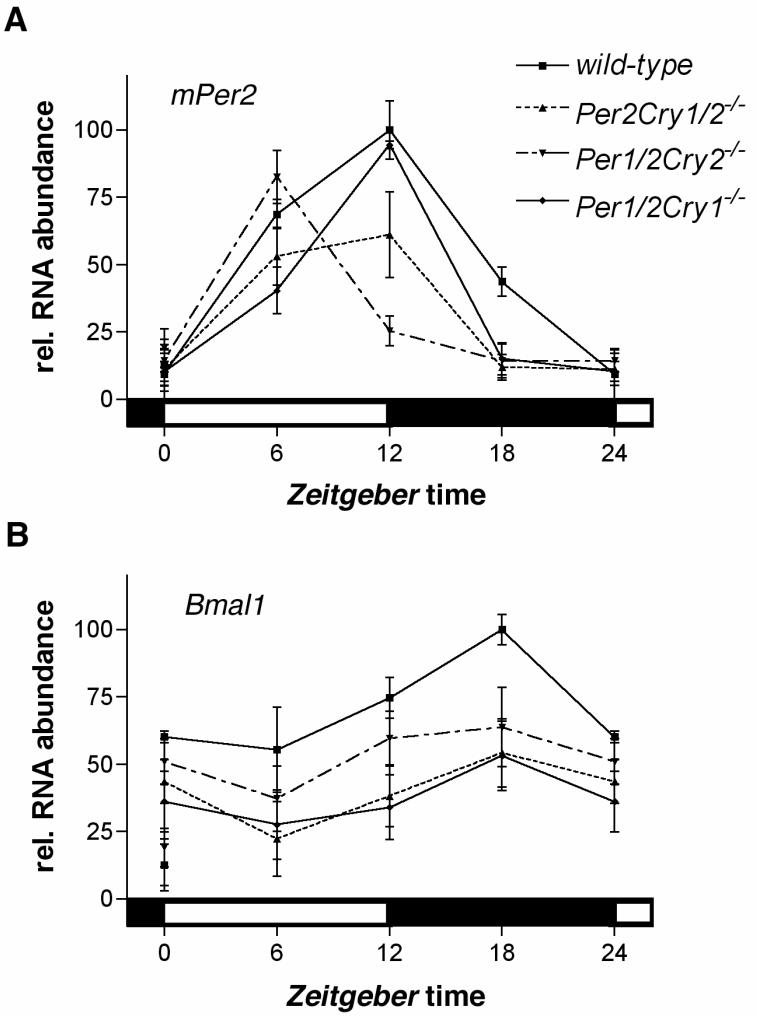

Fig. 33: *mPer2* and *Bmal1* expression in the SCN of *mPer/ mCry* triple mutant mice. (A) Diurnal mRNA profile of *mPer2* in wild-type and *mPer/ mCry* triple mutant mice. (B) Diurnal mRNA profile of *Bmal1* in wild-type and *mPer/ mCry* triple mutant mice. Black and white bars on x-axis indicate dark and light phase.

To further investigate the role of the truncated mPER2 protein in the mutant clockwork we examined mPER2 protein localization in wild-type, *mPer2*, *mPer2/ mCry1* and *mPer2/ mCry2* mutant mice by immunofluorescence. These four strains represent different configurations with regard to the role of mPER2. Wild-type animals are rhythmic and have a non-mutated mPER2 protein. *mPer2*^{Brdm1} animals become arrhythmic after some time in DD and have a mutated mPER2 protein. *mPer2*^{Brdm1}*/ mCry1*$^{-/-}$ animals become immediately arrhythmic in DD and have a mutated mPER2 protein. *mPer2*^{Brdm1}*/ mCry2*$^{-/-}$ animals are rhythmic but have a mutated mPER2 protein. We found mPER2 immunofluorescence predominantly in the nucleus in all four strains and at all time points examined.

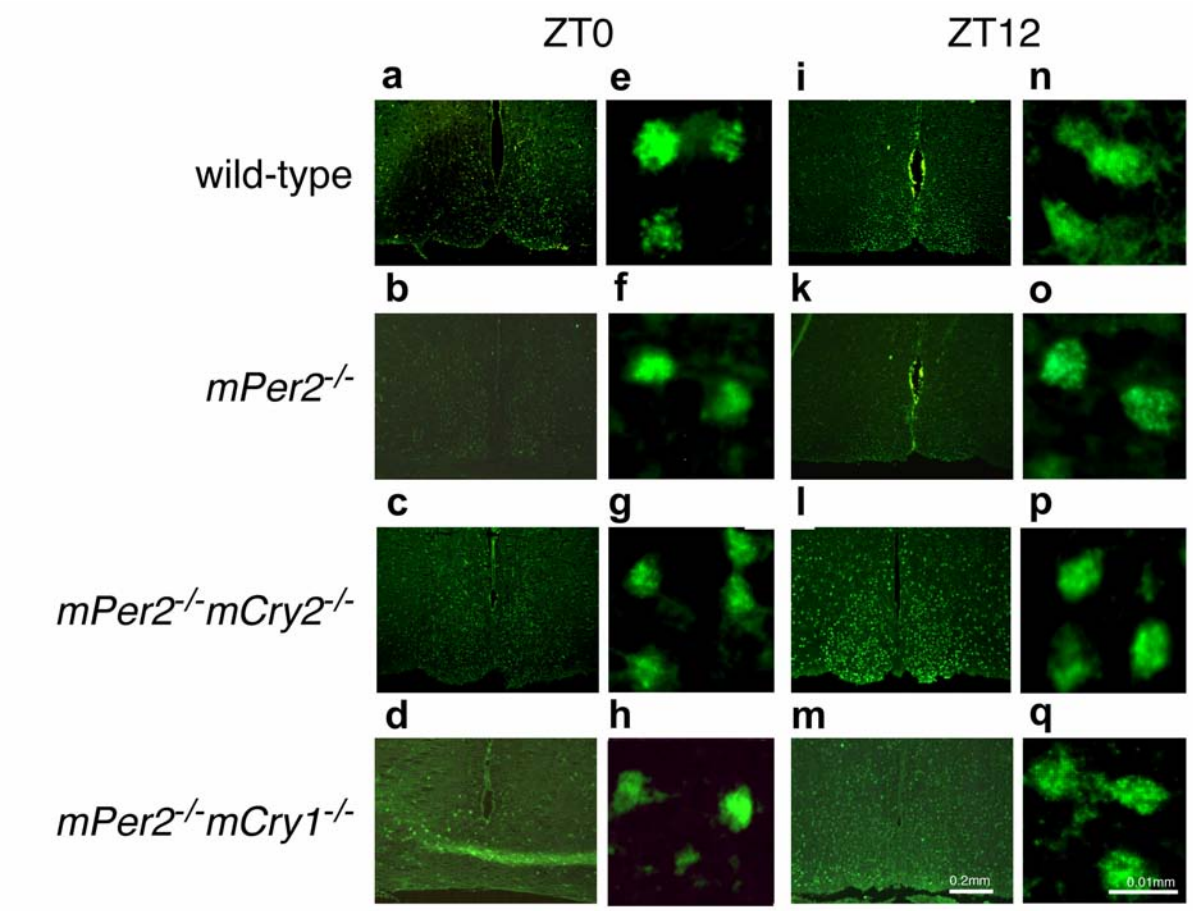

Fig. 34: mPER2 immunofluorescence in the SCN of *mPer2/mCry* mutant mice. Shown are representative micrographs from ZT0 (a-d, e-h) and ZT12 (i-m, n-q) from wild-type (first row), *mPer2*^{Brdm1} (second row), *mPer2*^{Brdm1} *mCry2*$^{-/-}$ (third row), and *mPer2*^{Brdm1} *mCry1*$^{-/-}$ mice (fourth row). Second and fourth column show magnifications of the micrographs to the left.

2.3.4. Output genes

In the last set of experiments we examined clock output in double and triple mutant mice. We chose *AVP* and *Dbp* as two genes with prominent diurnal and circadian oscillation in the SCN of wild-type mice. Both genes have been shown to be directly clock controlled (Jin et al., 1999; Ripperger et al., 2000). However the exact regulation of these genes in the SCN and the periphery still needs to be elucidated .

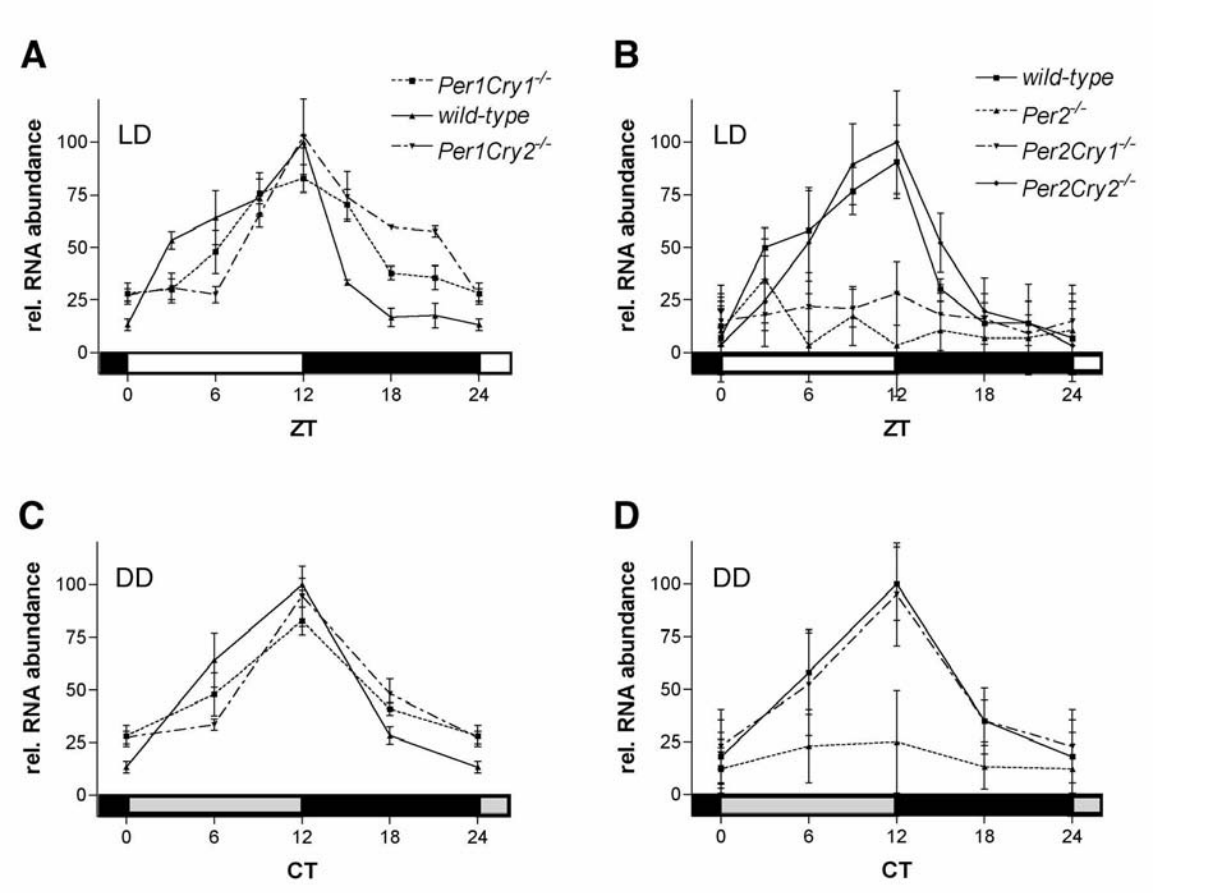

Fig. 35: AVP expression in *mPer/ mCry* double mutant mice. (A, B) Diurnal expression profiles of AVP transcript in the SCN. Black and white bars indicate dark and light phase. (C, D) Circadian expression of AVP transcript in the SCN. Grey and black bars indicate subjective day and night respectively. Data are mean +/- SD of three different experiments.

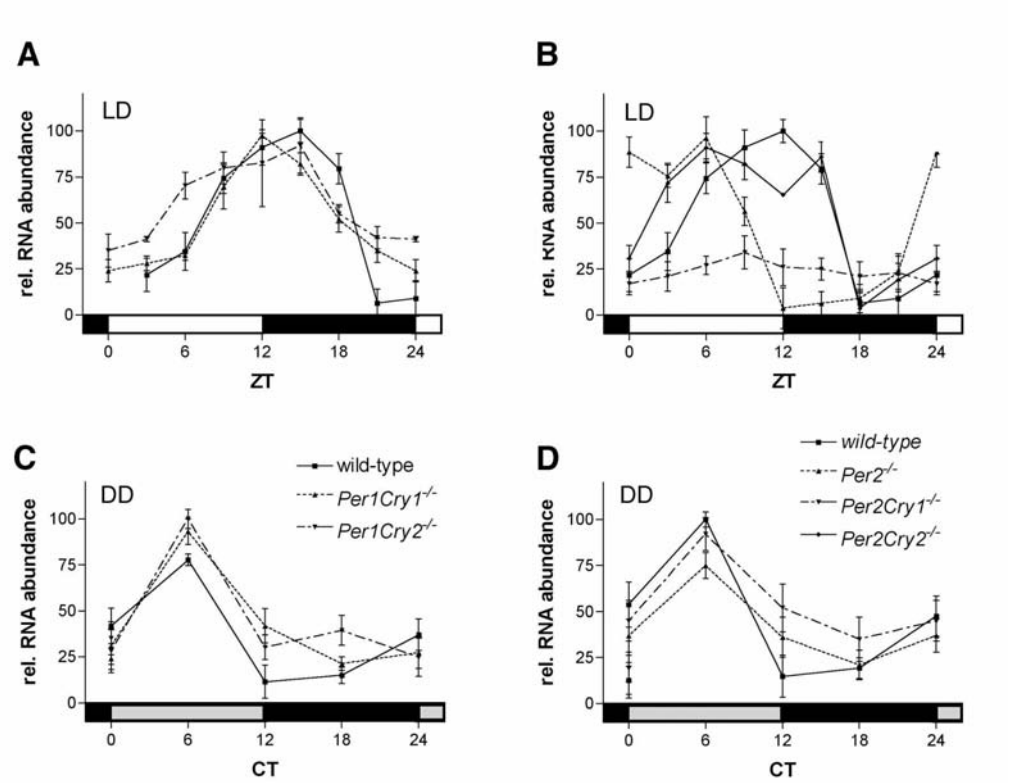

Fig. 36: *Dbp* expression in *mPer/ mCry* double mutant mice. (A, B) Diurnal expression profiles of *Dbp* transcript in the SCN. Black and white bars indicate dark and light phase. (C, D) Circadian expression of *Dbp* transcript in the SCN. Grey and black bars indicate subjective day and night respectively. Data are mean +/- SD of three different experiments.

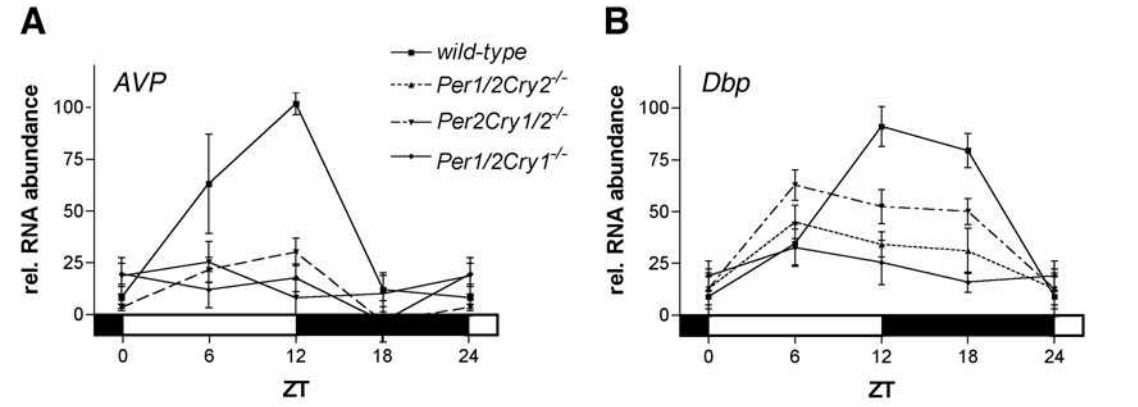

Fig. 37: AVP and *Dbp* expression in *mPer/ mCry* triple mutant mice. Diurnal expression profiles of AVP (A) and *Dbp* (B) transcript in the SCN. Black and white bars indicate dark and light phase.

AVP and *Dbp* seem to be differentially influenced by the *mPer* and *mCry* genes. While AVP expression is low and arrhythmic in *Per2* mutants in LD and DD, *Dbp* levels are still clearly cycling (see as well (Albrecht and Oster, 2001)). In the arrhythmic mutants like *mPer2mCry1*$^{-/-}$ and the triple mutants output gene rhythms are all blunted and generally low indicating that the LD cycle cannot substitute or re-induce clock oscillation to signalize rhythmicity to the body.

In the second project of my Ph.D. thesis I studied the molecular circadian clockwork of the blind mole rat *Spalax ehrenbergi*. This work was performed in collaboration with Dr. Aaron Avivi and Prof. Eviatar Nevo from the Institute of Evolution at Haifa University, Mount Carmel, Israel. While they performed all the animal work and sequence analysis we focused on the analysis of clock gene expression in different conditions and tissues.

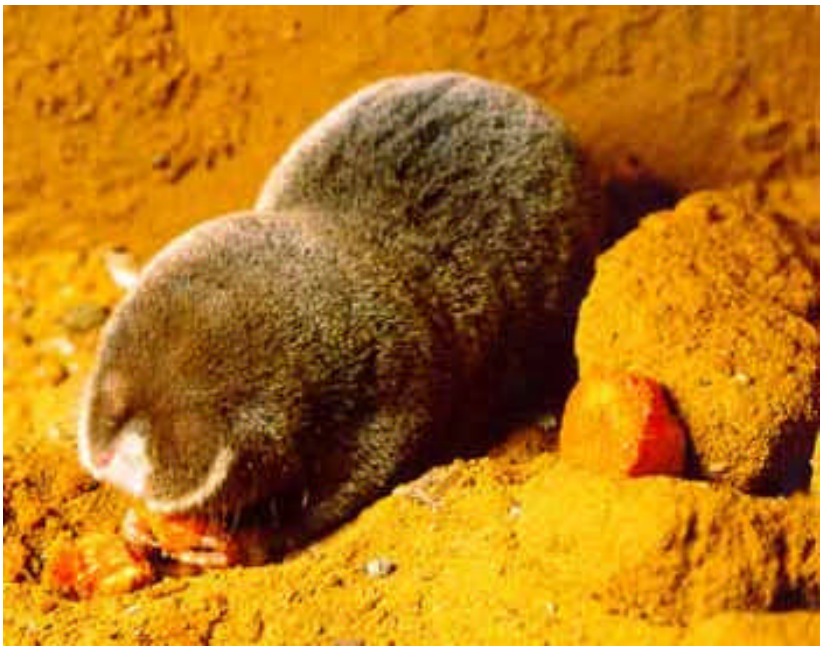

Fig. 38: ***Spalax ehrenbergi***

The *Spalax ehrenbergi* superspecies is a family of four actively speciating chromosomal subspecies (2n = 52, 54, 58, and 60 (Nevo, 1991)). *Spalax* is a solitary subterranean herbivore that spends more than 95% of his life in underground burrows, rarely coming to the surface. It represents an extreme example of natural eye and brain reorganization in mammals (Nevo, 1999). It is completely blind (Haim et al., 1983), yet the retina of the atrophied subcutaneous eye functions in photoentrainment of locomotor activity and thermoregulatory rhythms (Pévet et al., 1984; Rado et al., 1991). The eye is surrounded by a extremely hypertrophic Harderian gland which plays a role in the integration of photoperiodic changes (Pévet et al., 1984) and probably represents an adaptation of the mole rat's circadian system to its specialized ecotope. Despite its subterranean habitat and its degenerated visual system Spalax has a functional SCN, that can receive light/dark information from the retina via the hypothalamic tract and generate circadian rhythmicity (Ben-Shlomo et al., 1995; Nevo et al., 1982; Rado et al., 1991).

Another unique feature of *Spalax* is its polymorphic activity pattern with predominantly diurnal as well as predominantly nocturnal active individuals in the same populations (Nevo

et al., 1982). Nevertheless, activity rhythms can be entrained to changing light dark cycles in the laboratory (Tobler et al., 1998), indicating that the circadian clock of this animals retained its sensitivity to light.

When we started this project only few data was available on the molecular aspects of clocks from diurnal animals. Additionally, the ability of *Spalax* to change its activity pattern from nocturnal to diurnal and *vice versa* offered the opportunity to look for differential mechanisms of light entrainment in one species.

2.4. Publication: “Biological clock in total darkness: The Clock/MOP3 circadian system of the blind subterranean mole rat”

Aaron Avivi, Urs Albrecht, Henrik Oster, Alma Joel, Avigdor Beiles, and Eviatar Nevo

Proceedings of the National Academy of Sciences of the USA, 98 (24), 2001

Biological clock in total darkness: The *Clock/MOP3* circadian system of the blind subterranean mole rat

Aaron Avivi*, Urs Albrecht†, Henrik Oster†, Alma Joel*, Avigdor Beiles*, and Eviatar Nevo*‡

*Institute of Evolution, University of Haifa, Mount Carmel, Haifa 31905, Israel; and †Max Planck Institute for Experimental Endocrinology, 30625 Hannover, Germany

Contributed by Eviatar Nevo, September 20, 2001

Blind subterranean mole rats retain a degenerated, subcutaneous, visually blind but functionally circadian eye involved in photoperiodic perception. Here we describe the cloning, sequence, and expression of the circadian *Clock* and *MOP3* cDNAs of the *Spalax ehrenbergi* superspecies in Israel. Both genes are relatively conserved, although characterized by a significant number of amino acid substitutions. The glutamine-rich area of Clock, which is assumed to function in circadian rhythmicity, is expanded in *Spalax* compared with that of humans and mice, and is different in amino acid composition from that of rats. We also show that MOP3 is a bona fide partner of *Spalax* Clock and that the *Spalax* Clock/MOP3 dimer is less potent than its human counterpart in driving transcription. We suggest that this reduction in transcriptional activity may be attributed to the *Spalax* Clock glutamine-rich domain, which is unique in its amino acid composition compared with other studied mammalian species. Understanding *Clock/MOP3* function could highlight circadian mechanisms in blind mammals and their unique pattern as a result of adapting to life underground.

Biological Clocks Underground

The behavior of all eukaryotic organisms is characterized by a 24-h cycle of rest and activity, as a fundamental adaptation to the solar cycle of light and darkness (1–4). In mammals, the pacemaker of this circadian rhythm is localized in the central nervous system (5) and it is entrained by light signals in the eye. An intriguing question is how a subterranean, naturally blind mammal with a subcutaneous degenerated eye maintains its circadian system, and whether its examination can illuminate circadian rhythmicity of sighted mammals above ground.

The underground adaptive ecogeographical radiation of the *Spalax ehrenbergi* superspecies in Israel involves four sibling species: *Spalax galili*, *Spalax golani*, *Spalax carmeli*, and *Spalax judaei*, with diploid chromosome numbers $2n = 52$, 54, 58, and 60, respectively (6), displaying progressive stages of final ecological speciation (7, 8). Their adaptive radiation in Israel, from early Pleistocene to Recent times, is closely associated with increasing aridity stress, hence, with distinct climatic diversity. *S. galili*, radiated in the cool-humid northern upper Galilee Mountains; *S. golani*, in the cool-semidry northeastern Golan Heights; *S. carmeli*, in warm-humid central Israel; and *S. judaei*, in warm-dry southern Samaria, Judea, and the northern Negev mountains and plains.

Spalax represents an extreme example of natural eye and brain reorganization in mammals (8, 9). The animal is completely blind (10), yet the retina of the atrophied subcutaneous eye functions in photoentrainment of locomotor activity and thermoregulatory rhythms (11–13). Ocular regression of thalamic sight structures conceals adaptive progression of the photoperiodic system (14, 15). Retinal rhodopsin (16) and coneopsin participate in photoentrainment (17, 18). *Per*-homologous ACNGGN sequence comprising poly(Thr-Gly) shows hypothalamic circadian oscillation (19). Thus, *Spalax* displays behavioral circadian rhythm adapted to life underground.

Activity patterns were tested in the four sibling species of the *S. ehrenbergi* superspecies (20). Activity patterns were found to be polyphasic and polymorphic (19, 20), with a remarkable intra- and interspecies diversity in circadian patterns (refs. 21 and 22—no species is identified in the latter study) coupled with seasonal shifts.[§] This complex pattern is unique in mammals analyzed to date. These patterns may display an adaptive strategy of a subterranean mammal, safeguarded from above-ground predation.

Molecular Genetic Basis of Circadian Rhythms

In recent years, tremendous progress has been achieved in revealing the molecular-genetic basis of circadian activity in different organisms across phylogeny, including cyanobacteria, plants, fungi, insects, and mammals (1, 23). All show homologous circadian molecules, both structurally and functionally (23). The circadian genes identified in mammals are *Clock*, *MOP3*, *Per1*, *Per2*, *Per3*, *Tim*, *Cry1*, and *Cry2* (23), all interacting in circadian rhythmicity. In *Drosophila*, the sex-linked period (*Per*) gene affects rhythmicity in circadian (24-h), ultradian (<24-h), and infradian (>24-h) time domains (24). Work in *Drosophila* and mice suggested a mechanism in which expression of *Per* genes is driven by a CLOCK/MOP3 heterodimer, which, through their basic helix–loop–helix (bHLH) motif and the PAS domains, binds to the E-box present in the *Per* promoter, thereby activating *Per* transcription. PER/TIM and PER/CRY complexes probably block the activation of *Per* transcription by interfering with the activity of Clock/MOP3 (25). Indeed, it was recently proven (26) that the loss of PAS protein MOP3 in mice results in immediate and complete loss of circadian rhythmicity. Recent studies (27) more specifically clarify the detailed mechanism of the regulation of the circadian rhythm. Studying mutant *Clock*, *Per2*, and *Cry* of mice, Shearman *et al.* (27) showed that *Per2* has a dominant role in the positive regulation of the *MOP3*, whereas the *Crys* are the negative regulators of the *Per* and *Cry* cycles. *Clock* mutants appear to positively alter the regulation of *MOP3* gene expression in the suprachiasmatic nucleus (SCN), but not the regulation of *Clock* itself. As the oscillations of the *Pers* and *Crys* RNA are down-regulated in the *Clock* mutant mice, the effect of Clock on MOP3 levels is probably indirect and may occur through the Pers and/or the Crys proteins; the reduced levels of one or more of these genes may cause the reduced levels of *MOP3* in the *Clock* mutant mice through loss of the positive control of *MOP3* transcription.

The underlying genetic basis of circadian rhythms in the blind, subterranean mole rats may be different from that of strictly diurnal or nocturnal and sighted mammals, such as humans and mice, which presumably lack multiphasic, polymorphic, and

EVOLUTION

Abbreviations: RT, reverse transcriptase; bHLH, basic helix–loop–helix; SCN, suprachiasmatic nucleus; RLU, relative light unit; polyQ, polyglutamine; h*Clock*, human *Clock*; s*Clock*, *Spalax Clock*.

Data deposition: The sequences reported in this paper have been deposited in the GenBank database (accession nos. AJ318057–AJ318060).

‡To whom reprint requests should be addressed. E-mail: nevo@research.haifa.ac.il.

§Kushnirov, D., Beolchini, F., Lombardini, F. & Nevo, E. (1998) Euro-American Mammal Congress, July 19–24, 1998, Santiago de Compostela, Spain, abstr. 381.

The publication costs of this article were defrayed in part by page charge payment. This article must therefore be hereby marked "*advertisement*" in accordance with 18 U.S.C. §1734 solely to indicate this fact.

seasonal biological circadian patterns. The coupled ecological and phylogenetic uniqueness of *Spalax* makes it an intriguing model organism for assessing the molecular-genetic machinery of the biological clock.

Our objectives in this study were to compare and contrast the structure and the expression of the *Clock* gene in the blind subterranean mole rat with those of other mammals, and suggest experiments for its potential effects on the unique circadian rhythmicity of these species. We show differences in *Clock* structure and expression between mole rats, rats, mice, and humans. We also demonstrate differences among three mole rat species whose significance may derive from the ecological differences of the species—a testable hypothesis.

Materials and Methods

Animals. Animals used for the cloning of the mole rat *Clock* belong to three species of the *S. ehrenbergi* superspecies in Israel (6–8). The species name is followed by the diploid chromosome number, population name, and the geographic region: *S. galili*, $2n = 52$, Kerem Ben Zimra, Upper Galilee; *S. carmeli*, $2n = 58$, Muhraka, Mt. Carmel; *S. judaei*, $2n = 60$, Anza, Samaria. The *S. galili* was also used for the cloning of *MOP3*. All of the animals used in these experiments were captured in the field and kept in our animal facility for at least 3 months before use. Animals were housed in individual cages, each species in a separate room. They were kept under controlled conditions of 22–24°C with seasonal light/dark hours and fed with carrots and apples. Animals used in this study were adults and of similar weight (100–150 g).

Cloning. By reverse transcriptase (RT)-PCR (28), we cloned the complete ORF of *Clock* from three individuals each belonging to a different species as described above. The oligonucleotides used for the RT-PCR cloning were designed according to the published sequence of human *Clock* (GenBank accession no. AF011568) and that of the mouse (GenBank accession no. AF000998). These were a 5′ sense oligonucleotide 5′-ACAAGACGAAAAC(GA)TA-(GA)T(AG)TGTTATG (the 3′ ATG is the initiation codon), and a 3′ antisense oligonucleotide 5′-AGAGAGGAAG(CT)(AG)-(CT)GTGTGCTA (the 3′ CTA is the termination codon).

To construct the *S. galili Clock* cDNA with a replaced human Q-rich (glutamine-rich) domain (*sClock*-hQ) and the human equivalent (h*Clock*-sQ), *Clock* cDNA fragments from both species, equivalent to *Spalax* amino acids numbers 1–744 and 736–865 (see GenBank accession no. AJ318057) were amplified and joined by PCR.

Spalax MOP3 cDNA was also cloned by RT-PCR from *S. galili* brain tissue by using oligonucleotides designed according to the published sequence of human *MOP3* (GenBank accession no. AF044288) and that of the mouse (GenBank accession no. AB015203). These were a 5′ sense oligonucleotide 5′-TG(T/C)(G/A)A(C/G)(T/C)(T/A)C(A/C)G(A/T)(T/C)C(A/T)TCCAATG (the 3′ ATG is the initiation codon) and a 3′ antisense oligonucleotide 5′GCCAAAGCAACATGTAGTGT(T/C)(T/C)A. The (T/C)(T/C)A is a combination of the three possible termination codons. The tissues used in this study for the RT-PCR experiments were collected at the same time from all individuals.

Similarity Tree. The tree presented is a protein (amino acids)-based tree using Kimura's protein distance (29). The tree is derived by using the Wisconsin package version 10 (Genetics Computer Group, Madison, WI), using the neighbor-joining method. We chose this method after Weir (30), who summarized the simulation studies and showed that this method is among the best methods based on distance matrices.

Transcriptional Activity. The entire ORFs of *Spalax* (s) and human (h) *Clock* as well as *sClock*-hQ and h*Clock*-sQ were cloned into the pTARGET expression vector (Promega). Plasmids expressing these constructs were cotransfected with an h*MOP3* or s*MOP3*-expressing plasmid and the M34RE-luciferase reporter plasmid into the human hepatoma cell line Hep3b. The M34RE-luciferase has three E-box elements (the CACGTG sequence), a transcription factor-binding site found in the *Per1* promoter region, in tandem upstream of the luciferase gene (25). Transfections were performed by means of Lipofectamine (Life Technologies). In all experiments, the luciferase reporter activity was normalized to β-galactosidase expression resulting from cotransfection of a control plasmid [a cytomegalovirus (CMV) promoter that drives the expression of the β-galactosidase gene]. Cells were incubated for 20 h before harvest. The luciferase activity was determined as described (25). The relative light units (RLUs) were calculated from the luciferase activity divided by the β-galactosidase activity for each assay.

***In Situ* Hybridization.** Animals used for testing the brains were kept in a controlled environment of 12-h light/12-h dark. All specimens came from diurnal animals, as was proven by monitoring their locomotor activity. *Spalax* brains were removed under sterile conditions at Zeitgeber times ZT0, ZT6, ZT12, and ZT18 (ZT0 is when lights are turned on, and ZT12 is when lights are turned off) and fixed in ice-cold 4% paraformaldehyde/PBS for 16–20 h. Tissues were dehydrated, embedded in paraffin, and sectioned at a thickness of 10 μm. *In situ* hybridization was performed as described (31). The *Clock* probes corresponded to nucleotides 423-1290 of *Spalax* cDNA (amino acids 141–430 in accession no. AJ318057) and the *MOP3* probes to nucleotides 1–864 of *Spalax* cDNA (amino acids 1–288 in accession no. AJ318060). Antisense and sense riboprobes were synthesized with T3 or T7 RNA polymerase in the presence of 5′-α^{35}S-UTP (1,250 Ci/mmol; 1 Ci = 37 GBq; DuPont/NEN). Hybridization was done overnight at 55°C. Stringency washes were performed at 64°C. Slides were dipped in NTP-2 emulsion and exposed for 6 days. Tissue was visualized by fluorescence of Hoechst dye 33258-stained nuclei (blue color in figure). Silver grains were visualized by dark-field illumination. Image is a videograph captured with ADOBE PHOTOSHOP. Experiments were performed in duplicate.

Results

***Spalax Clock* and *MOP3* cDNA Structure.** A full length *Spalax* cDNA for *Clock* was isolated from three of the Israeli species, namely *S. galili*, *S. carmeli*, and *S. judaei*. A full-length cDNA of *Spalax MOP3* was isolated from *S. galili*. The clones were obtained by RT-PCR of brain tissue by using oligonucleotides from the translational initiation and termination sites of the previously published human and mouse counterparts.

The *Spalax Clock* cDNA is over 90% similar to the genes of mice, rats (accession no. NM021856), and humans (for the complete cDNA sequences and the deduced amino acids of the three *Spalax* species see accession nos. AJ318057, AJ318058, and AJ318059). Translated, however, *Spalax Clock* cDNA encodes a protein of 865 aa compared with 855 in mice, 846 in humans, and 862 in rats (32). The Gly-Met-Asn-Thr at positions 610–613 in human, missing in mouse, occur in the three *Spalax* species, though Thr is replaced by Ala in all *Spalax* species. Glutamine at position 629 in mice is missing in humans, and occurs in all *Spalax* species. Table 1 summarizes the synonymous and nonsynonymous mutations among the three *Spalax* species studied and then between them and humans and mice. *Spalax* has 18–26 amino acid substitutions compared with humans, and 35–42 substitutions compared with mice. *S. judaei* (S60) and *S. carmeli* (S58), geographically adjacent species, differ in 8 amino acids and 12 mutations. *S. judaei* differs from the more northern species, *S. galili* (S52), in 10 amino acids and in a total of 13 mutations. *S. galili* and *S. carmeli*, which are geographical neighbors, differ in 3 amino acids and 7 mutations. The bHLH domain and the two PAS domains of *Clock* cDNA are similar in

Table 1. Summary of mutations in *Clock* cDNA

	S52	S58	S60	Mus	Hu
S52	—				
S58	3ns + 4s (7)	—			
S60	10ns + 3s (13)	8ns + 4s (12)	—		
Mus	37ns + 148s (185)	35ns + 150s (185)	42ns + 151s (193)	—	
Hu	18ns + 154s (172)	26ns + 147s (173)	26ns + 152s (178)	25ns + 193s (218)	—

The distances in *Clock* cDNA sequence among the three *Spalax* species studied (S52, S58, and S60), mouse (Mus), and humans (Hu). The distance is expressed in number of synonymous (s) and nonsynonymous (ns) substitutions. The total number of substitutions appears in parentheses. Note the larger number of substitutions between *Spalax* and humans than that between *Spalax* and mouse. Also noteworthy is the unusual larger number of nonsynonymous mutations compared with the synonymous substitutions among the *Spalax* species, indicating interspecies functional changes.

all studied species. The most impressive difference between *Spalax* and humans and mice is in the Q-rich domain as can be seen in Fig. 1. The *Spalax* repeat is 18 aa longer than that found in humans and 5 aa longer than that of mice and it is different in amino acid composition from rats.

The *S. galili MOP3* cDNA (accession no. AJ318060) is also very similar to those of mouse and human. The putative peptide encodes 626 amino acids. Like human *MOP3* (accession no. AF044288), it misses the Leu-Asp-Asp-Phe-Ala-Phe-Glu, which appears in the mouse (position 48 to 54 in the mouse peptide, accession no. AB015203). There are 8 unique amino acid substitutions in the *Spalax* peptide (positions 304, 306, 330, 332, 334, 338, 476, and 580). However, the activity domains bHLH and PAS are completely identical in the three species.

The *Clock* Similarity Trees. We have used the Kimura distances (30) to generate two trees. One is based on the distances between nucleic acids and the other is based on distances between amino acids (Fig. 2). The method examines each pair of aligned sequences item by item and counts the number of exact matches, partial matches, and gap symbols. If the sequences are nucleic acids, transitions and transversions are also tallied. The *Clock* similarity trees show that *S. judaei*, the youngest species, seems to evolve faster than its older sibling species. Furthermore, *Spalax* is somewhat closer to humans than to mice in CLOCK protein structure (see also Table 1). This result is in contrast with all other phylogenetic trees of *Spalax* derived from other sets of data (6–8).

Function of the Clock/MOP3 Dimer. As already stated above, *Spalax* has a distinctly different polyglutamine (polyQ) repeat (Fig. 1). The *Spalax* MOP3 is very similar to the human MOP3 repeat, but also to the mouse protein. To functionally test whether the difference in the Q-repeat affects *Spalax* Clock activity, we compared *S. galili* Clock with human Clock, which is shorter by 18 aa at the polyQ domain. This was done by an assay that measures transactivation by Clock/MOP3 heterodimer of E-box elements, a type of transcription factor-binding site found adjacent to *Per1* and important for *Per1* expression (25). We found that *Spalax* Clock is a bona fide partner of MOP3 as shown by this E-box/luciferase reporter assay. Note too that its activity is only 30%, hence, it is significantly lower ($P < 0.001$) compared with human protein (Fig. 3). Dimerizing human or *Spalax* Clock with human or *Spalax* MOP3 does not influence their relative activity. However, replacing the Q-rich domain between the two species does invert their relative activity. That is to say, that hClock-sQ as a dimer of either hMOP3 or sMOP3 is as active as sClock, and sClock-hQ as a dimer of either hMOP3 or sMOP3 is as active as hClock (Fig. 3).

The Expression of *Spalax Clock* and *MOP3*. *In situ* hybridization localizes *Spalax Clock* and *MOP3* expression to the SCN in the brain (Fig. 4), the center of the mammalian circadian clock (5). *Spalax Clock* does not oscillate, but its *MOP3* does oscillate, which is similar to what is found in other species studied (23). Furthermore, RT-PCR demonstrates (Fig. 5) that *Spalax Clock* is expressed in several different organs, i.e., in the brain, retina, and harderian gland, as well as in the peripheral tissues kidney and liver. *MOP3* is expressed in all tissues studied. Its expression is quite low in kidney and spleen; however, like *Clock*, it is expressed in those tissues that

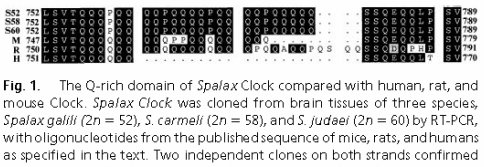

Fig. 1. The Q-rich domain of *Spalax* Clock compared with human, rat, and mouse Clock. *Spalax Clock* was cloned from brain tissues of three species, *Spalax galili* (2*n* = 52), *S. carmeli* (2*n* = 58), and *S. judaei* (2*n* = 60) by RT-PCR, with oligonucleotides from the published sequence of mice, rats, and humans as specified in the text. Two independent clones on both strands confirmed each sequence. The figure depicts a Prettybox of the Clock Q-rich domain of the three *Spalax* species (S52, S58, and S60), humans (H), mice (M), and rats (R). Numbers at both sides represent the amino acids aligned. The figure displaces multiple-sequence alignment in postscript format; shading represents regions that agree with a calculated consensus sequence (Wisconsin package version 10). □, amino acids not similar among the compared species.

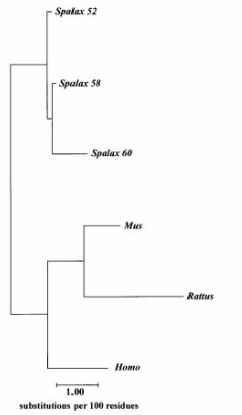

Fig. 2. Similarity tree of the Clock protein. The unrooted tree describes the similarity relationships among the Clock of the three *Spalax* species (S52, S58, and S60), mice (*Mus*), rats (*Rattus*), and humans (*Homo*). The calculated distances show a somewhat closer relationship of *Spalax* Clock to human than to mouse Clock and a faster evolution of the younger *S. judaei* (2*n* = 60) than its older sibling species *S. galili* (2*n* = 52) and *S. carmeli* (2*n* = 58).

EVOLUTION

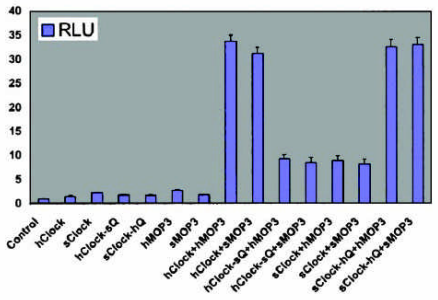

Fig. 3. A comparison of the transcriptional activities of *Spalax*(s) and human (h) *Clock/MOP3* dimer. Human hepatoma Hep3b cells were cotransfected with 1 μg of each plasmid expressing the *sClock* or h*Clock*, *sClock*-hQ or h*Clock*-sQ, h*MOP3* or *sMOP3*, and the different dimers as specified under the *x* axis of the graph. The M34RE-driven luciferase reporter plasmid (0.2 μg) was also transfected, along with 0.1 μg of the β-galactosidase control plasmid. The luciferase and β-galactosidase activities were measured as described in the text. Relative light units (RLU) were defined as the activity of luciferase divided by that of β-galactosidase (*y* axis). The data represent the mean ± SE of triplicate samples. The difference in activity between the h*Clock* or *sClock*-hQ with either *sMOP3* or h*MOP3* and the other combinations is highly significant ($P < 0.001$).

are involved in the maintenance of the circadian system, namely brain, eye, and harderian gland. As demonstrated in Fig. 6, *MOP3* also oscillates in the harderian gland, and although its oscillatory pattern is different from its pattern in the SCN, the peak of its expression is identical in both tissues.

Discussion

Circadian rhythm is localized in the central nervous system and is entrained by light signals in the eye. Lightless habitats lead to structural regressive eye evolution (8). Is function also lost? Maintenance of eye rudiments after millions of years in darkness suggests functionality. Blind subterranean mole rats, *S. ehrenbergi* superspecies (Spalacidae, Rodentia) in Israel, have undergone evolutionary tinkering that has optimized molecular and structural reductions and expansions presumably through loss-and-gain of homeotic mutations in organizing a photoperiodic system, adapting to life in total darkness underground (8). In our current work we present data on the cloning, structure, and expression of circadian genes from a visually blind, subterranean mammal.

***Spalax Clock* and *MOP3* Structure.** Despite being a rodent, *Spalax*, an old rodent offshoot (7, 8), is somewhat closer to humans than to mice in *Clock* structure, as was already manifested for some other genes, i.e., *Mhc* loci (33), VEGF cDNA (34), and HMG1 genes (preliminary results). *Spalax* presumably still retains early rodent patterns reorganized and adapted to life underground. *Spalax Clock* demonstrates distinct interspecies polymorphism and *S. judaei*, the youngest species of the *Spalax ehrenbergi* superspecies in Israel (6, 7), seems to evolve faster than the relatively older *S. galili* and *S. carmeli* species, suggesting distinct interspecies divergence across very short geographic distance (≈80 km). This may be due to its unique xeric ecology with large territories and its polyphasic activity pattern in a stressful climate (6–8). Note that already in our first study of activity patterns of different *S. ehrenbergi* species (20), we found that *S. judaei*, which inhabits a significantly warmer and drier environment than the northern species, *S. galili* and *S. carmeli*, has a significantly different activity profile in both levels and patterns. *S. judaei* is less active and has more, albeit shorter, periods of activity, displaying an adaptive strategy of increasing fitness in xeric environments (20).

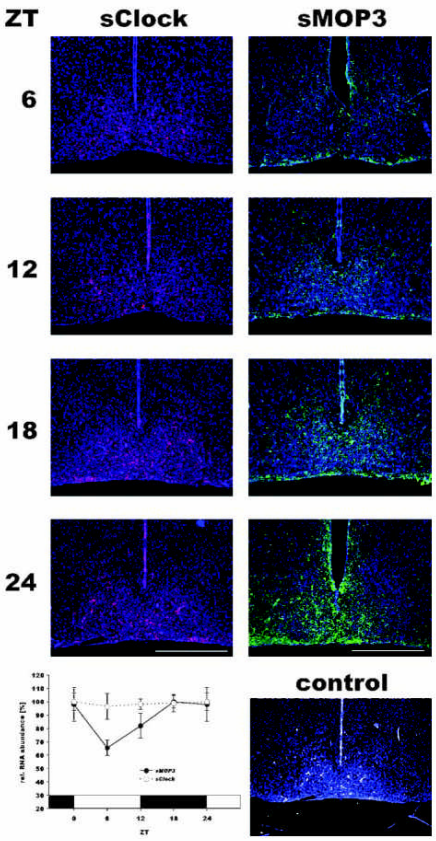

Fig. 4. *In situ* hybridization of *Clock* and *MOP3* in the SCN of *Spalax*. *S. judaei* ($2n = 60$) were killed, and brains were treated as described in *Materials and Methods*. ZT, Zeitgeber time (h). The red grains depict the *Clock*-hybridization areas and the yellow grains depict the *MOP3*-hybridization areas. The control panel (*Bottom Right*) is a negative control carried out with identical, but sense, riboprobes. Notice that, contradictory to *Clock*, *MOP3* is oscillating as can be seen in the intensity of the colored grains. (Bar = ZT) The graph (*Bottom Left*) is a quantified representation of the *in situ* hybridization. Values are densitometric data done with NIH IMAGE. Maxima are 100% for each gene. Error bars are SD.

Evolution of the *Clock* Gene in *Spalax* Species. The phylogenetic relationship of the four *Spalax* species was analyzed earlier by allozymes (35), mtDNA (36, 37), and DNA–DNA hybridization (38). The tree presented here displaying the interspecies *Clock* similarity relationship of the three *Spalax* species is different from the phylogenetic trees derived from allozymes, mtDNA, and DNA–DNA hybridization. Like the tree derived from cytochrome *b* (39), the *Clock* tree seems to represent not chronological relationships, but a gene tree that describes the rate of ecological evolution of the *Clock* gene in different species. This assumption is supported by the comparison between silent and nonsilent substitutions presented in Table 1. This table shows that the distances with human and mouse *Clock* involves 3 to 7 times more silent substitutions than nonsilent

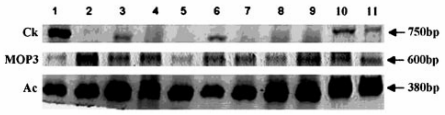

Fig. 5. Tissue distribution of *Clock* and *MOP3* expression in *Spalax*. The distribution of *Clock* (Ck) and *MOP3* expression was characterized by RT-PCR of a fragment of each cDNA, on total RNA samples prepared from the following *S. galili* tissues: kidney (lane 1); intestine (lane 2); liver (lane 3); heart (lane 4); spleen (lane 5); brain (lane 6); muscle (lane 7); testis (lane 8); lung (lane 9); harderian gland (lane 10); and eye (lane 11). The *Clock* gene (*Top*, Ck) is expressed in brain tissue, retina, and harderian gland, as well as in peripheral tissues: kidney and liver. *MOP3* (*Middle*, MOP3) is expressed in all tissues examined, although its relative expression in the kidney (lane 1) and spleen (lane 5) is low. An internal 380-bp fragment of actin cDNA (*Bottom*, Ac) was amplified by RT-PCR in the same reaction tubes as *Clock* or *MOP3*, with actin-specific primers as an internal control.

mutations, which is the usual result when comparing sequences. However, a comparison of the three *Spalax* species exhibits 2 to 3 times more substitutions that cause amino acid changes than those that are synonymous. This is a very unusual observation in phylogenetic trees. The dramatic divergence of the youngest species, *S. judaei*, which displays much faster evolution (more amino acid changes) cannot be reconciled with its relatively recent divergence (6–8, 40). It appears more plausible that *ecological* factors were involved, such as spatiotemporal increasing stressful aridity, which may indirectly affect the circadian pattern, as was demonstrated by radiotracking in time.[§]

Expression and Function of the *Clock*/*MOP3* Dimer. Circadian oscillators appear to be highly conserved throughout evolution and involve transcription-translation negative feedback loops (3, 23). The observation that PAS proteins play an important role in maintaining circadian rhythms supports this idea (41, 42). A distinguishing characteristic of the *Clock* gene is the presence of several functional domains in its amino acid sequence. These are the bHLH (amino acids 34–81), the PAS A direct repeat (amino acids 115–163), the PAS B direct repeat (amino acids 272–318), and the Q-rich domain at the C terminus. Although the bHLH and PAS domains are very conserved among the different *Clock* cDNAs that have been cloned, the most striking difference is in the significant variation in the Q-repeat near the C terminus of Clock. The Q-repeat characterizes the activation domains of many transcription factors (43), and it has been shown to influence circadian rhythmicity (44). It has been shown that A → T nucleotide transversion in a splice donor site, which results in exon skipping and a deletion of 51 aa from the Q-repeat area in the mouse protein, appears to be the cause of a number of changes in the circadian phenotype (45). Most notably, mice homozygous for this deletion manifest a 3–4 h longer period (27–28 h) on initial placement in the dark and then become arrhythmic after a few weeks in darkness. A 6-h exposure to light of these arrhythmic mice restores the long-period rhythmicity. Hence, in addition to a bHLH region (DNA binding domain) and PAS region (protein dimerization domain) Clock also contains a transcriptional activation domain (the Q-rich region). The mutant protein can therefore compete with nonmutant Clock for binding partners and/or DNA binding sites, which explains the dominant negative nature of the mutant allele (44).

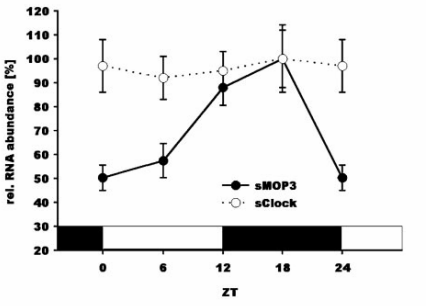

Fig. 6. Expression of *MOP3* and *Clock* in the harderian gland of *Spalax*. *S. galili* ($2n = 52$) kept in a 12-h light/12-h dark cycle were killed at different Zeitgeber time points. Harderian glands were treated as described in *Materials and Methods*. The graph is a quantified representation of the *in situ* hybridization. Values are the densitometric data done with NIH IMAGE. Maxima are 100% for each gene. Notice that contradictory to *Clock*, *MOP3* is oscillating. Bars are SD.

Evidence demonstrates that proper activity of the circadian system requires heterodimerization of two bHLH-PAS proteins: Clock and MOP3 (25, 26, 46). Our results prove that there is a reduced transcriptional activity ($P < 0.001$) of the *Spalax* Clock/MOP3 dimer compared with humans, possibly increasing metabolic economy (15). The fact that this pattern is retained after interchanging the Q-rich domains of the two species supports an assumption that it is this domain that causes the difference in transcriptional activity. It was already shown that mutant Clock could form heterodimers with MOP3 that bound DNA but failed to activate transcription (46). Moreover, such a mutant, probably by down-regulating the oscillations of *Pers* and *Crys* RNA, leads to reduced levels of *MOP3* transcription, hence limiting the available Clock/MOP3 heterodimers at the appropriate circadian time to drive *Per*/*Cry* transcription and restart the cycle (27). This suggests that Clock, after binding to a specific transcription activation site (the E-box), upstream the initiation site of *Per*, appears to drive the positive component of *Per* transcriptional oscillations, which are thought to underlie circadian rhythmicity. Thus, the *Spalax*-unique Clock may partially inactivate transcription, while retaining the ability to bind DNA and dimerize with partners. Further studies are essential to directly relate the unique polyQ repeat of *Spalax* Clock, with the reduced transactivation by *Spalax* Clock or with its unique polytypic (20), polymorphic (19), and seasonal[§] differences in circadian rhythms. Nevertheless, other differences in the *Spalax Clock* or *MOP3* sequence, although evolutionarily impressive, cannot be related to any presently known functional sites. Hence, the reduced activity of *Spalax* Clock may be cautiously attributed to the different polyQ of its protein. Transgenic mice with *Spalax Clock* may elucidate its direct function.

Tissue Distribution and Oscillation of *Spalax Clock* and *MOP3* Expression. As in other mammals, *Spalax Clock* does not oscillate, but *Spalax MOP3* does oscillate (23). Notably, the oscillatory pattern of *MOP3* in the *Spalax* SCN is a mirror image of that of the mouse *Per1* (32) as well as the *Spalax* equivalent (preliminary results). That is, *MOP3* expression is at its minimum at ZT6, when *Per1* expression is at its maximum. This observation may be explained by Shearman's *et al.* (27) interpretation of the feedback mechanism between Clock/MOP3 heterodimer level and the transcription drive of *Per*/*Cry*.

The tissue distribution of *Spalax Clock* is not restricted to tissues directly related to the maintenance of the biological clock, as was reported in mice (44). It may be involved, as was shown in *Drosophila*, in both circadian (47) and noncircadian oscillations in nonpacemaker tissues (48), or as hypothesized by Yamazaki *et al.* (49) in transgenic rats, that a self-sustained circadian pacemaker in the SCN entrains circadian oscillations in the peripheral tissues. *MOP3* is expressed in all tissues studied, which is similar to what was demonstrated in mice and may reflect its involvement as an orphan dimerizing protein in other transcription activation systems, like the hypoxia-inducible factor (25).

***Clock* and *MOP3* Expression in the Harderian Gland.** We are aware of no other report of expression of circadian genes in the harderian gland. Although the oscillatory pattern of *MOP3* is different from its pattern in the SCN, the peak of its expression is identical in both tissues. This may indicate a unique synchronization of these two tissues that has yet to be clarified, because in other tissues there is always a lag in the peak of expression of oscillatory circadian genes between the SCN and peripheral tissues. The expression of *Clock* and *MOP3* in the harderian gland of *Spalax* is remarkable and should be emphasized: the harderian gland of *Spalax* is tremendously hypertrophied, occupying the entire eye-socket, whereas the eye is degenerated (0.7 mm in diameter), subcutaneous, and embedded in that huge harderian gland. It was previously suggested that the harderian gland of *Spalax* is a possible photoreceptor and photoperiodic organ (11).

Circadian Genes in a Blind Subterranean Mammal. Expression of circadian genes in blind *Spalax* may highlight the genetic basis of its behavioral pattern of circadian rhythmicity (19–22). We have already cloned the *Spalax* cDNA homologs of *Per1*, *Per2*, *Per3*, *Tim*, *Cry1*, and *Cry2* (unpublished results). We plan to evaluate their function and their potential convergence in other subterranean mammals. Likewise, the *Spalax* photoreceptor pigment rhodopsin (16) and long-wavelength coneopsin (17, 18, 50) have been cloned and sequenced, and their unique *Spalax* function in photoentrainment was evaluated, presumably as adaptations to life underground by significant enrichment for wavelengths greater than 500 nm, maximizing photon capture, but minimizing the effects of heat (18).

The mosaic evolution of the *Spalax* eye (7, 14, 15), harderian gland (51), and brain (52), and its circadian genes provides a dramatic model of tinkering evolution at both the molecular and organismal levels. From an evolutionary perspective, the genetic basis of circadian rhythms in blind subterranean mole rats may be different from that of strictly diurnal or nocturnal and sighted mammals. The identification of the blind *Spalax Clock* might help, together with its other circadian genes, highlighting the structure and evolution of the circadian organization in mammals, including humans, at the molecular level and their ecological causation. Furthermore, it may highlight both adaptive evolution linking structure and function and behavioral–molecular interactions of regression, progression, and convergence in subterranean mammals generally, and especially in the Pleistocene ecological speciation of the *Spalax ehrenbergi* superspecies caused by increasing ecological aridity stresses (6–8), which in turn affect the patterns of circadian rhythmicity. It could also elucidate, by transgenic studies in mice, the control of the *Spalax*-unique polyphasic, polymorphic, and seasonal cycles, as well as sleeping disorders, work shifts, and jetlag in humans.

We thank Dr. J. Takahashi for the mouse *Clock* probe and Dr. C. Bradfield for his experimental help and advice with the transcriptional activation assay. We are also grateful to Mr. Michael Margulis for his help with the computer graphic work. This work was supported by a grant from Human Frontier Science Program and by the Ancell–Teicher Research Foundation for Genetics and Molecular Evolution.

1. Feldman, J. F. (1982) *Annu. Rev. Plant Physiol.* **33,** 583–608.
2. Edmunds, L. N., Jr. (1988) *Cellular and Molecular Bases of Biological Clocks: Models and Mechanisms for Circadian Timekeeping* (Springer, New York).
3. King, D. P. & Takahashi, J. S. (2000) *Annu. Rev. Neurosci.* **23,** 713–742.
4. Wager-Smith, K. & Kay, S. A. (2000) *Nature (London)* **26,** 23–27.
5. Ralph, M. R., Foster, R. G., David, F. C. & Menaker, M. (1990) *Science* **247,** 975–978.
6. Nevo, E., Ivanitskaya, E. & Beiles, A. (2001) *Adaptive Radiation of Blind Subterranean Mole Rats* (Backhuys, Leiden, The Netherlands)
7. Nevo, E. (1991) *Evol. Biol.* **25,** 1–125.
8. Nevo, E. (1999) *Mosaic Evolution of Subterranean Mammals: Regression, Progression, and Global Convergence* (Oxford Univ. Press, Oxford).
9. Nevo, E. (1998) in *Principles of Animal Design: The Optimization and Symmorphosis Debate*, eds. Weibel, E. R., Taylor, C. R. & Bolis, C. (Cambridge Univ. Press, Cambridge, U.K.), pp. 288–298.
10. Haim, A., Heth, G., Pratt, H. & Nevo, E. (1983) *J. Exp. Biol.* **107,** 59–64.
11. Pevet, P., Heth, G., Haim, A. & Nevo, E. (1984) *J. Exp. Zool.* **232,** 41–50.
12. Rado, R., Gev, H., Goldman, B. D. & Terkel, J. (1991) in *Photobiology*, ed. Riklis, E. (Plenum Press, New York), pp. 323–331.
13. Sanyal, S., Jansen, H. G., de Grip, W. G., Nevo, E. & de Jong, W. W. (1990) *Invest. Ophthalmol. Visual Sci.* **31,** 1398–1404.
14. Cooper, H. M., Herbin, M. & Nevo, E. (1993) *Nature (London)* **361,** 156–159.
15. Cooper, H. M., Herbin, M. & Nevo, E. (1993) *J. Comp. Neurol.* **328,** 313–350.
16. Janssen, J. W. H., Bovee-Geurts, P. H. M., Peeters, Z. P. A., Bowmaker, J. K., Cooper, H. M., David-Gray, Z. K., Nevo, E. & DeGrip, W. J. (2000) *J. Biol. Chem.* **275,** 38674–38679.
17. David-Gray, Z. K., Janssen, J. W. H., Nevo, E & Foster, R. G. (1998) *Nat. Neurosci.* **12,** 655–656.
18. David-Gray, Z. K., Cooper, H. M., Jenssen, J. W. H., Nevo, E. & Foster, R. G. (1999) *FEBS Lett.* **461,** 343–347.
19. Ben-Shlomo, R., Ritte, U. & Nevo, E. (1995) *Behav. Genet.* **25,** 239–245.
20. Nevo, E., Guttman, R., Haber, M. & Erez, E. (1982) *J. Mammal* **63,** 453–463.
21. Tobler, I., Nevo, E. & Hermann, M. (1998) *Behav. Brain Res.* **96,** 173–183.
22. Goldman, B. D., Goldman, S. L., Riccio, A. P. & Terkel, J. (1997) *J. Biol. Rhythms* **12,** 348–361.
23. Dunlap, J. C. (1999) *Cell* **96,** 271–290.
24. Kyriacou, C. P. (1990) *Behav. Genet.* **20,** 191–211.
25. Hogenesch, J. B., Gu., Y. Z., Jain, S. & Bradfield, C. A. (1998) *Proc. Natl. Acad. Sci. USA* **95,** 5474–5479.
26. Bunger, M. K., Wilsbacher L. D., Moran, S. M., Clendenin, C., Radcliffe, L. A., Hogenesch, J. B., Simon, M. C., Takahashi, J. S. & Bradfield, C. A. (2000) *Cell* **103,** 1009–1017.
27. Shearman, L. P., Sriram, S., Weaver, D. R., Maywood, E. S., Chaves, I., Zheng, B., Kume, K., Lee, C. C., van der Horst, G. T., Hastings, M. H. & Reppert, S. M. (2000) *Science* **288,** 1013–1019.
28. Veres, G., Gibbs, R. A., Scherer, S. E. & Caskey, C. T. (1987) *Science* **237,** 415–417.
29. Kimura, M. (1983) *The Neutral Theory of Molecular Evolution* (Cambridge Univ. Press, Cambridge, U.K.).
30. Weir, B. S. (1996) in *Genetic Data Analysis II* (Sinauer Associates, Sunderland, MA), p. 356.
31. Albrecht, U., Sun, Z., Eichele, G. & Lee, C. (1997) *Cell* **91,** 1055–1064.
32. Abe, H., Honma, S., Namihira, M., Takahasi, Y., Ikeda, M., Yu, W. & Honma, K. (1999) *Brain Res. Mol. Brain. Res.* **20,** 104–110.
33. Schopfer, R., Figueroa, F., Nizetic, D., Nevo, E. & Klein, J. (1987) *Mol. Biol. Evol.* **4,** 287–299.
34. Avivi, A., Resnick, M. B., Nevo, E., Joel, A. & Levy, A. P. (1999) *FEBS Lett.* **452,** 133–140.
35. Nevo, E., Filippucci, M. G. & Beiles, A. (1994) *Heredity* **72,** 465–487.
36. Nevo, E., Honeycutt, R. L., Yonekawa, H., Nelson, K. & Hanzawa, N. (1993) *Mol. Biol. Evol.* **10,** 590–604.
37. Nevo, E. & Beiles, A. (1992) *Biol. J. Linn. Soc.* **47,** 385–405.
38. Catzeflis, F. M., Nevo, E., Ahlquist, J. E. & Sibley, C. G. (1989) *J. Mol. Evol.* **29,** 223–232.
39. Nevo, E., Beiles, A. & Spradling, T. (1999) *J. Mol. Evol.* **49,** 215–226.
40. Nevo, E., Tchernov, E. & Beiles, A. (1988) *Z. Zool. Syst. Evol. Forsch.* **26,** 286–314.
41. Kay, S. A. (1997) *Science* **276,** 753–754.
42. Gu, Y. Z., Hogenesch, J. & Bradfield, C. (2000) *Annu. Rev. Pharmacol. Toxicol.* **40,** 519–561
43. Mitchell, P. J. & Tjian, R. (1989) *Science* **245,** 371–378.
44. Antoch, M. P., Song, E. J., Chang, A. M., Vitaterna, M. H., Zhao, Y., Wilsbacher, L. D., Sangoram, A. M., King, D. P., Pinto, L. H. & Takahashi, J. S. (1997) *Cell* **89,** 656–667.
45. King, D. P., Zhao, Y., Sangoram, A. M., Wilsbacher, L. D., Tanaka, M., Antoch, M. P., Steeves, T. D., Vitaterna, M. H., Kornhauser, J. M., Lowrey, P. L., *et al.* (1997) *Cell* **89,** 641–653.
46. Gekakis, N., Stakins, D., Nguyen, H. B., Davis, H. B., Wilsbacher, L. D., King, D. P., Takahashi, J. S. & Weitz, C. J. (1998) *Science* **280,** 1564–1569.
47. Darlington, T. K., Wager-Smith, K., Ceriani, M. F., Staknis, D., Gekakis, N., Steeves, T. D. L., Weitz, C. J., Takahashi, J. S. & Kay, S. A. (1998) *Science* **280,** 1599–1603.
48. Kyriacou, C. P. & Hall, J. C. (1980) *Proc. Natl. Acad. Sci. USA* **77,** 6929–6933.
49. Yamazaki, S., Numano, R., Abe, M., Hida, A., Takahashi, R. Ueda, M., Block, G. D., Sakaki, Y., Menaker, M. & Tei, H. (2000) *Science* **288,** 682–685.
50. Argamaso, S. M., Froehlich, A. C., McCall, M. A., Nevo, E., Provencio, I. & Foster, R. G. (1995) *Biophys. Chem.* **56,** 3–11.
51. Balemans, M. G. M., Pevet, P., Legerstee, W. C. & Nevo, E. (1980) *J. Neural Transm.* **49,** 247–255.
52. Rehkamper, G., Necker, R. & Nevo, E. (1994) *J. Comp. Neurol.* **347,** 570–584.

2.5. Publication: "Circadian genes in a blind subterranean mammal II: Conservation and uniqueness of the three *Period* homologs in the blind subterranean mole rat, *Spalax ehrenbergi* superspecies"

Aaron Avivi*, Henrik Oster*, Alma Joel, Avigdor Beiles, Urs Albrecht, and Eviatar Nevo

***** these authors contributed equally to this work

Proceedings of the National Academy of Sciences of the USA, 99 (18), 2002

Circadian genes in a blind subterranean mammal II: Conservation and uniqueness of the three *Period* homologs in the blind subterranean mole rat, *Spalax ehrenbergi* superspecies

Aaron Avivi*†‡, Henrik Oster†§¶, Alma Joel*, Avigdor Beiles*, Urs Albrecht§¶, and Eviatar Nevo*

*Laboratory of Animal Molecular Evolution, Institute of Evolution, University of Haifa, Mount Carmel, Haifa 31905, Israel; §Max-Planck-Institute for Experimental Endocrinology, Feodor-Lynen-Strasse 7, 30625 Hannover, Germany; and ¶Department of Medicine, Division of Biochemistry, University of Fribourg, Rue du Musée 5, 1700 Fribourg, Switzerland

Contributed by Eviatar Nevo, July 10, 2002

We demonstrated that a subterranean, visually blind mammal has a functional set of three *Per* genes that are important components of the circadian clockwork in mammals. The mole rat superspecies *Spalax ehrenbergi* is a blind subterranean animal that lives its entire life underground in darkness. It has degenerated eyes, but the retina and highly hypertrophic harderian gland are involved in photoperiodic perception. All three *Per* genes oscillate with a periodicity of 24 h in the suprachiasmatic nuclei, eye, and harderian gland and are expressed in peripheral organs. This oscillation is maintained under constant conditions. The light inducibility of *sPer1* and *sPer2*, which are similar in structure to those of other mammals, indicates the role of these genes in clock resetting. However, *sPer3* is unique in mammals and has two truncated isoforms, and its expressional analysis leaves its function unresolved. *Per*'s expression analysis in the harderian gland suggests an important partidpation of this organ in the stabilization and resetting mechanism of the central pacemaker in the suprachiasmatic nuclei and in unique adaptation to life underground.

Life on Earth is adapted to cyclical phenomena imposed by the external environment (1). Most organisms have circadian systems that synchronize physiological events to the external 24-h cycle (2). The underlying molecular-genetic mechanisms of these clocks exhibit an extraordinary evolutionary conservation from cyanobacteria through plants, fruit flies, and mammals. All of these clock systems consist of autoregulatory transcriptional/translational feedback loops with positive/negative regulatory elements and similar genetic machinery (3, 4).

Two basic helix–loop–helix PAS (PER-ARNT-SIM) transcription factors, CLOCK and MOP3 (BMAL1), form the positive elements of the system and drive transcription of three *Period* (*Per 1, 2, 3*) and two *Cryptochrome* (*Cry 1, 2*) genes. The protein products of these genes are thought to be components of a negative feedback complex that inhibits the CLOCK/MOP3 heterodimer, thereby closing the circadian loop.

The enigma of circadian rhythms in a blind subterranean mammal is intriguing (5–7). We have already shown that a CLOCK/MOP3-driven clock exists in *Spalax* (8). Here we continue to decipher its circadian machinery.

The Evolutionary Model of Blind Subterranean Mammals

The blind subterranean mammals, mole rats of the *Spalax ehrenbergi* superspecies in Israel, consist of four species that have been studied multidisciplinarily as an evolutionary model of speciation and adaptation (5–7). *Spalax* lives in total darkness, yet, it perceives the daily and seasonal temporal cycles underground (9). Behaviorally, *Spalax* displays polyphasic and polytypic day-night activity patterns (10, 11) coupled with polymorphic (12) and seasonal‖ variation, supported by a unique photoperiodic perception mechanism (9). *Spalax* has a degenerated s.c. functional eye (13, 14), which, together with the harderian gland, participates in photoperiodic perception (9, 15–18). The retina harbors *Rhodopsin* (19, 20) and *Coneopsin* (21), adaptively effective in photoperiodic perception (22, 23), and expresses *alfa-B-crystallin* (24). The photic signals entrain *c-fos* in the suprachiasmatic nuclei (SCN) Zeitgeber (25) and can possibly activate circadian genes.

Evolutionarily, *Spalax*'s perceptive brain structures (SCN and striatum) were expanded and sight pathways were drastically (>90%) reduced. The visual cortex was replaced by somatosensory cortex (26–28), *Per* homologous ACNGGN-repeats cycle in the hypothalamus (29) and melatonin precursors occur in the harderian and pineal glands and retina (30).

What is the genetic basis of circadian rhythmicity in *Spalax*? We cloned, sequenced, and unraveled the expression of the circadian *Clock* and *MOP3* cDNAs of three species of the *S. ehrenbergi* superspecies in Israel (8). Both genes are relatively conserved, yet *Clock* displays a unique Q-rich area as compared with other mammals, assumed to function in circadian rhythmicity, and *Spalax* CLOCK/MOP3 dimer is less potent than its human counterpart in driving transcription.

Here we describe the cloning, sequencing, and expression of the three *Period* cDNAs of *Spalax*. Its three *Per* cDNAs are conserved, yet they show features unique to *Spalax* especially in *Per3*, *Per1*, and *Per2* cycles in the SCN, eye, and harderian gland. *Per3* is structurally unique among studied sighted mammals and awaits functional elucidation.

Materials and Methods

Animals. We analyzed adults (100–150 g), belonging to *Spalax judaei*, ($2n = 60$) from Anza, Samaria (7). Field-trapped animals were kept at 22–24°C with seasonal photoperiod. We selected diurnal animals that were kept under a 12-h light/12-h dark cycle. For analysis of *Per* transcriptional activity in constant darkness, light was turned off at Zeitgeber time (ZT) 12, and animals were kept in the dark for at least 2 days before being killed under dim illumination (15-W safety red light). Light inducibility experiments were done on animals kept in light/dark for a week with a short light pulse (15 min, >200 Lx) at specified ZT followed by release into constant darkness. For gene induction analysis brains were taken 1 h after illumination. Each experiment was done on three sets of animals.

Abbreviations: SCN, suprachiasmatic nuclei; ZT, Zeitgeber time; RT-PCR, reverse transcription–PCR; ISH, *in situ* hybridization; CK1ε, casein kinase 1ε.

Data deposition: The sequences reported in this paper have been deposited in the GenBank database (accession nos. AJ345059–AJ345062).

†A.A. and H.O. contributed equally to this work.

‡To whom reprint requests should be addressed. E-mail: aaron@esti.haifa.ac.il.

‖Kushnirov, D., Beolchini, F., Lombardini, F. & Nevo, E., Euro-American Mammal Congress, July 24–28, 1998, Santiago de Compostela, Spain, p. 381.

www.pnas.org/cgi/doi/10.1073/pnas.182423299

Cloning of *Spalax Per* cDNAs. We cloned the three *Spalax Per* cDNAs by reverse transcription–PCR (RT-PCR) (31). Oligos were synthesized according to the ORF of the known human and mouse homologous sequences (GenBank accession nos. AF022991, AB002370, and AB047686 for human *Per1, Per2*, and *Per3*, respectively and AF022992, AF036893, and AB013605 for mouse *Per1, Per2*, and *Per3*, respectively). Whole brain total RNA was prepared by using the TriReagent RNA isolation reagent (Molecular Research Center, Cincinnati). First-strand cDNA was synthesized with oligo(dT) as a primer and Super-Script II reverse transcriptase enzyme (GIBCO/BRL). This cDNA product was taken for PCR by using *Taq*DNA polymerase (Appligene, Strasbourg, France). The annealing temperature, elongation time, and $MgCl_2$ concentration were adjusted for each specific PCR. In the case of *sPer3* isolation, we verified our RT-PCR results by also cloning through cDNA library screening (32). *Spalax* brain cDNA library in Lambda-TripleEx was screened by using a partial *mPer3* cDNA as a probe. Sequencing was determined by thermocycling sequencing using di-deoxy nucleotide terminators (3700 DNA Analyzer, Perkin–Elmer/Applied Biosystems) at the sequencing unit of the Weizmann Institute of Science (Rehovot, Israel).

Evolutionary Analysis. The evolutionary analysis of the *Per* cDNAs presented here is based on distances and divergence calculations (Wisconsin package version 10, GCG).

The DISTANCES program (33) calculates pairwise distances between aligned sequences expressed as substitutions per 100 bases or amino acids. To correct the distances for multiple substitutions at a site, we used Kimura's nucleic acid (33) and protein (34) methods.

The DIVERGE program estimates the pairwise number of synonymous and nonsynonymous substitutions per site between two or more coding aligned nucleic acid sequences (35, 36).

***In Situ* Hybridization (ISH).** Tissues used for ISH were treated and examined as described in Albrecht *et al.* (37). The *Spalax Per1* probe corresponded to nucleotides 615-1300, the *sPer2* probe corresponded to nucleotides 85–605, and the probe of *sPer3* corresponded to nucleotides 1751–2590.

Quantification was performed by densitometric analysis of hybridization signals on x-ray films with Scion (Frederick, MD) IMAGE 4.0.2 software. For silver grain images, tissue was visualized by fluorescence of Hoechst dye-stained nuclei, and silver grain signals were artificially colored for clarity. Quantitation of ISH results was analyzed with GraphPad (San Diego) PRISM software. Data sets were compared by ANOVA with subsequent Bonferroni correction for multiple comparisons, with $P < 0.05$ as the criterion of significance.

Quantitative RT-PCR. For quantitation of the *sPer* genes expression in the harderian gland and the liver of *Spalax*, a quantitative RT-PCR was performed. Equal amounts of total RNA from animals killed at the relevant ZT points were taken for first-strand cDNA synthesis (see above). The cDNAs were synthesized by adding equal traces of [^{32}P]dCTP to ensure equal amounts of cDNA templates in the PCRs. For the PCR we used oligos synthesized according to the sequence of the different *sPer* isolated clones. For each *Per* gene quantitation we used one sense 5′ oligo and two antisense 3′ oligos (3′[1] and 3′[2]), giving rise to two distinct products (450–600 bp). One set of oligos (5′ and 3′[1]) was used for the harderian gland and the other (oligos 5′ and 3′[2]) for the liver, in the same PCR tube. A second PCR was carried out by changing the 3′ oligo between the harderian and liver tissues. In each PCR, a 300-bp fragment of actin, as an internal control, was also synthesized, using specific actin oligos. Each cDNA was first tested for different PCR amplification cycles with the different sets of oligos. The final experimental PCRs were performed at the logarithmic phase of the reaction for each specific cDNA of interest (18–22 cycles). Each experiment was carried out on two RNA samples taken from two different individuals, and each PCR was repeated three times. The PCR products were then run on ethidium bromide/1.3% agarose gels. The gels were subjected to quantitation of the specific bands by the Eagle Eye II system (Stratagene). The system integrates the density of the ethidium bromide of a rectangle limiting a specific band in pixel values. The values received for the specific *Per* bands were normalized according to the values received for the actin bands (which were statistically equal in the different tissues and in the different reactions).

Results

Cloning and Structural Analysis of the Three *Spalax Per* (*sPer*) Genes. Analysis of the ORFs of *Spalax Per* cDNAs revealed transcripts of 1,062 aa residues for *sPER1* (GenBank accession no. AJ345059) and 1,248 aa for *sPER2* (GenBank accession no. AJ345060). For *sPER3* we isolated two truncated deduced proteins, one with 489 aa (isoform a, GenBank accession no. AJ345061) and the other with 583 aa (isoform b, GenBank accession no. AJ345062). Identified functional domains like the PAS domain and the basic helix–loop–helix motif are highly similar in sPER1 and sPER2, but the homology in sPER3 is low. The recently identified casein kinase 1ε (CK1ε) binding site of human PER2 and the five putative phosphorylation sites (AA 668, 671, 674, 677, and 680) (38) are conserved in PER proteins of *Spalax*, mice, and humans with the exception of sPER3. Hence sPER3 is probably not a substrate for the *Spalax* CK1ε ortholog.

Evolutionary Analysis of the *Spalax Per* Genes. Protein trees of PER1, PER2, and PER3 in *Spalax*, mice, rats, and humans appear in Fig. 1. The *Drosophila* Per (GenBank accession no. X03636) was also compared, but it was very different from the three mammalian Per proteins. The computer program used (GCG10) estimated the distance of the dPer from its mammalian counterparts as maximal and beyond the accuracy of the method.

The estimated divergence time between *Spalax* and other rodents is much shorter than the divergence between humans and rodents. Therefore, we expected that the genetic distance between *Spalax* and mice or rats would be considerably smaller than between humans and these two rodents. We also expected that the distance between humans and *Spalax* and between humans and mice or rats would be similar. Any divergence from these expectations can suggest that additional factor(s) influence the rate of evolution of the *Per* genes of *Spalax* and, therefore, deviate from the phylogenetic divergence time.

Below we present the evolutionary analysis for each *Per* gene separately.

Per1. There is agreement between the above evolutionary expectations and the PER1 proteins (Fig. 1 *Top*) and *Per1* nucleotide sequence (tree not shown). The relative distances in protein and nucleotides between *Spalax* and mice are 75% (6.85 vs. 9.12) and 80% (10.51 vs. 13.18) of the distances between *Spalax* and humans, respectively. The distances between rodents (*Spalax* and mice) and humans are similar: 9.12 and 8.04 in the protein and 13.18 and 13.26 in the nucleotide sequence.

Per2. Rat PER2 (GenBank accession no. MN031678) was also included and expected to be similar to mouse PER2. As in Per1, PER2 results were in agreement with the phylogenetic expectations (Fig. 1 *Middle*). The relative distances between *Spalax* and mice were 42% (11.55 vs. 27.54) or 59% (13.07 vs. 22.09) of the distances between *Spalax* and humans in protein and nucleotides, respectively. The distances between *Spalax* and rats were 46% (12.69 vs. 27.54) or 66% (14.6 vs. 22.09) of the distances between *Spalax* and humans in protein and nucleotides, respectively. The distances between rodents (mice, rats, and *Spalax*)

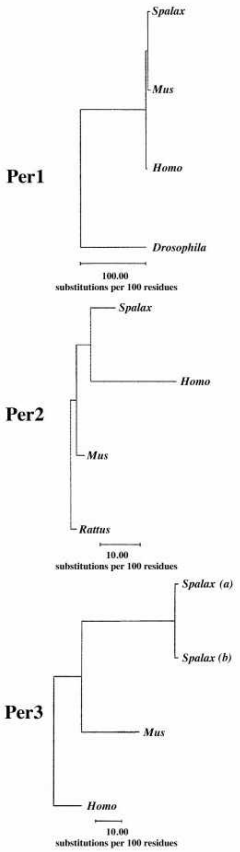

Fig. 1. Similarity tree of the three Per-deduced proteins. The unrooted tree depicts the similarity relationships of the three PER proteins (amino acids) in *Spalax*, mice, rats, humans, and *Drosophila*.

and humans were also similar: 27.00, 27.70, and 27.54 for protein and 22.56, 23.58, and 22.09 for nucleotides, respectively.

Per3. As mentioned, we cloned two truncated clones of *Spalax Per3* (named a and b). Both clones start at the equivalent of mouse 468 bp (110 bp 3′ to the mouse ATG initiation codon). We could not isolate any further 5′ sequences either through RT-PCR or cDNA library screening. Both clones contain an insertion of 198 bp at position 1211 bp of mice that interrupts the ORF. Furthermore, *sPer3*a has two deletions, the prominent one is 432 bp in length starting at position 1478 bp of the mouse sequence. At the starting point of this deletion in *sPer3*a, *sPer3b* has a cluster of termination codons at any of the three reading frames. The apparent initiation ATG is located immediately after the deletion in the *sPer3*a or these termination codons in *sPer3b*. Omitting the changes in the *sPer3b* clone yielded a *Spalax Per3* ORF, which is similar to that of mice and humans. It should be emphasized that similar products have never been obtained in negative control amplifications with templates generated

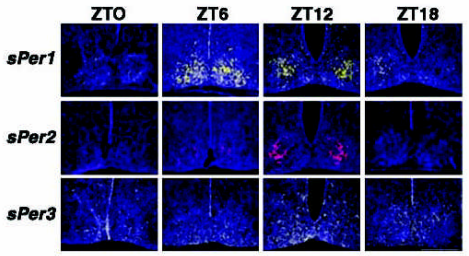

Fig. 2. Diurnal expression of *sPer1*, *sPer2*, and *sPer3* of *Spalax* in the SCN: coronal sections through the brain. Blue color represents Hoechst-stained nuclei. (*Top*) The yellow signal shows the expression of *Spalax Per1* over 24 h measured at 6-h time intervals (ZT0: lights on; ZT12: lights off). Maximal expression is seen at ZT6. (*Middle*) The red signal shows the expression of *sPer2* in representative sections. Maximal expression is seen at ZT12. (*Bottom*) The green signal shows the expression of *sPer3* in representative sections. Maximal expression is at ZT12. Note that *sPer1* and *sPer2* expression is mainly in the SCN, whereas *sPer3* expression is weaker and spreads in different areas of the brain. (Magnification: ×20.)

without reverse transcriptase enzyme, eliminating the possibility of genomic DNA contamination. Furthermore, the *sPer3* clones that were isolated from the *Spalax* brain cDNA library contain a shorter 3′ untranslated region than those of mice and humans, and in contrast to them, contain an adenylation site 940 bp 3′ to the termination TAA codon. The published 3′ untranslated regions of mice (1,164 bp) and humans (2,421 bp) do not reach the adenylation site. Southern blot analyses suggest that the *Spalax sPer3* is probably a pseudogene (results not shown).

The nucleotide distances between *Spalax Per3* and that of mice or humans are similar. The protein distances (Fig. 1 *Bottom*) between the two *Spalax* PER3 and mice or humans were 56.21 vs. 57.20 for sPER3a, respectively and 60.41 vs. 57.74 for sPER3b, respectively. Kimura's two-parameter nucleotide distance analysis (33) gave more than two substitutions per bp. Thus, the exact calculated value is meaningless and depends heavily on the assumptions of the correction factors. Nevertheless, the calculated distance of *Spalax* vs. mice is even larger than the calculated distance of *Spalax* vs. humans. The same is true for the distances calculated separately for synonymous and nonsynonymous substitutions.

Synonymous vs. Nonsynonymous Substitutions in the *Per* Family. Our calculations show that *Per2* has a ratio around 0.2, indicating that it attained optimum function before the divergence of the species. *Per1* and *Per3* have a ratio of 0.43 to 0.75, a relatively high ratio suggesting adaptive evolution. The *Drosophila Per* showed a ratio >1.0, indicating positive selection for a functional change.

sPer Genes Oscillate in the *Spalax* SCN. ISH with antisense riboprobes in the brain revealed a rhythmic pattern of expression for *sPer1* and *sPer2*, mainly in the SCN but *sPer3* is widely spread in the brain (Fig. 2). Maximal expression for *sPer1* was at ZT6 and for *sPer2* and *sPer3* at ZT12. The amplitude of *sPer3* expression was markedly lower ($P < 0.05$) than that of *sPer1* and *sPer2*. The sense (control) riboprobes of the three *sPer* had a reproducible background hybridization that did not overlap with the antisense probe. No rhythmic expression with the sense riboprobe hybridization intensity was noted.

sPer Genes Exhibit a Diurnal Oscillation in *Spalax* Peripheral Tissues. Significant expression of the three *sPer* genes was noted, using RT-PCR, in lung, intestine, liver, harderian gland, eye, brain, and skeletal muscle (data not shown).

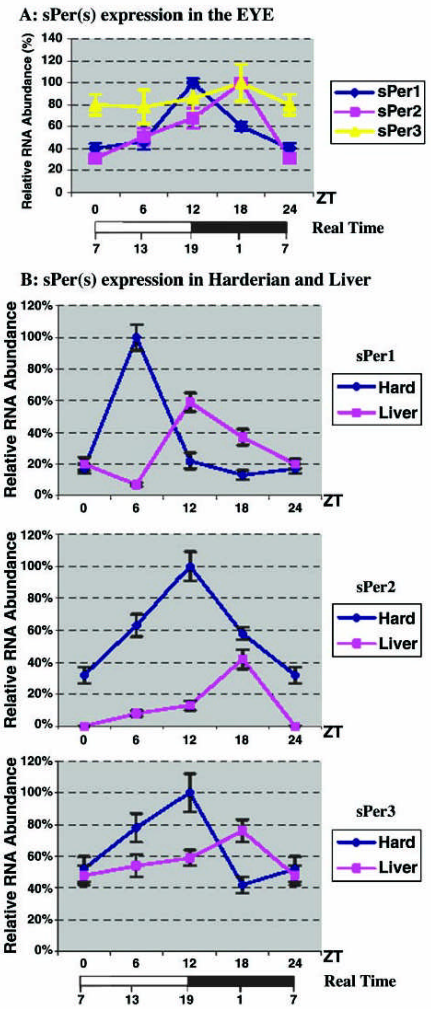

Fig. 3. Expression of *Spalax Per* genes in peripheral tissues. (*A*) Densitometric analysis of silver grain *in situ* staining in the eye. The maximal expression in the eye shows that the expression of the three *sPer* genes is shifted by 6 h as compared with their expression in the SCN (Fig. 2). The oscillation of *sPer3* is very weak ($P > 0.05$). (*B*) Expression of the three *sPER* genes in the harderian gland and liver quantitated by RT-PCR. The expression peaks of all three *sPer* genes in the harderian gland are synchronized with the SCN (see Fig. 2), whereas the peak of expression in the liver is shifted by 6 h. As in the SCN, the difference in *sPer3* expression in ZT6 and ZT12 is very small ($P > 0.05$).

The *Spalax* Eye. In the *Spalax* eye (Fig. 3*A*) ISH revealed a shift of 6 h in the expression maxima of all three *Per* genes compared with the expression in the SCN. Expression of *sPer1* was maximal at ZT12 and of *sPer2* and *sPer3* at ZT18, but for *sPer3*, the amplitude of expression was very small. Thus the RNA rhythms for all three *Per* genes of *Spalax* are present in the photoperiodic retina, the site of light detection.

The *Spalax* Harderian Gland. Expression maxima in the harderian gland could be observed by quantitative RT-PCR (Fig. 3*B*) and ISH (data not shown) at the following ZTs: *sPer1* at ZT6 and *sPer2* and *sPer3* at ZT12. Quantitative RT-PCR analysis in the liver (Fig. 3*B*) revealed rhythmic expression of *sPer* genes with maxima of *sPer1* at ZT12 and of *sPer2* and *sPer3* at ZT18. The oscillation in the *Spalax* liver, as in its eye, shows a 6-h delay compared with the *Spalax* SCN. However, the circadian rhythm in the *Spalax* harderian gland is synchronous with the expression pattern in the *Spalax* SCN.

The Circadian Oscillation of *sPer* Genes Is Maintained in Constant Darkness. *sPer* gene RNA levels in the SCN, eye, and harderian gland were studied at four time points over a 24-h period, on the second day in constant darkness (not shown). ISH revealed that RNA levels of all three *sPer* genes were rhythmic and the oscillation pattern under constant darkness was similar to that under 12-h light/12-h dark conditions. Highest levels were observed during the subjective day in the SCN at circadian time 6 for *sPer1* and circadian time 12 for *sPer2* and *sPer3*. The peak levels of mRNA in the eye were 6 h later than in the SCN, but were synchronized with the SCN in the harderian gland. The amplitude of *sPer3* rhythmicity was markedly lower than that of *sPer1* and *sPer2* in all three tissues studied and only nearly significant ($P > 0.05$).

Differential Light Regulation of *Spalax Per* Genes. Previous studies have shown that *mPer1* and *mPer2* expression in the SCN is induced by exposure to light at night (39, 40), whereas *mPer3* is unaffected (41). We examined inducibility of the *sPer* genes in the SCN, eye, and harderian gland by nocturnal light pulses at ZT14 and ZT22 (Fig. 4). These time points were chosen for study as light pulses at these times produce phase delays and advances in locomotor activity.

Quantitation of the *in situ* results showed that 1 h after a light pulse at ZT14, *sPer1* and *sPer2* were significantly induced in all three tissues. Remarkably, the level of *sPer1* induction in the harderian gland was significantly ($P < 0.05$) higher than in the SCN or the eye, reinforcing its great importance for the *Spalax* clock. One hour after the light pulse at ZT22 only *sPer1* was significantly induced in the three tissues examined. Like the *sClock* gene, *sPer3* gene was not light inducible either at ZT14 or ZT22 in the three tissues tested.

Discussion

Adaptive Selection on *Per* Genes in *Spalax* to Life Underground in Total Darkness. Like other mammals, the subterranean blind *Spalax* has three *Per* genes.

The distances between *sPer1* and *sPer2* and those of other rodents or humans are as expected from their divergence time, which is estimated to be 40 million years ago and 80 million years ago, respectively (6). The distances between *Spalax* or mice and humans are similar, as expected. Generally, the distances calculated for *Per2* are larger than the distances for *Per1*. In our analysis of synonymous vs. nonsynonymous substitutions we relied on Liberles *et al.* (42), who suggested using this ratio to reveal selection for change in enzymatic function. Data of Makalowski and Boguski (43) show that most rodents and human sequences have a ratio of 0.2. This finding indicates that such proteins, selected over millions of years, attained an optimum function before the divergence of rodents and primates and subsequent evolution was relatively conservative. They also considered ratios between 0.6 and 1.0 as suggesting a relaxation of functional constraint and selection. Our results show that *sPer1* and *sPer3* have a ratio of 0.4 to 0.6 and *sPer2* has a ratio of about 0.2. Hence, presumably, *sPer2* has not been changed to

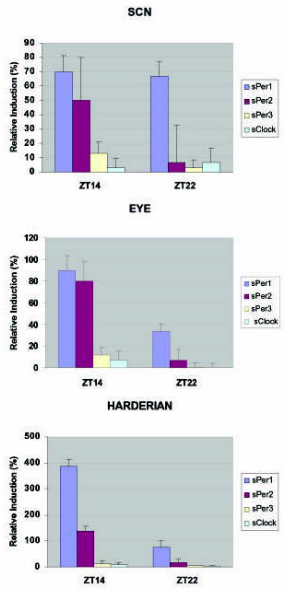

Fig. 4. Light inducibility of the three *Spalax Per* genes' expression. Animals were given a 15-min light pulse at ZT14 and ZT22 and killed 1 h later. Coronal sections through the brain and ISH were performed on treated (ZT14 pulse and ZT22 pulse) and control animals that were killed at the same time. Relative mRNA induction was analyzed by densitometric analysis of *in situ* silver grain staining. *sClock* inducibility is given as negative control. (*Top*) In the SCN, *sPer1* is equally inducible at ZT14 and ZT22. *sPer2* is inducible only at ZT14, whereas *sPer3* gene shows no measurable changes in expression levels at the two time points. (*Middle*) Inducibility of *sPer1*, *sPer2*, and *sPer3* in the eye is similar to that in the SCN. (*Lower*) In the harderian gland, *sPer1* is highly inducible at ZT14 and less at ZT22 whereas *sPer2* expression is light sensitive only at ZT14. *sPer3* shows no light inducibility at either time point. Note the significantly ($P < 0.01$) higher induction of *sPer1* in the harderian gland compared with the other tissues after light pulse at ZT14. Note the different *y*-axis scales in SCN, eye, and harderian.

function in a visually blind mammal living in a dark environment with negligible light cues. However, the figures obtained for *sPer1* and *sPer3* may suggest that molecular changes in these genes were necessary to fulfill their expected adaptive function in darkness. If we combine the calculated distances and the high ratio of nonsynonymous substitutions, the result supports the hypothesis of adaptive changes caused by natural selection, possibly in response to life in darkness underground.

sPer3 evinces a different situation. First, this locus in *Spalax* underwent major changes of deletions and insertions, resulting in two isoforms exhibiting truncated coding regions; somewhat similar results were reported for the *hPer4* pseudogene (44). However, *sPer3* is very different from *hPer4*. Its insertion could not be identified with any known sequence, in contrast to the fossil MER-2 mobile element that is within the *hPer4* locus (44). When the changes in the *sPer3* are omitted, an ORF similar to *mPer3* is obtained. When the distances were calculated from the aligned shortened sequences the phylogenetic expectations were not met. The distances between *sPer3* and *mPer3* are similar or even larger than the distances between *sPer3* and *hPer3*. This finding may support adaptive selective changes in the evolution of this gene and not just the neutral accumulation of substitutions over time. The comparison of *sPer3* expression patterns with *sPer1* and *sPer2*, which was described here and is discussed below, raises questions as to the role that *sPer3* plays in the *Spalax* circadian system.

The Functional Circadian Domains of *Spalax Per* Genes. *sPer1* and *sPer2* contain all functionally relevant domains discovered in other mammalian PER proteins so far. The basic helix–loop–helix motif as well as the PAS domain consisting of PAS A, PAS B (39, 45), and PAC CK1ε binding and phosphorylation sites (38) are conserved, suggesting their role as a CK1ε substrate in the central mechanism of the *Spalax* circadian clockwork. Remarkably, the whole putative CK1ε binding site as well as the N-terminal basic helix–loop–helix motif are missing in *sPer3*. This finding supports a speculation about its role in the biological clock (45).

Because *Spalax* is visually blind and lives entirely underground, hence denied outside Zeitgeber information (6), a robust and precise internal clock is necessary for the animal to keep track of time under negligible light cues. Indeed, *in situ* data revealed that *Spalax Per* genes' expression is clearly rhythmic and maintained under constant conditions and in constant darkness. *sPer1* and *sPer2* expression in the *Spalax* brain is concentrated mainly in the SCN. However *sPer3* is widely spread in different areas of the brain, similar to what has been reported for the mouse *Per3* (41), and its oscillation levels are less prominent than those of *sPer1* and *sPer2*. These findings raise a question as to the role of *Per3* in the circadian system. The central pacemaker of the SCN signals time to the retina and peripheral clocks, as in the liver, where the circadian genes' expression follows its rhythm with a delay of 4–6 h (41, 46). The blind *Spalax Per* genes' expression is similar, and our results also show a lag of 6 h in the peak expression of the *Per* genes in the retina and liver. Although the exact role of *Spalax Per3* in the maintenance of the circadian rhythm remains unresolved, it may prove substantial for time keeping underground.

The Harderian Gland: A Circadian Center in *Spalax*. Noteworthy, mRNA levels in the *Spalax* hypertrophic harderian gland oscillate synchronously with the SCN. Similar synchronization in the peak levels of mRNA in the SCN and the harderian gland was seen also for *Spalax MOP3* gene (8), the dimerization partner of the CLOCK protein (47) and an essential component of the circadian pacemaker in mammals (48). Furthermore, *sPer1* inducibility in the harderian gland after light pulse during the dark phase of the clock cycle is much higher than in the SCN. The harderian gland of *Spalax* is extraordinarily enlarged and occupies the entire eye socket, presumably as an adaptation to life underground. Previous studies (15) suggested that the harderian gland of *Spalax* is a possible photoreceptor and photoperiodic organ. Given its exposed position directly behind the atrophied minute eye, it seems likely that the harderian gland has a prominent role in the *Spalax* clock mechanism. This gland may demonstrate the extreme of evolutionary progression during the adaptive morphological and molecular reorganization for life underground (6).

Differential Regulation of *Spalax Per* Genes. Light inducible experiments in *Spalax* reveal that *sPer1* is light inducible both early (ZT14) and late (ZT22) at night, whereas *sPer2* is light inducible only at the beginning of the night. This result is in accordance with the findings of Albrecht *et al.* (39). *sPer3* levels are unresponsive to light pulses applied throughout the dark phase of the circadian cycle. This differential regulation among the three *sPer* genes suggests that each has a different regulatory function in the SCN. The behavioral effects of photic stimuli at these two time points (ZT14 and ZT22) have been characterized in mice (49, 50). Light pulse at ZT14 causes phase delays in behavioral rhythms and light pulse at ZT22 causes phase advances. Our results indicate a role of *sPer1* in both phases and of *sPer2* in the phase-delay mechanism. Our *in situ* data provide a molecular confirmation of previous

behavioral studies in *Spalax* (11) and link the activity pattern of these species with the cellular cycling in sighted animals. The poor *sPer3* oscillation and the absence of light influence on *sPer3* expression levels may suggest a role for *sPer3* outside the central pacemaker. This finding is consistent with data from *Per3*-deficient mice (51, 52) but may prove an adaptation to life underground and deserves further critical studies.

All three *Spalax Per* genes are expressed in a wide variety of nonneural tissues as previously shown in *Drosophila* (53, 54) and mice (39, 41). In three of these tissues (liver, eye, and harderian gland) we found that the RNA levels for the three *sPer* genes oscillate. Oscillation of *sPer* genes in the eye, the target organ of light absorption, is rational. As we already suggested, the oscillation of the *sPer* genes in the *Spalax* harderian gland is in accordance with previous results, suggesting an important role of this tissue in circadian maintenance (15) and merits further intensive study. The oscillation in the liver and the widespread expression in other peripheral tissues that were examined suggest the existence of clocks outside the SCN.

Molecular-Genetic Tinkering of Circadian Genes in a Blind Mammal. This study substantiates the claim that the blind subterranean *Spalax* needs a photoperiodic system to perceive daily and seasonal cycles. It has retained a functional retina with effective visual pigment genes signaling to the SCN (14, 17–20, 23, 24) presumably induced by the small amount of photons that penetrate underground to an otherwise dark environment. Circadian genes in the retina, harderian gland, SCN, and other tissues, including *Clock* (8) and the three *Per* genes described here, process the light signals and translate them into the unique behavioral repertoire of *Spalax*, including polyphasic, polymorphic, and seasonal behavioral phenotypes. In this respect we should emphasize that *Spalax* exhibits naturally occurring predominantly either diurnal or nocturnal individuals. Currently we are studying the expression pattern of the *Per* genes in naturally occurring nocturnal animals or on diurnal animals after a phase shift of light. The mosaic evolution of the *Spalax* eye (17, 18), harderian gland (30), and brain (26–28) and its circadian genes provide a striking model of tinkering evolution at both the molecular and organismal levels. From an evolutionary perspective the genetic basis of circadian rhythms in the blind subterranean *Spalax* may be different from that of strictly diurnal or nocturnal and sighted mammals. Identification of the circadian genes of blind *Spalax* might advance insights into the structure and evolution of the circadian organization in mammals, including humans, at the molecular level and their ecological causation. Remarkably, the colonization of the subterranean dark ecological zone by *Spalax* did not obliterate the conservative circadian rhythmicity and its genetic basis of photoreceptiveness and clock genes. All of the circadian machinery was adaptively transformed to perceive light in darkness.

We thank Dr. Z. S. Sun for his initial help with the cloning of the *Spalax Per1* probe. We are also grateful to Mr. Michael Margulis for his help with the computer graphic work. This work was supported by the Max Planck Society and Deutsche Forschungsgemeinschaft Grant AL549/1-1 (to U.A.) and the Ancell-Teicher Research Foundation for Genetics and Molecular Evolution (to E.N.).

1. Lowrey, L. P. & Takahashi, J. S. (2000) *Annu. Rev. Genet.* **34,** 533–562.
2. Pittendrigh, C. S. (1993) *Annu. Rev. Physiol.* **55,** 15–54.
3. Dunlap, J. C. (1999) *Cell* **96,** 271–290.
4. Hastings, M. & Maywood, E. S. (2000) *BioEssays* **22,** 23–31.
5. Nevo, E. (1991) *Evol. Biol.* **25,** 1–125.
6. Nevo, E. (1999) *Mosaic Evolution of Subterranean Mammals: Regression, Progression, and Global Convergence* (Oxford Univ. Press, Oxford).
7. Nevo, E., Ivanitskaya, E. & Beiles, A. (2001) *Adaptive Radiation of Blind Subterranean Mole Rats* (Backhuys, Leiden).
8. Avivi, A., Albrecht, U., Oster, H., Joel, A., Beiles, A. & Nevo, E. (2001) *Proc. Natl. Acad. Sci. USA* **98,** 13751–13756.
9. Nevo, E. (1998) in *Principles of Animal Design*, eds. Weibel, E. R., Taylor, C. R. & Bolis, C. (Cambridge Univ. Press, Cambridge, U.K.), pp. 288–298.
10. Nevo, E., Guttman, R., Haber, M. & Erez, E. (1982) *J. Mamm.* **63,** 453–463.
11. Tobler, I., Herrmann, M., Cooper, H. M., Negroni, J., Nevo, E. & Achermann, P. (1998) *Behav. Brain Res.* **96,** 173–183.
12. Ben-Shlomo, R., Ritte, U. & Nevo, E. (1995) *Behav. Genet.* **25,** 239–245.
13. Haim, A., Heth, G., Pratt, H. & Nevo, E. (1983) *J. Exp. Biol.* **107,** 59–64.
14. Sanyal, S., Jansen, H. G., de Grip, W. G., Nevo, E. & De Jong, W. W. (1990) *Invest. Ophthalmol. Visual Sci.* **31,** 1398–1404.
15. Pevet, P., Heth, G., Haim, A. & Nevo, E. (1984) *J. Exp. Zool.* **232,** 41–50.
16. Rado, R., Gev, H., Goldman, B. D. & Terkel, J. (1991) in *Photobiology*, ed. Riklis, E. (Plenum, New York), pp. 581–589.
17. Cooper, H. M., Herbin, M. & Nevo, E. (1993) *Nature (London)* **361,** 156–159.
18. Cooper, H. M., Herbin, M. & Nevo, E. (1993) *J. Comp. Neurol.* **328,** 313–350.
19. DeGrip, W. J., Janssen, J. J. M., Foster, R. G., Korf, H. W., Rothschild, K. J., Nevo, E. & de Caluwe, G. L. J. (1992) in *Signal Transduction in Photoreceptor Cells*, eds. Hargrave, P. A., Hofmann, K. P. & Kaupp, U. B. (Springer, Berlin), pp. 43–59.
20. Janssen, J. W. H., Bovee-Geurts, P. H. M., Peeters, Z. P. A., Bowmaker, J. K., Cooper, H. M., David-Gray, Z. K., Nevo, E. & DeGrip, W. J. (2000) *J. Biol. Chem.* **275,** 38674–38679.
21. Argamaso, S. M., Froehlich, A. C., McCall, M. A., Nevo, E., Provencio, I. & Foster, R. G. (1995) *Biophys. Chem.* **56,** 3–11.
22. David-Gray, Z. K., Janssen, J. W. H., Nevo, E. & Foster, R. G. (1998) *Nat. Neurosci.* **12,** 655–656.
23. David-Gray, Z. K., Cooper, H. M., Jannsen, J. W. H., Nevo, E. & Foster, R. G. (1999) *FEBS Lett.* **461,** 343–347.
24. Avivi, A., Joel, A. & Nevo, E. (2001) *Gene* **264,** 45–49.
25. Vuillez, P., Herbin, M., Cooper, H. M., Nevo, E. & Pevet, P. (1994) *Brain Res.* **654,** 81–84.
26. Rehkamper, G., Necker, R. & Nevo, E. (1994) *J. Comp. Neurol.* **347,** 570–584.
27. Frahm, H. D., Rehkamper, G. & Nevo, E. (1997) *J. Brain Res.* **38,** 209–222.
28. Mann, M. D., Rehkamper, G., Reinke, H., Fraham, H. D., Necker, R. & Nevo, E. (1997) *J. Brain Res.* **38,** 47–59.
29. Ben-Shlomo, R., Ritte, U. & Nevo, E. (1996) *Behav. Genet.* **26,** 177–184.
30. Balemans, M. G. M., Pevet, P., Legerstee, W. C. & Nevo, E. (1980) *J. Neural Transm.* **49,** 247–255.
31. Veres, G., Gibbs, R. A., Scherer, S. E. & Caskey, C. T. (1987) *Science* **237,** 415–417.
32. Maniatis, T., Fritsch, E. F. & Sambrook, J. (1982) *Molecular Cloning: A Laboratory Manual* (Cold Spring Harbor Lab. Press, Plainview, NY).
33. Kimura, M. (1983) *The Neutral Theory of Molecular Evolution* (Cambridge Univ. Press, Cambridge, U.K.).
34. Kimura, M. (1980) *J. Mol. Evol.* **16,** 111–120.
35. Li, W. H., Wu, C. I. & Luo, C. C. (1985) *Mol. Biol. Evol.* **2,** 150–174.
36. Li, W. H. (1993) *J. Mol. Evol.* **36,** 96–99.
37. Albrecht, U., Lu, H.-C., Revelli, J.-P., Xu, X.-C., Lotan, R. & Eichele, G. (1998) *Human Genome Methods* (CRC, New York), pp. 93–119
38. Toh, K. L., Jones, C. R., He, Y., Eide, E. J., Hinz, W. A., Virshup, D. M., Ptacek, L. J. & Fu, Y. H. (2001) *Science* **291,** 1040–1043.
39. Albrecht, U., Sun, Z. S., Eichele, G. & Lee, C. C. (1997) *Cell* **91,** 1055–1064.
40. Shearman, L. P., Zylka, M. J., Weaver, D. R., Kolakowski, L. F. & Reppert, S. M. (1997) *Neuron* **19,** 1261–1269.
41. Zylka, M. J., Shearman, L. P., Weaver, D. R. & Reppert, S. M. (1998) *Neuron* **20,** 1103–1110.
42. Liberles, D. A., Schreiber, D. R., Govindarajan, S., Chamberlin, S. G. & Benner, S. A. (2001) *Genome Biol.* **2,** 1–6.
43. Makalowski, W. & Boguski, M. S. (1998) *Proc. Natl. Acad. Sci. USA* **95,** 9407–9412.
44. Gotter, A. L. & Reppert, M. S. (2001) *Mol. Brain Res.* **92,** 19–26.
45. Zheng, B., Larkin, D. W., Albrecht, U., Sun, Z. S., Sage, M., Eichele, G., Lee, C. C. & Bradley, A. (1999) *Nature (London)* **400,** 169–173.
46. Sun, Z. S., Albrecht, U., Zhuchenko, O., Bailey, J., Eichele, G. & Lee, C. C. (1997) *Cell* **90,** 1003–1011.
47. Hogenesch, J. B., Gu, Y. Z., Jain, S. & Bradfield, C. A. (1998) *Proc. Natl. Acad. Sci. USA* **95,** 5474–5479.
48. Bunger, M. K., Wilsbacher, L. D., Moran, S. M., Clendenin, C., Radcliffe, L. A., Hogenesch, J. B., Simon, M. C., Takahashi, J. S. & Bradfield, C. A. (2000) *Cell* **103,** 1009–1017.
49. Schwartz, W. J. & Zimmerman, P. (1990) *J. Neurosci.* **10,** 3685–3694.
50. Albrecht, U., Zheng, B., Larkin, D., Sun, Z. S. & Lee, C. C. (2001) *J. Biol. Rhythms* **16,** 100–104.
51. Shearman, L. P., Jin, X., Lee, C., Reppert, S. M. & Weaver, D. R. (2000) *Mol. Cell. Biol.* **20,** 6269–6275.
52. Bae, K., Jin, X., Maywood, E. S., Hastings, M. H., Reppert, S. M. & Weaver, D. R. (2001) *Neuron* **30,** 525–536.
53. Hardin, P. E. (1994) *Mol. Cell. Biol.* **14,** 7211–7218.
54. Plautz, J. D., Kaneko, M., Hall, J. C. & Kay, S. A. (1997) *Science* **279,** 1632–1635.

2.6. Publication: "A Switch from Diurnal to Nocturnal Activity in the Mole Rat *Spalax Ehrenbergi* Superspecies is Accompanied by an Uncoupling of the Light Input and the Circadian Clock"

Henrik Oster*, Aaron Avivi*, Alma Joel, Urs Albrecht, and Eviatar Nevo

***** these authors contributed equally to this work

Current Biology, Vol. 12, 1919-1922, November 19, 2002

Current Biology, Vol. 12, 1919–1922, November 19, 2002, ©2002 Elsevier Science Ltd. All rights reserved. PII S0960-9822(02)01263-0

A Switch from Diurnal to Nocturnal Activity in *S. ehrenbergi* Is Accompanied by an Uncoupling of Light Input and the Circadian Clock

Henrik Oster,[1,4] Aaron Avivi,[2,4,5] Alma Joel,[2] Urs Albrecht,[1,3] and Eviatar Nevo[2]
[1]Department of Medicine
Division of Biochemistry
University of Fribourg
1700 Fribourg
Switzerland
[2]Institute of Evolution
University of Haifa
Mount Carmel
Haifa 31905
Israel

Summary

The subterranean mole rat *Spalax ehrenbergi* superspecies represents an extreme example of adaptive visual and neuronal reorganization [1, 2]. Despite its total visual blindness, its daily activity rhythm is entrainable to light-dark cycles [3], indicating that it can confer light information to the clock. Although most individuals are active during the light phase under laboratory conditions (diurnal animals), some individuals switch their activity period to the night (nocturnal animals) [3, 4]. Similar to other rodents [5], the *Spalax* circadian clock is driven by a set of clock genes, including the *period* (*sPer*) genes [6, 7]. In this work, we show that diurnal mole rats express the *Per* genes *sPer1* and *sPer2* with a peak during the light period. Light can synchronize *sPer* gene expression to an altered light-dark cycle and thereby reset the clock. In contrast, nocturnal *Spalax* express *sPer2* in the dark period and *sPer1* in a biphasic manner, with a light-dependent maximum during the day and a second light-independent maximum during the night. Although *sPer1* expression remains light inducible, this is not sufficient to reset the molecular clockwork. Hence, the strict coupling of light, *Per* expression, and the circadian clock is lost. This indicates that *Spalax* can dissociate the light-driven resetting pathway from the central clock oscillator.

Results and Discussion

The circadian clock coordinates the body's physiological, endocrinological, and behavioral status and enables the organism to maximally benefit from temporally available natural resources [8]. At the molecular level, the clock is based on transcriptional/translational feedback loops (TTLs), a principle that is conserved throughout all *phyla*, even though the single components of the loops vary [9]. In mammals, the master circadian clock is located in the hypothalamic *suprachiasmatic nuclei* (SCN) [10]. From here, subordinated clocks in the peripheral organs of the body are synchronized to generate a concerted rhythm for the whole organism [11]. Among the genes driving the clock in the SCN are the two *Period* genes *Per1* and *Per2* [12–14]. Both homologs show a circadian rhythm of activation within the SCN and can serve as markers for the phase of the circadian clock [15–17].

Recent data indicate that, at both the behavioral and the molecular levels, the blind mole rat *Spalax ehrenbergi* superspecies has a functional circadian clock despite its isolated subterranean ecotope [3, 6, 7]. Twenty-five million years of selective adaptation to this environment have resulted in a radical degeneration of its visual system, leading to atrophied (600 μm wide), totally fur-covered eyes that lack any image-forming ability [18]. Interestingly, the degenerated retina contains opsins and melanopsin, which might be responsible for light detection [19, 20]. The SCN, however, is well developed and receives clock-related signals from the retina via the retinohypothalamic tract [7, 18, 21].

Mole rats show a unique polyphasic activity pattern in that they can switch from day activity (diurnal animals) to night activity (nocturnal animals) depending on environmental conditions [4, 22]. Although the majority of all populations studied are more active during the day, activity patterns seem to be highly influenced by temperature and aridity [23]. Compared with above-ground mammals, for a totally blind subterranean herbivore, a change in the time of activity is less crucial for its ability to find food or for its susceptibility to predators. Therefore, the polyphasic nature of *Spalax* rhythmicity may have been evolutionarily stabilized by balancing the need for social interaction in the mating season on one hand and metabolic economy on the other [24].

In the laboratory, activity of animals can be entrained to shifted light-dark cycles, indicating a sensitivity of the circadian clock to light [3, 25]. At the molecular level, three *Period* genes (*sPer1*, *sPer2*, *and sPer3*) as well as a *Clock* and a *MOP3* homolog have been characterized and show circadian expression rhythms and light inducibility similar to their counterparts in other rodents like mice, rats, and hamsters [6, 7]. Experiments with diurnal species like *Arvicanthis niloticus* and *Spermophilus tridecemlineatus* revealed that clock gene expression in these animals is the same as in nocturnal animals; this indicates that the center managing activity is located downstream from the core pacemaker [26, 27].

The great majority of *Spalax* individuals (~80% of 63 total) used in this study displayed a diurnal activity pattern (see [22] as well). To test whether the behavioral adaptation to a shifted light-dark cycle [3] is reflected at the molecular level, we looked for *sPer* gene expression in the SCN of diurnal animals before and after an inversion (12 hr shift) of a 12 hr light/12 hr dark (LD) cycle. As has been shown before [7], in diurnal animals, *sPer1* expression rises during the early day, with a maximum around noon, and has a steady decline throughout the night (Figures 1A and 2C). The *sPer2* expression peaks at the day-night transition, with low levels during

[3]Correspondence: urs.albrecht@unifr.ch
[4]These authors contributed equally to this work.
[5]To whom reprint requests should be addressed.

Current Biology
1920

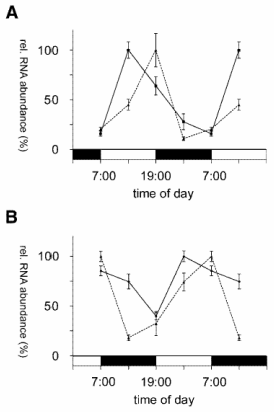

Figure 1. *sPer* Gene Expression in the SCN

(A and B) Expression in (A) diurnal animals and (B) diurnal animals entrained to a 12 hr-shifted LD cycle. Diurnal animals were adapted to a 12 hr light/12 hr dark (LD) cycle and were sacrificed at four different time points throughout the day (7:00, ZT0; 13:00; 19:00; and 1:00). The phase-shift animals were exposed to a 12 hr-shifted LD cycle (19:00, ZT0) and were sacrificed after behavioral adaptation (~1 week, data not shown). Quantitative analysis of *sPer1* (solid line) and *sPer2* expression (dotted line) in the SCN is shown. All values are mean ± SD of three different experiments. Black and white bars indicate dark and light phases, respectively.

the dark period and the early morning (Figures 1A and 2C). Similar expression patterns have been observed in mice [15–17].

After the shift of the LD cycle ("lights on" at 19:00), we examined *sPer1* and -*2* expressions in the SCN after the animals' activity patterns were synchronized to this new light schedule. We found an inverted rhythm in *Period* gene expression, with peaks at 1:00 and 7:00, indicating that the molecular clockwork is reacting to light and adapts readily to new environmental conditions.

Since the *Spalax* clock is light sensitive, what is the explanation for the nocturnal activity pattern of some animals when most are diurnal? To pursue this question, we scanned our colonies for night-active animals. About 20% of all individuals tested displayed a stable nocturnal activity rhythm and were chosen for further experiments (Figures 2A and 2B). We examined *Period* gene expression in these animals to determine whether the observed phenotype was caused by an event in, up-, or downstream of the central oscillator. In LD, *sPer1* shows a biphasic expression — with two maxima, one in the middle of the day and the other at midnight — in nocturnal animals (Figures 2D and 2F). As in diurnal animals, *sPer2* expression shows only one peak of expression, occurring at the end of the activity phase, in nocturnal mole rats (Figures 2C–2F). Maximal *sPer2* expression for nocturnal animals is at *Zeitgeber* time (ZT) 0 (7:00). Hence, in relation to the light/dark cycle, the expression patterns for *sPer1* and *sPer2* are inverted in nocturnal *Spalax* as compared to diurnal *Spalax*, except for the second *sPer1* maximum at ZT6 (13:00).

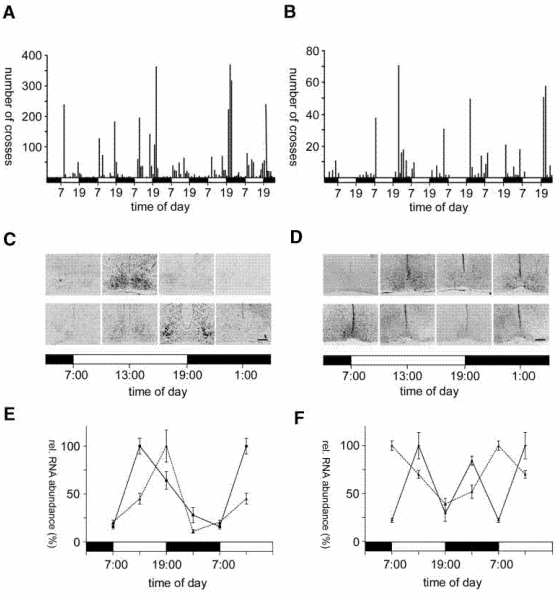

Figure 2. Activity and *sPer* Gene Expression of Nocturnal Animals

(A and B) Typical activity plots of (A) day- and (B) night-active animals measured by crossing events of an infrared beam in the animal's cage.

(C and D) Representative bright-field micrographs of ^{35}S liquid film autoradiographs on coronal brain sections probed for *sPer1* (upper row) and *sPer2* (lower row). (C) Diurnal animals; (D) nocturnal animals in LD. The localization of the SCN was verified by bisbenzimide costaining (not shown).

(E and F) Quantitative analysis (n = 3) of *sPer1* (solid line) and *sPer2* expression (dotted line) in the SCN of (E) day- and (F) night-active animals kept in LD (7:00, ZT0). The scale bar represents 100 μm.

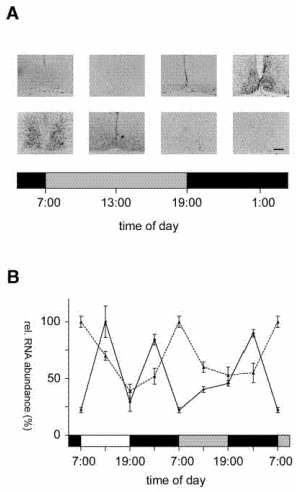

Figure 3. *sPer* Gene Expression in Nocturnal Animals in DD

(A) Night-active animals were released into constant darkness (DD) and were sacrificed every 6 hr of the first day in constant conditions (CT 0, 7:00, with the gray bar approximately indicating subjective day). Upper row: micrographs of *sPer1* in situ hybridization; lower row: *sPer2* probe.

(B) Densitometric analysis (n = 3) of *sPer1* (solid line) and *sPer2* (dotted line) expression in night-active animals released into DD (white bar: light phase of the last LD cycle; gray bar: approximate subjective day of the first DD cycle). The scale bar represents 100 μm.

The two distinct *sPer1* activity maxima in nocturnal animals could be the consequence of an uncoupling of different cell groups within the individual SCN or of an uncoupling of the two SCNs oscillating in anti-phase. Thorough examination of the whole SCN, however, did not reveal any clusters of cells with just one expression maximum or differences between the left and the right nucleus, as has been shown in the mouse SCN [28] and in hamsters with a split activity pattern [29].

To test whether the second *sPer1* peak was clock driven or induced by the LD cycle, we released nocturnal animals into constant darkness (DD) and looked for the *Period* gene expression on the first day in constant conditions (Figure 3). While *sPer2* gene expression continues to oscillate in a circadian manner, the morning peak in *sPer1* expression vanishes in DD. This demonstrates that, in animals with a predominantly nocturnal activity pattern, the molecular clock is shifted for 12 hr, with the activity pattern clearly following gene expression in the SCN. Under normal LD conditions, *sPer1* is regularly induced at dawn. This induction, however, is not sufficient to reset the clock (Figure 2B).

As a rapidly light-inducible gene in mice, *Per1* is thought to integrate light-driven signaling pathways from the retina via the retinohypothalamic tract and the intergeniculate leaflet [30, 31]. The PER proteins would then phase shift the oscillation of the circadian clock, thereby synchronizing it to the environment [5, 32]. Here, we give the first example of a mammalian species in which *Per1* is, under some circumstances, not sufficient to shift the circadian pacemaker. We show that, in the laboratory, the molecular circadian clock of the diurnal *Spalax* is light responsive and that diurnal animals can adapt to changes in the external light cycle. However, in animals with a nocturnal activity pattern, photic signaling can be overruled by factors other than light. We propose that the variability of the mole rat's circadian clock to react to light reflects its subterranean ecotope.

Radiotracking field studies revealed that mole rats are predominantly diurnal during the rainy, short-day winter (mating season) and are predominantly nocturnal during the dry, long-day, hot summer seasons [33]. We tried to simulate this natural ambience by applying different photoperiods, e.g., long day/short night environments, to diurnal animals but failed to induce transition into a nocturnal activity profile by varying only one environmental parameter (light; data not shown). This indicates that other factors like temperature and humidity could have an impact on resetting the *Spalax* clock.

The results indicate that the *Spalax* clock contains a switch controlling the preference for diurnal to nocturnal activity that is located in the input pathway upstream from the core clock mechanism. This is in marked contrast to other mammalian species in which the mechanism that determines the activity phase lies downstream from the clock, because, in all diurnal and nocturnal species studied so far, *Per* gene expression is invariant with maxima during the light phase. We suggest that the *Spalax* clock can vary its sensitivity to light-induced input signals, probably as a response to changes in humidity or temperature. Our findings give a good example for the highly adaptive nature of the clock entrainment mechanism with regard to a species-specific environment.

Experimental Procedures

Animal Handling and Activity Monitoring

We analyzed 63 adults (100–150 g) belonging to *Spalax judaei* (2n = 60) from Anza, Samaria [34]. Field-trapped animals were kept at 22°C–24°C under a 12 hr light/12 hr dark (LD) cycle. Selection of animals was done after monitoring their activity: the animals were kept in 20 × 20 cm cages supplied with two 80 cm, transparent tubes. Each tube was equipped with two infrared-beam sensors that signaled whenever the animal crossed the sensor. For analysis of *sPer* RNA levels in total darkness (DD), light was turned off at *Zeitgeber* time (ZT) 12 for at least 2 days before animals were sacrificed.

In Situ Hybridization

Animals were sacrificed by cervical dislocation under ambient light conditions at 13:00 and 19:00 in LD and under a 15 W safety red light at all other indicated time points. Specimen preparation, ^{35}S-UTP-labeled riboprobe synthesis, and hybridization steps were performed as described in [35]. The probes for *sPer1* and *sPer2* were as described in [7]. Quantification was performed by densitometric analysis of autoradiograph films (Amersham Hyperfilm MP) by using the NIH Image 1.6 program after conversion into the relative optical densities by the ^{14}C-autoradiographic microscale (Amersham). Data from the SCN were normalized with respect to the signal intensities in an equal area of the lateral hypothalamus. Three sections per SCN were analyzed. "Relative mRNA abundance" values were calculated by defining the highest value of each experiment as 100%.

Current Biology
1922

Acknowledgments

We'd like to thank Dr. Adrian Streit, Robin Permut, and Gurudutt Pendyala for comments on the manuscript. This work was supported by grants from the Israeli Academy of Sciences and the Ancell-Teicher Research Foundation to A.A. and E.N. and the German Research Foundation DFG (AL549/3-1), the Swiss National Science Foundation, and the State of Fribourg to U.A.

Received: August 7, 2002
Revised: September 5, 2002
Accepted: September 5, 2002
Published: November 19, 2002

References

1. Bronchti, G., Rado, R., Terkel, J., and Wollberg, Z. (1991). Retinal projections in the blind mole rat: a WGA-HRP tracing study of a natural degeneration. Brain Res. Dev. Brain Res. *58*, 159–170.
2. Nevo, E. (1999). Mosaic Evolution of Subterranean Mammals: Regression, Progression, and Global Convergence (New York: Oxford University Press).
3. Tobler, I., Herrmann, M., Cooper, H.M., Negroni, J., Nevo, E., and Achermann, P. (1998). Rest-activity rhythm of the blind mole rat *Spalax ehrenbergi* under different lighting conditions. Behav. Brain Res. *96*, 173–183.
4. Ben-Shlomo, R., Ritte, U., and Nevo, E. (1995). Activity pattern and rhythm in the subterranean mole rat superspecies *Spalax ehrenbergi*. Behav. Genet. *25*, 239–245.
5. Albrecht, U. (2002). Invited review: regulation of mammalian circadian clock genes. J. Appl. Physiol. *92*, 1348–1355.
6. Avivi, A., Albrecht, U., Oster, H., Joel, A., Beiles, A., and Nevo, E. (2001). Biological clock in total darkness: the Clock/MOP3 circadian system of the blind subterranean mole rat. Proc. Natl. Acad. Sci. USA *98*, 13751–13756.
7. Avivi, A., Oster, H., Joel, A., Beiles, A., Albrecht, U., and Nevo, E. (2002). Circadian genes in a blind subterranean mammal II: conservation and uniqueness of the three Period homologs in the blind subterranean mole rat, *Spalax ehrenbergi* superspecies. Proc. Natl. Acad. Sci. USA *22*, 11718–11723.
8. Pittendrigh, C.S. (1993). Temporal organization: reflections of a Darwinian clock-watcher. Annu. Rev. Physiol. *55*, 16–54.
9. Harmer, S.L., Panda, S., and Kay, S.A. (2001). Molecular bases of circadian rhythms. Annu. Rev. Cell Dev. Biol. *17*, 215–253.
10. Klein, D.C., Moore, R.Y., and Reppert, S.M. (1991). Suprachiasmatic Nucleus: The Mind's Clock (New York: Oxford University Press).
11. Herzog, E.D., and Tosini, G. (2001). The mammalian circadian clock shop. Semin. Cell Dev. Biol. *12*, 295–303.
12. Zheng, B., Larkin, D.W., Albrecht, U., Sun, Z.S., Sage, M., Eichele, G., Lee, C.C., and Bradley, A. (1999). The mPer2 gene encodes a functional component of the mammalian circadian clock. Nature *400*, 169–173.
13. Zheng, B., Albrecht, U., Kaasik, K., Sage, M., Lu, W., Vaishnav, S., Li, Q., Sun, Z.S., Eichele, G., Bradley, A., et al. (2001). Nonredundant roles of the mPer1 and mPer2 genes in the mammalian circadian clock. Cell *105*, 683–694.
14. Bae, K., Jin, X., Maywood, E.S., Hastings, M.H., Reppert, S.M., and Weaver, D.R. (2001). Differential functions of *mPer1*, *mPer2* and *mPer3* in the SCN circadian clock. Neuron *30*, 525–536.
15. Sun, Z.S., Albrecht, U., Zhuchenko, O., Bailey, J., Eichele, G., and Lee, C.C. (1997). RIGUI, a putative mammalian ortholog of the *Drosophila* period gene. Cell *90*, 1003–1011.
16. Tei, H., Okamura, H., Shigeyoshi, Y., Fukuhara, C., Ozawa, R., Hirose, M., and Sakaki, Y. (1997). Circadian oscillation of a mammalian homologue of the *Drosophila* period gene. Nature *389*, 512–516.
17. Albrecht, U., Sun, Z.S., Eichele, G., and Lee, C.C. (1997). A differential response of two putative mammalian circadian regulators, mper1 and mper2, to light. Cell *91*, 1055–1064.
18. Cooper, H.M., Herbin, M., and Nevo, E. (1993). Visual system of a naturally microphthalmic mammal: the blind mole rat, *Spalax ehrenbergi*. J. Comp. Neurol. *328*, 313–350.
19. David-Gray, Z.K., Cooper, H.M., Janssen, J.W., Nevo, E., and Foster, R.G. (1999). Spectral tuning of a circadian photopigment in a subterranean "blind" mammal (*Spalax ehrenbergi*). FEBS Lett. *461*, 343–347.
20. Hannibal, J., Hindersson, P., Nevo, E., and Fahrenkrug, J. (2002). The circadian photopigment melanopsin is expressed in the blind subterranean mole rat, *Spalax*. Neuroreport *13*, 1411–1414.
21. Negroni, J., Nevo, E., and Cooper, H.M. (1997). Neuropeptidergic organization of the suprachiasmatic nucleus in the blind mole rat (*Spalax ehrenbergi*). Brain Res. Bull. *44*, 633–639.
22. Nevo, E., Guttman, R., Haber, M., and Erez, E. (1982). Activity patterns of evolving mole rats. J. Mammal. *63*, 453–463.
23. Nevo, E. (1991). Evolutionary theory and processes of active speciation in subterranean mole-rats, *Spalax ehrenbergi* superspecies in Israel. In Evolutionary Biology, M.K. Hecht, B. Wallace, and R.J. MacIntyre, eds. (New York: Plenum), pp. 1–125.
24. Ben-Shlomo, R., Ritte, U., and Nevo, E. (1996). Circadian rhythm and the per ACNGGN repeat in the mole rat, *Spalax ehrenbergi*. Behav. Genet. *26*, 177–184.
25. Goldman, B.D., Goldman, S.L., Riccio, A.P., and Terkel, J. (1997). Circadian patterns of locomotor activity and body temperature in blind mole-rats, *Spalax ehrenbergi*. J. Biol. Rhythms *12*, 348–361.
26. Novak, C.M., Smale, L., and Nunez, A.A. (2000). Rhythms in Fos expression in brain areas related to the sleep-wake cycle in the diurnal *Arvicanthis niloticus*. Am. J. Physiol. Regul. Integr. Comp. Physiol. *278*, R1267–1274.
27. Mrosovsky, N., Edelstein, K., Hastings, M.H., and Maywood, E.S. (2001). Cycle of period gene expression in a diurnal mammal (*Spermophilus tridecemlineatus*): implications for nonphotic phase shifting. J. Biol. Rhythms *16*, 471–478.
28. Jagota, A., de la Iglesia, H.O., and Schwartz, W.J. (2000). Morning and evening circadian oscillations in the suprachiasmatic nucleus in vitro. Nat. Neurosci. *3*, 372–376.
29. de la Iglesia, H.O., Meyer, J., Carpino, A., Jr., and Schwartz, W.J. (2000). Antiphase oscillation of the left and right suprachiasmatic nuclei. Science *290*, 799–801.
30. Challet, E., Scarbrough, K., Penev, P.D., and Turek, F.W. (1998). Roles of suprachiasmatic nuclei and intergeniculate leaflets in mediating the phase-shifting effects of a serotonergic agonist and their photic modulation during subjective day. J. Biol. Rhythms *13*, 410–421.
31. Jacob, N., Vuillez, P., Lakdhar-Ghazal, N., and Pevet, P. (1999). Does the intergeniculate leaflet play a role in the integration of the photoperiod by the suprachiasmatic nucleus? Brain Res. *828*, 83–90.
32. Reppert, S.M., and Weaver, D.R. (2001). Molecular analysis of mammalian circadian rhythms. Annu. Rev. Physiol. *63*, 647–676.
33. Kushnirov, D., Beolchini, F., Lombardini, F., and Nevo, E. (1998). Radiotracking studies in the blind mole rat. In Abstracts Euro-American Mammal Congress, (Santiago de Compostela, Spain), p. 381.
34. Nevo, E., Ivanitskaya, E., and Beiles, A. (2001). Adaptive Radiation of Blind Subterranean Mole Rats: Naming and Revisiting the Four Sibling Species of the *Spalax ehrenbergi* superspecies in Israel: *Spalax galili* (2n=52), *S. golani* (2n=54), *S. carmeli* (2n=58), and *S. judaei* (2n=60) (Leiden, The Netherlands: Backhuys).
35. Albrecht, U., Lu, H.-C., and Revelli, J.-P. Xu X-C-, Lotan R, Eichele G. (1998). Studying gene expression on tissue sections using *in situ* hybridization. In Human Genome Methods, K.S. Adolph, ed. (New York: CRC Press), pp. 93–119.

Additional Data

To conclude the work on the central circadian clock of *Spalax* we examined *sCry1* and *2* expression in the SCN, the Harderian gland and the eye. From a *Spalax* brain cDNA library Dr. Avivi extracted two different fragments for both *sCry* genes. We looked for daily expression profiles with different probes for all four fragments by *in situ* hybridization.
The two probes for *sCry1* were named 5' and 3'-probe since they aligned to the 5' and 3' region of the corresponding mouse gene. The two probes for *sCry2* were named 'S' (for 'short') and 'L' (for 'long') because of the different lengths of the two fragments extracted from the cDNA library.

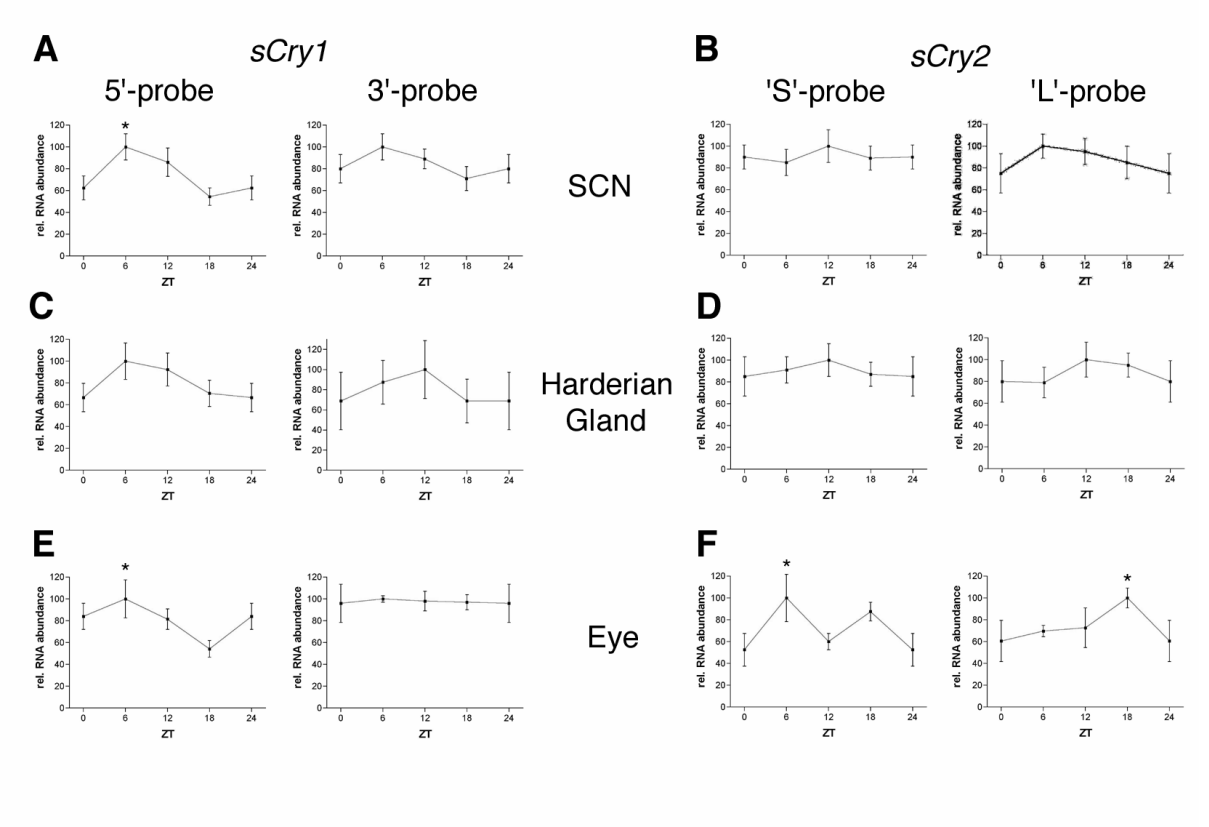

Fig. 52: Daily *sCry* expression profiles in the SCN, the Harderian gland and the eye. Shown are *in situ* hybridization data for *sCry1* (left columns) and *sCry2* (right columns) in the SCN (upper row), the Harderian gland (middle row), and the eye (bottom row). Data are mean +/- SD of three different experiments. Asterisks indicate significant differences between highest and lowest value (unpaired ANOVA, $p < 0.05$).

While only the 5' probe of *sCry1* showed a diurnal oscillation, the 3' probe showed stable expression throughout the day. This might indicate a post-transcriptional modification of the mRNA with the 5' part but not the 3' (more stable) part used for circadian function in the central TTL. *sCry2* transcripts did not cycle prominently as expected from other rodents

(Vitaterna et al., 1999). Interesting however, is the rather high level of the 'S' probe signal with a significant double peak at the light/ dark and dark/ light transitions in the eye. One might speculate about a role of the 'S' fragment in light reception like it is still proposed for the mammalian *Crys* (Sancar, 2000; Thresher et al., 1998) while the 'L' fragment serves in the central oscillator. This would reflect the situation in zebrafish, where some of the *Cry* genes act as photoreceptors while others drive the feedback of the TTL (Kobayashi et al., 2000).

Chapter 3

Conclusion and Perspectives

Most of the interpretations that arise from the work presented here have been elaborated in the included publications. Therefore I will focus in this part on some comprehensive conclusions drawn from the phenotypical data derived from the *mPer/ mCry* double mutants with special regard to the free-running period lengths in DD. I will introduce a new model emphasizing the repressive action of the mPER and mCRY proteins in the TTL as a variation of the limit cycle model suggested in the second double mutant publication (chapter 2.2.).

On the mixed genetic background we used for the double mutants we generated several

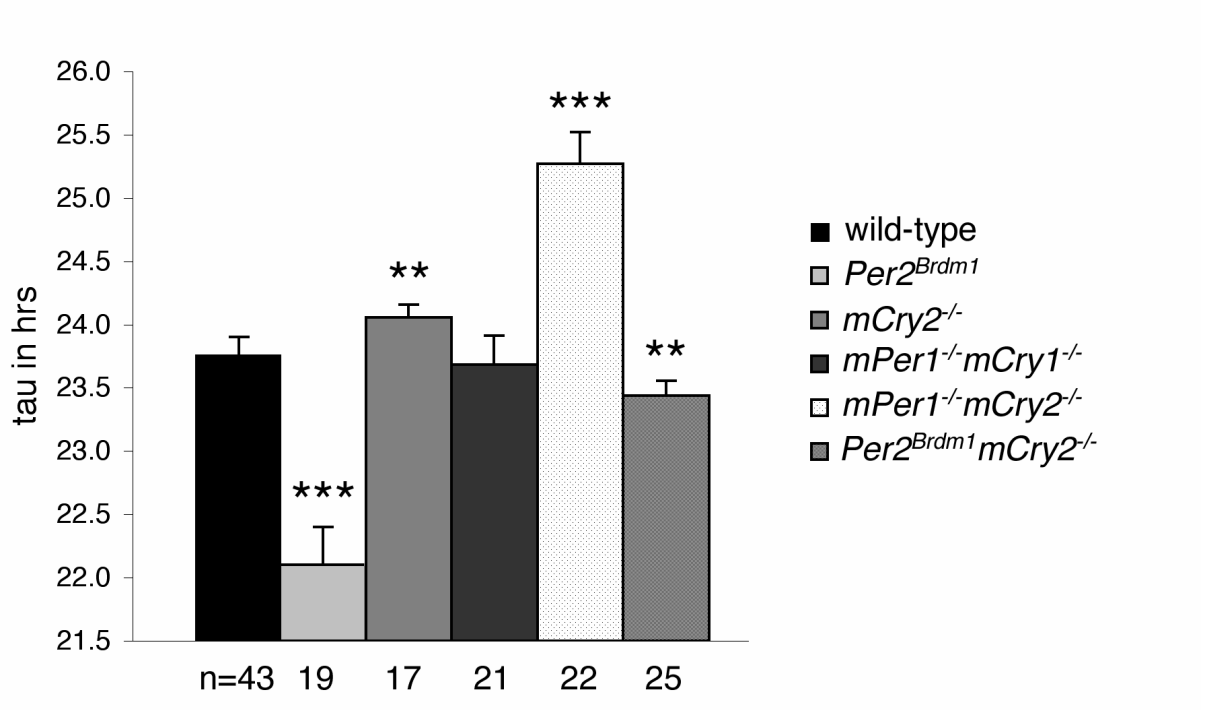

Fig. 53: Free running period lengths of clock mutant mice (from the mixed genetic background used in this study) in DD. Data presented are mean +/- SD; total numbers of animals used are given below the x-axis; significance was determined by one way ANOVA followed by Bonferroni post-test (, p< 0.01; ***, p< 0.001).**

different mutant lines of which five were rhythmic for at least some time in DD. Four of these lines showed a period length significantly different from that of the corresponding wild-type controls (see figure 53).

From the current understanding of the central circadian oscillator (see chapter 1.4.) a major role of the PER and CRY proteins is to form a multi-protein complex which interacts with the CLOCK/ BMAL1 transcriptional activator thereby inhibiting the transcription of their own genes. If one or more of the PER and/ or CRY proteins are removed from this complex by genetic disruption of the corresponding gene *loci*, the overall activity of the remaining complex is changed.

If we define the efficiency of the PER/ CRY protein complex by its ability to accelerate the pace of the oscillator (by its efficiency to inhibit transcription of CLOCK/ BMAL1 induced genes), all components of this complex contribute to the overall potential of the Cluster. The easiest way to separately define the contributions of the single PER and CRY proteins is to assign 'accelerator potentials' (APs) to each gene/ protein with the sum of all four single unit potentials being the overall accelerator potential of the multimeric complex. This overall accelerator potential (OAP) determines the pace of the central oscillator under constant conditions measured as the internal period τ. A high overall accelerator potential speeds up the clock resulting in a short period length (like in *mCry1* mutants) while a low OAP decelerates the clock which corresponds to a long τ in DD (like in *mCry2* mutants). To have a measure of the OAPs we subtracted the experimentally defined mutant free-running period from that of the wild-type. This results in positive values for mutants with a shortened τ and negative values for mutants with a longer τ as given in the table below (termed "experimental accelerator potentials" or EAPs).

mutant	τ in DD (in hours)	experimental accelerator potential (in min)
wild-type	23.8	0
mPer2	22.1	102
mPer1/ mCry1	23.7	6
mPer1/ mCry2	25.3	-90
mPer2/ mCry2	23.4	24
mCry2	24.1	-18

Tab. 6: Period lengths and EAPs of clock gene mutant mice from this study. Internal period length τ was determined as described (chapter 4.1.3.3.3.). Experimental accelerator potentials (ERPs) were calculated as the difference between mutant and wild-type τ. Only mice of the mixed genetic background that was used throughout this study are shown.

From the assumptions above one can derive formulas to calculate theoretically expected OAPs (theoretical overall activator potentials; TAPs) from the single APs. For the mutants examined in this study the formulas to calculate the TAPs would be:

wild-type:	$(RP_{Per1} + RP_{Per2} + RP_{Cry1} + RP_{Cry2})$
mPer2 mutant:	$(RP_{Per1} + RP_{Cry1} + RP_{Cry2})$
mPer1/ mCry1 mutant:	$(RP_{Per2} + RP_{Cry2})$
mPer1/ mCry2 mutant:	$(RP_{Per2} + RP_{Cry1})$
mPer2/ mCry2 mutant:	$(RP_{Per1} + RP_{Cry1})$
mCry2 mutant:	$(RP_{Per1} + RP_{Per2} + RP_{Cry1})$

To calculate optimized accelerator potentials for the single genes/ proteins we determined a regression error (RE) with RE as the square root of the sum of the squares of the differences comparing the TAPs to the EAPs in all mutant strains.

$$RE = \sqrt{\sum (TAP - EAP)^2}_{for\,all\,different\,strains}$$

We now assigned random values for the single gene/ protein APs, calculated the TAPs and subsequently RE. Now we applied the Solver routine of the Excel program (Microsoft) using a Newton regression algorithm to minimize RE by changing the values for the single gene/ protein accelerator potentials. After 100 iterations the values were as follows:

gene/ protein	optimized accelerator potential.
mPer1	62,50
mPer2	-51,00
mCry1	-39,00
mCry2	47,00

Tab. 7: Optimized accelerator potentials (APs) for *Per* and *Cry* genes/ proteins after Newton regression using the Solver routine of the Excel program (100 iterations).

If we applied these optimized APs to the different mutants using the formulas given above we get the following theoretical overall accelerator potentials (TAPs):

Mutant	optimized TAPs	EAPs	Difference
wild-type	19,5	0	-19,5
mPer2-/-	70,5	80	9,5
mPer1mCry1-/-	-4,0	6	10,0
mPer1mCry2-/-	-90,0	-90	0,0
mPer2mCry2-/-	23,5	24	0,5
mCry2-/-	-27,5	-18	9,5

Tab. 8: Optimized theoretical overall accelerator potentials for clock mutants used in this study. The difference between optimized TAPs and the experimental results (EAPs) visualizes the quality of the iteration.

From the regression we get a clearly defined ranking of accelerator potentials (APs) with *mPer1* and *mCry2* as the most potent accelerator – a fact reflected in the *mCry2* mutant, which shows the longest τ of all single mutants (van der Horst et al., 1999; Vitaterna et al., 1999) – followed by *mCry1* with *mPer2* being the weakest accelerator. This was expected from the short free running period of the $mPer2^{Brdm1}$ mutant in DD (Zheng et al., 1999).
To compare our model with results from other groups we applied the obtained TAPs to different clock gene mutants previously published:

Mutant	Source	EAPs	Difference
mCry1-/-	v.d. Horst et al., 1999	76	17,50
mCry2-/-	"	-52	-24,50
mCry1-/-	Vitaterna et al., 1999	41	-17,50
mCry2-/-	"	-61	-33,50
mPer1-/-	Zheng et al., 2001	66	109,00
mPer2-/-	", 1999	96	25,50
mPer1-/-	Bae et al., 2001	32	75,00
mPer2-/-	"	10	-60,50
mPer1-/-	Cermakian et al., 2001	35	78,00

Tab. 9: Comparison between calculated (TAP) and experimental determined accelerator potentials (EAP) from the literature

As expected, the differences between theoretical and experimental results are higher than in our own studies. However, most of the free-running periods are comparable to the predictions from the model. For example the predicted τ of the *mCry1* mutant lies exactly between the two values published before (van der Horst et al., 1999; Vitaterna et al., 1999). The same is true for the *mCry2* mutant, where the published mutants (van der Horst et al., 1999; Vitaterna

et al., 1999) both have longer period lengths than predicted but our own mCry2 mutant shows a shorter τ. Again, in the *mPer2* mutant the predicted value is located between two different versions of published data (Bae et al., 2001; Zheng et al., 1999).

The only mutation the model completely fails to predict is *mPer1*. This is somehow expected since *mPer1* single mutants show a normal or slightly shortened τ (Bae et al., 2001; Cermakian et al., 2001; Zheng et al., 2001) while we could show that an additional mutation of *mPer1* in *mCry1* or *mCry2* mutants leads to an elongation of the internal period. This may as well reflect the posttranslational role of mPER1 protein in the circadian pacemaker which cannot be taken into consideration by a simple model of accelerator potentials (Bae et al., 2001; Lee et al., 2001; Zheng et al., 2001).

But what happens in the *mPer2*, the *mPer2/mCry1* and the *mPer1/mCry2* mutants which become arrhythmic immediately or after some time in DD? Calculating the TAPs for these three strains we get very high or very low values (71, 110 and –90min respectively) indicating corresponding short or long internal periods respectively. If the circadian clockwork functions as a stabilized oscillator the disturbance introduced by the deletion of these genes in the negative component of the TTL might overwhelm the compensation capacities of the clockwork. With the loss of stability the oscillation dampens and ultimately reaches equilibrium or arrhythmicity.

Taken together we demonstrate in this work that the finely tuned interaction of both *Per* and *Cry* genes creates a stabilized negative branch of the transcriptional/ translational feedback loop at the heart of the circadian pacemaker. Although there is some redundancy in these components when looking at mere rhythmicity, every gene has its specific function in the whole clock mechanism. Together they ensure the stability and adaptivity the internal pacemaker needs to serve as a reliable time-teller and synchronizer for the complex mammalian organism.

With the discovery of *Rev-Erbα* as the transcription factor controlling *Bmal1* expression (Preitner et al., 2002) most of the genes which are supposed to be necessary to build up the mammalian cellular clockwork have been discovered. Some questions remain on the physical interactions of the clock proteins and especially their spatio-temporal organization. Novel animal models like transgenic mice carrying reporter genes tagged to clock controlled promoters will probably help to elucidate the exact time course of clock organization in the living animal (Wilsbacher et al., 2002).

With the discovery of peripheral oscillators and the identification of clock gene relatives in several tissues outside the hypothalamus much work has been spent on these body clocks and

their connections to the SCN (reviewed in Balsalobre, 2002). Although some signaling candidates have been discovered like glucocorticoids (Balsalobre et al., 2000a), retinoids (McNamara et al., 2001) or *Prokineticin 2* (Cheng et al., 2002), the pathway by which the SCN synchronizes the body to the environment is still not clear.

The quest for these signaling molecules and the properties of the peripheral clocks organizing the metabolism of the body will most probably be the main focus of molecular chronobiology in the upcoming years. It will offer us the pharmacological tools to manipulate these oscillators thereby providing new strategies for the treatment of diseases caused or complicated by desynchronization or misentrainment of circadian clocks.

Chapter 4

Material and Methods

4.1. Animal Handling and Breeding

All animal work was performed according to the guidelines of the Bundestierschutzgesetz (BGBl. I S. 1105, ber. S. 1818, Abschnitt 2 (§2+3) 5 (§7-9) and 8(§11) for Hannover and the Schweizer Tierschutzgesetz (TSchG, SR455, Abschnitt 2 (Art. 5 und 7), 5 (Art. 11) and 6 (Art. 12-19) for Fribourg.

4.1.1. Mouse Strains

Colony founders for the *mPer/mCry* multiple mutant lines came from two different genetic backgrounds. We started with *mPer1*$^{-/-}$ and homozygous *mPer2*^{Brdm2} mice carrying a targeted gene from a 129S5/S7 genomic library in a C57BL/6 background (Zheng et al., 2001; Zheng et al., 1999) and *mCry1*$^{+/-}$/*mCry2*$^{+/-}$ heterozygous mice carrying a targeted gene from a Ola129 derived genomic library in a C57BL/6 background (van der Horst et al., 1999). While in the *mPer1*, the *mCry1* and the *mCry2* targeting vectors almost all of the translated coding sequence was deleted the *Per2*^{Brdm2} mutants lack a major part of their PAS domain responsible for protein protein interaction resulting in a truncated non-functioning protein (Oster et al., 2002; Zheng et al., 1999).

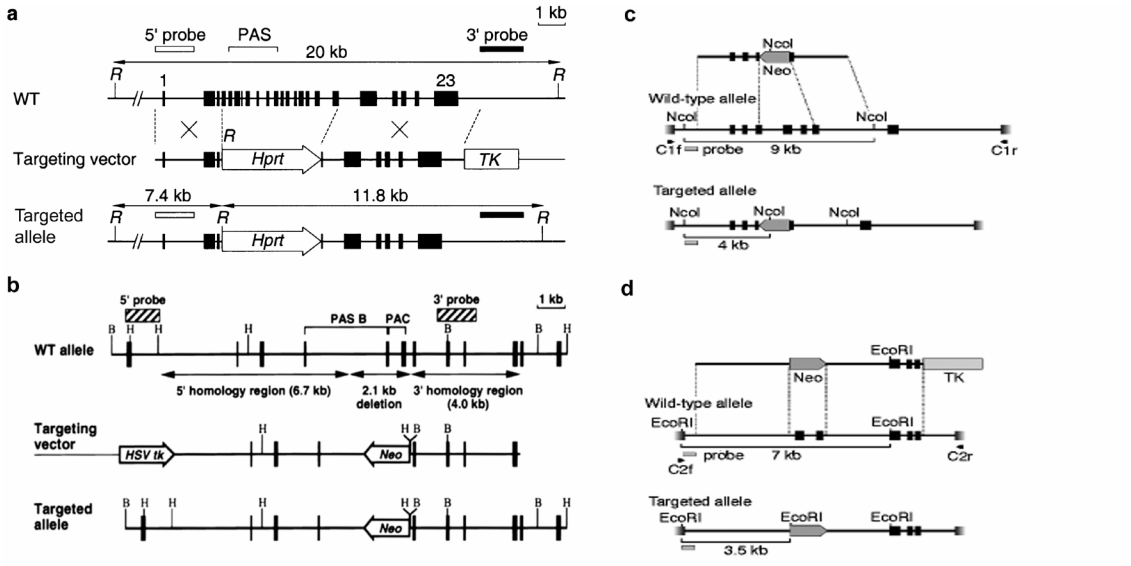

Fig. 54: Targeted disruption of the *Per* and C*ry* genes (a) Genomic structure of the murine *mPer1* gene, the targeting vector, and the predicted structure of the targeted allele. Exons are indicated by vertical black bars with the first and last exons numbered. WT, wild-type; *R*, *Eco*RI; *Hprt*, hypoxanthine phosphoribosyltransferase gene; *TK*, *Herpes Simplex Virus thymidine kinase* gene. A 1.6 kb 3' external probe that detects a 20 kb wild-type *EcoRI* fragment and an 11.8 kb mutant *Eco*RI fragment were used to detect targeted ES cell clones and to genotype test mutant mice. (b) Genomic structure of a portion of the mouse *mPer2* gene, the targeting vector and the predicted structure of the targeted allele. H, *Hin*dIII; B, *Bam* HI; *Neo*, neomycin resistance gene. Figure 1 Targeted disruption of the *cry* genes and generation of Cry-deficient mice. (c) Physical map of the wild-type *Cry1* locus, the targeting construct and the disrupted *Cry1* locus. Exons are indicated by black filled boxes. Note that the use of PCR-derived genomic DNA does not allow proper exon numbering. The probe used for screening homologous recombinants and genotyping mice, localized external to the construct, is represented by a gray box. Primers used for RNA analysis by RT-long-range PCR are depicted as black arrowheads. (d) Physical map of the wild-type *Cry2* locus, the targeting construct and the disrupted *Cry2* locus (from van der Horst et al., 1999; Zheng et al., 2001; Zheng et al., 1999).

4.1.2. Mouse Breeding

Mice were bred in BioZone ventilated caging systems (Cage Model CA20, VR Classic TM, BioZone, Margate, UK) in Hannover and in filter top open cages (Type 2 Polycarbonate Cage with top wiring, Tecniplast, Italy) in custom made racks in Fribourg in a 12h Light 12h dark cycle. Matings were normally setup as pairs or triples with rotation of the females in a one to two week turn during the expansion of the colonies. Litters were weaned three to four weeks after birth and separated for their gender. Store cages held up to 6 animals. Genotype was determined by Southern Blot Hybridization with genomic DNA extracted from tail tissue before weaning.

4.1.3. Activity Monitoring

4.1.3.1. Facilities and General Guidelines

Animals were housed individually in transparent plastic cages (Tecniplast 1155M) that were equipped with a steel running wheel of 115 mm in diameter (Trixie 6083, Trixie GmbH, Germany). The axis of the wheel was equipped with a plastic disc holding a small magnet (article number 34.6401300702, Fehrenkemper Magnetsysteme, Germany). The magnet opens and closes a magnetic switch (Reed-Relais 60, Conrad Electronic, Germany) upon rotation of the running wheel. The switch was connected to a computer that counts the revolutions of the wheel (using the Activity Counting System Program, Simon Fraser University, Burnaby, Canada in Hannover and ClockLab, Actimetrics, Austin St. Evanston, USA in Fribourg). Twelve cages of this type were placed in one isolation cabinet (custom made, length = 180cm; height = 54cm; depth = 69cm). Running data analysis was performed using the Circadia Program (Simon Fraser University) in Hannover and ClockLab plug-in for MatLab (The Mathworks, Natick, USA) in Fribourg (Albrecht and Foster, 2002).
Mice used for activity monitoring were generally 2 to 6 month old males (except stated otherwise). An equal number of wild-type controls was included in each isolation chamber. Animals were provided food and water *ad libitum* at all times. Cages were changed every three to four weeks at the beginning of the activity phase to minimize phase shifts induced by a new environment (Mrosovsky, 1996).

4.1.3.2. Publication: “The Circadian Clock and Behavior”

Urs Albrecht and Henrik Oster

Behavioural Brain Research 125 (2001)

ELSEVIER

Behavioural Brain Research 125 (2001) 89–91

BEHAVIOURAL BRAIN RESEARCH

www.elsevier.com/locate/bbr

The circadian clock and behavior

Urs Albrecht *, Henrik Oster

Max-Planck-Institute for Experimental Endocrinology, Feodor-Lynen-Strasse 7, 30625 Hannover, Germany

Received 29 June 2000; accepted 28 March 2001

Abstract

Temporal organization is a fundamental feature of all living systems. Timing is essential for development, growth and differentiation and in the mature organism, it is essential to maintain normal physiology and behavior. The biological entity that permits an organism's day night organization is the circadian system. In the following, we describe how daily or circadian activity is measured in mice, and what such activity measurements can tell us about the state of the animal. © 2001 Elsevier Science B.V. All rights reserved.

Keywords: Circadian clock; Wheel-running; Zeitgeber time; Circadian time; Phase-shift; *Per* genes; Vasopressin; NOS1

1. Introduction

Activity in rodents is evaluated either by monitoring general movement (e.g., with photosensors), or by measuring wheel-running activity. Assessment by photosensors or infrared sensors registers general activity including movement that occurs during feeding or grooming. In contrast, wheel-running activity represents only intended running of the animal and therefore provides activity patterns lacking background activity. This is one of the reasons, why this type of activity measurement is preferred over infrared monitoring. In the following, we will focus only on wheel-running activity and describe general protocols.

In our wheel-running experiments, animals are housed individually in transparent plastic cages (280 mm long × 105 mm wide × 125 mm high, Techniplast 1155M) that are equipped with a steel running wheel of 115 mm in diameter. The axis of the wheel is equipped with a magnet that opens and closes a magnetic switch upon rotation of the running wheel. The switch is hooked up to a computer that counts the revolutions of the wheel. Twelve cages are placed in a black, light-tight box, which is ventilated and containing fluorescent light that can be controlled via a timer from the outside. The box is placed in a room that is controlled for temperature, humidity, light and free of noise and vibrations. If environmental noise is not well under control, a constant background sound (white noise) should be installed to drown any outside noise, e.g., traffic or trains. Living conditions that lead to disease can be readily observed. Outbursts of viral infections are reflected in daily wheel-running activity. After the viral burst, the circadian activity returns to the normal nocturnal activity until the next viral burst occurs. Hence, abnormal activity patterns can be a result of infections.

Wheel-running activity in mice is measured under a standard light–dark (LD) cycle that consists of 12 h of light (we use 500 lux, but 50 lux is sufficient, light intensity is measured with a lux-meter, Testo 0500, Lenzkirch, Germany) and 12 h of darkness, e.g., lights on 07:00, lights off 19:00. Activity recording is usually started just before lights off (e.g., 19:00) when mice are at the beginning of their activity phase. Hyperactivity due to the placement in a novel environment (arousal) has then a minimal effect on the animals clock [3]. It is important that at this point the data transmission is checked to correct problems that occur with data acquisition. If adjustments are necessary later on in the experiment, it is advisable to do them just before lights off, e.g., 19:00. This is also the guideline for food and

* Corresponding author. Present address: Institute of Biochemistry, University of Fribourg, Rue du Musée 5, 1700 Fribourg, Switerland. Tel.: +41-26-300-8636; fax: +41-26-300-9735.

E-mail address: urs.albrecht@unifr.ch (U. Albrecht).

0166-4328/01/$ - see front matter
PII: S0166-4328(01)00288-1

water supply, which is necessary every 3–4 weeks. Important to note here is that the cage and the wheel should not be replaced by a new cage, because a new wheel is a novel stimulus that can phase-shift the clock [5]. After the animals have been held in the LD 12/12 cycle for at least 10 days, they are 'entrained' and adjusted to this particular LD cycle and the measurements from that point on are reliable. These animals are still under the daily influence of light and therefore can use the light as a Zeitgeber or timegiver. Measurements under these conditions are determined by the Zeitgeber time (ZT), where ZT0 is lights on. The specification of the LD cycle determines the ZT for lights off, e.g., ZT12 in an LD 12/12 cycle. Animals held under these conditions can also be used for molecular analysis. Good markers for the circadian clock are the *mPer* genes [1,7], which are expressed in a diurnal manner and remain expressed in a circadian manner under constant conditions (see next paragraph).

To investigate the circadian clock, mice have to be held under constant darkness conditions. Their clock is then 'free-running' and independent of light changes. After animals were in an LD 12/12 cycle for at least 10 days, the lights are not turned on the next day and remain off for the rest of the experiment. The first 5 days show an unstable period length of a particular animals clock, because the animal is in transition and has to adjust to the constant darkness or dark–dark (DD) conditions. The period (*tau*) of an animal is established by analyzing 10 days of stable circadian data using the Chi-squared periodogram. A wild type (WT) animal has a period length of ~23.8 h (depending on the strain), which is close to a day of 24 h. In contrast, an *mPer2* mutant animal has a period length of only 22 h [9]. To study arrhythmicity, animals are left undisturbed for 28 days in DD. For example, an *mPer2* mutant animal can take 14–20 days until its circadian rhythm is lost [9]. After the period length has been determined, the circadian times (CT) for an animal are defined and time measurements under DD conditions are described by CT. For example, CT24 is at the end of the period of the animals clock, hence, after 23.8 h for a WT animal or after 22 h for an *mPer2* mutant animal. Times given in CT indicate constant darkness conditions and are strictly speaking animal specific. Given that the individual variation in *tau* for a strain is not very large, the CT is based on the average *tau* of that strain and can be used for all individuals. Strains that immediately lose circadian rhythmicity in DD, like the *mPer1/mPer2* double mutants [8] cannot be temporally defined by a CT, because no *tau* can be determined.

Phase shifts are the consequence of disturbance of the clock by an external signal, such as light, noise or providing a new running wheel. To study the effects of light on the phase shifting of the circadian clock, light pulses are applied to the animals. We apply a light pulse that has a duration of 15 min and an intensity of 500 lux. The animals that are investigated must establish a clear stable rhythm in DD for 10–12 days before a light pulse is applied. Animals that become arrhythmic in DD have to establish a stable rhythm in LD. A light pulse has only an effect on the clock if it is applied in the activity phase of the mouse, i.e., between CT12 and CT24 (subjective night) or ZT12 and ZT24, respectively [3]. To evoke a phase delay of the clock, the light pulse must be applied in the early night (between CT12 and CT18–20). For phase advances, the light pulse is applied in the late night (between CT18–20 and CT24). These are just approximate CT values, because they

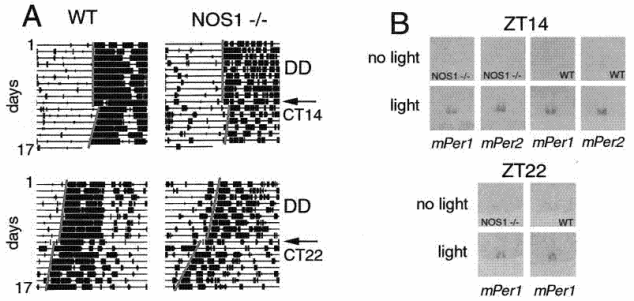

Fig. 1. (a) Wheel-running activity of WT and NOS1 – / – mice before and after a 15 min light pulse. Mice were entrained for 10 days to an LD 12/12 cycle and then released into constant darkness (DD). Shown are 10 days of activity in DD before a light pulse was applied at CT14 (top arrow) or at CT22 (bottom arrow), respectively. The vertical grey lines indicate activity onset. The light pulse at CT14 causes a delay of wheel-running activity (vertical line moves to the right), whereas a light pulse at CT22 causes onset of activity at earlier times (vertical line shifted to the left). WT and NOS1 – / – mice did not behave differently in response to a light pulse, but wheel-running activity was more fragmented in NOS1 – / – mice. (b) Induction of *mPer1* and *mPer2* in NOS1 – / – mice by a light pulse. NOS1 – / – and WT mice were exposed to 500 lux of light for 15 min at ZT14 and ZT22, respectively. Induction of *mPer1* and *mPer2* after 1 h in NOS1 – / – animals was comparable to WT animals indicating that lack of NOS1 has no influence on *mPer* gene light inducibility. Induction of *mPer1* and *mPer2* in WT animals at ZT14 is similar to *mPer1* induction at ZT22. *mPer2* is not inducible by light at ZT22 [1].

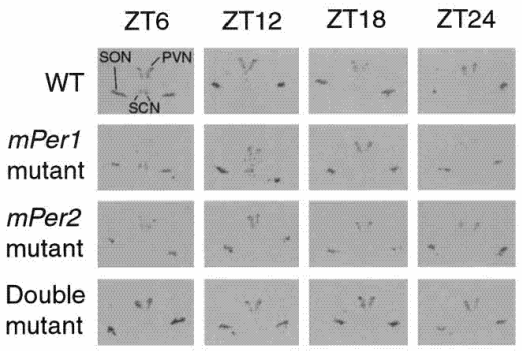

Fig. 2. Expression of vasopressin prepropressophysin mRNA in WT, *mPer1*, *mPer2* and *mPer1/2* mutant mice that were kept in an LD 12/12 cycle. Constitutive expression is detected in the SON and PVN. In the SCN, diurnal expression is observed in WT and *mPer1* mutant animals with a maximum at ZT6, but this diurnal expression is absent in *mPer2* and *mPer1/2* mutant animals. SON – supraoptic nucleus, PVN – paraventricular nucleus, and SCN – suprachiasmatic nucleus.

vary depending on the mouse strain [2,6]. After the light pulse, the animals are left in DD. Phase delays can already be recognized 1 day after the light pulse has occurred, but phase advances take up to 6 days to be recognizable and they are smaller than phase delays. At least seven consecutive days have to be measured to determine the amount of the phase advance or delay, respectively. Fig. 1 shows that NOS1 knock-out animals behave like WT animals in clock resetting ([4], Fig. 1(a)). In molecular terms, NOS1 $-/-$ mice displayed *mPer1* and *mPer2* light inducibility comparable to WT animals (Fig. 1(b)). Thus, NOS1 is not necessary for *Per1* and *Per2* gene induction, which is consistent with the normal resetting behavior in NOS $-/-$ mice. However, it cannot be ruled out that NO is synthesized by other isoforms of NOS, like endothelial NOS or unknown NOS isoforms.

The *mPer1* and *mPer2* genes are important components of the mammalian circadian clock [1,7–9]. Disturbance of the circadian clock can lead to a derailment of an organism's physiology. To illustrate this point, we examined the transcriptional regulation of the clock-controlled vasopressin prepropressophysin in the suprachiasmatic nucleus (SCN). We found that the vasopressin mRNA rhythm was severely blunted in the SCN of *mPer2* mutant and in *mPer1/2* double mutant animals, but not in *mPer1* mutants (Fig. 2). This indicates that vasopressin mRNA is positively regulated by *mPer2*, but not by *mPer1*. Vasopressin is well known for its peripheral effects on salt and water balance and has a number of distinct actions within the central nervous system. Therefore, a number of physiological abnormalities can be expected in *mPer2* and *mPer1/2* mutants. This clearly shows that in a WT animal the physiological state of the organism is not constant throughout the day. We recommend that behavioral studies are accompanied by a ZT with the corresponding LD cycle to ensure reproducibility of behavioral measurements.

Acknowledgements

We would like to thank Prof. Stefan Steinlechner for critically reading the manuscript and Prof. Gregor Eichele for support. This work was supported by the DFG to U.A. (AL 594/1-1).

References

[1] Albrecht U, Sun ZS, Eichele G, Lee CC. A differential response of two putative mammalian circadian regulators, *mper1* and *mper2*, to light. Cell 1997;91:1055–64.
[2] Daan S, Pittendrigh CS. A functional analysis of circadian pacemakers in nocturnal rodents. II. The variability of phase response curves. J Comp Physiol 1976;106:253–66.
[3] Hastings MH, Best JD, Ebling FJP, Maywood ES, McNulty S, Schurov I, et al. Entrainment of the circadian clock. Prog Brain Res 1996;111:147–74.
[4] Kriegsfeld LJ, Eliasson MJL, Demas GE, Blackshaw S, Dawson TM, Nelson RJ, et al. Nocturnal motor coordination deficits in neuronal nitric oxide synthase knock-out mice. Neuroscience 1999;89:311–5.
[5] Mrosovsky N. Locomotor activity and non-photic influences on circadian clocks. Biol Rev 1996;71:343–72.
[6] Pittendrigh CS, Daan S. A functional analysis of circadian pacemakers in nocturnal rodents. IV. Entrainment: pacemaker as clock. J Comp Physiol 1976;106:291–331.
[7] Sun ZS, Albrecht U, Zhuchenko O, Bailey J, Eichele G, Lee CC. RIGUI, a putative mammalian ortholog of the *Drosophila period* gene. Cell 1997;90:1003–11.
[8] Zheng B, Albrecht U, Sage M, Vaishnav S, Sun ZS, Eichele G, Bradley A, Lee CC. Requirement for the *mPer1* and *mPer2* genes in maintaining the mammalian circadian clock, submitted for publication.
[9] Zheng B, Albrecht U, Kaasik K, Sage M, Lu W, Vaishnav S, Li Q, Sun ZS, Eichele G, Bradley A, Lee CC. Nonredundant roles of the mPer1 and mPer2 genes in the mammalian circadian clock. Cell 2001;105:683–94.

4.1.3.3. Experiments

4.1.3.3.1. Light/ Dark (LD) Cycle Entrainment

Animals were kept in a 12h light (250-300 Lx bright white light)/ 12h dark cycle ("Lights on" = ZT0 at 7:00 in summer and 6:00 in winter; "Lights off" = ZT12 at 19:00 and 18:00 respectively) for three to five weeks (LD12:12). After one week of training activity profiles were taken for characterizing the entrainment of the animals. We studied the following criteria:

a. Activity onset: A minimum of 100 wheel revolutions per 5min bin after a minimum of 240min of rest. The average was taken for 7 consecutive days after one week of adaptation.
b. Overall activity: average number of wheel evolutions and approximate covered distance in 24h
c. Night time activity: like b. but only during the dark phase
d. Day time activity: like b. but only during the light phase
e. Activity phase (α): time between onset and offset of activity

4.1.3.3.2. Shifted LD Cycles

After entrainment to an LD12:12 cycle for at least 10 days lights were not turned on at 7:00/ 6:00 the next day but 8h later (15:00/ 14:00). From there a shifted light cycle was presented to the animals ("Lights on" = ZT0 at 15:00 in summer and 14:00 in winter; "Lights off" = ZT12 at 3:00 and 2:00 respectively). We measured the number of days needed for an animal to adapt to the new LD cycle by looking at the onset of activity. After another 10 days the LD cycle was shifted back again (with a long night at the transition, e.g. "lights off" at 3:00/ 2:00 and "lights on" at 7:00/ 6:00 on the following day.

4.1.3.3.3. Free Running in Constant Darkness

After entrainment to an LD12:12 cycle for at least 10 days lights were not turned on again at the following morning and animals were kept in constant darkness for several weeks (DD). We studied the following criteria:

a. Internal period (τ): Length of a subjective day determined by the time points of activity onset on two consecutive days. The average was taken from at least 7 consecutive days of stable rhythmicity in DD.
b. Overall activity: average number of wheel evolutions and approximate covered distance in 24h
c. Activity phase (α): time between onset and offset of activity

4.1.3.3.4. Free Running in Constant Light

Activity monitoring in constant light (LL) was performed like described for DD. In some experiments increasing light intensities were applied (as given in the diagrams). Therefore isolation boxes were equipped with dimmable halogen lamps (one for each cage). Light intensity was measured with a Luxmeter (Testo, Germany) and averaged for all cages (deviations were less than 10% in all cases).

4.1.3.3.5. Phase Shifting Experiments

Two different protocols were used for determining light induced phase shifts (Pittendrigh and Daan, 1976). For Type 1 mice were kept in DD for at least 10 days before a 15min Light pulse (300Lx) was applied to every single animal at CT14 (2 subjective hours after activity onset) or at CT22 (10 subjective hours after activity onset). For that the animals were removed from the isolation box and placed under a fluorescent light after replacing the lid of the cage with an empty wiring lid to ensure equal illumination of the whole cage area. The phase shift was determined by fitting a line through the onsets of activity before and after the light pulse with ignoring the first days after the treatment when the clock is still in transition. The difference between the two lines at the day after the pulse depicts the phase shift. Phase delays count as negative while phase advances count as positive phase shifts.
For the Type 2 protocol mice were kept in LD 12:12 for at least 10 days. A nocturnal light pulse (at ZT14 or at ZT22) was applied for 15min to all animals in one chamber and the lights

remained turned off on the following days. Two lines were drawn through the onsets of activity before and after the light pulse. The line after the light treatment was elongated to the day of the pulse. The difference between the two lines was determined. The same procedure was performed with control animals by applying the same LD/ DD schedule without the light pulse. The difference between treated and control animals was determined as the phase shift.
These values are generally very similar to the ones obtained with a Type 1 experiment with slightly smaller numbers. An advantage of Type 2 are the easy and efficient treatment of many animals of different strains since no τ has to be taken into consideration for the timing of the light pulse and the animals need not to be removed from the isolation chamber for illumination. Additionally this protocol is applicable to mutants which eventually become arrhythmic in DD like the *mPer2*^{Brdm1} mutant used in this work or the *Clock* mutant (Vitaterna et al., 1994).

4.1.4. Cross Breeding

mCry1$^{+/-}$/ *mCry2*$^{+/-}$ animals were crossed with *mPer1*$^{-/-}$ and homozygous *mPer2*^{Brdm1} animals respectively. From the f1 offspring *mPer/ mCry* double heterozygous animals (e.g. *mPer1*$^{+/-}$/ *mCry1*$^{+/-}$) were selected and cross-bread to yield double mutants and corresponding wild-type animals in the f2 generation.
For *mPer/ mCry* triple mutants homozygous animals from two double mutant strains sharing one mutation were chosen (e.g. for *mPer1*/ *mCry1*/ *mCry2* mutants we started with *mPer1*$^{-/-}$ /*mCry1*$^{-/-}$ and *mPer1*$^{-/-}$/ *mCry2*$^{-/-}$ mice). The double heterozygous f1 offspring was intercrossed to yield the desired triple mutant strain in the f2 generation. As wild-type controls we chose the same animals as used for the double mutants (depicted “PC-WT”).

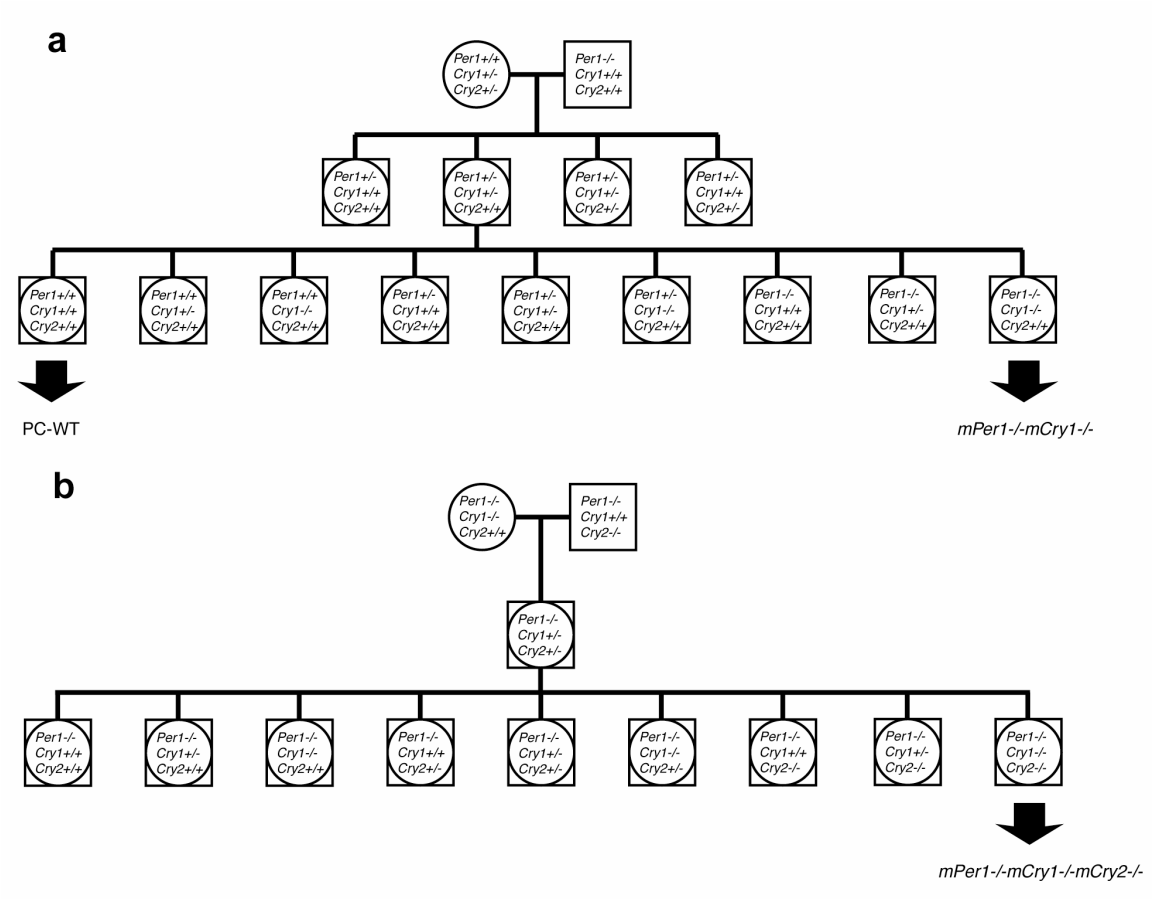

Fig. 57: Breeding schemes for double and triple mutant mice. (a) Breeding scheme *for mPer1/ mCry1* mutants (b) breeding scheme for *mPer1/ mCry1/ mCry2* mutants.

4.1.5. *Spalax* Strains

All animal work with *Spalax* was performed in collaboration with Dr. Aaron Avivi at the Institute of Evolution, University of Haifa, Israel. For the work on *sClock* and *sMOP3* we used brain tissue, eyes and Harderian glands from *Spalax S. judaei* (*2n*= 60) *and Spalax S. galili* (*2n*= 52). For the studies on the *sPers* and the *sCrys* we used only *Spalax S. judaei* (*2n*= 60). Animals were trapped in the field, kept under specific lighting conditions in the lab and sacrificed at the depicted time points. We received fixed and dehydrated tissue for *in situ* Hybridization.

4.2. Molecular Biological Experiments

4.2.1. Genotyping

4.2.1.1. DNA Templates

The *mPer2* probe hybridizes to a 12kb wild-type and a 10kb mutant fragment of *BamH I* digested genomic DNA. The *mCry1* probe detects a 9kb wild-type and a 4kb *Nco I* digested fragment of the targeted locus. In *mCry2* mutants the wild-type allele is detected by hybridization of the probe to a 7kb *EcoR I* fragment whereas the mutant allele yields a 3.5kb fragment. For further descriptions see (van der Horst et al., 1999; Zheng et al., 2001; Zheng et al., 1999).

4.2.1.2. Probe Preparation

Templates for southern probes were as described for *mPer1*$^{-/-}$ (Zheng et al., 2001), *mPer2*^{Brdm1} (Zheng et al., 1999) and for *mCry1*$^{-/-}$ and *mCry2*$^{-/-}$ (van der Horst et al., 1999). Probes were labeled with ^{32}P-dCTP (NEN, Boston, USA) using the Rediprime II Random Prime Labeling Kit (Amersham Pharmacia, Little Chalfont, UK). Unincorporated nucleotides were removed with ProbeQuant G-50 Micro Columns (Amersham Pharmacia). Incorporation efficiency was assessed by measuring the activity of the probe with a liquid scintillation counter (Canberra Packard, Zürich, Switzerland).

4.2.1.3. DNA Extraction

Tail tips (~1cm) taken at the age of weaning (3-4 weeks) were used as tissue samples with a sharp scalpel blade or scissors. Excessive bleeding was stopped by holding a flamed blade briefly to the truncated tail. Tips were digested in a roller bottle over night at 55-60°C in 500µl of 100mM Tris/HCl, 5mM EDTA, 200mM NaCl, 0.2% SDS, 100µg/ml Proteinase K (pH 8.5). Genomic DNA was precipitated with Ethanol. The cloudy DNA was transferred to a new tube using a pipette tip and washed once with 70% Ethanol and 100% Ethanol before drying. The pellet was then dissolved in 50µl TE buffer (10mM Tris/ HCl, 1mM EDTA, pH 7.5) and stored at 4°C.

4.2.1.4. Southern Blotting and Hybridization

- start with 10µg genomic DNA in TE buffer
- + water up to 20µl
- + 2.5µl 10x restriction enzyme buffer (New England Biolabs, Boston, USA)
- + 2.5µl (50U) restriction enzyme (*EcoRI* for *Per1* and *Cry2*, *BamH1* for *Per2*, *Not1* for *Cry1*, all from NEB)
  Incubation ON at 37°C
- + 5µl 6x DNA Loading Buffer (0.25% (w/v) bromophenol blue, 0.25% (w/v) xylene cyanol FF, 30% (v/v) glycerol)
  mix gently with the pipette tip to avoid shearing of the genomic DNA
- load samples on a 0.7% agarose gel (no ethidium bromide!) in a Gibco Sunrise electrophoresis chamber (Invitrogen, San Diego, USA)
- run at 60V (~ 6-8h) until the bromophenol blue band hits the next loading slot row
- cut gel and mark orientation
- incubate gel for 10min in 0.05‰ ethidium bromide in TE buffer
- photograph gel on a UV screen (Vilber Lourmat, Marne Le Valée, France)
- partly hydrolyze the DNA in 0.25M hydrochloric acid (exactly 2x 5min!)
- denature in 0.4M sodium hydroxide (20min)
- assemble blotting chamber (from bottom to top: 0.4M sodium hydroxide for transfer, blotting paper, gel (turn upside down for better transfer efficiency), blotting membrane (Hybond$^+$, NEN), blotting paper, paper towels, weight) and leave ON
- disassemble chamber, mark membrane and cross-link (Stratagene Linker, Stratagene, La Jolla, USA)
- wash 2x with water and put into hybridization bottle
- add appropriate volume of hybridization buffer (QuikHyb, Stratagene) and rotate at 68°C (minimum 20min) prior to hybridization
- denature probe and hybridize 1h at 68°
- remove excess buffer and wash three times with 2xSSC (0.3M sodium chloride, 0.03M sodium citrate, pH 7), 0.1% SDS
- wash 2x 15min with 2xSSC, 0.1% SDS at RT
- wash 2x 20min with 0.1xSSC, 0.1%SDS at 60-63°C in a shaking water bath

- wrap membrane with Saran and expose on film (-80°C with enhancer screen (Amersham Pharmacia)) ON

4.2.2. RNA Blotting

4.2.2.1. cDNA Templates

The probes for *mPer1* and *mPer2* were as described (Albrecht et al., 1997b). The *mPer1* probe corresponds to nucleotides 1 to 619 (GenBank accession number AF022992). The *mPer2* probe was made from a cDNA corresponding to nucleotides 229–768 (AF036893). The *mPer2* probe is located outside the region deleted in the mutant. The *c-Fos* probe was made from a mouse cDNA whose nucleotide sequence corresponds to amino acid positions 237–332. The *AVP* probe was made from a cDNA corresponding to nucleotides 1 to 480 (GenBank M88354). The *mCry1* probe was made from a cDNA corresponding to nucleotides 190-771 (accession number AB000777) and the *Bmal1* probe corresponding to nucleotides 654-1290 (accession number AF015953).
cDNA was obtained by RT-PCR from brain total RNA (for preparation see below) using Superscript II (Gibco/ Invitrogen) and Taq Polymerase (Qiagen, Hilden, Germany) and standard protocols (Sambrook and Russel, 2001). PCR product was cloned into pCR II Topo vector using TOPO TA Cloning Kit (Invitrogen). Single colonies were picked and grown in LB medium (1% (w/v) tryptone, 0.5% (w/v) yeast extract, 1% (w/v) sodium chloride, 0.1 mg/ml ampicillin) for Maxi preparation of plasmid DNA using QIAfilter Plasmid Maxi Kit (Qiagen). Inserts were cut from the vector with *EcoRI* and extracted from an agarose gel (1%, with ethidium) using QIAEX II Gel Extraction Kit (Qiagen).

4.2.2.2. Probe Preparation

See probe preparation for genotyping (4.2.1.2.).

4.2.2.3. RNA Purification

Animals were killed by cervical dislocation and tissue removed and transferred into RNAzol B (WAK Chemie, Bad Soden, Germany; ~1ml per 0.25g of tissue) on ice. After

homogenization (Polytron PT 1200, Kinematica, Littau, Switzerland) 1/10 volumes chloroform was added and mixed before incubation on ice for 5min. After centrifugation (15min, 13k rpm, 4°C) supernatant was transferred to a fresh tube and RNA precipitated with an equal volume of 2-Propanol (15min on ice). Total RNA pellets were stored at –80°C under 50% 2-Propanol and dissolved in water before use. For mRNA preparation we used Oligotex mRNA Kit (Qiagen) according to the protocol of the manufacturer.
To remove excess glycogen from liver total RNA pellets were washed in 4M lithium chloride before use.

4.2.2.4. Northern Blotting and Hybridization

- start with 20µg total RNA or up to 10µg mRNA in 5µl water
- + 2.2µl 5x Running Buffer (0.1M MOPS (pH 7), 25mM sodium acetate, 5mM EDTA)
  + 3.9µl 37% (w/v) formaldehyde
  + 11.1µl formamide
  + 2.2µl 6x RNA Loading Buffer (see DNA Loading Buffer but without xylene cyanol FF)
- incubation for 15min at 65°C
- load samples on a 1% agarose gel (no ethidium!) containing formaldehyde (see (Sambrook and Russel, 2001))
- run at 10-15V (ON) until the bromophenol blue band hits the end of the gel
- cut gel and mark orientation
- incubate gel for 5min in water
- partly hydrolyze the RNA in 50mM sodium hydroxide, 10mM sodium chloride (45min)
- neutralize in 0.1M Tris/HCl (pH 7.5) for 45min
- equilibrate gel in 20xSSC (see above) for 1h
- assemble blotting chamber (from bottom to top: 10xSSC for transfer, blotting paper, gel (turn upside down for better transfer efficiency), blotting membrane (Hybond$^+$, NEN), blotting paper, paper towels, weight) and leave ON
- disassemble chamber, mark membrane and UV crosslink
- wash 2x with water and put into hybridization bottle
- add appropriate volume of hybridization buffer (QuikHyb, Stratagene or UltraHyb, Ambion, Austin, USA) and rotate at 68°C (QuikHyb, minimum 20min) or 42°C (UltraHyb, 1-2h) prior to hybridization

- denature probe and hybridize 1-2h at 68° (QuikHyb) or at 42°C (UltraHyb)
- remove excess buffer and wash three times with 2xSSC, 0.1% SDS
- wash 20min with 2xSSC, 0.1% SDS at RT
- wash 2x 20min with 0.1xSSC, 0.1%SDS at 60°C in a shaking water bath
- wrap membrane with Saran and expose on film (-80°C with enhancer screen (Amersham Pharmacia)) or on phosphoimager screen.

4.2.2.5. Quantification

Exposed phosphoimager plates (Bio-Rad, Hercules, USA) were scanned with a phosphoimager (Bio-Rad) and quantified using Quantity One V3.0 software (Bio-Rad).

4.2.3. *In situ* Hybridization

In situ Hybridization was performed according to Albrecht et al., 1997a.

4.2.3.1. cDNA Templates

For most templates see 4.2.2.1. The *c-Fos* probe was made from a mouse cDNA whose nucleotide sequence corresponds to amino acid positions 237–332. The *AVP* probe was made from a cDNA corresponding to nucleotides 1 to 480 (GenBank M88354).

4.2.3.2. Probe Preparation

^{35}S-UTP (NEN) labeled RNA probes were made using RNA Transcription Kit (Stratagene) with T7, T3 or SP6 RNA polymerases (Stratagene, NEB and Promega, Madison, USA). 1µg linearized plasmid template was used in a 30µl setup sufficient for 24 slides according to the manufacturer's protocol.
Incorporation was determined by liquid scintillation and probes were diluted to 2-6M cpm per slide in HybMix (25% (v/v formamide, 0.3M NaCl, 20mM Tris/HCl (pH 8), 5mM EDTA, 10% (w/v) dextrane sulfate, 0.02% Ficoll, 0.02% BSA, 0.02% polyvinylpyrolidone, 0.5mg/ml yeast RNA, 0.1M DTT, 250µM αS-ATP).

4.2.3.3. Tissue Preparation

Either paraffin embedded or frozen tissue was used. For paraffin embedding animals were killed by cervical dislocation, tissue was removed and immersion fixed in 4% paraformaldehyde (PFA) in PBS (pH 7.4) at 4°C for 12-18h. Tissues were then dehydrated with ethanol (30, 50, 70 and 100%, 3h each at 4°C) and transferred to xylene. Xylene was changed once and replaced by 50% xylene/ 50% paraffin and 3x paraffin at 60°C before pouring the samples in embedding forms. Tissues were cut on the following day or later using a microtome (R. Jung, Hamburg, Germany) at 7µm thickness and stored at RT before use.
For cryo-sections tissue was shock frozen in liquid nitrogen, cut embedded in TissueTek (Sakura Finetec, Zoeterwoude, The Netherlands) on a cryostat (Leica Microsystems, Wetzlar, Germany) at 20µm thickness and stored at –80°C before use.

4.2.3.4. Hybridization

All de-waxing steps were performed with paraffin embedded sections in Tissue Tek II cuvette racks (Sakura Finetec,).

- 2x Histoclear (Vogel, Giessen, Germany) 10min
- 2x 100% Ethanol 2min
- re-hydrate with ethanol 20s each (95/80/70/50/30%)
- 0.9% sodium chloride 5min
- PBS 5min
- 4% PFA (pH7.4 in PBS) 20min
- 2x PBS 5min
- Proteinase K (20µg/ml in 50mM Tris/HCl, 5mM EDTA pH8.5) 5min
- PBS 5min
- 4% PFA pH7.4 20min
- acetylation in 0.1M Triethanolamine/HCl pH8: add 600µl acetic anhydride on 250ml; stir 3min; add another 600µl acetic anhydride and stir 7min
- PBS 5min
- 0.9% sodium chloride 5min
- de-hydrate with ethanol 20sec each (30/50/70/80/95/100%)

- let slides air-dry at a RNase-free place

Frozen sections were fixed in PFA and treated like paraffin sections subsequently. Hybridization was performed in humidified chambers (5x SSC, 50% (v/v) formamide) in a hybridization oven ON at 55-58°C. Probe was put on the slides and spread over the whole area using a pipette tip before covering with a cover slip. Post-hybridization was performed in Tissue Tek II cuvettes (Sakura Finetec).

- Removal Wash: 30min in 5xSSC/ 20mM mercaptoethanol (ME) at 64°C in a shaking water bath; after 10min cover slips were removed using forceps
- 2xSSC/ 50% formamide/ 40mM ME 30min at 64°C
- 3x NTE (50mM sodium chloride, 10mM Tris/ HCl, 5mM EDTA, pH 8) 15min at 37°C
- RNase A (20µg/ml in NTE) 30min at 37°C
- NTE 15min at 37°C
- 2xSSC/ 50% formamide/ 40mM ME 30min at 64°C
- 2xSSC 15min at RT
- 0,1xSSC 15min
- de-hydration with ethanol 30sec each (30/60/80% EtOH/ 0.3M ammonium acetate, 95/100/100% EtOH)
- let slides air-dry before exposure to film or coating with liquid film (Kodak)

4.2.3.5. Quantification

Exposed films were scanned with a flatbed scanner (Hewlett Packard, Palo Alto, USA). SCN cut outs were selected using Adobe PhotoShop (Adobe, San Jose, USA) and analyzed densitometrically with NIH Image 1.62 (National Institutes of Health, USA). Three sections per brain were used and background subtracted from adjacent hypothalamic areas on the same slide. Measurements from different animals/ experiments were combined for statistical analysis performed with GraphPad Prism software (GraphPad Software, San Diego, USA).

4.3. Immunological Experiments

4.3.1. Immunohistochemistry and –fluorescence

4.3.1.1. Antibodies

Antigen / Antibody	Company	Catalog Number	Working dilution
Rabbit-αPER2 (mouse)	Alpha Diagnostics	PER21-A	1:200
Rabbit-αCRY1 (mouse)	Alpha Diagnostics	CRY11-A	1:200
Rabbit-αCREB (mouse)	Cell Signalling Tech	9192S	1:500
Rabbit-αP^{133}-CREB (mouse)	New England Biolabs	9191S	1:500
Biotinylated Goat-αIgG (rabbit)	Vector Laboratories	PK6101	1:200

Tab. 10: Used Antibodies and Dilutions.

The secondary antibodies were included in the Vectastain Elite Kit used for all immunostaining protocols (Vector Laboratories, Burlingame, USA).

4.3.1.2. Tissue Preparation

Tissue was prepared as described for *in situ* hybridization (4.2.2.3.).

4.3.1.3. Immunohistochemistry

- 2x 10min xylene
- 2min ethanol
- re-hydration with ethanol (100/70/50/30%) 20sec each
- 2min water
- 10min 3% (v/v) hydrogen peroxide in methanol
- 3x 2min water
- 2min 0,01M sodium citrate (pH6)
- 10min boiling in citrate (s.a.)
- 10min cool down
- 2min TNT (0.1M Tris/ HCl pH 7.5, 150mM sodium chloride, 0.05% Tween20); put slides in flow chambers (Rediflow, Tecan, Durham, USA)
- 2x 2min TNT

- 1h normal goat serum (Vectastain Kit, in TNT)
- 1st antibody ON at RT (in TNT; store horizontally in a humidified chamber)
- 3x 5min TNT
- 2nd antibody 1h at RT (Vectastain Kit, in TNT)
- 3x 5min TNT
- 1h AB-Complex (Vectastain Kit, in TNT) RT
- 3x 5min TNT
- 10min Ni/DAB (1g nickel ammonium sulfate;17.5mg diaminobenzidine/HCl (both from Fluka, Germany) in 100ml 0.1M sodium acetate (pH 6)
- add 100µl 30% H_2O_2; incubate for 5min
- 3x 5min TNT
- 2x 20sec water
- air dry
- apply cover slips with Canada Balsam

4.3.1.4. Immunofluorescence

All steps for immunofluorescence follow the immunohistochemistry protocol up to the incubation with the AB-Complex. Further protocol as follows:

- 3x 5min TNT
- 20min Tyramide-Fluoresceine in NEN amplification buffer (Tyramide Amplification Kit, NEN)
- 3x 5min TNT
- dehydrate with ethanol 20sec each (30/50/70/100% ethanol)
- 2min xylene
- mount coverslips with DPX (Fluka, Germany)

4.3.1.5. Quantification

Semiquantitative analysis of immunohistochemistry was performed with NIH Image software 1.62 (National Institutes of Health). In selected slice areas positively stained nuclei were counted after thresholding. Three slices per SCN of similar regions were selected and the average value determined. Values from multiple experiments were taken for statistical analysis with GraphPad Prism software (GraphPad Software).

4.4. Histological Experiments

4.4.1. Nissl Staining

To visualize cell nuclei in brain and eye slices samples were stained with Cresyl Violet according to Nissl:
Slides were de-waxed and re-hydrated and subsequently colorised 5min in Cresyl Violet (0.15g in 250ml 0.3M sodium acetate buffer, pH 5.5, 60°C). After de-hydration slides were incubated in xylene and coverslips mounted with DPX.

4.4.2. Gomori's Trichrome Staining

Slides were de-waxed and re-hydrated and post-fixated in Bouin's Fluid (70% (v/v) saturated picric acid, 10% (w/v) formaldehyde and 5% (v/v) acetic acid) for 30min at 56°C (. After washing with water slides were stained for 15-20min with Trichrome Stain (0.6% (w/v) Chromotrope 2R, 0.3% (w/v) Light Green, 1% (v/v) acetic acid and 0.8% (w/v) phosphotungstic acid). Subsequently samples were washed with 0.5% (v/v) acetic acid for 2min and 1% (v/v) acetic acid containing 0.7% (w/v) phosphotungstic acid if the staining was still too dark. After that slides were de-hydrated, incubated in xylene and coverslips were mounted with DPX.

4.4.3. Lipofuscin Staining

Slides were de-waxed and re-hydrated with decreasing concentrations of ethanol. After a brief rinsing in distilled water they were incubated for 5min in 0.75% (w/v) ferric chloride/ 0.1%

(w/v) potassium ferricyanide. Subsequently they were transferred to 1% (v/v) acetic acid (5min), washed in distilled water (10min) and colonized with neutral red (1% (w/v) for 3.5min. After another wash with distilled water slides were de-hydrated in increasing ethanol concentrations. After incubation with xylene coverslips were applied using DPX embedding medium.

4.4.4. Congo Red Staining

Congo red staining was performed using Accustain Amyloid Stain, Congo Red (Sigma Diagnostics, St. Louis, USA). Slides were de-waxed and re-hydrated with decreasing concentrations of ethanol. After a brief rinsing in distilled water they were incubated for 10min in Mayer's hematoxylin. Subsequently slides were incubated for 5min in distilled water, for 20min in 0.01% (w/v) sodium hydroxide in saturated sodium chloride solution, and for 20min in 0.01% (w/v) sodium hydroxide, 0.2% (w/v) Congo red in 80% saturated sodium chloride solution. After that slides were washed three times (1min each) with ethanol and two times with xylene. Coverslips were applied using DPX embedding medium.

Chapter 5

References

Akashi, M., and Nishida, E. (2000). Involvement of the MAP kinase cascade in resetting of the mammalian circadian clock, Genes Dev *14*, 645-9.

Akhtar, R. A., Reddy, A. B., Maywood, E. S., Clayton, J. D., King, V. M., Smith, A. G., Gant, T. W., Hastings, M. H., and Kyriacou, C. P. (2002). Circadian cycling of the mouse liver transcriptome, as revealed by cDNA microarray, is driven by the suprachiasmatic nucleus, Curr Biol *12*, 540-50.

Albrecht, U., Eichele, G., Helms, J. A., and Lu, H.-C. (1997a). Visualization of gene expression patterns by in situ hybridization. In Human Genome Methods, K. W. Adolph, ed. (Boca Raton, CRC Press), pp. 93-120.

Albrecht, U., and Foster, R. G. (2002). Placing ocular mutants into a functional context: A chronobiological approach, Methods *in press*.

Albrecht, U., and Oster, H. (2001). The circadian clock and behavior, Behav Brain Res *125*, 89-91.

Albrecht, U., Sun, Z. S., Eichele, G., and Lee, C. C. (1997b). A differential response of two putative mammalian circadian regulators, mper1 and mper2, to light, Cell *91*, 1055-64.

Albrecht, U., Zheng, B., Larkin, D., Sun, Z. S., and Lee, C. C. (2001). MPer1 and mper2 are essential for normal resetting of the circadian clock, J Biol Rhythms *16*, 100-4.

Allen, G., Rappe, J., Earnest, D. J., and Cassone, V. M. (2001). Oscillating on borrowed time: diffusible signals from immortalized suprachiasmatic nucleus cells regulate circadian rhythmicity in cultured fibroblasts, J Neurosci *21*, 7937-43.

Alleva, J. J., Waleski, M. V., and Alleva, F. R. (1971). A biological clock controlling the estrous cycle of the hamster, Endocrinology *88*, 1368-79.

Avivi, A., Albrecht, U., Oster, H., Joel, A., Beiles, A., and Nevo, E. (2001). Biological clock in total darkness: the Clock/MOP3 circadian system of the blind subterranean mole rat, Proc Natl Acad Sci U S A *98*, 13751-6.

Bae, K., Jin, X., Maywood, E. S., Hastings, M. H., Reppert, S. M., and Weaver, D. R. (2001). Differential Functions of *mPer1*, *mPer2* and *mPer3* in the SCN Circadian CLock, Neuron *30*, 525-536.

Balsalobre, A. (2002). Clock genes in mammalian peripheral tissues, Cell Tissue Res *309*, 193-9.

Balsalobre, A., Brown, S. A., Marcacci, L., Tronche, F., Kellendonk, C., Reichardt, H. M., Schutz, G., and Schibler, U. (2000a). Resetting of circadian time in peripheral tissues by glucocorticoid signaling, Science *289*, 2344-7.

Balsalobre, A., Damiola, F., and Schibler, U. (1998). A serum shock induces circadian gene expression in mammalian tissue culture cells, Cell *93*, 929-37.

Balsalobre, A., Marcacci, L., and Schibler, U. (2000b). Multiple signaling pathways elicit circadian gene expression in cultured Rat-1 fibroblasts, Curr Biol *10*, 1291-4.

Barinaga, M. (1999). Circadian rhythms. CRY's clock role differs in mice, flies, Science *285*, 506-7.

Ben-Shlomo, R., Ritte, U., and Nevo, E. (1995). Activity Pattern and Rhythm in the Subterranean Mole Rat Superspecies *Spalax Ehrenbergii*, Behav Genet *25*, 239-45.

Berson, D. M., Dunn, F. A., and Takao, M. (2002). Phototransduction by retinal ganglion cells that set the circadian clock, Science *295*, 1070-3.

Biello, S. M., Janik, D., and Mrosovsky, N. (1994). Neuropeptide Y and behaviorally induced phase shifts, Neuroscience *62*, 273-9.

Bosler, O., and Beaudet, A. (1985). VIP neurons as prime synaptic targets for serotonin afferents in rat suprachiasmatic nucleus: a combined radioautographic and immunocytochemical study, J Neurocytol *14*, 749-63.

Bradbury, M. J., Dement, W. C., and Edgar, D. M. (1997). Serotonin-containing fibers in the suprachiasmatic hypothalamus attenuate light-induced phase delays in mice, Brain Res *768*, 125-34.

Brown, M., and Vale, W. (1979). Trends Neurosci *April*, 95-97.

Buijs, R. M., and Kalsbeek, A. (2001). Hypothalamic integration of central and peripheral clocks, Nat Rev Neurosci *2*, 521-6.

Bunger, M. K., Wilsbacher, L. D., Moran, S. M., Clendenin, C., Radcliffe, L. A., Hogenesch, J. B., Simon, M. C., Takahashi, J. S., and Bradfield, C. A. (2000). Mop3 is an essential component of the master circadian pacemaker in mammals, Cell *103*, 1009-17.

Cagampang, F. R., and Inouye, S. T. (1994). Diurnal and circadian changes of serotonin in the suprachiasmatic nuclei: regulation by light and an endogenous pacemaker, Brain Res *639*, 175-9.

Castel, M., and Morris, J. F. (2000). Morphological heterogeneity of the GABAergic network in the suprachiasmatic nucleus, the brain's circadian pacemaker, J Anat *196*, 1-13.

Cermakian, N., Monaco, L., Pando, M. P., Dierich, A., and Sassone-Corsi, P. (2001). Altered behavioral rhythms and clock gene expression in mice with a targeted mutation in the Period1 gene, Embo J *20*, 3967-74.

Cermakian, N., Pando, M. P., Thompson, C. L., Pinchak, A. B., Selby, C. P., Gutierrez, L., Wells, D. E., Cahill, G. M., Sancar, A., and Sassone-Corsi, P. (2002). Light Induction of a Vertebrate Clock Gene Involves Signaling through Blue-Light Receptors and MAP Kinases, Curr Biol *12*, 844-8.

Cermakian, N., and Sassone-Corsi, P. (2000). Multilevel regulation of the circadian clock, Nat Rev Mol Cell Biol *1*, 59-67.

Cheng, M. Y., Bullock, C. M., Li, C., Lee, A. G., Bermak, J. C., Belluzzi, J., Weaver, D. R., Leslie, F. M., and Zhou, Q. Y. (2002). Prokineticin 2 transmits the behavioural circadian rhythm of the suprachiasmatic nucleus, Nature *417*, 405-10.

Cooper, H. M., Herbin, M., and Nevo, E. (1993). Visual system of a naturally microphthalmic mammal: the blind mole rat, Spalax ehrenbergi, J Comp Neurol *328*, 313-50.

Damiola, F., Le Minh, N., Preitner, N., Kornmann, B., Fleury-Olela, F., and Schibler, U. (2000). Restricted feeding uncouples circadian oscillators in peripheral tissues from the central pacemaker in the suprachiasmatic nucleus, Genes Dev *14*, 2950-61.

Darlington, T. K., Wager-Smith, K., Ceriani, M. F., Staknis, D., Gekakis, N., Steeves, T. D. L., Weitz, C. J., Takahashi, J. S., and Kay, S. A. (1998). Closing the circadian loop: CLOCK-induced transcription of its own inhibitors per and tim, Science *280*, 1599-603.

de la Iglesia, H. O., Meyer, J., Carpino, A., Jr., and Schwartz, W. J. (2000). Antiphase oscillation of the left and right suprachiasmatic nuclei, Science *290*, 799-801.

Ding, J. M., Faiman, L. E., Hurst, W. J., Kuriashkina, L. R., and Gillette, M. U. (1997). Resetting the biological clock: mediation of nocturnal CREB phosphorylation via light, glutamate, and nitric oxide, J Neurosci *17*, 667-75.

Dunlap, J. C. (1999). Molecular bases for circadian clocks, Cell *96*, 271-90.

Eide, E. J., Vielhaber, E. L., Hinz, W. A., and Virshup, D. M. (2002). The circadian regulatory proteins BMAL1 and cryptochromes are substrates of casein Kinase I epsilon (CKIepsilon), J Biol Chem *1*, 1.

Field, M. D., Maywood, E. S., O'Brien, J. A., Weaver, D. R., Reppert, S. M., and Hastings, M. H. (2000). Analysis of clock proteins in mouse SCN demonstrates phylogenetic divergence of the circadian clockwork and resetting mechanisms, Neuron *25*, 437-47.

Francois-Bellan, A. M., and Bosler, O. (1992). Convergent serotonin and GABA innervation of VIP neurons in the suprachiasmatic nucleus demonstrated by triple labeling in the rat, Brain Res *595*, 149-53.

Gannon, R. L., and Rea, M. A. (1995). Twelve-hour phase shifts of hamster circadian rhythms elicited by voluntary wheel running, J Biol Rhythms *10*, 196-210.

Gau, D., Lemberger, T., von Gall, C., Kretz, O., Le Minh, N., Gass, P., Schmid, W., Schibler, U., Korf, H. W., and Schutz, G. (2002). Phosphorylation of CREB Ser142 Regulates Light-Induced Phase Shifts of the Circadian Clock, Neuron *34*, 245-53.

Gekakis, N., Staknis, D., Nguyen, H. B., Davis, F. C., Wilsbacher, L. D., King, D. P., Takahashi, J. S., and Weitz, C. J. (1998). Role of the CLOCK protein in the mammalian circadian mechanism, Science *280*, 1564-9.

Gillette, M. U., and Mitchell, J. W. (2002). Signaling in the suprachiasmatic nucleus: selectively responsive and integrative, Cell Tissue Res *309*, 99-107.

Gillette, M. U., and Tischkau, S. A. (1999). Suprachiasmatic nucleus: the brain's circadian clock, Recent Prog Horm Res *54*, 33-58.

Glass, J. D., Selim, M., Srkalovic, G., and Rea, M. A. (1995). Tryptophan loading modulates light-induced responses in the mammalian circadian system, J Biol Rhythms *10*, 80-90.

Goldman, B. D. (2001). Mammalian photoperiodic system: formal properties and neuroendocrine mechanisms of photoperiodic time measurement, J Biol Rhythms *16*, 283-301.

Goldman, B. D., Goldman, S. L., Riccio, A. P., and Terkel, J. (1997). Circadian patterns of locomotor activity and body temperature in blind mole-rats, Spalax ehrenbergi, J Biol Rhythms *12*, 348-61.

Gooley, J. J., Lu, J., Chou, T. C., Scammell, T. E., and Saper, C. B. (2001). Melanopsin in cells of origin of the retinohypothalamic tract, Nat Neurosci *4*, 1165.

Gotter, A. L., Manganaro, T., Weaver, D. R., Kolakowski, L. F., Jr., Possidente, B., Sriram, S., MacLaughlin, D. T., and Reppert, S. M. (2000). A time-less function for mouse Timeless, Nat Neurosci *3*, 755-756.

Griffin, E. A., Jr., Staknis, D., and Weitz, C. J. (1999). Light-independent role of CRY1 and CRY2 in the mammalian circadian clock, Science *286*, 768-71.

Groos, G., and Hendriks, J. (1982). Circadian rhythms in electrical discharge of rat suprachiasmatic neurones recorded in vitro, Neurosci Lett *34*, 283-8.

Gu, Y. Z., Hogenesch, J. B., and Bradfield, C. A. (2000). The PAS superfamily: sensors of environmental and developmental signals, Annu Rev Pharmacol Toxicol *40*, 519-61.

Hastings, M. H. (2000). Circadian clockwork: two loops are better than one, Nat Rev Neurosci *1*, 143-6.

Hastings, M. H., Duffield, G. E., Ebling, F. J., Kidd, A., Maywood, E. S., and Schurov, I. (1997). Non-photic signalling in the suprachiasmatic nucleus, Biol Cell *89*, 495-503.

Hastings, M. H., Ebling, F. J., Grosse, J., Herbert, J., Maywood, E. S., Mikkelsen, J. D., and Sumova, A. (1995). Immediate-early genes and the neural bases of photic and non-photic entrainment, Ciba Found Symp *183*, 175-89.

Hastings, M. H., Field, M. D., Maywood, E. S., Weaver, D. R., and Reppert, S. M. (1999). Differential Regulation of mPER1 and mTIM Proteins in the Mouse Suprachiasmatic Nuclei: New Insights into a Core Clock Mechanism, J Neurosci *19*, RC11.

Hattar, S., Liao, H. W., Takao, M., Berson, D. M., and Yau, K. W. (2002). Melanopsin-containing retinal ganglion cells: architecture, projections, and intrinsic photosensitivity, Science *295*, 1065-70.

Hermes, M. L., Coderre, E. M., Buijs, R. M., and Renaud, L. P. (1996). GABA and glutamate mediate rapid neurotransmission from suprachiasmatic nucleus to hypothalamic paraventricular nucleus in rat, J Physiol *496*, 749-57.

Herzog, E. D., and Tosini, G. (2001). The mammalian circadian clock shop, Semin Cell Dev Biol *12*, 295-303.

Hogenesch, J. B., Gu, Y. Z., Jain, S., and Bradfield, C. A. (1998). The basic-helix-loop-helix-PAS orphan MOP3 forms transcriptionally active complexes with circadian and hypoxia factors, Proc Natl Acad Sci U S A *95*, 5474-9.

Hogenesch, J. B., Gu, Y. Z., Moran, S. M., Shimomura, K., Radcliffe, L. A., Takahashi, J. S., and Bradfield, C. A. (2000). The basic helix-loop-helix-PAS protein MOP9 is a brain-specific heterodimeric partner of circadian and hypoxia factors, J Neurosci (Online) *20*, RC83.

Honma, S., Ikeda, M., Abe, H., Tanahashi, Y., Namihira, M., Honma, K., and Nomura, M. (1998). Circadian oscillation of BMAL1, a partner of a mammalian clock gene Clock, in rat suprachiasmatic nucleus, Biochem Biophys Res Commun *250*, 83-7.

Ikeda, M., Sagara, M., and Inoue, S. (2000). Continuous exposure to dim illumination uncouples temporal patterns of sleep, body temperature, locomotion and drinking behavior in the rat, Neurosci Lett *279*, 185-9.

Jacob, N., Vuillez, P., Lakdhar-Ghazal, N., and Pevet, P. (1999). Does the intergeniculate leaflet play a role in the integration of the photoperiod by the suprachiasmatic nucleus?, Brain Res *828*, 83-90.

Janik, D., and Mrosovsky, N. (1994). Intergeniculate leaflet lesions and behaviorally-induced shifts of circadian rhythms, Brain Res *651*, 174-82.

Jin, X., Shearman, L. P., Weaver, D. R., Zylka, M. J., de Vries, G. J., and Reppert, S. M. (1999). A molecular mechanism regulating rhythmic output from the suprachiasmatic circadian clock, Cell *96*, 57-68.

Jones, C. R., Campbell, S. S., Zone, S. E., Cooper, F., DeSano, A., Murphy, P. J., Jones, B., Czajkowski, L., and Ptacek, L. J. (1999). Familial advanced sleep-phase syndrome: A short-period circadian rhythm variant in humans, Nat Med *5*, 1062-5.

Kalsbeek, A., and Buijs, R. M. (2002). Output pathways of the mammalian suprachiasmatic nucleus: coding circadian time by transmitter selection and specific targeting, Cell Tissue Res *309*, 109-18.

Kay, S. A. (1997). As time PASses: the first mammalian clock gene, Science *276*, 1093.

Keesler, G. A., Camacho, F., Guo, Y., Virshup, D., Mondadori, C., and Yao, Z. (2000). Phosphorylation and destabilization of human period I clock protein by human casein kinase I epsilon, Neuroreport *11*, 951-5.

King, D. P., Zhao, Y., Sangoram, A. M., Wilsbacher, L. D., Tanaka, M., Antoch, M. P., Steeves, T. D., Vitaterna, M. H., Kornhauser, J. M., Lowrey, P. L., *et al.* (1997). Positional cloning of the mouse circadian clock gene, Cell *89*, 641-53.

Klein, D. C., Moore, R. Y., and Reppert, S. M. (1991). Suprachiasmatic Nucleus: The Mind's Clock (New York, Oxford University Press).

Kobayashi, Y., Ishikawa, T., Hirayama, J., Daiyasu, H., Kanai, S., Toh, H., Fukuda, I., Tsujimura, T., Terada, N., Kamei, Y., *et al.* (2000). Molecular analysis of zebrafish photolyase/cryptochrome family: two types of cryptochromes present in zebrafish, Genes Cells *5*, 725-738.

Konopka, R. J., and Benzer, S. (1971). Clock mutants of Drosophila melanogaster, Proc Natl Acad Sci U S A *68*, 2112-6.

Kow, L., and Pfaff, D. W. (1984). Brain Res *297*, 275-286.

Kume, K., Zylka, M. J., Sriram, S., Shearman, L. P., Weaver, D. R., Jin, X., Maywood, E. S., Hastings, M. H., and Reppert, S. M. (1999). mCRY1 and mCRY2 are essential components of the negative limb of the circadian clock feedback loop, Cell *98*, 193-205.

Lee, C., Etchegaray, J. P., Cagampang, F. R., Loudon, A. S., and Reppert, S. M. (2001). Posttranslational mechanisms regulate the mammalian circadian clock, Cell *107*, 855-67.

Lowrey, P. L., Shimomura, K., Antoch, M. P., Yamazaki, S., Zemenides, P. D., Ralph, M. R., Menaker, M., and Takahashi, J. S. (2000). Positional syntenic cloning and functional characterization of the mammalian circadian mutation tau, Science *288*, 483-92.

Low-Zeddies, S. S., and Takahashi, J. S. (2001). Chimera analysis of the Clock mutation in mice shows that complex cellular integration determines circadian behavior, Cell *105*, 25-42.

Malpaux, B., Migaud, M., Tricoire, H., and Chemineau, P. (2001). Biology of mammalian photoperiodism and the critical role of the pineal gland and melatonin, J Biol Rhythms *16*, 336-47.

Maywood, E. S., Smith, E., Hall, S. J., and Hastings, M. H. (1997). A thalamic contribution to arousal-induced, non-photic entrainment of the circadian clock of the Syrian hamster, Eur J Neurosci *9*, 1739-47.

McNamara, P., Seo, S. P., Rudic, R. D., Sehgal, A., Chakravarti, D., and FitzGerald, G. A. (2001). Regulation of CLOCK and MOP4 by nuclear hormone receptors in the vasculature: a humoral mechanism to reset a peripheral clock, Cell *105*, 877-89.

Meijer, J. H. (1991). Integration of visual information by the suprachiasmatic nucleus. In Suprachiasmatic Nucleus - The Mind's Clock, D. Klein, R. Y. Moore, and S. M. Reppert, eds. (New York, Oxford University Press), pp. 107-119.

Moga, M. M., and Moore, R. Y. (1997). Organization of neural inputs to the suprachiasmatic nucleus in the rat, J Comp Neurol *389*, 508-34.

Moore, R. Y., and Eichler, V. B. (1972). Loss of a circadian adrenal corticosterone rhythm following suprachiasmatic lesions in the rat, Brain research *42*, 201-6.

Moore, R. Y., and Lenn, N. J. (1972). A retinohypothalamic projection in the rat, J Comp Neurol *146*, 1-14.

Moore, R. Y., Speh, J. C., and Leak, R. K. (2002). Suprachiasmatic nucleus organization, Cell Tissue Res *309*, 89-98.

Motzkus, D., Albrecht, U., and Maronde, E. (2002). The human PER1 gene is inducible by interleukin-6, J Mol Neurosci *18*, 105-9.

Motzkus, D., Maronde, E., Grunenberg, U., Lee, C. C., Forssmann, W., and Albrecht, U. (2000). The human PER1 gene is transcriptionally regulated by multiple signaling pathways, FEBS Lett *486*, 315-319.

Mrosovsky, N. (1996). Locomotor activity and non-photic influences on circadian clocks, Biol Rev Camb Philos Soc *71*, 343-72.

Nakamura, W., Honma, S., Shirakawa, T., and Honma, K. I. (2002). Clock mutation lengthens the circadian period without damping rhythms in individual SCN neurons, Nat Neurosci *5*, 399-400.

Negroni, J., Nevo, E., and Cooper, H. M. (1997). Neuropeptidergic organization of the suprachiasmatic nucleus in the blind mole rat (Spalax ehrenbergi), Brain Res Bull *44*, 633-9.

Nevo, E., Guttman, R., Haber, M., and Erez, E. (1982). Activity patterns of evolving mole rats, J Mammal *63*, 453-463.

Nonaka, H., Emoto, N., Ikeda, K., Fukuya, H., Rohman, M. S., Raharjo, S. B., Yagita, K., Okamura, H., and Yokoyama, M. (2001). Angiotensin II induces circadian gene expression of clock genes in cultured vascular smooth muscle cells, Circulation *104*, 1746-8.

Obrietan, K., Impey, S., and Storm, D. R. (1998). Light and circadian rhythmicity regulate MAP kinase activation in the suprachiasmatic nuclei, Nat Neurosci *1*, 693-700.

Oishi, K., Fukui, H., and Ishida, N. (2000). Rhythmic expression of BMAL1 mRNA is altered in Clock mutant mice: differential regulation in the suprachiasmatic nucleus and peripheral tissues, Biochem Biophys Res Commun *268*, 164-71.

Oishi, K., Sakamoto, K., Okada, T., Nagase, T., and Ishida, N. (1998). Humoral signals mediate the circadian expression of rat period homologue (rPer2) mRNA in peripheral tissues, Neurosci Lett *256*, 117-9.

Okamura, H., Abitbol, M., Julien, J. F., Dumas, S., Berod, A., Geffard, M., Kitahama, K., Bobillier, P., Mallet, J., and Wiklund, L. (1990). Neurons containing messenger RNA encoding glutamate decarboxylase in rat hypothalamus demonstrated by in situ hybridization, with special emphasis on cell groups in medial preoptic area, anterior hypothalamic area and dorsomedial hypothalamic nucleus, Neuroscience *39*, 675-99.

Panda, S., Antoch, M. P., Miller, B. H., Su, A. I., Schook, A. B., Straume, M., Schultz, P. G., Kay, S. A., Takahashi, J. S., and Hogenesch, J. B. (2002a). Coordinated transcription of key pathways in the mouse by the circadian clock, Cell *109*, 307-20.

Panda, S., Hogenesch, J. B., and Kay, S. A. (2002b). Circadian rhythms from flies to human, Nature *417*, 329-35.

Pennartz, C. M., Bierlaagh, M. A., and Geurtsen, A. M. (1997). Cellular mechanisms underlying spontaneous firing in rat suprachiasmatic nucleus: involvement of a slowly inactivating component of sodium current, J Neurophysiol *78*, 1811-25.

Pennartz, C. M., De Jeu, M. T., Geurtsen, A. M., Sluiter, A. A., and Hermes, M. L. (1998). Electrophysiological and morphological heterogeneity of neurons in slices of rat suprachiasmatic nucleus, J Physiol *506*, 775-93.

Pickard, G. E., and Turek, F. W. (1983). Brain Res *268*, 201-210.

Pittendrigh, C. S. (1993). Temporal organization: reflections of a Darwinian clock-watcher, Annu Rev Physiol *55*, 16-54.

Pittendrigh, C. S., and Daan, S. (1976). A Functional Analysis of Circadian Pacemakers in Nocturnal Rodents, Journal of comparative Physiology *106*, 291-331.

Preitner, N., Damiola, F., Lopez-Molina, L., Zakany, J., Duboule, D., Albrecht, U., and Schibler, U. (2002). The Orphan Nuclear Receptor REV-ERBalpha Controls Circadian Transcription within the Positive Limb of the Mammalian Circadian Oscillator, Cell *110*, 251-60.

Provencio, I., Rollag, M. D., and Castrucci, A. M. (2002). Photoreceptive net in the mammalian retina. This mesh of cells may explain how some blind mice can still tell day from night, Nature *415*, 493.

Rado, R., and Terkel, J. (1989). Circadian activity of the blind mole rat, *Spalax ehrenbergii*, monitored by radio telemetry, in seminatural and natural conditions, Environmental Quality and Ecosystem Stability *IV*, 391-400.

Ralph, M. R., and Menaker, M. (1988). A mutation of the circadian system in golden hamsters, Science *241*, 1225-7.

Reick, M., Garcia, J. A., Dudley, C., and McKnight, S. L. (2001). NPAS2: an analog of clock operative in the mammalian forebrain, Science *293*, 506-9.

Rensing, L., Meyer-Grahle, U., and Ruoff, P. (2001). Biological timing and the clock metaphor: oscillatory and hourglass mechanisms, Chronobiol Int *18*, 329-69.

Reppert, S., and Weaver, D. (2001). Molecular analysis of mammalian circadian rhythms, Annu Rev Physiol *63*, 647-76.

Reppert, S. M. (1998). A clockwork explosion!, Neuron *21*, 1-4.

Ripperger, J. A., Shearman, L. P., Reppert, S. M., and Schibler, U. (2000). CLOCK, an essential pacemaker component, controls expression of the circadian transcription factor DBP, Genes Dev *14*, 679-89.

Rutter, J., Reick, M., Wu, L. C., and McKnight, S. L. (2001). Regulation of clock and NPAS2 DNA binding by the redox state of NAD cofactors, Science *293*, 510-4.

Sambrook, J., and Russel, D. W. (2001). Molecular Cloning, Vol 1, 3 edn (Cold Spring Harbour, USA, Cold Spring Harbour Laboratory Press).

Sancar, A. (2000). Cryptochrome: the second photoactive pigment in the eye and its role in circadian photoreception, Annu Rev Biochem *69*, 31-67.

Sangoram, A. M., Saez, L., Antoch, M. P., Gekakis, N., Staknis, D., Whiteley, A., Fruechte, E. M., Vitaterna, M. H., Shimomura, K., King, D. P., *et al.* (1998). Mammalian circadian autoregulatory loop: a timeless ortholog and mPer1 interact and negatively regulate CLOCK-BMAL1-induced transcription, Neuron *21*, 1101-13.

Schibler, U., Ripperger, J. A., and Brown, S. A. (2001). Circadian rhythms. Chronobiology--reducing time, Science *293*, 437-8.

Schwartz, W. J., de la Iglesia, H. O., Zlomanczuk, P., and Illnerova, H. (2001). Encoding le quattro stagioni within the mammalian brain: photoperiodic orchestration through the suprachiasmatic nucleus, J Biol Rhythms *16*, 302-11.

Shearman, L. P., Jin, X., Lee, C., Reppert, S. M., and Weaver, D. R. (2000a). Targeted Disruption of the mPer3 Gene: Subtle Effects on Circadian Clock Function, Mol Cell Biol *20*, 6269-6275.

Shearman, L. P., Sriram, S., Weaver, D. R., Maywood, E. S., Chaves, I., Zheng, B., Kume, K., Lee, C. C., van der Horst, G. T., Hastings, M. H., and Reppert, S. M. (2000b). Interacting Molecular Loops in the Mammalian Circadian Clock, Science *288*, 1013-1019.

Shearman, L. P., Zylka, M. J., Weaver, D. R., Kolakowski, L. F., Jr., and Reppert, S. M. (1997). Two period homologs: circadian expression and photic regulation in the suprachiasmatic nuclei, Neuron *19*, 1261-9.

Shigeyoshi, Y., Taguchi, K., Yamamoto, S., Takekida, S., Yan, L., Tei, H., Moriya, T., Shibata, S., Loros, J. J., Dunlap, J. C., and Okamura, H. (1997). Light-induced resetting of a mammalian circadian clock is associated with rapid induction of the mPer1 transcript, Cell *91*, 1043-53.

Shinohara, K., Tominaga, K., Fukuhara, C., Otori, Y., and Inouye, S. I. (1993). Processing of photic information within the intergeniculate leaflet of the lateral geniculate body: assessed by neuropeptide Y immunoreactivity in the suprachiasmatic nucleus of rats, Neuroscience *56*, 813-22.

Silver, R., LeSauter, J., Tresco, P. A., and Lehman, M. N. (1996). A diffusible coupling signal from the transplanted suprachiasmatic nucleus controlling circadian locomotor rhythms, Nature *382*, 810-3.

Stephan, F. K., and Zucker, I. (1972). Proc Natl Acad Sci U S A *69*, 1583-1596.

Storch, K., Lipan, O., Leykin, I., Viswanathan, N., Davis, F., Wong, W., and Weitz, C. (2002). Extensive and divergent circadian gene expression in liver and heart, Nature *417*, 78-83.

Sumova, A., Ebling, F. J., Maywood, E. S., Herbert, J., and Hastings, M. H. (1994). Non-photic circadian entrainment in the Syrian hamster is not associated with phosphorylation of the transcriptional regulator CREB within the suprachiasmatic nucleus, but is associated with adrenocortical activation, Neuroendocrinology *59*, 579-89.

Sun, Z. S., Albrecht, U., Zhuchenko, O., Bailey, J., Eichele, G., and Lee, C. C. (1997). RIGUI, a putative mammalian ortholog of the Drosophila period gene, Cell *90*, 1003-11.

Swanson, L. W., and Cowan, W. M. (1975). The efferent connections of the suprachiasmatic nucleus of the hypothalamus, J Comp Neurol *160*, 1-12.

Swanson, L. W., Mogenson, G. J., Simerly, R. B., and Wu, M. (1987). Anatomical and electrophysiological evidence for a projection from the medial preoptic area to the 'mesencephalic and subthalamic locomotor regions' in the rat, Brain Res *405*, 108-22.

Takumi, T., Matsubara, C., Shigeyoshi, Y., Taguchi, K., Yagita, K., Maebayashi, Y., Sakakida, Y., Okumura, K., Takashima, N., and Okamura, H. (1998). A new mammalian period gene predominantly expressed in the suprachiasmatic nucleus, Genes Cells *3*, 167-76.

Tei, H., Okamura, H., Shigeyoshi, Y., Fukuhara, C., Ozawa, R., Hirose, M., and Sakaki, Y. (1997). Circadian oscillation of a mammalian homologue of the Drosophila period gene, Nature *389*, 512-6.

Thresher, R. J., Vitaterna, M. H., Miyamoto, Y., Kazantsev, A., Hsu, D. S., Petit, C., Selby, C. P., Dawut, L., Smithies, O., Takahashi, J. S., and Sancar, A. (1998). Role of mouse

cryptochrome blue-light photoreceptor in circadian photoresponses, Science *282*, 1490-4.

Tobler, I., Herrmann, M., Cooper, H. M., Negroni, J., Nevo, E., and Achermann, P. (1998). Rest-activity rhythm of the blind mole rat Spalax ehrenbergi under different lighting conditions, Behav Brain Res *96*, 173-83.

Toh, K. L., Jones, C. R., He, Y., Eide, E. J., Hinz, W. A., Virshup, D. M., Ptacek, L. J., and Fu, Y. H. (2001). An hPer2 phosphorylation site mutation in familial advanced sleep phase syndrome, Science *291*, 1040-3.

van den Pol, A. N. (1980). The hypothalamic suprachiasmatic nucleus of the rat: intrinsic anatomy, J Comp Neurol *191*, 661-702.

van den Pol, A. N. (1991). The suprachiasmatic nucleus: morphological and chemical substrates for cellular interaction. In Suprachiasmatic Nucleus: The Mind's Clock, D. C. Klein, R. Y. Moore, and S. M. Reppert, eds. (New York, Oxford University Press), pp. 17-50.

van den Pol, A. N., Finkbeiner, S. M., and Cornell-Bell, A. H. (1992). Calcium excitability and oscillations in suprachiasmatic nucleus neurons and glia in vitro, J Neurosci *12*, 2648-64.

van der Horst, G. T., Muijtjens, M., Kobayashi, K., Takano, R., Kanno, S., Takao, M., de Wit, J., Verkerk, A., Eker, A. P., van Leenen, D., *et al.* (1999). Mammalian Cry1 and Cry2 are essential for maintenance of circadian rhythms, Nature *398*, 627-30.

van Reeth, O., and Turek, F. W. (1989). Stimulated activity mediates phase shifts in the hamster circadian clock induced by dark pulses or benzodiazepines, Nature *339*, 49-51.

Vielhaber, E., Eide, E., Rivers, A., Gao, Z. H., and Virshup, D. M. (2000). Nuclear Entry of the Circadian Regulator mPER1 Is Controlled by Mammalian Casein Kinase I epsilon, Mol Cell Biol *20*, 4888-4899.

Vitaterna, M. H., King, D. P., Chang, A. M., Kornhauser, J. M., Lowrey, P. L., McDonald, J. D., Dove, W. F., Pinto, L. H., Turek, F. W., and Takahashi, J. S. (1994). Mutagenesis and mapping of a mouse gene, Clock, essential for circadian behavior, Science *264*, 719-25.

Vitaterna, M. H., Selby, C. P., Todo, T., Niwa, H., Thompson, C., Fruechte, E. M., Hitomi, K., Thresher, R. J., Ishikawa, T., Miyazaki, J., *et al.* (1999). Differential regulation of mammalian period genes and circadian rhythmicity by cryptochromes 1 and 2, Proc Natl Acad Sci U S A *96*, 12114-9.

Watts, A. G. (1991). The efferent projections of the suprachiasmatic nucleus: anatomical insights into the control of circadian rhythms. In Suprachiasmatic Nucleus - The Mind's Clock, D. C. Klein, R. Y. Moore, and S. M. Reppert, eds. (New York, Oxford University Press), pp. 77-106.

Welsh, D. K., Logothetis, D. E., Meister, M., and Reppert, S. M. (1995). Individual neurons dissociated from rat suprachiasmatic nucleus express independently phased circadian firing rhythms, Neuron *14*, 697-706.

Wickland, C. R., and Turek, F. W. (1991). Phase-shifting effects of acute increases in activity on circadian locomotor rhythms in hamsters, Am J Physiol *261*, R1109-17.

Wilsbacher, L. D., Yamazaki, S., Herzog, E. D., Song, E. J., Radcliffe, L. A., Abe, M., Block, G., Spitznagel, E., Menaker, M., and Takahashi, J. S. (2002). Photic and circadian expression of luciferase in mPeriod1-luc transgenic mice invivo, Proc Natl Acad Sci U S A *99*, 489-94.

Xia, Z., Dudek, H., Miranti, C. K., and Greenberg, M. E. (1996). Calcium influx via the NMDA receptor induces immediate early gene transcription by a MAP kinase/ERK-dependent mechanism, J Neurosci *16*, 5425-36.

Yagita, K., and Okamura, H. (2000). Forskolin induces circadian gene expression of rPer1, rPer2 and dbp in mammalian rat-1 fibroblasts, FEBS Lett *465*, 79-82.

Yagita, K., Tamanini, F., van Der Horst, G. T., and Okamura, H. (2001). Molecular mechanisms of the biological clock in cultured fibroblasts, Science *292*, 278-81.

Yagita, K., Tamanini, F., Yasuda, M., Hoeijmakers, J. H., van der Horst, G. T., and Okamura, H. (2002). Nucleocytoplasmic shuttling and mCRY-dependent inhibition of ubiquitylation of the mPER2 clock protein, Embo J *21*, 1301-14.

Yagita, K., Yamaguchi, S., Tamanini, F., van Der Horst, G. T., Hoeijmakers, J. H., Yasui, A., Loros, J. J., Dunlap, J. C., and Okamura, H. (2000). Dimerization and nuclear entry of mPER proteins in mammalian cells, Genes Dev *14*, 1353-63.

Young, M. W., and Kay, S. A. (2001). Time zones: a comparative genetics of circadian clocks, Nat Rev Genet *2*, 702-15.

Yu, W., Nomura, M., and Ikeda, M. (2002). Interactivating feedback loops within the mammalian clock: BMAL1 is negatively autoregulated and upregulated by CRY1, CRY2, and PER2, Biochem Biophys Res Commun *290*, 933-41.

Zheng, B., Albrecht, U., Kaasik, K., Sage, M., Lu, W., Vaishnav, S., Li, Q., Sun, Z. S., Eichele, G., Bradley, A., and Lee, C. C. (2001). Nonredundant roles of the mPer1 and mPer2 genes in the mammalian circadian clock, Cell *105*, 683-94.

Zheng, B., Larkin, D. W., Albrecht, U., Sun, Z. S., Sage, M., Eichele, G., Lee, C. C., and Bradley, A. (1999). The mPer2 gene encodes a functional component of the mammalian circadian clock, Nature *400*, 169-73.

Zylka, M. J., Shearman, L. P., Levine, J. D., Jin, X., Weaver, D. R., and Reppert, S. M. (1998a). Molecular analysis of mammalian timeless, Neuron *21*, 1115-22.

Zylka, M. J., Shearman, L. P., Weaver, D. R., and Reppert, S. M. (1998b). Three period homologs in mammals: differential light responses in the suprachiasmatic circadian clock and oscillating transcripts outside of brain, Neuron *20*, 1103-10.

Chapter 6

Curriculum Vitae

Henrik Oster

* 23.04.1973	in Trier/ Germany
08.83-07.92	High school attendance at the Treviris Gymnasium Trier and the Detlefsenschule Glückstadt/ Germany
06.92	Abitur at the Detlefsenschule Glückstadt
08.92-10.93	Public service at the Diakonie-Sozialstation Glückstadt
10.93-06.99	University courses in biochemistry at the University of Hannover/ Germany
05.96-01.97	Project work in the group of Prof. G. Brabant at Hannover Medical School (MHH) on cell adhesion molecules and DNA methylation in human thyroid carcinoma
03.97-05.97	Project work in the group of Prof. T.J. Jentsch at the Center for Molecular Neurobiology Hamburg/ Germany (ZMNH) on the morphological and functional characterization of the voltage regulated chloride channel hCLC-1
03.98-05.98	Project work in the group of Prof. J. Barber at the Imperial College for Science, Medicine and Technology London/ UK on the structural characterization of CP43 in the plant photosystem II
11.98-06.99	Graduation project in the group of Dr. R. Bauerfeind (Institue of Physiological Chemistry, Prof. H.H. Niemann) at Hannover Medical School on molecular interactions of Amphiphysin 1 in the endocytosis machinery
06.99	Diploma in biochemistry at Hannover Medical School
since 09.99	Ph.D. studentship in the group of Prof. U. Albrecht at the Max Planck Institute for Experimental Endocrinology Hannover and the University of Fribourg/ Switzerland on the interactions of *Per* and *Cry* genes in the mammalian circadian clock

Chapter 7

Acknowledgements

First of all I would like to thank Urs Albrecht for supervision and all the help and advice he gave me throughout the laborious years I spent at his group in Hannover and in Fribourg. I really appreciate that he always was open for all my small and big problems and worries.
I would like to thank Erik Maronde for the fruitful and amicable collaboration and for accepting the correference of my thesis.
Ueli Schibler I would like to thank for the inspiring comments he made on some of the publications presented in this work and for accepting correference of my thesis, too.
I thank Aaron Avivi and Eviatar Nevo for the long-standing and fruitful collaboration on the blind mole rat presented in the second part of this thesis.
Thanks to all the people at the Max Planck Institute in Hannover who helped me in finishing this work, especially Friederike Kruse, Uwe Herzig, Hans-Otto Bader, Karola Neubert, Heidi Kruppa, Pablo Szendro, Michael Leitges, Carsten Moeller and most of all to Nadine Naujokat for her support and her patience. I am very grateful to Gregor Eichele who generously supported my work in Hannover as well as in Fribourg.
I would like to thank all the people at the Biochemistry Department of the Universtiy of Fribourg, especially Andreas Conzelmann, Matthias Wymann, Catherine Marin, Gurudutt Pendyala, Jean-Luc Baeriswyl, Maria Chiara Magnone and Stéphanie Aebischer, who was a great help at work and in organizing all those essential things outside the lab.

Most of all I thank my family, my mother Ilse and my father Peter as well as my sisters Maike, Susanne and my brother David for their support and for offering me a secure haven to return to throughout all these years.

Henrik.

Fribourg, the 22nd of October 2002